

1. Nano Science and Engineering in Mechanics and Smart Materials



Ken P. Chong, National Science Foundation (USA)

Nano science and engineering is one of the frontiers in transformative research. It is the creation of new materials, devices and systems at the molecular level - phenomena associated with atomic and molecular interactions strongly influence macroscopic material properties with significantly improved mechanical, optical, chemical, electrical and other properties. Nobelist Richard Feynman back in 1959 had the foresight to indicate, "there is plenty of room at the bottom". National Science Foundation former Director Rita Colwell in 2002 declared, "nanoscale technology will have an impact equal to the Industrial Revolution". The transcendent technologies include nanotechnology, microelectronics, information technology and biotechnology as well as the enabling and supporting mechanical and civil infrastructure systems and smart materials. These technologies are the primary drivers of the twenty first century and the new economy. Mechanics and materials are essential elements in all of the transcendent technologies. Bio sensing, drug delivery systems, efficient molecular dynamics, modeling and simulation are also some of the challenging areas. Efficient civil and mechanical infrastructure systems as well as high performance smart materials are essential for these technologies. By promoting research and development at critical points where these technological areas intersect, we can foster major developments in engineering. The solid mechanics and materials engineering (M&M) communities will be well served if some specific linkages or alignments are made toward these technologies. Some thoughtful examples for the M&M and other engineering communities are:

- Bio-mechanics/materials
- Thin-film mechanics/materials
- Wave Propagation/NDT
- Nano-mechanics/materials
- Nano-electro-mech'cal (NEMS)
- Multi-scale Simulations/modeling
- Micro-electro-mechanical systems
- Smart materials/structures
- Designer materials
- Fire Retardant Materials and Structures

Research opportunities, education and challenges in mechanics and materials, including experimental, numerical and analytical methods in multi-scale modeling, nanomechanics, carbon nano-tubes, bio-inspired materials, smart materials, as well as improved engineering and design of materials will be presented and discussed.

2. Nanogenerators and Nanopiezotronics Based on Smart Structures



Zhonglin Wang, Georgia Institute of Technology (USA)

Developing novel technologies for wireless nanodevices and nanosystems are of critical importance for sensing, medical science, defense technology and even personal electronics. It is highly desired for wireless devices and even required for implanted biomedical devices to be self-powered without using battery. Therefore, it is essential to explore innovative nanotechnologies for converting mechanical energy (such as body movement, muscle stretching), vibration energy (such as acoustic/ultrasonic wave), and hydraulic energy (such as body fluid and blood flow) into electric energy that will be used to power nanodevices without using battery. We have demonstrated novel approaches for converting nano-scale mechanical energy into electric energy by piezoelectric zinc oxide nanowire (NW) arrays. The

operation mechanism of the electric generator relies on the unique coupling of piezoelectric and semiconducting dual properties of ZnO as well as the elegant rectifying function of the Schottky barrier formed between the metal tip and the NW. Based on this mechanism, we have developed DC nanogenerator driven by ultrasonic wave, fiber nanogenerator driven by tiny mechanical movement, and muscle driven nanogenerator for energy harvesting. Finally, a new field on nano-piezotronics is introduced, which uses piezoelectric-semiconducting coupled property for fabricating novel and unique electronic devices and components.

3. Research and Practice of Smart Materials and Structures in the Mainland of China

Jinping Ou, Dalian University of Technology (China)



In mainland China, research on smart materials first originated from the end of 1980s in the aerospace field, and then expanded to other areas. Basically speaking, the smart materials and structures have capability of self-sensing or/and controlling their shape, deformation or response, or/and repairing/curing their damage or/and self-adaptability. Therefore, they have four essential characteristics, i.e. self-sensing, self-control, self-curing and self-adaptability. The first two issues have been made great progresses, while the last two issues are still in early stage. The state-of-the-art and practice in the mainland of China are summarized in the paper.

The optical fibre-based sensing technology (strain, temperature and acoustic emission sensors, demodulators, software for data collection and products with optical fibre sensors) has been systematically developed and extensively used in civil infrastructures, composites structures and industries because this technology can provide distributed sensor networks with good durability and compatibility with fibre reinforced polymer composites. For concrete structures, the short carbon fibre reinforced cement mixed with conductive materials and cement-based composites containing carbon blacks have been proposed. Their strain self-sensing properties, electromechanical models, effects on electromechanical properties of temperature and water-proof measures have been experimentally and theoretically investigated. The monitoring for whole loading process of concrete members embedded with these kinds of sensors is studied. The PZT array has been extensively used as positive monitoring techniques for cracks, debonding, loosening and delamination. Besides the sensors for response monitoring, a sensor for corrosion monitoring is also developed. The advanced signal process approaches for corrosion detection based on wavelet analysis are proposed.

In intelligent structural control area, the magnetorheological fluid (MR fluid) is a type of smart fluid with a number of advantages. The fabrication procedures of MR fluids, sediment of MR fluids and prevention measures are developed. The MR dampers and their electromechanical properties and models are studied. The control of MR dampers to stay cables, offshore platforms and nonlinear structures is systematically studied. The shape memory alloys (SMA) are used as an integrated sensor and damper. The seismic response of buildings are measured and controlled simultaneously by SMA dampers. Recent years, shape memory polymer is also developed and its shape memory effects and damping properties are investigated. The magnetostrictive composites are developed and their magnetostrictive effects are studied. A smart damping device using these composites is fabricated and used to control vibration of cables. The design approach of intelligent control systems is also presented.

A crack self-repairing concrete and its structures have been proposed. The performance of the structure after self-repairing

has been experimentally verified.

4. Recent Advances on Developing Bio-Inspired Galfenol Nanowire Sensors



Alison Flatau, University of Maryland (USA)

Galfenol ($\text{Fe}_{100-x}\text{Ga}_x$, $10 < x < 25$ at. %) nanowires have been fabricated into close packed arrays through the process of electrochemical deposition. These structures exhibit a unique combination of size, elasticity, and magnetostrictive transduction that make them well suited for use as artificial cilia in biomimetic sensor devices. The cantilevered nanowires deflect in response to excitation (acoustic, tactile, flow, etc.), and the resultant bending or compressive stresses can produce a magnetization change that can be measured using conventional magnetic field sensor technologies. This presentation will provide an overview of the fabrication nanowire process and will discuss details of strategies used to overcome some of the specific challenges in making the nanowires, e.g. maintaining uniform composition along the length of a nanowire. We also review details the complete magneto-mechanical characterization of these nanowires. Results on the mechanical properties of individual Galfenol nanowires are shown from experimental measurements taken using a custom nanomanipulator mounted inside of a scanning electron microscope (SEM). Data shows drastically improved elasticity and tensile strength in the nanowires compared with the bulk material. Magnetic force microscopy (MFM) results are shown and used to visualize the magnetic domain structure, which are in excellent agreement with micro-magnetic models. The implications of these results with regards to the influence of shape anisotropy on nanowire responses to stress and optimization of sensor design are discussed. The presentation will conclude with a summary of some of the potential applications for the proposed nanowires as critical transduction components in a sensor.

5. Energy Harvesting Systems a Key to Self-Powered Systems



Ephraim Garcia, Cornell University (USA)

A new class of systems is just beginning to emerge in engineering, self-powered systems. In these systems, energy is harvested locally, while information is transmitted to and from the system wirelessly. Power harvesting is a key to this technology and smart materials, and in particular piezoelectrics, offer us new ways to create power from the vibratory motion from the surroundings. Piezoelectrics utilize strain in the transducer device to create a free charge or voltage field across the transducer's capacitive element. Discussed will be competing methods of harvesting this power using nonlinear switching circuitry. A number of methods have been created and the advantages and disadvantages of each will be explored. Piezoelectric systems are being created for structures undergoing base excitation and flutter conditions; both will be presented. Issues of harvesting power from different converters types will also be presented and discussed; types of converters of interest are DC and AC type that harvest power from different sources in the environment. Most recently, we have created useful electrical power from living organism, i.e., *Manduca sexta*, which was able to carry a piezoelectric structure weighing less than 300 milligrams and demonstrated useful power generation.

6. Durability of nanostructured silicate concrete in aggressive media



Oleg Figovsky, International Nanotechnology Research Center Polymate (Israel)

Nanostructured silicate concrete was elaborated by using a principle forming nanostructures during technological process. Significant increasing of silicate matrix strength and toughness was reached by incorporation of special liquid additives, such as tetrahydrofuryloxysilane -TFS, which effect as a microcrystallizing nucleator on the technological stage and later they colmatage the pores of silicate matrix. Our last elaborations are mainly applying a novel type of soluble silicate contained organic cations, for example, the DABCO-based organic alkali soluble silicate that also give the possibility additional modification of silicate concretes different polymers, such dimethylhudantoine epoxy resins and water dispersion of chlorine-sulfonated polyethylene. As was shown in our experimental investigation adding nanostructured agent TFS dramatically increased durability of silicate concretes in aggressive media and more that 10 time decreasing penetration of water solutions of acids into such silicate concrete. Nanostructured silicate concrete floor covering was tested – shock flooring test give more than 3 times increasing shock resistant of a new type silicate concrete before exposition in aggressive media and 4-5 increasing shock resistant after 12 months exposition in many aggressive media.

7. Toward a Bio-inspired Flapping UAV: Efficient Fluid-structure Interaction Analysis



Jae-Hung Han, Korea Advanced Institute of Science of technology (Korea)

The flapping-wing flight has superior maneuverability and aerodynamic advantages in a low Reynolds number regime. Recent research trends on UAV (Unmanned Air Vehicle) developments and numerous efforts to discover the principles of nature's flyers have been focused on the design and development of the flapping UAV. The flapping UAV generates aerodynamic forces and moments from the various wing motions such as flapping, pitching, twisting and lagging to fly and sustain its flight stability. Bio-inspired design of flapping UAV is one of the effective ways to exploit such a complex system. The morphological and kinematic parameters of nature's flyers are actually quite essential in the bio-inspired design process as input parameters. However the flapping aerodynamics has been investigated recently using computational fluid dynamics and wind tunnel testing but not fully understood yet. This makes hard to estimate the performance of the final flapping UAV design. In this talk, we propose a bio-inspired flapping UAV design framework considering fluid-structure interaction of flexible flapping-wing and efficient flapping-wing aerodynamic model for low Reynolds number flow. Moreover, we will briefly introduce the trimmed flapping-wing flight characteristics.

8. Structural Health Monitoring in Japan



Zhishen Wu, Ibaraki University (Japan)

This plenary presentation intends to first give an overview on the current status and point out developments of the element technologies such as sensing technology, data communication and information technologies and modeling feature selection and diagnosis technologies for

structural health monitoring/Management in Japan. Moreover, some application examples, major challenges and technology gaps will be discussed. In addition, the distributed dynamic and static monitoring techniques, and the related structural identification theories, structural performance evaluation and SHM design methodology based on the achievements from the speaker's research group will be also introduced.

001

A Comparison of Interrogation Schemes for Impact Event Monitoring Using Fiber Bragg Gratings

C. S. Shin, B. L. Chen, Department of Mechanical Engineering, National Taiwan University (Twain, China).

Composite structures are prone to develop internal damage caused by impact of tool drop, bird-strike, hailstorm and so on. These insidious defects may grow during service and eventually lead to catastrophic failures. Although non-destructive examination techniques for the detection of internal damages are available, they are limited in resolution. Moreover, to stage a thorough examination on a large scale structure can be highly time and resource consuming. The problem can be much alleviated if one knows where to look at and what to look for. Such information may be provided by an impact event monitoring and locating system. It has been established that when interrogated by appropriate energy modulation schemes, Fiber Bragg gratings (FBGs) are capable of acquiring transient impact signals and are suitable for the above application. Moreover they also enjoy excellent compatibility with common polymeric materials and may be embedded inside a composite structure without inducing significant weakening of the material. FBGs.

In order to minimize the number of FBGs deployed, the sensitivity of the interrogation system has to be optimized. In this work, we compared the performance of three interrogation systems for impact event monitoring on a large aluminum plate and a wind turbine blade. The configuration with an ASE light source is the least sensitive but remained stable under all impact conditions. In the other two configurations which comprise a ring laser scheme, the one with the sensing FBG being part of the laser ring is extremely sensitive and is capable of detecting the impact of a 70g projectile from a height of 0.1mm at a distance of 60cm. However, with increasing impact severity, the system may become unstable. A third configuration where the sensing FBG is not part of the laser ring gives a good compromise between sensitivity and stability. Based on the above results, the implications on the sensitivities and limitations of the three different configurations when used for impact event monitoring on large structures will be discussed.

002

A Design of Piezoelectric Sensors and Actuators for Active Control Vibrating Piezolaminated Plate, Application to Oceanographic Instrumentation

Mustapha Sanbi, Lalla Aicha Faik and Miloud Rahmoune, Moulay Ismail University (Morocco)

The concept of piezoelectric smart materials and structural systems with highly integrated sensors and actuators has led to a revolution in control of complex flexible structures. By integrating distributed piezoelectric sensors/actuators and advanced composites, the potential exists for forming high-strength, high-stiffness, light-weight structures capable of self-monitoring and self-controlling. To control such a structure an accurate estimation of voltage sensed by the piezoelectric sensors is necessary to provide the exact remedial actuation voltage. The coupled electromechanical properties of piezoelectric materials and their availability in the form of thin sheets make them well suited for use as distributed sensors and actuators for controlling structural response. In this paper, we present a generalized formulation for dynamic analysis of piezoelectric structures. The formulation is extended to include the electromechanical coupling.

004

A New Reddy-Levinson Beam Model Incorporating the Size Effect

H. M. Ma, X.L. Gao, J. N. Reddy, Texas A&M University (USA).

Thin beams widely used in sensors, probes and other micro/nano-scale devices have been experimentally observed to exhibit microstructure-dependent size effects, which cannot be explained by applying beam theories based on classical elasticity due to the lack of a material length scale parameter. This motivated the development of non-classical beam models using higher-order (non-local) elasticity theories that contain microstructure-dependent length scale parameters and are capable of interpreting the size effects. Two such models have recently been developed for the Bernoulli-Euler beam [1] and for the Timoshenko beam [2] using a modified couple stress theory [3, 4] which contains one material length scale parameter. In the current study, this higher-order elasticity theory is employed to develop a microstructure-dependent model for the Reddy-Levinson beam.

The classical elasticity based Reddy-Levinson beam theory was developed for beams with rectangular cross-sections using a third-order displacement field that satisfies the shear-free conditions on the upper and lower beam surfaces and accounts for the parabolically distributed transverse shear strain on the beam cross-section. A major advantage of the Reddy-Levinson beam theory is that a shear correction factor, which is inherently present in the Timoshenko beam theory and is typically an empirical parameter, is no longer needed.

In the current non-classical Reddy-Levinson (R-L) beam model, the governing equations and boundary conditions are obtained by using a variational formulation based on Hamilton's principle. The use of the modified couple stress theory enables the new beam model to capture the size effect. Also, the Poisson effect is incorporated in the current model, which differs from other R-L beam models. The newly developed non-classical R-L model reduces to the existing classical elasticity based R-L model when the material length scale parameter and Poisson's ratio are both taken to be zero. In addition, the current R-L beam model recovers the non-classical Bernoulli-Euler beam model based on the same modified couple stress theory when the normality assumption is reinstated.

To illustrate the new R-L beam model, the static bending and free vibration problems of a simply supported beam under a concentrated load are analytically solved by directly applying the general formulas derived. The numerical results for the static bending problem reveal that both the deflection and rotation predicted by the current non-classical R-L model are smaller than those predicted by the classical R-L model. Also, the differences in both the deflection and rotation predicted by the two models are very large when the beam thickness is small, but they are diminishing with the increase of the beam thickness. For the free vibration problem, the numerical results show that the natural frequency predicted by the current R-L model is higher than that by the classical R-L model, and the difference is significant only for very thin beam. These predicted trends of the size effect at the micron scale agree with those observed in experiments.

005

A Nondestructive Study on Porosity Content and Fiber Orientation in CFRP Composite Laminates Using Ultrasonic Through-Transmission Method

Je-Woong Park, Do-Jung Kim, Chosun University (Korea); Kwang-Hee Im, Woosuk University (Korea); David K. Hsu, Iowa State University (Korea); Sun-Kyu Kim, Iksan National College (Korea); Kil-Sung Lee, Yong-Jun Yang and In-Young Yang, Chosun University (Korea).

It is found that a pitch-catch signal was more sensitive than normal incidence backwall echo of longitudinal wave to subtle flaw conditions in the composites (damages, fiber orientation, low level porosity, ply waviness, and cracks). The depth of the sampling volume where the pitch-catch signal came from was relatively shallow with the head-to-head miniature Rayleigh probes, but the depth can be increased by increasing the separation distance of the transmitting and receiving probes. Also, a method was utilized to determine the porosity content of a composite lay-up by processing micrograph images of the laminate. The porosity content of a composite structure is critical to the overall strength and performance of the structure. The image processing method developed utilizes a free software package to process micrograph images of the test sample. The results from the image processing method are compared with existing data. Beam profile was characterized in unidirectional CFRP (Carbon fiber reinforced plastics) with using pitch-catch Rayleigh probes and the one-sided and two-side pitch-catch technique was utilized to produce C-scan images with the aid of the automatic scanner.

006

A Nonlinear Scalable Model for Designing Ionic Polymer-Metal Composite Actuator Systems

A. J. McDaid, K.C Aw, S.Q. Xie, E. Haemmerle, The University of Auckland (New Zealand).

In order to make full use of the significant potential of IPMC transducers and to have them widely accepted as a viable alternative to traditional actuators, accurate models must be developed to describe their behaviour so engineers can simulate and evaluate their performance in real world applications.

The proposed model addresses all the requirements of a useful design tool for IPMC actuators. Applied voltage is the single input and mechanical outputs are modelled in the rotational coordinate system, 'angle to tip' and 'torque output', to give more practical results for the design and simulation of mechanisms. The interaction between the IPMC and external loads are also modelled making it extremely useful in designing complete engineering systems. The model is geometrically scalable for different sizes of actuator, accurate for a large range of angle and torque outputs and is designed for operation in air.

It is largely accepted that the response of an IPMC when a potential is applied is in three stages, as so the model is split into three parts, (i) a nonlinear equivalent electrical model to predict the current draw for the applied signal, (ii) an electro-mechanical coupling term, which represents the conversion of the flow of ions to a stress generated in the polymer membrane and (iii) an equivalent mechanical circuit which includes an electrically induced torque, a passive stiffness term for the polymer and an equivalent beam model which outputs the angle and torque of the actuator.

The model is intended for robotic and bio-mimetic applications which operate at low frequencies, the model parameters are therefore obtained using the dynamic time response of a number of samples, sizes and input voltages. The model is similarly verified and results are presented to show the correspondence between the model and experimental results.

007

A Novel Micro Aerial Vehicle Made from Smart Material

Shijun Guo, Daochun Li, Cranfield University (UK).

A micro aerial vehicles (MAV) is defined as a semiautonomous airborne vehicle, measuring less than 15 cm in any dimension, weighing not more than 140g, which can fly up to 2h for range of 10km. As demonstrated by flying birds and insects, flapping flight

is advantageous for its superior manoeuvrability and lifting capability at low flight speeds. Different mechanisms such as pneumatic and motor-driven actuators have been applied to mimic this complex flapping motion, but these mechanisms often suffer from heavy weight and mechanical system complexity.

In this paper, investigation was made into the design, analysis and experiment of a smart material flapping wing devices for MAV. Attention was mainly focused on the design of a simple, reliable and lightweight flapping mechanism to achieve two most challenging objectives. Firstly enlarge the piezoelectric actuator motion for adequate flapping amplitude for forward flight; secondly achieve hovering or very low speed flight. Apart from the traditional rigid lever mechanism and symmetrical flapping wing configuration, this current research produced a couple of new design concepts including a compliant joint and a flapping rotor MAV configuration. Structural resonance and aeroelastic beneficial effect have been considered in the system design to reduce power demand and enhance aerodynamic performance.

The results have shown that the compliant joint amplification mechanism is simple and effective. The flapping wing rotation angle can reach up to 50 deg in the traditional mechanism and the frequency up to 9 Hz. For the compliant joint mechanism, the flapping wing can rotate up to 28 deg at 6.8 Hz and produce a powerful aerodynamic force. The test result of a 9 gm micro flapping wing rotorcraft prototype shows that the innovative design concept for hovering and very low speed flight is feasible.

009

A Numerical Study on the Effect of Sweep Angle on Flapping-Wing Flight Using Fluid-Structure Interaction Analysis

Dae-Kwan Kim, Korea Aerospace Research Institute (Republic of Korea); Jun-Seong Lee, and Jae-Hung Han, Korea Advanced Institute of Science and Technology (Republic of Korea).

Biological flyers such as birds, bats and insects have spanwise-chordwise anisotropic flexible wings. In flapping-wing flight, the flyers utilize the deformation of the wings to attain an appropriate effective angle of attack during up and down strokes. This means that the chordwise deformation, twisting motion, characterizes the efficient flapping flight. In particular, the amplitude and phase angle of the twisting motions are the main factors that affect the aerodynamic performance, and these values depend on the geometrical shape as well as the chordwise bending stiffness of the wing. Actually, most birds and bats have swept wings to increase the distance between the pressure center and the elastic axis, so that the twisting motion is increased. Therefore, the sweep angle of a flapping wing can be an important design parameter for artificial flapping-wing vehicles.

In the present study, the effect of sweep angle on flapping-wing flight is investigated through an aeroelastic analysis of a flexible flapping wing. The numerical analysis is carried out by using the efficient FSI (fluid-structure interaction) analysis tool based on the modified strip theory and flexible multibody dynamics, which was proposed in our previous research for an optimal design of a flexible flapping wing. To investigate the effect of sweep angle, several FSI analyses are performed on a swept flapping wing according to the variation of the sweep angle and the position at which the wing is swept. From the analysis results, the optimal sweep angle and position with respect to aerodynamic performance are determined, and the effect of the sweep angle on the aeroelastic characteristics of the flapping wing are discussed in detail.

010

A Photocatalyst Prepared with Functionalized Diatom Frustules by the Liquid Phase Deposition

K. Umemura, Tokyo University of Science (Japan); Y. F. Gao, Chinese Academy of Sciences (China); T Nishikawa, The Hyogo Prefectural Technology Center for Agriculture, Forestry and Fisheries (Japan).

Frustules that are cell walls of diatom cells are natural nanoporous silica. The frustules have been widely used for various industrial applications such as water filters, building materials, etc. Recently the frustules are becoming one of the most attractive nanobiomaterials by combining the nanoporous structures of the frustules with the nanotechnology. In this paper, we demonstrated production of a photocatalyst using functionalized diatom frustules by the liquid phase deposition (LPD) method.

Firstly, the frustules of *Coscinodiscus wailesii* were prepared by cultivation of the isolated diatom cells. Then, the purified frustules were incubated in boric acid and ammonium hexafluorotitanate in order to deposit TiO_2 film on the frustules surface. Scanning electron microscopy and optical microscopy revealed the frustule surfaces were well covered with TiO_2 thin film. Activity of the functionalized frustules as a photocatalyst was examined by decomposition of methylene blue molecules.

When suspension of the native diatom frustules was mixed with the methylene blue solution, some amount of methylene blue molecules was rapidly adsorbed to the frustules. However, even after irradiating for 3 hours by a black light, absorbance at 664 nm was not decreased. It suggests that the methylene blue molecules were not decomposed on the native frustule surface. In the case of the functionalized frustules with TiO_2 , absorbance at 664 nm was gradually decreased according to the irradiation. The result indicated that the functionalized frustules had activity as a photocatalyst.

011

A Rotary Joint Sensor Using Ionic Polymer Metallic Composite

A. van den Hurk, X.J. Chew, K.C. Aw, S.Q. Xie, The University of Auckland (New Zealand).

Ionic Polymer Metallic Composite (IPMC) is a type of smart material that has the potential of being used as sensors for various applications. This paper investigates how IPMC is used as a rotary joint sensor, which offers many advantages over conventional sensing methods. Previous studies have identified the sensing properties of IPMC that would be useful for this purpose, but the testing methods are still inadequate, and more work needs to be carried out so that IPMC sensors can be used in measuring rotary motion.

A mathematical model is developed to relate the voltage response of the sensor to the motion of the joint from numerous experimental results. This model has been used to develop calibration and prediction routines which calculate the bending angle and bending rate of the joint, based on the voltage response of the IPMC sensor. Experimental results show that the model has an accuracy of 1.5° for measuring bending angles. The accuracy of the measured bending rate is closely related to the joint motion; with errors ranging from $0.8\%/s$ at a slow turning rate ($\leq 150^\circ/s$) for a large bending angle ($\geq 50^\circ$) up to an error of $65.2\%/s$ at fast bending rate ($\geq 200^\circ/s$) for a small bending angle ($\leq 30^\circ$).

It is concluded that the methods developed in this study provide a more complete description of the relationship between IPMC sensor voltage and joint motion than has previously been documented. This model shows a good accuracy for measuring bending angles and also for measuring bending rate up to $150^\circ/s$.

The current model still has limitations that will require further investigation for IPMC to become a realistic option for use as a rotary joint sensor.

013

A Study of Optimum Configuration of the Injection Molded Plastic Gear by the Modification of Gear Tooth

Dae-Suep Lee, Yeungjin College (Korea); Jin-Wook Do, Young-Doo Kwon, Kyungpook National University (Korea).

This study is an optimization of gear system modifying tooth configuration of injection molded plastic gears. The applied range of the injection molded plastic gear is wide in the field of industrial machine elements like the electric and electronic parts, auto-motive parts, etc. When the injection molded plastic gear is used instead of the steel gear, as the weak points, capabilities of the injection molded plastic gear are low in load transmission, durability and reliability in prediction of life. However, as the strong points, light weight, low-noise, operation without lubricant, shock absorption, and anti-corrosion can be mentioned.

This study has carried out the calculation and analysis of gear characteristics by FEM tool, and compared the characteristics of the common normal gear system and the modified gear system at the contacting condition in each system. When torque is applied to these gear systems, the system using the modified gear has the effect of slow-contact between gears. So, the noise of modified gear system exhibits lesser than common normal gear system. And also, load sharing of the modified system is better than the common system because of increased contact ratio to recover decreased form factor. To calculate and analyze the simulation of gear matching, we used the commercial tools like CATIA, Pro/Engineer for simulation and ANSYS, MARC for calculation.

015

A Study on Preparation and Mechanical Properties of UHMWPE/Nylon Wrap Yarn

WeiHua Yao, Oriental Institute of Technology(Twain, China); Jen-Taut Yeh, National Taiwan University of Science and Technology(Twain, China); Wen-Li Chou, Nanya Institute of Technology(Twain,China); Yao-Chi Shu, Vanung University(Twain, China).

The preparation of UHMWPE/NYLON wrap yarn which is composed of ultra-high molecular weight polyethylene (UHMWPE) filament and nylon filament was fabricated via hollow spindle machine. Among the UHMWPE filament (Spectra 1000) which was purchased from Honeywell of USA was treated as core filament and the nylon filament which was purchased from factory of Taiwan was treated as sheath yarn. The mechanical properties of UHMWPE/NYLON wrap yarn were investigated through experiments of evenness, wrap yarn denier, tensile strength, tensile tenacity, tensile elongation and tensile strain. The properties of tensile strength, tensile tenacity, tensile elongation and tensile strain of UHMWPE/NYLON wrap yarn were tested by tensile testing frame; for the wrap yarn denier of UHMWPE/NYLON wrap yarn was experimented by accurate balance, a vacuum oven and calculated by direct system formula of yarn count and the wrap yarn qualities of evenness (U% or CV%) was measured by Uster Testing Instrument. The wrap nylon denier, nylon type and wrap number of nylon filament around onto UHMWPE filament (degree of twist, TPM) were chosen as the experiment's parameters in this study, Meanwhile, the parameters of nylon filament denier is chosen the both of 40D and 70D, nylon type is chosen the both of nylon6, 6 and a nylon6; and twist degree is chosen from 700TPM to 1000TPM (turn per meter). The resulted properties of UHMWPE/NYLON wrap yarn are indicated that the U% and CV%

of yarns evenness aren't affected by those parameters and always kept below 3%. The denier of wrap yarn was increased with the increase of denier and twist degree of wrap nylon. The tensile strength was also increased with the increase of denier and twist degree of wrap nylon and the wrap nylon66 was higher tensile strength than wrap nylon6. For the tensile strength of UHMWPE/NYLON wrap yarn, the tensile tenacity was decreased with the increase of wrap nylon denier, when wraps nylon 40 deniers, the tensile tenacity was kept constant with wrap in any nylon type, and twist degree, whereas wrap nylon 70 deniers, the tensile tenacity was increased with increasing of twist degree in both of wrap nylon6 or nylon66. For the elongation and elongation% (tensile strain) of wrap yarn were shown to increase with increasing both of denier and twist degree of wrap nylon, this phenomena was more obviously wrap nylon 40 deniers than wrap 70 deniers, whereas there was not difference between wrap nylon6 and nylon6,6.affected the elongation and elongation% (tensile strain) of wrap yarn

In summary, the UHMWPE filament was wrapped with nylon to fabricate the UHMWPE/nylon warp yarn via hollow spindle frame, although the tensile strength of UHMWPE/Nylon wraps yarn would be decreased, in contrast with UHMWPE filament, the UHMWPE/Nylon wraps yarn is a great tensile elongation and tensile strain as well as the dyeing and the weaving would be improved; The optimum parameters to prepared UHMWPE/Nylon wraps yarn is respectively chose nylon66, 70D and 1000TPM.

016

A Study on Radiated-Heat Plate for a Use of Electronic Component Cooling Using Engineering Plastics

Young Tae Cho, Jeonju Univ (Korea).

Recently, the electronic parts are to be thinner plate, smaller size, light weight material and CPU, HDD and DRAM in all the parts have been produced on the basis of the high speed and greater capacity. Also, conventional goods have replaced a LED (Light-Emitting Diode) in lighting products so; such industry devices need to have cooling. To maximize all the performance on the heat-radiated products, the area of heat-radiated parts is required to be cooled for keeping the life time extension and performance of product up.

Existing cooling systems are using radiant heat plate of aluminum, brass by extrusion molding, heat pipe or hydro-cooling system for cooling. There is a limitation for bringing the light weight of product, cost reduction, molding of the cooling system. So it is proposed that an alternative way was made for bringing to the cooling system.

EP (Engineering Plastic) of low-cost ABS(Acrylonitrile butadiene styrene Resin) and PC (Polycarbonate) was coated with brass and the coating made the radiated heat go up. The performance of radiant heat plate is the similar to the existing part. We have studied analytically and experimentally on the radiated heat plate for the light-weight, molding improvement and low-cost.

From now on, we are going to develop the way to replace the exiting plate with exterior surface of product as a cooling system. It is thought that approximately 10% of the radiated-heat rate for the brass-coated ABS is decreased more that the existing aluminum plate in natural convection state through the simulation results. The similar performance is expected for keeping forced convection state and optimum shape design of radiated-heat plate.

017

A Study on the Adhesive Strength of Cfrp/Aluminum Composite Using Surface Treatment

H.J.Chung, K.Y.Rhee, B.S.Han, Y.M. Ryu, Harbin Institute of Technology (China).

Aluminum foam is light-weight porous material and its manufacturing process is simple. Aluminum foam material has immense potential for application in the automobile and architectural industries. In the present study, the effect of oxygen plasma treatment on the adhesive strength of CFRP/Aluminum foam composites was investigated. CFRP and aluminum foam were plasma treated in a plasma cleaner using oxygen gas. The result showed when the CFRP was plasma-treated, the shear strength were improved 650%, when compared to cases without plasma treatment or plasma treatment of aluminum foam. AFM result showed that R_q prior to the plasma treatment was 22.99 nm, while after treatment it was 27.86 nm, meaning that the surface roughness of CFRP increased by more than 20% as a result of the plasma treatment. It is known that as the higher a surface roughness becomes, the larger a bonding area between adhesive and an adherend becomes. Thus, it is believed that the increased surface roughness of CFRP played a role in improving the bending and shear strengths of the adhesive CFRP/aluminum foam composites.

018

A Thermo-Viscoelastic Model for Amorphous Shape Memory Polymers

H. Jerry Qi, Francisco Castro, University of Colorado at Boulder (USA).

Shape memory polymers can offer a large shape change as the environment changes. For thermally induced shape memory polymers, an SMP can be pre-deformed from an initial shape to a deformed shape by applying an external mechanical load at temperature T_d . A subsequently lowering down the temperature to T_s will freeze this deformed shape after the external mechanical load is removed. The shape memory effect is then activated by increasing the temperature to T_r , where the initial shape is recovered. In general, T_d and T_r are in the vicinity of the glassy transition temperature T_g , whilst T_d is above T_g and T_s is below T_g . In such a shape-frozen and shape-recovery cycle, the sample needs to go through its T_g twice. For polymers, as the temperature traverses the T_g , the mechanical behaviors of the polymer will change from a rubbery behavior to a glassy behavior which is a direct result of the transition in the polymer structure, a process that is strongly dependent on time. In this paper, a constitutive model based on thermoviscoelasticity is presented to capture the thermo-mechanical behaviors of amorphous shape memory polymers. The model simulations compare well with experiments under different thermomechanical loading conditions.

019

Beam Vibration Control Using Electro-Active Paper Sensor

Heung Soo Kim, Ho Cheol Lee, Catholic University of Daegu; Jaehwan Kim, Inha University (South Korea).

Cellulose-based Electro-Active Paper (EAPap) has been discovered as a smart material that can be used as a sensor and an actuator. Its advantages include low voltage operation, light weight, low power consumption, biodegradability and low cost. EAPap is made of cellulose paper coated with thin electrodes. EAPap shows a reversible and reproducible bending movement as well as longitudinal displacement under electric field and vice versa. Piezoelectricity is one of major driving mechanism of a cellulose-based EAPap. Although the potential of EAPap as a piezoelectric sensor is promising, the application of EAPap as a piezoelectric sensor has not been clearly studied yet. In order to use EAPap as a useful sensor, it is important to demonstrate EAPap as an actual piezoelectric sensor. Therefore, beam vibration control using EAPap sensor is investigated in the present paper. The

EAPap sensor and piezoceramic patch will be attached on top and bottom surfaces of an aluminum cantilever beam. The beam vibration data will be obtained from EAPap sensor and the piezoceramic patch will suppress the beam vibrations as an actuator. Simple velocity feedback control algorithm will be used to control beam vibration. The final paper will present effective vibration suppression of the cantilever beam with EAPap sensor and propose EAPap as a promising piezoelectric sensor.

020

Adhesion Strength of Norbornene-based Self-healing Agents to an Amine-cured Epoxy

Guang Chun Huang, Jong Keun Lee, Michael R. Kessler.

Self-healing is triggered by crack propagation through the microcapsules, which then release the liquid healing agent into the crack plane. Subsequent exposure of the healing agent to the chemical catalyst initiates ring-opening metathesis polymerization (ROMP) and bonding of the crack faces. In order to improve self-healing functionality, it is necessary to enhance adhesion of polymerized healing agent within the crack to the matrix resin. In this study, shear bond strength between different norbornene-based healing agents and an amine-cured epoxy resin was evaluated using the single lap shear test method (ASTM D5868). The healing agents tested include endo-dicyclopentadiene (endo-DCPD), 5-ethylidene-2-norbornene (ENB) and DCPD/ENB blends. 5-Norbornene-2-methanol (NBM) was used as an adhesion promoter, containing hydroxyl groups to form hydrogen bonding with the amine-cured epoxy. A custom synthesized norbornene-based crosslinking agent was also added to improve adhesion for ENB forming a linear chain structure after ROMP. The healing agents were polymerized with varying loadings of the first generation Grubbs catalyst at different reaction times and temperatures.

021

Ambient Thermal Response Based Damage Detection in Beam-Like Structure

N.H.M. Kamrujjaman Serker, Md. Robiul Awal, Md. Kumruzzaman, Tarif Uddin Ahmed.

Detecting damage in structure is an important and active research area. Numerous damage detection techniques have been proposed based on the responses measured under static or dynamic loading. Some of the proposed techniques utilize the response of the monitored structure measured under ambient loading. However, most of the techniques require some external sources of excitation causing interruption to the normal operation of the monitored subject. In this regard, ambient thermal response can also be a good choice for damage detection, especially, in civil structures. Under solar radiation excitation, thermal response of structure takes place slowly, periodically and the magnitude of the response is large enough to measure using conventional measuring devices. Moreover, monitoring of structures using thermal responses can be performed continuously under the normal operating condition of the monitored structure. This paper presents a methodology for the use of ambient thermal response as a damage detection tool for structural health monitoring of beam-like structures. To develop a damage detection methodology, a simple supported prestressed concrete beam was exposed to normal environmental condition and structural responses due to thermal loading were measured. Experimental results show that the damage stage due to cracking can be identified successfully and distinctly by analyzing thermal responses.

022

An Investigation on the Cryogenic Ball Milling to Multi-Walled Carbon Nanotubes

J. H. Lee, M. T. Kim, and K. Y. Rhee.

A cryogenic ball milling process is widely applied to reduce particle size of metal, metal alloys, and ceramics at extremely low temperature environment. Also, this process provides a more simple and efficient than other method. In this study, cryogenic ball milling was performed on CNTs in chamber at a temperature of -180°C or lowers to reduce the agglomeration of CNTs. The effect of cryogenic process on the de-agglomeration of CNTs was investigated. SEM examination was made to analyze the shape and size of particles before and after ball milling. The chemical changes by the cryogenic ball milling process were examined through x-ray diffraction (XRD) analysis. The results showed that the agglomeration of CNTs was reduced considerably by the cryogenic ball milling. The cryogenic ball milling yielded only a reduction of agglomeration without chemical changes of CNTs.

023

Analysis of Flexural Wave in Double-Walled Carbon Nanotubes Using Continuum Mechanics and Molecular Dynamic Simulations

Y.G. Hu, K.M. Liew and Q. Wang

Flexural wave in single-walled carbon nanotubes (SWCNTs) has been studied through the beam model and molecular dynamic (MD) simulation. The transverse and torsional wave in single- and double-walled carbon nanotubes have also been studied using shell model and MD simulations. The flexural wave in double-walled carbon nanotubes (DWCNTs) is still not available.

This paper investigates the dispersion of flexural waves in DWCNTs, focusing on the effect of carbon nanotube microstructure on wave dispersion. The DWCNTs are modeled as nonlocal double elastic beam model. Molecular dynamics (MD) simulations are used to simulate the flexural wave in DWCNTs. The van der Waals force between the inner and outer walls is described by the Lennard-Jones potential. The nonlocal elastic beam theory is expected to provide a better prediction of the dispersion relationships than the classical beam theory when the wave number is large enough for the carbon tube microstructure to have a significant influence on the flexural wave dispersion. Because of the different small-scale effects of SWCNTs with different diameters and the interlayer van der Waals interaction of DWCNTs, the noncoaxial vibration of DWCNTs will be investigated through the MD simulations in the flexural wave propagation at high frequency.

024

Application of Swift Heavy Ions Irradiated Conducting Polymers in EMI Shielding

Amarjeet Kaur, Anju, University of Delhi(India); D.K. Avasthi, Inter University Accelerator Center (India).

The irradiation of conducting polymers by swift heavy ion (SHI) is a recent technique for physical and chemical modifications of the polymers. In present investigations, three different polymers viz. polypyrrole (PPY), poly (3-hexyl thiophene) (P3HT) and Poly(3,4-ethylenedioxythiophene)-polystyrene sulfonic acid (PDOT:PSS) have been chosen to study the effect of 100 MeV silver (Ag^{8+}) ion radiations and to explore their possible applications. PDOT: PSS was procured from Sigma-Aldrich. PPY films have been prepared by electrochemical polymerization where as P3HT has been prepared by chemical oxidation i.e. Sugimoto method. Appropriate thickness of all the polymeric films have been

selected by Monte-Carlo simulation program SRIM so as to be thin enough to allow the 100MeV ions to completely pass through it. The samples were irradiated with different fluences (10^{10} , 10^{11} , 10^{12} ions/cm²) of 100 MeV silver (Ag^{8+}) ions. A comparative study between the samples, before and after irradiation has been performed by various characterization techniques, such as surface electron microscopy (SEM), atomic force microscopy (AFM), X-ray diffraction (XRD). The temperature dependence of dc conductivity of irradiated as well as unirradiated samples has been investigated in 77-300K. It has been observed that surface structure becomes smooth and polymer chains get more organized due to irradiation. The conductivity increases by two orders. The increased degree of crystallinity leads to higher values of conductivity due to decreased scattering of charge carriers. The conductivity of all the irradiated samples remain stable under atmospheric conditions, for more than one year whereas the conductivity of unirradiated samples, changes by $\pm 15\%$, when kept under atmospheric conditions, over a period of time. The conductivity here can be assumed to consist of two components, namely σ_B and σ_H such that the total dc conductivity $\sigma_{dc} = \sigma_B + \sigma_H$. The intrachain conductivity σ_B can be described by the mechanism for band conduction model whereas σ_H is contribution due to charge transport between the chains. With the organization of the polymer chains under the influence of silver ion radiation the contribution of σ_H increases. By trying different combinations of high energy heavy ions, the conductivity can be further increased, which leads to their application in EMI shielding. Fully undoped samples of PPY and P3HT were chosen, so that there should not be any interference of the results from dopant and that due to irradiations. SE in decibel is a measure of the reduction of EMI at a specific frequency achieved by a shield. Better values of SE are obtained by increasing the conductivity by doping. But the conductivity of doped conducting polymers decay over the period of time, but in this case structural modification of the polymers is done so as to increase the conductivity, without using any dopant ion and there is no decay in conductivity over a period time.

025

Active Vibration Control of a Composite Wing Model Using PZT Sensors/Actuators & Virtex – 4 FPGAs

Shashikala Prakash, D.V. Venkatasubramanyam, Bharath Krishnan, Aravind Pavate, Hemant Kabra NAL, Bangalore (India).

The reduction of vibration in Aircraft/Aerospace structures as well as helicopter fuselage is becoming increasingly important. A traditional approach to vibration control uses passive techniques which are relatively large, costly and ineffective at low frequencies. Active Vibration Control (AVC) overcomes these problems & uses additional sources (secondary) to cancel vibration from primary source based on the principle of superposition theorem. AVC, apart from having benefits in size, weight, volume and cost, efficiently attenuates low frequency vibration. Since the characteristics of the vibration source and environment are time varying, an AVC system must be adaptive. Hitherto this was being achieved using high speed Digital Signal Processors (DSPs). But the throughput requirements of these systems have strained the abilities of general purpose DSPs so much that the Field Programmable Gate Arrays (FPGAs) have emerged as an alternative. FPGAs incorporate arrays of dedicated multipliers, embedded memory & high speed I/O. The silicon resources of an FPGA lead to staggering performance gains i.e. they are 100 times faster than DSPs.

In the present paper Active Vibration Control of a Composite Research Wing Model is investigated using Piezo electric patches as sensors and PZT bimorph actuators collocated on the bottom surface as secondary actuators. Attempt has been made to realize the State – of – the – Art Active Vibration Controller using the

Xilinx System Generator on VIRTEX - 4 FPGA. The control is achieved by implementing the Filtered-X Least Mean Square (FXLMS) based adaptive filter on VIRTEX – 4 FPGA. Single channel real time control has been successfully implemented & tested on the composite research wing model. The methodology & results of this novel study are brought out in this paper.

026

Bio-inspired Methods to Self-Assemble 3D Micro-/Nano-Structures for Energy Harvesting

Xiaoying Guo, Huan Li, Ralph Nuzzo, K. Jimmy Hsia, University of Illinois at Urbana-Champaign (USA).

No matter how complex the structures of a living organism are, the building blocks of such a structure are often amazingly simple. Self-assembly at the micro- and nanoscales is a powerful tool to construct such complex structures. Water, among all things, plays a critical role in the self-assembling processes. In particular, such processes often involve surface phenomena, such as capillary interactions and surface adhesion. Many scientific issues of these surface phenomena during self-assembly can be best understood using the mechanics approach. In this presentation, we will demonstrate that mechanics can indeed be a useful tool to help understand surface phenomena-driven self-assembly by considering the self-assembly of a 3-D photovoltaic device made of thin silicon foil. We will describe the strategy for fabricating 3D single crystalline Si structures and suggests a new route to 3D light trapping in photovoltaic applications. It combines photolithography for fabrication of planar, patterned Si sheets with self-assembly driven by capillary forces. A model has been developed to identify the mechanisms controlling the behavior of these processes. Critical parameters emerge naturally from the analysis which can be used to guide the device formation and manufacturing of nanoscale components.

027

Bio-molecules Detection Sensor Using Silicon Nanowire

P.K. Kim, H.S. Oh, Korea Electrotechnology Research Institute (Korea); G. Lim, Postech-Pohang University of Science and Technology (Korea).

Schottky barrier-Silicon nanowire field effect transistor (SB-SiNWFET) sensor for detecting a bio-molecule was fabricated by combining the E-beam lithography and the conventional MEM technique. The detection of few numbers of bio-molecules is enabled by realizing the gold nanodots on SiNW.

Silicon nanowire-Schottky barrier field effect transistor sensor has few advantages that would enable to detect a small signal from the bio molecules. Since main detection area is the nano size channel, because of its small size, almost one dimensional flow of electrons is possible. Significance is this phenomenon is that because such a small number of electrons are flowing in the electron, it would be very sensitive to external charge and very small charge of bio-molecule can make the signal change between the channel ends. Additionally, to detect the small number of bio-molecules, it is necessary to place the binding sites on the sensor which is close to the size of the single molecule. By careful establishing the nanodot fabrication condition and reducing the signal noise, single bio-molecule will be possible. The current-voltage (I-V) properties of Schottky barrier silicon nanowire FET (SB-SiNWFET) were measured using semiconductor analyzer. Drain current was measured against applied drain voltage for the gate voltage of 0 ~ 4V. SB-SiNWFET that exhibits the normal FET behavior at around tens nano ampere range, and at low gate bias, the current flow is significantly suppressed. When SB-SiNWFET is exposed with different pH buffer solution, it responds with current change. Because ions in pH solution cause the change of charge density on

the SiNW surface, it disturbs the current flow. From this result, we conclude that our sensor responses to small signal change that would be used to detect the bio-molecules.

028

Carbon-Nanotube/Semiconducting Polymer Nanocomposites for Application in OTFTs

Silvia Janietz, Tatjana Egorov-Brening, Björn Gruber, Fraunhofer Institute Applied Polymer Research (Germany).

It is widely acknowledged that for application in organic electronics solution processing of organic semiconductors on flexible substrates will offer a significant advantage over established silicon technology for new types of consumer products. A key advantage of organic semiconductors over inorganic semiconductors is their printability, so the use is possible of large scale, low cost processing technologies. Here are present a generic approach to disperse and processing carbon nanotubes into conjugated polymer materials to be used as active organic material. Therefore chemical functionalisation was done onto the surfaces of carbon nanotubes (CNTs) to improve the compatibility between the conjugated matrix and the nanoscale objects. Surfaces of multiwall carbon nanotubes (MWCNTs) as well as single wall carbon nanotubes (SWCNTs) were chemically modified. Favourable non-covalent interactions of the conjugated units with the nanoscale objects are enable dispersion of these species in solvents suitable for low-cost processing. The films produced are being composites of well-dispersed carbon nanotubes and high performance organic soluble semiconductor. The formation of polymer /CNT composites were investigated with different amounts of carbon nanotubes into the semiconducting poly(3-hexylthiophene) with 5% of tetrafluorobenzene as an electron accepting unit in the main chain. These blend systems were studied in different OTFT structures. In one approach PET-foil substrates were utilized with pre-deposited metal source and drain electrodes in a “bottom contact” and “top gate” structure with polymeric dielectric and evaporated Al gate. In dependence of the amount of carbon nanotubes which where integrated in the semiconducting matrix improvement was achieved for the OTFT parameters like field effect mobility in the range of one order of magnitude, On/Off ratio and threshold voltage. The relationship between the composition of the blend system and the achieved OTFT device parameters will be discussed in detail.

029

Coarse-Grained Molecular Dynamics Simulations of Shape Transitions of Red Blood Cells

Hongyan Yuan, Changjin Huang, and Sulin Zhang, Pennsylvania State University (Panama).

The shape of the human red blood cells (RBC) has been the subject of many biophysical investigations over the past half century. Human RBCs generally take a biconcave shape under normal conditions. When passing through narrow vessels, or being stimulated by certain bioagents, RBCs may undergo drastic shape transitions. Continuum theories based on curvature elasticity have been employed to determine the stable configurations of RBCs under the constraint of fixed volume and area on the basis of free energy minimization. However, continuum models are incapable of taking into account the effect of thermal fluctuations, which have been proven to be essential for such a soft matter. In addition, the energy-minimization method is unable to extract the dynamic evolution of the shape transition. Methods to the other end of length spectrum, i.e., all-atom molecular dynamics (MD) simulations are computationally too costly to model such shape transitions.

The limitations of all-atom atomistic simulations and continuum approaches along with the practical needs to treat the heterogeneous nature of biomembranes have motivated a continual search for coarse-grained (CG) methods that bridge atomistic and continuum models. We have recently developed such a coarse-grained biomembrane model that facilitates the simulations of shape transitions of RBCs. In this model, a coarse-grained particle represents a cluster of lipid molecules and proteins with a diameter on the order of membrane thickness and carries both translational and rotational degrees of freedom. The model is solvent-free and the inter-grain interaction is anisotropic characterized by a Lennard-Jones type potential. The model also allows free diffusion of membrane particles. Combining with a volume and area control mechanisms by tessellating the membrane surface, this coarse-grained model enables us to simulate a broad range of physiological phenomena involving a closed membrane of laboratory size. We have successfully reproduced a series of experimentally observed shape transitions of RBCs. Our simulations identify that the shape transitions of RBCs are governed by the volume, temperature, and the spontaneous curvature.

031

Compressive Properties of Am50 and Az91d Alloys Using Hopkinson Bar (SHPB)

Iram Raza Ahmad, DongWei SHU, Nanyang Technological University (Singapore).

Magnesium alloys being the lightest structural materials are very attractive for aerospace and automobile industries. In the present study two magnesium alloys AM50 and AZ91D have been investigated for their potential to be used in above industries. The compressive stress-strain relation of AM50 and AZ91D has been obtained at the strain rates range between 0.002 s^{-1} and 1500 s^{-1} . The high strain rate experiments have been conducted using the split Hopkinson pressure bar (SHPB) apparatus. For both alloys, a substantially higher work hardening is observed at higher strain rates as compare to their quasi-static tests. Furthermore, higher compressive stresses are observed at higher strain rates. A higher yield stress is observed for AZ91D as compare to AM50. A comparison has also been made with aluminum alloys.

032

Constraint Super-elastic SMA Based Experimental Study of Self-Monitoring and Repairing of Concrete Beam Crack

Weipan HUA, Shengwei JI, Lanzhou University of Technology (China); DI Sheng-kui, Steve Zou, Dalhousie University (Canada)

Taken advantages of the characteristics of super-elasticity and restoring forces while the shape memory alloy(SMA) was excited, concrete modal beams were established, embedded different pre-stretching length, different numbers Ni-Ti SMA under martensitic state into the concrete tensile zone before the concrete casted under environmental temperature, the relationship between the resistance rate of SMA and the cracks width of beams was studied under loaded process, and the variety regulation of restoring force of the SMA with the cracks width of beam while excited by electrifying. The impact of slip and bond between the concrete and SMA was taken into account by embedded the anchor at both ends of the beam to prevent the slip of the SMA, the process was simulated considered the influence of additional resistance coming from the anchor, the result is good agreement with the experimental result. It was shown that SMA increased the deformation capacity of the beam significantly, the crack closed almost completely and the deformation recovered suddenly after the SMA was excited by electrifying, the drive effect can be

improved by growing in quantity of SMA, but the existence of residual deformation of rebar play a very negative role while recovering of the residual deformation.

033 Continuum Modeling of Interfaces in Carbon Nanotube-Reinforced Composites Based on Van Der Waals Forces and Chemical Bonds

Liyang Jiang, the University of Western Ontario (USA).

Carbon Nanotube-Reinforced Composites possess a large amount of interfaces due to the small (nanometer) size of carbon nanotube reinforcements. The interface behavior can significantly affect the mechanical properties of nanocomposites. However, modeling of CNT/polymer interfaces has been a challenge in the continuum modeling of CNT-reinforced composites. It is, therefore, the objective of the current work to model the CNT/polymer interfaces via an interfacial cohesive law. In addition to the van der Waals forces, the influence of the chemical bond due to carbon nanotube functionalization is considered, thus the interface load transfer is governed by both van der Waals force and chemical covalent bond. This developed cohesive law provides an analytical expression for the cohesive stress in terms of the interface opening displacement. All cohesive law properties (e.g., cohesive strength, cohesive energy) are obtained in terms of atom area density of carbon nanotube and volume density of polymer molecules, as well as the parameters in the van der Waals force and Tersoff-Brenner potential. It is found that the cohesive strength increases with the addition of chemical bond along the interface, and the interface debonding may be hindered by the existence of chemical bond. This simple and analytical cohesive law provides a direct link between the macroscopic behavior of nanocomposites and nanoscale behavior of interfaces, and therefore an assessment whether the interface behavior is indeed responsible for the macroscopic properties of nanocomposites.

034 Coupling of Physical Domains at the Nanoscale

Aman Haque, Pennsylvania State University (USA).

The first part of this presentation deals with the challenges in characterization of nanoscale materials. The issues of specimen preparation and mechanical testing are discussed for different classes of materials with varied morphology and dimensionality. Particular attention is given on the concept of in-situ testing of materials, with examples shown for both scanning and transmission electron microscopes. It is shown that in-situ testing not only enhances the measurement resolution, but also adds valuable insights on the fundamentals of deformation and failure mechanisms dominant at the nanoscale. Experimental results will be presented on metallic, ceramic and carbon-based materials and interfaces.

In the second part of the presentation, we will investigate how physical domains are coupled at the nanoscale. When the physical dimensions are on the same order as the mean free paths of electrons or phonons, pronounced coupling in thermal, electrical and mechanical domains. We will introduce a novel experimental technique that can perform such coupled domain experiments. The technique uses a nanofabricated chip with uniaxial tensile testing, four probe electrical and 3- thermal conductivity testing on nanoscale thin films of one dimensional materials. For aluminium, we observe 40% reduction in thermal conductivity at 0.25% mechanical strain. Similar pronounced coupling in carbonaceous and polymeric materials will also be presented.

The findings of this study will be useful in developing a unified theory of materials in multi-domains and also help discover new

physical characteristics in current materials by tuning their properties rather than developing new materials.

035 Damage Detection in Composite Laminates Containing Delaminations Using Fiber-Optic Sensor

Fucai Li, Kazuro Kageyama, Hideaki Murayama, Kiyoshi Uzawa, Isamu Osawa, The University of Tokyo (Japan).

In this paper, carbon fiber reinforced epoxy (CF/EP) laminates (intact and delaminated) are addressed for the purpose of damage assessment. A piezoceramic (PZT) wafer and a Doppler effect-based fiber-optic (FOD) sensor were bonded on the surface of each composite beam to generate and acquire guided waves propagating in the specimens, respectively. Characteristics of the fundamental symmetric (S_0) wave and asymmetric (A_0) wave in captured guided wave signals were extracted by taking advantage of the well-developed signal processing algorithms (linear-phase finite impulse response filter and Hilbert transform), so as to investigate the influence of the delaminations to the guided wave propagation. When the guided waves are incident on the discontinuities, mode conversion may occur as a result of satisfying the boundary conditions along the discontinuities. Both the dispersive characteristics of multi-mode guided waves and features of the A_0 wave-excited fundamental shear horizontal (SH_0) wave were applied for damage evaluation and multiple-damage detection.

036 Damage Detection in Hexagonal Honeycomb Sandwich Composite Using Guided Wave Propagation

G. L. Huang, F. Song and K. Hudson, University of Arkansas at Little Rock (USA).

This paper gives numerical and experimental analyses of elastic wave propagation phenomena in sandwich panels with a honeycomb core, especially when the frequency domain of interest is relative high. Finite element method is based on using exact models and considering the electromechanical coupling behavior. The reliability of the simulated wave will be verified with the experimental results. Specific attention will be paid on the relationship of transmission ultrasonic energy in the honeycomb sandwich composite under different wave frequencies. The study of guided wave excitation and propagation will provide quantitative information for the mode selection by using piezoelectric actuators and sensors and then be used for damage detection. This research will establish a solid theoretical foundation for the study of the structural health monitoring in the honeycomb composites.

038 Decentralised Information Management in Facility Management Using RFID Technology

ZiXiang Cong, Hang Yin, Farhan Manzoor, Karsten Menzel, Brian Cahll, Yang Gao, University College Cork (Ireland).

Facility Management (FM) is part of the operational phase of a building's life cycle, which includes management of building systems and their services. One aspect of FM is the responsibility to detect building system faults and provide diagnosis. All buildings require FM operations to ensure that all systems within the building are working to their full potential. At the same time, facility managers need specific building management information to solve problems and control building performance. Currently this information is provided by Smart Buildings that have mechanisms in place to inform building management of installed equipment behaviour. For example, a building's Heating, Ventilation, and Air

Conditioning (HVAC) system frequently needs to be checked by a facility manager for safe, reliable and efficient operation. The heating system of a building can include many sub-systems and equipment which require regular checking and occasional maintenance.

Effective management of system maintenance can be extremely difficult due to the physical location of FM devices within buildings. Not all FM devices provide convenient methods for data extraction. Our research emphasises the integration of Radio Frequency Identification (RFID) with FM. One aspect of this research is the accurate identification of equipment faults within a building, assessment of the fault characteristics, and how to update a building's central management system with fault data. The research also contributes to how this information is propagated to maintenance technicians, facility managers and building owners.

In order to take predictive building control decisions, among other parametric data requirements, there is a need for measuring occupant density and assessing occupancy patterns in a building. Occupant density represents the number of people in a specific building space at a specific time. Occupancy patterns represent the use of building space over a specific period of time. Based on these two parameters, decisions can be made to support building space usage, to identify occupant capacity limitations and building space services required for adequate user comfort. The occupancy patterns in this context provide a perspective into how a particular space in a building is used, and hence the behaviour of occupants in that specific building space. Based on these patterns, different building systems can be controlled intelligently.

In our paper, we envisage to (1) discuss the principle of a facility manager being able to detect faults in building devices and equipment using RFID technology, (2) discuss different hardware and software challenges offered by the use of RFID systems in the FM sector, and (3) present a prototype demonstrator currently deployed at University College Cork (UCC) to examine building space usage.

039

Deep Ultraviolet Light-Emitting Organosoluble Polyimides Derived from Siloxane-Containing Aliphatic Dianhydride and Various Aromatic Diamines

Shouming Wu, Tohru Tsuruoka, Tsuyoshi Hasegawa, International Center for Materials Nanoarchitectonics (MANA), National Institute for Materials Science; Ziyi Ge, Teruaki Hayakawa, Masa-aki Kakimoto, Tokyo Institute of Technology (Japan).

We synthesized a new class of polyimides containing siloxane unit in the main chain and showing an intense photoluminescence (PL) in the deep ultraviolet (DUV) region at room temperature. The PL emissions of the sample in solution were observed around 310 nm with excitation at 266 nm. The polyimide **3 (a-e)** solution emission intensity remained very stable. This result indicates that the siloxane and imide units act as a non-conjugated spacer, providing excellent resistance to UV radiation of the polyimide. In particular, polyimide **3e** of intensity became two orders of magnitude greater than that of the PL emission from other polyimides in around 310 nm. The fluorescence quantum yield (FQY) of **3e** was estimated to be 0.35. The polyimide **3e** in the film state also exhibited a strong PL emission around 328 nm. The FQY of the solution state was estimated to be 0.35, which is the highest possible value for a UV light-emitting polymer. This is the first report of the synthesis of a polyimide with an intense DUV emission. Moreover, by introducing the siloxane units into the main chain, the film gains several characteristics, such as good mechanical properties, outstanding thermal resistance, and high organosolubility. Thus, the synthesized polyimide can be an attractive candidate for high performance DUV solid-state light sources.

040

Degradation of Thermal Barrier Coated Superalloy Component during Service

Han-sang Lee and Keun-bong Yoo, Korea Electric Power Research Institute (Korea).

The time dependent degradation of first-stage blades for gas turbine was investigated. The specimens were prepared from the operating facilities, in the Bo-ryoung combined-cycle plant, and their equivalent operating hours were 24,000 and 52,000hrs, respectively. Although there are many investigations of superalloys and coatings in the laboratory, it is important that practical failures during service also be analyzed. The components in the hot gas section of turbine such as combustors, blades and vanes are subjected to the high gas velocity and temperatures causing excessive oxidation and corrosion.

A microstructural investigation of TBC (thermal barrier coating) and substrate, Ni-based superalloy, showed the degradation process of TBC and single crystal superalloy strengthened by intermetallic compounds precipitation, $r'(Ni_3(Al,Ti))$, less than 1 μm . Microstructural comparison of coating surface showed that exposure to the environment increased thickness of TGO (Thermal Grown Oxide) and β depletion region, and then debonding and spallation of TBC were occurred finally. In the case of substrate, Ni-based superalloy, the shape and size of r' were changed with increasing operating time. Especially, in the leading and trailing edges of blades, the size of r' was bigger and the shape was more circular than other region. It can be thought that the leading and trailing edges of blades can be the degradation starting point of first-stage blades.

041

Design of Lath-Shaped Tool in Defective Nanostructure Removal from Digital Touch-Panel Surfaces

P.S.Pa, National Taipei University of Education (Taiwan, China)

An effective economic viability that uses micro electroremoval as a reclaim system was developed to remove the defective ITO nanostructure coatings from the optical PET surfaces of digital touch-panel. The low yield of ITO thin-film deposition is an important factor in semiconductor production. By establishing the reclaim process using the ultra-precise removal of the nanostructure coatings, the optoelectronic semiconductor industry can effectively reclaim defective products, minimizing both production costs and pollution. In the current experiment, a large lath-shaped cathode with a small gap-width between the cathode and the workpiece takes less time for the same amount of ITO removal. A small end radius of the cathode combines with enough electric power to drive fast machining. Pulsed direct current can improve the effect of dreg discharge, and it is advantageous to associate the workpiece with the fast feed rate. However, this improvement can increase the current rating. A high rotational speed of the electrodes, a higher temperature, or a large flow rate of the electrolyte corresponds to a higher removal rate for the ITO nanostructure. The micro electroremoval requires only a short period of time to remove the ITO thin-film coatings easily and cleanly.

042

Development of High Sensitive Long-gage FBG Sensor for Structural Health Monitoring

Zhishen Wu, N.H.M. Kamrujjaman Serker, Adekunle Philips Adewuyi, Ibaraki University (Japan).

Structural health monitoring (SHM) is an active field of research. For the monitoring of bridges, actual and future trends in this

domain require the use of very large arrays of sensors to construct a system similar to human nervous system and use of vibration signals under ambient, unknown excitation due to wind or traffic. Traditional sensors such as strain gage, accelerometer, velocimeter, displacement transducer, are essentially point sensors and usually capture the global behavior of the structure. However, recent developments in the field of fiber optic sensing technology have created the opportunity to measure the structural responses in a distributed manner. Novel packaging technique to obtain the long-gage length from point fiber Bragg grating (FBG) sensors is described in our previous work. One important issue regarding the distributed sensing under normal traffic condition is that the response measured is sometimes too small and highly affected by noise. This paper presents the development of an enhanced sensitive long-gage FBG sensor for the purpose of civil SHM. The sensitivity enhancement was achieved by reinforcing some part of the long-gage FBG sensors with fiber reinforced polymer composites. Laboratory as well as field test results of the proposed enhanced sensitive sensor show the potentials for practical applications.

043

Development of Polymer Electrolytes Based Resistive Switch

Shouming Wu, Tohru Tsuruoka, Kazuya Terabe, Tsuyoshi Hasegawa, Jonathan P. Hill, Katsuhiko Ariga, Masakazu Aono, International Center for Materials Nanoarchitectonics (MANA), National Institute for Materials Science (Japan).

The construction of an organic-electronic resistive switch based on polymer electrolytes is the basis to study the interfacial and bulk transport and the interaction between ions and electrons/holes at the nanoscale level. Moreover, it could also be potentially applied in novel nanoelectrochemical devices for sensors, fuel cells and batteries, and has attracted much attention in recent years. In this work, resistive switching devices based on silver-ion-conductive polymer electrolytes were fabricated and varieties of switching behaviors were observed via their current-voltage (I-V) response. The switching behavior is found to be related to the silver ion concentration from typical I-V characteristics. At the silver ion/polymer electrolyte ratio of 3 wt%, the switch shows the most stable switching behavior by sweeping a bias voltage from -1 to 2 V. A high resistance up to 1 G Ω in the "off" state and a low resistance of less than tens of k Ω in the "on" state can be achieved. It is believed that reversible electrochemical reactions led to the system working in the low and high resistance states respectively. By combining with the results of DSC, AC impedance, and higher temperature I-V measurements, the switching mechanism will be discussed.

044

Design and Construction of Pre-stressed Piezoelectric Unimorph for Trailing Edge Flap Actuation

Lae-Hyong Kang, Jong-Won Lee, Jae-Hung Han, Korea Advanced Institute of Science and Technology (Korea).

This paper presents a novel piezoelectric unimorph called PUMPS (Piezoelectric Unimorph with Mechanically Pre-stressed Substrate) that are made by a new and simple fabrication method. Generally, in order to make conventional pre-stressed curved shape unimorphs, high-temperature adhesion processes and the thermal expansion coefficient mismatch of their constituent layers are required. In the conventional methods, therefore, it is necessary to use the materials with different thermal expansion coefficients, high-temperature ovens or autoclaves and special adhesives. In addition, the conventional methods generally require the re-poling of the piezoceramic layer due to high-temperature adhesion near or above

the Curie temperature of the piezoceramic. In order to generate the stress mismatch between the metal and piezoelectric layers, the present method uses a mechanically, not thermally, pre-stressed metal layer. Using a mechanically pre-stressed substrate, the whole manufacturing process can be performed at room temperature so that the total fabrication time is significantly reduced compared with that of the conventional method. First, a substrate material is strained in the longitudinal direction, and then a piezoelectric material is attached to the substrate. A difference of mechanical strains between the substrate and the piezoelectric layer causes the final manufactured actuator to curve. In this way, a new type of curved shape pre-stressed piezoelectric unimorph, PUMPS, can be easily fabricated at room temperature and can be used as a sensor, an actuator, and an energy-harvesting element without the necessity of a re-poling process. A series of performance tests of the proposed PUMPS actuators were accomplished and the test results show that the actuation capability of PUMPS is comparable to that of conventional curved shape actuators, in spite of the much simpler manufacturing process. Finally, we applied the PUMPS to a simple trailing edge flap actuation mechanism and confirmed that actuation performance of the PUMPS satisfied the flap actuation requirements of the present model.

045

Durability of Nanostructured Silicate Concrete in Aggressive Media

Oleg Figovsky, Dmitry Beilin, International Nanotechnology Research Center Polymate (Israel); Yuri Borisov, Voronezh State Architecture and Building University (Russia).

Nanostructured silicate concrete was elaborated by using a principle forming nanostructures during technological process. Significant increasing of silicate matrix strength and toughness was reached by incorporation of special liquid additives, such as tetrafururyloxisilane -TFS, which effect as a microcrystallizing nucleator on the technological stage and later they colmatage the pores of silicate matrix. Our last elaborations are mainly applying a novel type of soluble silicate contained organic cations, for



example, the DABCO ()-based organic alkali soluble silicate that also give the possibility additional modification of silicate concretes different polymers, such dimethylhudantoine epoxy resins and water dispersion of chlorine-sulfonated polyethylene .

As was shown in our experimental investigation adding nanostructured agent TFS dramatically increased durability of silicate concretes in aggressive media and more that 10 time decreasing penetration of water solutions of acids into such silicate concrete. Nanostructured silicate concrete floor covering was tested – shock flooring test give more than 3 times increasing shock resistant of a new type silicate concrete before exposition in aggressive media and 4-5 increasing shock resistant after 12 months exposition in many aggressive media.

047

Dynamic and Full-Field Deformation Measurement by Mechanoluminescence Sensing Film

Chenshu Li, Chao-Nan Xu, Kyushu University (Japan); Yusuke Imai, Nan Bu, National Institute of Advanced Industrial Science and Technology (AIST) (Japan).

Dynamic and full-field deformation measurement has been realized by coating the surface of the test object of metal with a upgrade mechanoluminescence sensing film of SrAl₂O₄: Eu (SAO). Mechanoluminescent materials are attractive smart materials that

can emit light induced by mechanical deformation. The sensing film of SAO has been developed to make possible to visualize dynamic feature of deformation. Consequently this visualization technique has become a promising experimental techniques to investigate full-field deformation analysis.

In this paper we report the application of this SAO sensing film to full-field deformation analysis on Al-alloy samples. Especially the moving features of strain-localized band that propagate over the sample are clearly seen and precisely investigated. A quantitative analysis by the correlation between mechanoluminescence intensity and deformation is presented.

049

Effect of Aging and Step –Quenched Heat Treatment on the Martensitic Transformation of CuZnAl Shape Memory Alloy

Abdul-Raheem K. AbidAli, Department of Material engineering College of engineering/Babylon university (USA).

There are many parameters affecting on the martensitic transformation of nonferrous alloys such as point defects, pores and heat treatment. In this paper, the effect of aging after direct quenching treatment and step-quenched treatment on the Martensitic transformation of porous CuZnAl alloy are studied. X-ray diffraction analysis is based to identify phases presence in the microstructure of examined specimens. Optical microscopy and scanning electron microscopy examinations have also studied for prepared samples. It has been shown that aging and step-queched heat treatment lead to precipitate some intermetallic compounds in the Martensite matrix which make the lower percentage of shape memory effects for prepared alloy.

050

Electrical Properties of Mos-Structures with Incrusted Nanoballs in Dielectrics

M.D. Efremov, A.Kh. Antonenko, S.A. Arzhannikova, A.V. Vishnyakov, V.A. Volodin, A.A. Gismatulin, G.N. Kamaev, D.V. Marin, A.A. Voschenkov, Russia Novosibirsk State University (Russia).

Separate nanoballs attract science attention due to unique properties of silicon with size about several nanometers. A both electrical and optical property is important, as well as promises for device application. For incrustation of nanoballs into silicon dioxide layers with thickness about several nanometers a method was chosen to prepare a suspension using silicon organic materials (hexametyldisilozan and hexametyldisiloxan)..

Series of nanopowder were manufactured using beam of relativistic electrons for evaporation of pure FZ-silicon in a result of silicon coagulation in gas flow of argon. 1.6MeV electron beam accelerator was used for evaporation. Size selection was as in stage of manufacturing by means of filtering, as in stage of preparation of a suspension for nanopowder. Sublayer, separating nanoballs from substrate, have a characteristic thickness about 5nm. Electrophysical properties for manufactured MOS- and MOS: NC – structures were investigated. There was discovered frequency dependent increasing of both differential capacity and conductivity in depletion regime, what was explained as exchange of charge between substrate and nanoballs. Calculations of single-electron IV were made taking into account diode characteristic for substrate and presence of parallel conductivity chains in dielectric layer. Instability of impedance observed for MOS: NC – structures at voltage above 7V was explained as possible variation of nanoballs electronic spectrum as influence of multi-electron effects. Increasing of frequency leads to approaching of characteristics to standard form for MOS-structures, what corresponds to retarding of charge exchange with substrate due to shortening period of voltage

applied. Thus, method was realized for creation of MOS:NC-structures with nanoballs in dielectric layer and researching of its electronic properties was provided.

051

Electrochemical Properties of Multilayer Film Assembled by Layer-By-Layer Adsorption of Redox Polymer

Tao Sun, Haitao Zheng, Pu Liu, Jingli Zhou, Tianjin Polytechnic University(China); Shin-ichiro Suye, University of Fukui(China).

A redox polymer, poly (ethylenimine) ferrocene (PEI-Fc) was prepared by attaching electroactive ferrocene groups to the backbone of a water soluble, biocompatible polyelectrolyte, poly(ethylenimine), and multilayer film composed of polystyrenesulfonate sodium and PEI-Fc was prepared on gold electrode surface by alternate layer-by-layer (LBL) self-assembly adsorption technique based on the electrostatic force between the opposite charges carried by these two polymers. UV-Vis spectra was used to monitored the LBL process, and the thickness and immobilization amount of each layer were characterized by quartz crystal microbalance (QCM), which showed the formation of nano-scale multilayer structure and linear mass increase dependent on the alternate adsorption cycles. The electrochemical properties of the multilayer film were investigated by cyclic voltammetry. It was observed clearly that the electrochemical properties of this multilayer film were strongly dependent on the layer number and the ferrocene content in PEI-Fc. The electrochemical kinetic was analyzed based on a general model for surface process, and the experimental data fitted well with that evaluated from the above model. This redox polymer showed potential for the construction of reagentless biosensor.

052

Electromagnetic Multi-Mode Shunt Damper for Flexible Beams Based on Current Flowing Circuit

Tai-Hong Cheng, Xuan-Lun Wang, Chonnam National University (Korea); Il-Kwon Oh, Chonnam National University (Korea).

In this paper, the multiple current flowing electromagnetic shunt damper was newly employed for the semi-active vibration suppression of the flexible structures. The electromagnetic shunt damper consists of a coil and a permanent magnet. The ends of the coil were connected to the multimode current flowing electromagnetic shunt circuit for vibration reduction of the cantilever beam employing energy dispersion method. The system was electro-magneto-mechanically coupled between the electrical circuit and mechanical vibrating cantilever beam with a electromagnetic transducer. The circuits were designed for first two mode control of the cantilever. The vibration and damping characteristics of the flexible beams with the electromagnetic shunt damper were investigated by tuning the circuit parameters. The time responses with initial displacement were investigated experimentally. The effect of the magnetic intensity on the shunt damping was studied with the variation of the gap between the aluminum beam and the permanent magnet. The resistances of the shunt circuit were used to investigate vibration damping effect of cantilever. The theoretical prediction of frequency response of the beam under multiple mode electromagnetic shunt damping method has a good agreement with experimental results. Present results show that the magnet shunt damper can be successfully applied to reduce the vibration of the flexible structures.

053

Electromechanical Characterization of Polypyrrole Bilayer Actuators

Ping Du, Xi Lin, Xin Zhang, Boston University (USA).

Conducting polymers are a novel class of electro active polymers that can generate mechanical output by applying electronic stimuli. The exhibited features make the polymer a promising candidate of the future actuator technology. A significant amount of research has been conducted both on theories and experiments in the last decade, but the relationship between input electrical input and mechanical output has yet to be fully described. This work is intended to characterize the electromechanical properties of conducting polymer actuators. A bilayer actuator of gold coated Kapton and dodecylbenzene sulfonate doped polypyrrole is first fabricated. The static characterization indicates the actuator has the highest mechanical output efficiency when stepping from -0.5 V to 0 V. After that a mathematical model to describe the actuator dynamic behavior has been established, using Timoshenko's bilayer theory and an analogy between thermal expansion and ion insertion. The results show that both the curvature and current changes along time share a similar tendency to exponential decay. This model is further verified by a FEA simulation. In the end, two distinct relaxation behaviors between reduced and oxidized CP actuator are also studied.

055

Electrorheological Properties of Organically Modified Nanolayered Laponite: Influence of Intercalation, Adsorption and Wettability

Baoxiang Wang, Min Zhou, Zbigniew Rozynek and Jon Otto Fossum, Norwegian University of Science and Technology (Norway).

Cethyl-Trimethyl-Ammonium Bromide (CTAB) modified synthetic laponite is synthesized by an ion exchange method and characterized by simultaneous small-angle x-ray scattering (SAXS) and wide angle x-ray scattering (WAXS), field emission scanning electron microscopy (FESEM), transmission electron microscopy (TEM), energy dispersive spectrometry (EDS), atomic force microscopy (AFM), thermal analysis and rheometry. Through the formation of the organoclay, the properties of clay change from hydrophilic to hydrophobic. Morphology results show that the hydrophilic particles are aggregating easily, where the suitable CTAB modified laponite can get near monodispersed nanoparticles due to its hydrophobic properties. It is proposed that CTAB is intercalated and adsorbed onto the laponite partially depending on the substituted concentration of the surfactant cation exchange capacity (CEC) (0.5CEC to 6CEC). The electrorheological (ER) effect is investigated for suspensions of CTAB modified laponite dispersed in silicone oil. The two-dimensional SAXS images from ER bundles of CTAB modified laponite exhibit marked anisotropy SAXS patterns, giving a measure for laponite particle alignment within the ER structure. An optimum electrorheological effect can be attained at a particular CEC substituted concentration. On the basis of the structure analysis and dielectric measurements, we attribute the enhancement of ER activity to the improvement in the dielectric properties that showed an increase in the dielectric constant and the dielectric loss at low frequency and their regular optimum change with CTAB modification.

056

Evaluation of Vibration-Based Damage Identification Methods Using Displacement and Distributed Strain Measurements

Adekunle Philips Adewuyi and Zhishen Wu, Ibaraki University (Japan)

Vibration-based damage identification (VBDI) methods have increasingly become an essential field of research due to their flexibility of measurement, cost-effectiveness and nondestructive approach of damage identification in global structure. Although most of the VBDI techniques have demonstrated various degrees of success in identifying damages in small structures, the inherent complexity of structures, the diversity as well as heterogeneity of material properties, the influence of noise and the variability of environmental conditions are basic challenges facing civil SHM. Also, the type and placement of sensors are very crucial for reliable damage identification and successful implementation of SHM programs.

With the development of measurement device and signal processing techniques, structural dynamic properties can be measured more conveniently and precisely, and the performance of some damage identification methods might be improved. This paper, through computer simulation and experimental investigation of a simply supported beam, comparatively evaluates the performance of typical damage localization techniques for practical civil SHM by using displacement modes from accelerometers and long-gage distributed strain measurements. Since experimentally measured modal properties are inevitably corrupted by measurement errors and environmental variability, different levels of random noise are introduced into the calculated displacement and distributed strain mode shapes and the performance of the vibration-based damage identification (VBDI) algorithms are comparatively examined.

Most of all the techniques proved unreliable for damage identification using noisy measurements from accelerometers, while successful with distributed strain measurements. The findings reveal that long-gage distributed strain measurements are much more efficient choice over the traditional measurement techniques for reliable civil SHM. It may therefore be concluded that the performance of some algorithms might be improved for application to civil infrastructure by using distributed strain fiber optic sensing measurement techniques.

057

Experimental Thermo-stress Analysis for a Bending Control of Composite Beams Embedded with SMA Wire Actuators

Gang Zhou, Department of Aeronautical and Automotive Engineering, Loughborough University (UK); Peter Lloyd, DSTL, the Ministry of Defence, Farnborough (UK)

Shape memory alloys (SMAs) such as nitinol have the ability to exhibit diffusionless solid-state phase transformations, which are induced either by mechanical stress or by temperature. Commercially, they are available in wire or ribbon form. The two solid-state crystalline phases involved are room temperature martensite and high temperature parent phase austenite. Their unique transformations from austenite to martensite are characterised by, martensitic finish temperature M_f , austenitic start four critical temperatures, i.e. martensitic start temperature M_s , M_f and austenitic finish temperature A_f . One type of transformation, called pseudoelasticity, temperature A_s superelasticity, or stress-induced martensite (SIM), occurs when SMAs in the isothermal austenitic condition are mechanically stressed into the plastic region so that their plastic strain is completely recovered on the removal of the stress. The other type of transformation, called the shape memory effect (SME), occurs when plastically deformed. If SMAs in the martensite state recovers their original shape (i.e. plastic strain), if heated electrically above their A_f the recovery of the plastic strain is constrained, a large recovery stress will be generated. Since their discovery in the early 60s, a great deal of effort has been devoted to characterising SMAs, exploiting these

two thermomechanical phenomena and developing new applications in aerospace, civil, mechanical and medical industries. In particular, as those transformation temperatures for any given SMAs can be tuned to suit a specific application via a change of the material composition and/or heat treatment, they can be developed into smart actuators through extensive exploitations of the recovery stress for smart adaptive structure technology.

To develop smart adaptive structural components by controlling their shapes in bending, SMA actuators in general need to be integrated with the host components such as composite structures, though some non-embedding approaches have also been investigated. Important performance parameters for such smart components include those associated with SMA actuators such as maximum strain, prestrain, wire diameter, energy density ratio, stiffness, bandwidth (including cooling rate) and actuation capability; and those associated with the host such as actuator volume fraction, actuator through-the-thickness location, host flexural rigidity, actuator-host interfacial strength and actuation cycle. For the smart components to be adaptive, the respective contributions of the aforementioned parameters to their functional performance must be synergistic, which can be a significant challenge. This is because the functional attributes of their performance contributions sometimes lead to significant conflicting consequences, which compromise the performance of the components, as well as undesirable 'side effects'. Although the literature abounds with individual endeavours of using SMAs for the shape control of smart adaptive structures, a synergistic set of the performance attributes from the aforementioned parameters seemed clearly application specific involving inevitable compromises. In particular, the experimental thermomechanical behaviour of embedded SMA actuators, underpinning and justifying those compromises, has not been understood. To this end, it is of paramount importance to develop a good understanding of actuation characteristics of SMA-based adaptive composite beams in terms of performance bounds of the aforementioned important parameters.

In the early paper, the experimental details of design and fabrication of smart composite beams embedded with prestrained nitinol wire actuators were discussed. The developed fabrication process allowed both quasi-isotropic E-glass/epoxy and carbon/epoxy beams of three different lengths made successfully. The preliminary study of both single-cycle and multi-cycle thermomechanical bending actuations with various levels of electric current aimed at the manufacturability and actuation repeatability of adaptive composite beam. In this paper we intend to develop an in-depth understanding of the actuation response characteristics of these smart composite beams in terms of recovery stress. Our focus will be on the understanding of the development of recovery stress during both single-cycle and multi-cycle thermomechanical bending actuations. The effect of beam/wire length on the actuation performance will also be discussed. Information generated and experience gained will be channelled into the subsequent examination of their multi-cycling characteristics and related heat damage.

060

Fabrication of Organic Solar Cells Based on a Blend of Poly (3-Octylthiophene-2, 5-Diyl) and Fullerene Derivative Using Inkjet Printing Technique

A. Shafiee, M.M. Salleh, University Kebangsaan Malaysia, M. Yahaya, University Kebangsaan Malaysia (USA).

Inkjet printing technique is a promising deposition method to fabricate low-cost organic solar cells. This paper reports the fabrication of organic solar cells using inkjet printing technique. The devices consist of an active layer sandwiched between ITO

bottom electrode and aluminum as top electrode. The active layer is made of a blend of a fullerene derivative [6, 6]-phenyl C61-butyric acid 3-ethylthiophene ester (PCBE) as acceptor and poly 3-octyl-thiophene (P3OT) as the donor. I-V curves of the devices were measured in the dark and under illumination of light. It was found that the device showed rectifier property in the dark and able to generate electrical current under light. Further improvements were studied by variations of donor and acceptor blend ratios, different number of printed active layers and annealing process using microwave oven.

061

Fatigue Crack Growth Characteristics of Base and Weld Metals of 9% Ni Steel for LNG Storage Tank

Young-Kyun Kim, Jae-Hoon Kim, Chungnam National University (South Korea).

The fatigue crack growth rate of 9% Ni steel and weld metal were studied over the temperature range -162°C to room temperature. Newly developed heavy thick plates of 9% Ni steel for large capacity of LNG tank were fabricated to conduct a fatigue crack growth test. Two types of 9% Ni steels were prepared by differentiate the fabrication procedure of heat treatment such as QT and QLT. Also the weld metal specimens were fabricated by taking the same weld procedure applied in actual LNG storage tank inner shell. Fatigue crack growth tests were conducted using compact tension specimen in accordance with ASTM E647.

062

Feasibility Investigation of Self-Healing Cementitious Composite Using Oil Core/Silica Gel Shell Passive Smart Microcapsules

Zhengxian Yang, Xiaodong He, Matthew Johnson, John Hollar, Montana State University (USA); Xianming Shi, Montana State University (USA).

The formation of microcracks is a major concern for the durability of concrete and other cementitious composites, since such microcracks cannot be easily controlled by the use of fibers. Formed during cement hydration or under environmental or mechanical loadings, the microcracks are difficult to detect before they develop, coalesce and lead to significant cracking and spalling of the materials and subsequent reduction in the strength, serviceability, and aesthetics of the structures. This paper presents our work in the concept exploration of a new family of self-healing materials that hold promise for truly "crack-free" concrete or other cementitious composites. This innovative system features the design of passive smart microcapsules with oil core and silica gel shell. Such smart microcapsules were prepared based on an interfacial self-assembly process and sol-gel reaction. Methylmethacrylate monomer and triethylborane were chosen as the polymeric healing agent and the catalyst for use in the system, and they were microencapsulated respectively. The microcapsules were dispersed in the cementitious matrix of fresh concrete. For hardened concrete, the self-healing can be triggered by crack propagation through the microcapsules, which then releases the healing agent and the catalyst into the microcracks through capillary action. Polymerization of the healing agent is then initiated by contact with the catalyst, bonding the crack face in a just-in-time manner at the micron level. The self-healing effect is demonstrated using electrochemical impedance spectroscopy (EIS), differential scanning calorimetry (DSC), Fourier transform infrared spectroscopy (FT-IR), and other surface analytical tools including optical microscope and scanning electron microscopy (SEM) coupled with energy dispersive x-ray spectroscopy (EDS).

063

Finite Element Modeling of Beam Bimorph Piezoelectric Power Harvesters Including Viscoelasticity and Viscopiezoelectricity

S. D. Yu, S. Y. He, Ryerson University (Canada).

This paper presents a finite element procedure for modeling beam bimorph piezoelectric power harvesters including viscoelasticity and viscopiezoelectricity. The symmetrically laminated bimorph piezoelectric structure consists of two identical layers of piezoelectric materials at the top and bottom and a non-active shim core. Due to the attachment of a large and heavy proof mass at the free end of the piezoelectric structure, the longitudinal and lateral deformations of the piezoelectric structure are coupled. As a result, the longitudinal and lateral deformations must be modeled simultaneously. To improve accuracy in determining the dynamic responses of the electromechanical system, a three node beam finite element is employed for both longitudinal and flexural deformations. Within a beam finite element, the proposed element permits a quintic polynomial shape function for lateral deformations and a quadratic polynomial shape function for the longitudinal deformation. The dynamic equations of the electromechanical system are established using the Lagrange equations method and solved for lateral harmonic base motions. Numerical results obtained are in good agreement with those published in the literature for example test cases.

065

Frequency Response Analysis of Fatigue Behaviour in NiTi Shape Memory Alloys

T. Liladomwit, P. Passaranon, P. Lekhakul, S. Wongs, D. Koolpiluck, University of Technology Thonburi (Thailand); Khantachawana, King Monkut's University of Technology Thonburi (Thailand).

This paper investigates the relationship between the functional fatigue level and the frequency response behaviour of NiTi Shape Memory Alloys. In this work, the functional fatigue is indicated as the reduction of working displacement with increasing thermal cycling. The specimens, which are SMAs with 0.7-millimeter diameter, were subjected to a constant stress under different number of thermal cycles, leading to different fatigue levels. The fatigued SMAs were tested in open-loop experiments, in ambient air at room temperature, with step inputs and sinusoidal inputs, and their frequency response were evaluated as the magnitude and phase of the wires' displacement, with respect to the input voltage signal. The results of the experimental study showed that over low frequency ranges under 0.1 Hz the gain of the specimens, subjected to ranges of stresses from 76 to 203 Mpa, decreased as the fatigue levels of SMAs increased. It is expected that these observations may provide insight into the dynamic response of SMAs suffering from fatigue, and could eventually lead to the development of an online fatigue detection method based on frequency response analysis for SMA actuators.

066

Fullerene Reinforced Ionic Polymer Transducer

J. H. Jung, T. H. Cheng, I. K. Oh.

The novel fullerene reinforced nano-composite transducer based on nafion was developed to improve the ionic polymer metal composite transducer. The fullerene reinforced nano-composite membranes are manufactured with 0.1 and 0.5 weight percentage of a nafion by recasting method. The tensile test was employed to define the stiffness and modulus of the nano-composite membranes. The ionic exchange capacity analysis and proton conductivity test were performed to calculate the electrical property of the composite

fil The water uptake was measured to know a tendency about the liquid containing of the membranes. Also, the tip displacement of the nano-composite membrane transducer was investigated under AC excitations with various magnitudes and frequencies. Furthermore, the generation energy was measured from the sinusoidal physical input vibration with several displacements and frequencies by using a mechanical shaker. As a result, the fullerene reinforced nano-composite membrane based on nafion shows higher stiffness and Young's modulus than the pure nafion membrane. Also, the nano-composite membrane has better water uptake and proton conductivity than the pure membrane. Furthermore, the fullerene reinforced nano-composite membrane transducer actuates much larger deformation than the pure nafion membrane transducer. In addition, the developed membrane transducer makes much larger energy from the physical input vibration than the previous pure membrane transducer.

067

Functional Measurement of Biological Parts

Matthew J. Lang, Massachusetts Institute of Technology (USA).

Biological systems can be thought of as forming from smaller functional components, or parts. Understanding these physical parts and fundamental interrelationships will form a foundation for forward engineering using Nature's fascinating structures. It will also provide a better understanding for disease and new targets for fighting disease. Several functional measurements to characterize parts such as connectivity parts, motor protein modules and cell based structural components such as actin filament networks will be discussed. Strategies to address challenges such as instrumentation advances and assay development will be presented.

068

Giant Dielectric Permittivity in Multiferroic BiFe_{1-x}Mn_xO₃ Ceramics

Wai Ping Suen, Haitao Huang and Helen L.W. Chan, the Hong Kong Polytechnic University (HongKong, China).

The effect of Mn doping on the dielectric properties of multiferroic BiFe_{1-x}Mn_xO₃ (BFM, x≤0.4) ceramics was studied. A giant dielectric permittivity in BFM system was found, which exhibits similar relaxational behavior to that of colossal dielectric constant material, CaCu₃Ti₄O₁₂. The dielectric relaxation peak shifts to higher frequencies with increasing amount of Mn doping. At the same time, the intrinsic antiferromagnetic BiFeO₃ became weak ferromagnetic with a small but nonzero remnant magnetization when Mn is doped into the structure. A mechanism of the giant dielectric permittivity in BFM was discussed and related to the microstructure of ceramics.

069

Guided Wave Propagation Based Damage Detection in Welded Rectangular Tubular Structures

Xi Lu, Limin Zhou, Zhongqing Su, Li Cheng, The Hong Kong Polytechnic University(HongKong, China); Lin Ye, The University of Sydney(Australia).

Structural health monitoring (SHM) has been widely accepted as a promising way to improve safety and whole lifecycle reliability of engineering structures. Among those technologies adopted for implementation of SHM, guided wave based methods have shown great potential to practical use and have been the object of many researches. However, most studies focused on simple plates or axial symmetrical structures. In this paper, complex welded steel structures with rectangular section, which are almost 1:1 scale models for bogie frame segment of train, were investigated using

both finite element method (FEM) and experimental analysis for the purpose of damage detection. Finite element models were established to simulate the propagation behavior of guided waves in the structure. An active sensor network consisted of different types of piezoelectric transducers (PZT), regarding as both actuator and sensor, was used to generate guided waves propagating in the structures and collect their response signals. Differ from previous studies, a special mode tuning strategy was utilized to minimize the effect due to the intrinsic multi-mode phenomenon of guided wave propagating in homogenous metallic medium to the consequent signal interpretation. Damage detection was then implemented by taking advantage of modern signal processing approaches, such as continuous wavelet transform (CWT), discrete wavelet transform (DWT) and Hilbert transform (HT), which were applied to the collected guided wave signals. The result indicated that such guided wave propagation based damage detection method is reasonable. Moreover, as part of the result, tuning curves for the purpose of mode choosing at certain frequency were gained.

070

Guided-Wave-Based Detections of Different Types of Cracks in Steel Plates

Mingyu Lu, Limin Zhou, Zhongqing Su, The Hong Kong Polytechnic University (China); Lin Ye, The University of Sydney (Australia).

The guided-wave-based damage detection technique using structurally integrated Lead-zirconate-titanate (PZT) patches for structural health monitoring have been developed for many years. However, the method is still in its formative years and one of the main challenges is the application in real-world complicated structures. It's very important to vastly study the guided-wave-based crack detections in the structures with simple geometries which can be used to construct more complicated structures for practical applications. In this paper, the guided-wave-based detections of different types of cracks in steel plates have been studied. Firstly, a steel plate of 600x200x10mm was used to find the needed wave mode. The PZT arrays were then used to detect a contact crack and a crack with 2mm gap on two different welded steel plates with same dimensions. To study the effects of different cracks on wave propagations, the conditions of loading and unloading for contact crack and different inclusions such as water, oil, epoxy inside the gap of the crack have been considered in this study. Advanced signal processing and pattern recognition techniques such as the wavelet transform (WT) including continuous wavelet transform (CWT), discrete wavelet transform (DWT) and Hilbert transform (HT) were used to enhance the efficiency of crack detections in the steel plates. The results from the experiments show the validity of the proposed methods and the effects of different factors on the crack detections of the steel plates.

071

Health Monitoring of Cfrp with Cnt Modified Matrix under Fatigue Loading via the Electrical Resistance Change Method

V. Kostopoulos, A.Vavouliotis, P. Karapappas, A.Baltopoulos, E.Fiamogou, University of Patras (Greece).

The goal of this work is to evaluate the effect of dispersed Multi-Wall Carbon NanoTubes (MWCNT) in the matrix of a Carbon Fibre Reinforced Plastic on the damage monitoring of the materials during fatigue loading with the use of the Electrical Resistance Change method. Furthermore the electromechanical response of CFRP under fatigue loading was investigated. A commonly used quasi-isotropic lay-up was used in order to emulate materials used in real aerospace structures. The longitudinal

resistance change of the specimens was monitored throughout the experiment. Three different stress levels were tested in order to investigate any connection between the electrical response and the mechanical stress. The frequency and the R ratio were kept the same for the different stress levels. The results of the CNT doped specimens were compared to the ones recorder from Neat epoxy CFRPs. Temperature of the specimen was also monitored throughout the process in order to decompose any possible effect of it on the electrical resistance of the specimen. For the evaluation and the safer extraction of the conclusions of the used method, Acoustic Emission recordings and analysis were also utilized. The electrical behavior of the quasi-isotropic CFRP was very interesting due to the fact that it deviated from the commonly observed electrical response of unidirectional or cross-ply CFRPs due to the presence of the 45° layers. A repeatable pattern was observed for both the neat and the CNT-doped specimens, with the latter having smoother electrical recordings. The material reached a Critical Damage State (CDS) which could be identified via the electrical measurements and the remaining life could be estimated with a high level of confidence. The results were verified with the findings from acoustic emission measurements and the mechanical response.

072

Highly Red Luminescence Properties From Ternary Zncdte Quantum Dots

Norhayati Abu Bakar, Akrajas Ali Umar, Muhamad Mat Salleh, Muhammad, Universiti Kebangsaan Malaysia; Yahaya, Universiti Kebangsaan Malaysia (USA).

There is an increasing interest in using quantum dots (QDs) in variety of applications such LED and solar cells due to their unique optoelectronics properties. Ternary QDs might be potentially used in currently existing application due to their novel properties in comparison to the binary system. Here, we report the synthesis of ternary QDs system by quick injection of chemical precursor into the reactor at moderate temperature (300°C). The ternary QDs have been synthesis using wet chemical process giving highly red emission with high photoluminescence after exposing under UV lamp (365 nm). The quantum dots were characterized using photoluminescence and UV-Vis spectroscopy.

073

High-Performance Piezoelectric Single Crystals-A Smart Material with Complex Nanostructure

Zuo-Guang Ye, Simon Fraser University (Canada).

Piezoelectrics can sense environmental mechanical forces by giving out electric signals and generate mechanical responses when driven by electric forces. They are inherently smart materials that have found applications in a wide range of electromechanical transducers, such as medical ultrasonic imaging, sonar, micro-/nano-positioning, environmental monitoring and aerospace. As the range of applications continues to grow, so does the demand for new materials with improved piezoelectric properties. Recently developed relaxor-based single crystals of complex perovskite solid solutions, $\text{Pb}(\text{Mg}_{1/3}\text{Nb}_{2/3})\text{O}_3$ - PbTiO_3 [PMN-PT] and $\text{Pb}(\text{Zn}_{1/3}\text{Nb}_{2/3})\text{O}_3$ - PbTiO_3 [PZN-PT], represent a breakthrough in the development of piezo-materials. They exhibit extraordinary piezoelectric performance (with extremely high piezoelectric coefficients, very large electromechanical couple factors and exceptionally high strain levels) that outperforms the currently used $\text{Pb}(\text{Zr}_{1-x}\text{Ti}_x)\text{O}_3$ [PZT] ceramics, making them the materials of choice for the next generation of electromechanical transducers for a broad range of advanced applications.

In this paper, recent major advances in the development of

piezocrystals are reviewed in terms of crystal growth, dielectric and piezoelectric properties, device applications and crystal chemistry and physics. Large and high-quality single crystals of PMN-PT and PZN-PT have become commercially available via improved flux method, top-seeded solution growth, solid state growth and especially modified Bridgman technique. Device testing has demonstrated the advantages these crystals can provide in realizing dramatic improvements in the efficiency, sensitivity, source level, bandwidth and cryogenic applicability for electromechanical sensing and actuating, leading to the commercialization of new ultrasonic transducers. The outstanding piezoelectric response of these crystals can be related to the complex structures of chemical nano domains and polar nano regions, the nature of morphotropic phase boundary and the peculiar domain states and phase components engineered through appropriate electric field poling. Single crystals of new ternary solid solution systems are also presented with further improved properties and broader prospective for transducer applications in the near future.

074

Hybrid Finite Element Formulation for Electrostrictive Materials: Static and Buckling Analysis of Beam

R. Jerome, N. Ganesan, Indian Institute of Technology Madras (India).

Electrostriction is the basis of electromechanical coupling in all insulators. When these electrostrictive materials are embedded in a complex structure and because of the complicated behavior of electrostrictive materials, analytical simulation of the electrostrictive material embedded structures are difficult. The finite element method is a potential tool for the simulation of these electrostrictive material embedded structures. There are only two distinct types of nonlinear finite element formulations available in the literature. The first type is the Hom and Shankar formulation which is based on the Toupin's elastic dielectric theory. Since this formulation is based on the very general Toupin's elastic dielectric theory, it contains many complicated terms which can be neglected in most of the practical cases and some of the terms are tedious to obtain. The second type is the J.C. Debus et al formulation which reduces the complications in the first type of formulation but this formulation is based on the assumption $\mathbf{P} \gg \mathbf{D}$ (i.e., polarization is approximately equal to electric displacement). This assumption is true when the relative dielectric permittivity of the material is very large and it is true for their case because their formulation is specifically for lead magnesium niobate electrostrictive materials. In this paper, we present a Hybrid Finite Element formulation for the static analysis of an electrostrictive material. This formulation relaxes the assumption $\mathbf{P} \gg \mathbf{D}$ so the formulation is generic and can be used for the analysis of electrostrictive materials having low relative dielectric permittivity. Though the present formulation relaxes the assumption $\mathbf{P} \gg \mathbf{D}$, it will not contain complicated terms as Hom and Shankar formulation. The present formulation is based on the Hom and Shankar constitutive model and it models full electromechanical coupling in solids. This formulation uses linear finite element analysis for stress and strain evaluation along with the numerical solution (modified Newton – Raphson) of the nonlinear constitutive equation within each element and hence this formulation is named as Hybrid Finite Element formulation. This formulation uses a specially modified Newton – Raphson technique for solving the nonlinear constitutive equation so that the convergence of the solution is guaranteed. A technique for obtaining the initial guess of the solution is also proposed which gives faster convergence of the solution. The present Hybrid Finite Element formulation along with the modified Newton – Raphson solution technique is computationally efficient procedure when compared to the other two types of available finite element

formulation and solution procedures. In the present formulation, the nonlinear constitutive equation is solved on each element which will be less than the nodes and the system of algebraic finite element equations are not iteratively solved.

The finite beam elements developed based on the Hybrid Finite Element formulation are subjected to patch test 'C' (O. C. Zienkiewicz) which will guarantee the necessary and sufficient condition for the convergence of the finite element analysis when the elements passes the test. The results of the patch test are shown in Figures 1 – 4 and it is clear from the Figures 1 – 4 that the finite beam elements passed the patch test 'C'. In addition, the finite element technique is demonstrated by solving the static and buckling problem of multilayered electrostrictive beam.

075

Hydrodynamics and Rheology of Active Suspensions

Zhenlu Cui, Department of Mathematics and Computer Science Fayetteville State University (USA).

Active soft materials are a challenging class of systems driven out of equilibrium by an internal or an external energy source. Examples are self-propelled particles in bacterial colonies, or the membrane and the cytoskeleton of eukaryotic cells, etc. In this talk, I will present a hydrodynamic theory of flowing active particle suspensions and discuss the flow and rheological behaviors of these materials. In sharp contrast to their passive counterparts, the flow is either permeative or oscillatory under weak external forcing and the rheological behaviors are altered due to the activity induced by the system.

076

Hysteresis in Dielectric Electroactive Polymers

B. Lassen, C. Melvad, G.R. Kristjnsdttir, R. Jones, The University of Southern Denmark (Denmark); L. Wang, Hangzhou Dianzi University (China).

Dielectric electroactive polymer (DEAP) actuators are expected to be an important future linear actuator technology due to its light weight, large actuation and relative low cost. These actuators are in principle large parallel plate ca-pacitors with a viscoelastic polymer material in between. In order to further develop these actuators a good understanding of their behavior is needed. In particular, the hysteretic behavior needs to be understood. It is clear that due to the DEAP's viscoelastic nature the actuators will exhibit dynamic hysteresis. However, some of these actuators, e.g., the rolled actuator developed by Danfoss Polypower, also show static hysteresis. In this work we investigate one possible source, namely, the static hysteretic behavior of DEAP materials.

In the first part we present experimental stress strain curves for the acrylic tape VHB 4910 produced by 3M. In these experiments the stress was measured while straining the material first linearly from 0 to around 300 (%) and then back to 0. These curves clearly show the presence of hysteresis. Furthermore, we have carried out a set of experiments with different stretching speeds. The results of these experiments show that indeed this material exhibit static hysteresis. In the second part we compare two hysteresis modeling approaches, the Bouc-Wen and the Preisach model. These models have been fitted to the experimental results using the particle swarm optimization scheme. Not surprisingly, the Preisach model fits the experimental results best as it is also the one with most fitting parameters. In order to have a simpler model that still reproduces the results, we propose a simplified Preisach model along the lines of Smith et al..

077

Improvement of Radiative Efficiency by Multi-Quantum Barriers in InGaN/GaN Multi-Quantum Well Light-Emitting Diodes

Ya-Fen Wu, Jeng-Kuang Huang, Tsang-Yen Hsieh, Ming Chi University of Technology (Taiwan, China); Jiunn-Chyi Lee, Yeu-Jent Hu, Ming-Zhi Lee, Technology and Science Institute of Northern Taiwan (Taiwan, China); Yi-Ping Wang, Chang Gung University (Taiwan, China).

InGaN/GaN multi-quantum wells (MQWs) are widely used as the active layers of high-brightness blue-green light-emitting diodes and laser diodes. The radiative recombination of InGaN-based MQWs has been attributed mainly to excitons localized at deep traps originating from indium-rich regions in the wells acting as quantum dots. However, the InGaN-based heterostructures display misfit dislocation in nanocrystalline structures, which lead to nonradiative recombination centers. The performance of such devices is limited by the thermally activated loss of electrons overflowing from the active layer to the nonradiative recombination centers, thus reducing the emission efficiency. To improve the radiative efficiency in light-emitting diodes, we introduce a structure of multi-quantum barriers (MQBs) into the MQW heterostructures. The InGaN/GaN MQW samples with and without MQBs were prepared by metal-organic vapor phase epitaxy system. The electroluminescence measurements were carried out over a temperature range from 20 to 300 K and an injection current level from 5 to 100 mA. Analyzing the experimental results of the InGaN/GaN MQW samples, we observe the enhancement of carrier confinement in the active layer and the inhibited carrier leakage over the barrier to the p-GaN regions for the sample with MQBs, which we attribute to the increase of effective barrier heights due to the quantum interference of the electrons within MQB. In addition, the sample possessing MQBs also exhibit less sensitive temperature dependence. It is confirmed experimentally and quantitatively that the well-designed MQBs can indeed improve the performance of light-emitting diodes significantly.

078

Influence of Electric Boundary Condition on the Interface Crack between Metal Electrode and Piezoelectric Ceramic

Qun Li, Einhard Kuna, Institute of Mechanics and Fluid Dynamics (Germany).

The interface crack problem between a metal electrode and a piezoelectric ceramic is researched based on the extended Stroh formalism. It is concluded that different electric boundary condition have significant influence on the crack tip energy release rate and in turn influences on the effect of the applied electric field on the interface crack stability between metal electrode and piezoelectric ceramic.

079

Influence of Smart Nano-materials on Properties of Fresh and Hardened Cement Paste

P.Hosseini, A.Booshehrian, A.Khalifei, S.Farshchi.

Nanotechnology has changed and will continue to change our vision, expectations and abilities to control the material world. These developments will definitely affect construction and also the field of construction materials. In addition, few researches in this field of technology have shown that nano-Fe₂O₃ is a smart material due to self monitoring stress.

In this study, different amounts of this material were used to investigate the effect of nano-Fe₂O₃ on properties of hardened

cement pastes. To study these properties, mechanical (Compressive and Flexural) and micro-structural (XRD and SEM) tests were done. Also consistency and setting time of fresh cement pastes were tested to investigate properties of fresh cement pastes.

080

Influence of Wc Target Power, N₂ Flux and Negative Bias Voltage on the Microstructures and Mechanical Properties of the Super Hard TiAlN-Wc Nanocomposite Films Deposited by the Hybrid Technique of Arc Ion Plating and Direct Current Magnetron Sputtering

Shi-Hong Zhang, Yun-Kon Joo, Jae-Young Cho, Jae-Hong Yoon, Tong-Yul Cho, Changwon National University (Korea).

TiAlN-WC films were prepared on Si substrate using the hybrid technique of arc ion plating and magnetron sputtering. The microstructure and mechanical properties of the films were investigated to find out a super hardening mechanism and nanostructured film growth mechanism.

The surface of the film became rougher with increasing the WC target power and N₂ flux. But, increasing the negative bias voltage contributed to improvement of roughness. The deposition efficiency of the film had a decrease with increasing the WC content, N₂ flux and negative bias voltage. The macro particle densities on the TiAlN-WC film surfaces were greatly eliminated by applying negative bias voltage to the substrates. Under various WC target power, N₂ flux and negative bias voltage, the films were comprised of TiN, Ti₂AlN and amorphous WC phases. The growth orientation was changed by different deposition conditions. The AIP TiAlN film was formed by TiN dendrite crystals of 5~10 nm with (111) orientation and Ti₂AlN phase with random orientation. With increasing the content of WC phase, the films were formed by amorphous WC and a part of TiN and Ti₂AlN phases. The columnar structure was replaced with a quasi-amorphous microstructure, with small distorted grains recrystallized in the amorphous background. The average hardness of the films had a dramatic increase with increasing the content of WC phase. In addition, with increasing the negative bias voltage to the substrates resulted in increase of compressive stress. Thus, the hardness also was enhanced. The max hardness was up to 45 GPa in the TiAlN-WC film with WC target power of 300 W, N₂ flux of 40 sccm and bias voltage of -400 V. At last, compared to AIP TiAlN film, the hardness and plastic resistance of the film added amorphous WC phase had an evidence increase, which indicates this novel film would possess great potential in the wear application.

081

Inorganic Nanoparticles Synthesis by Precipitation Route

Tkatchenko E.A., Fedorov P.P.

Soft chemistry route such as precipitation is well-known way to synthesize soluble compounds (hydroxides, borates, oxides, carbonates, fluorides etc.). Current research is the united research for borates and oxides precipitation and consequent powders heating that leads to amorphization and crystallization processes. Borates (RBO₃ for R=In, Sc, Y) and oxides (Y₂O₃, Fe₂O₃) were synthesized through calcination the precipitation after reacting ammonium hydroxide with an aqueous solution of metal nitrates (oxides has been solved in HNO₃), acetates, iron chromate and B₂O₃. White or brown (for Fe only) precipitates appear and settle during several hours. The precipitation finished at different pH value depending on metal ions. pH dependences were measured as a function of NH₄OH-solution volume. The precipitates were washed by distilled water several times. The dehydration up to 500°C for orthoborates and Y₂O₃ leads to the amorphous state.

Calcinating of Fe₂O₃-precursor at 500°C leads to crystallization. All samples were researched by X-ray powder, derivative thermal and scanning electron microscopy analyses.

082

In-Situ Synthesis and Thermal-Electrical Properties of CP2-Polyimide/Pristine and Amine-Functionalized Carbon Nanofiber Composites

David H. Wang, University of Dayton Research Institute; J. David Jacobs, University of Cincinnati(USA); Aaron Trionfi, Julia W. P. Hsu, Sandia National Laboratory(USA); Michael J. Arlen, University of Akron(USA); Richard A. Vaia, Loon-Seng Tan, Wright-Patterson Air Force Base(USA).

Vapor-grown carbon nanofibers (VGCNF) were functionalized with amine-containing pendants via Friedel-Crafts acylation reaction with 4-(3-aminophenoxy) benzoic acid. The resulting H₂N-VGCNF co-reacted during in-situ polymerization of 2,2-bis(phthalic anhydride)-1,1,1,3,3,3-hexafluoroisopropane (6FDA) and 1,3-bis(3-aminophenoxy)benzene (APB) in N,N-dimethylacetamide (DMAc) to afford a series of CP2-polyimide nanocomposite films, which contained 0.18-9.19 wt % of H₂N-VGCNF (corresponding to 0.10-5.0 wt % of pristine VGCNF), using the conventional poly(amic acid) precursor method. For comparison purposes, the pristine VGCNF (0.10-5.0 wt %) was also used in similar in-situ polymerization of 6FDA and APB. These two series of nanocomposite films were cast from the respective poly(amic acid)/VGCNF/DMAc solutions, followed by thermal imidization at curing temperatures up to 250 °C. Amine-functionalized VGCNFs enable direct formation of CP2 grafts on the VGCNFs, whereas pristine VGCNFs result in a relatively weak interface between the carbon nanofiber and CP2 matrix. Conducting-tip atomic force microscopy (C-AFM) showed that the electrical transport is solely carried by the carbon nanofiber networks in the nanocomposites. In addition, high-resolution C-AFM maps show non-uniform distribution of current along the length of some VGCNFs, suggesting the presence of a heterogeneously distributed, adsorbed polymer layer around nanofibers. In general, low-frequency ac impedance measurements are well described by the percolation bond model, yielding a percolation threshold below 1 vol % (0.24 and 0.68 vol % for PCNF-CP2 and FCNF-CP2, respectively). However, the design of the interface is determined to be crucial for controlling the electrical behavior in four substantial ways: magnitude of the limiting conductivity, linearity of the I-V response, magnitude and direction of temperature-dependent resistivity, and reproducibility of the absolute value of the resistivity with thermal cycling. These observations are consistent with a direct VGCNF-VGCNF contact limiting transport in the pristine VGCNF-CP2 system, whereas the CP2 grafts on FCNF form a dielectric layer between individual CNFs, limiting transport within the FCNF-CP2 system. Furthermore, the grafted CP2 chains on the H₂N-VGCNF reduce local polymer dewetting at the VGCNF surfaces when the temperatures exceed the CP2 glass transition. This appears to stabilize the structure of the percolation network and associated conductivity. The general behavior of these interfacial extremes (pristine and fully functionalized VGCNFs) set important bounds on the design of interface modification for CNFs when the intended use is for electrical performance at elevated temperatures or under extreme current loads. The combination of high thermomechanical performance of CP2 with the ability to tune electrical characteristics affords the creation of novel materials for a range of aerospace applications including smart materials, EMI shielding, morphing structures, and actuator controls.

083

Integrated Piezoceramic Transducers for Imaging Damage in Composite Laminates

Ching-Tai Ng, The University of Queensland (Australia); Martin Veidt, Cooperative Research Centre for Advanced Composite Structures Ltd.; Nik Rajic, 3Aeronautical and Maritime Research Laboratory (Australia).

This paper presents a two-phase damage imaging methodology to characterise damage in composite laminates using Lamb waves generated by integrated piezoelectric transducers. The proposed methodology uses the transducers to sequentially scan the composite laminates before and after the presence of damage by transmitting and receiving Lamb wave pulses. In phase one, the damage localisation image is reconstructed by analysing the cross correlation of the scatter signal with the excitation pulse for each transducer pair. A potential damage area is then reconstructed by superimposing the image observed from each actuator and sensor signal path. In phase two, plate wave diffraction tomography is used to reconstruct an image quantifying severity and shape of the damage based on the same set of measurement data used in phase one. One of the advantages of using the two-phase approach comparing to other diffraction tomography methodologies is that the number of required measurements can be gradually reduced due to the known damage location. This makes the proposed Lamb wave based imaging methodology very efficient and practical. The results of simulation and experimental investigations show that the proposed methodology is able to detect damage with locating inaccuracies of a few millimetres within inspection areas of around 150 x 150mm² and provides quantitative information on severity and shape of the damage.

084

Investigation of the Oxygen Depletion Properties of Low Density Polyethylene Resins Filled with Thermally Stable Oxygen Scavengers

Jen-taut Yeh, Li Cui, Yan-bin Sun, Li-ping Xu, Wei Wei, Fang-chang Tsai, Tao Jiang, Hubei University (China), Jen-taut Yeh, Ping Zhu, Wuhan University of Science and Engineering(China); Jen-taut Yeh, National Taiwan University of Science and Technology (Taiwan,China); Chien-Yu Yeh, National Taiwan University (Taiwan, China); Wei-Hua Yao, Oriental Institute of Technology (Taiwan, China).

The thermal stability, oxygen depletion and tensile properties of low density polyethylene (LDPE) resins filled with ascorbic acid (Vc), sodium ascorbate (SA), iron (Fe) and modified iron (MFe) oxygen scavengers were systematically investigated. Thermogravimetric analysis (TGA) results clearly suggest that the thermal stability of SA powder and L₉₅(SA)₅ specimen is significantly better than that of Vc powder and L₉₅(Vc)₅ specimen, respectively. The oxygen depletion efficiency of L₉₅(SA)₅ is significantly better than that of L₉₅(Vc)₅, L₉₅(Fe)₅ and L₉₅(MFe)₅ specimens, although the virgin SA powders exhibit worse oxygen depletion efficiency than Vc, Fe or MFe powders before melt blending. Moreover, at a fixed weight ratio of Vc (or SA) to MFe of the oxygen scavenger compounds, the oxygen depletion efficiency of L₉₅[SA_x(MFe)_y]₅ series specimens is always significantly better than that of L₉₅[Vc_x(MFe)_y]₅ series specimens. In fact, at weight ratios of Vc/MFe and SA/MFe higher than 3/7 and 5/5, respectively, the residual oxygen concentration values present in the airtight flask of L₉₅[Vc_x(MFe)_y]₅ and L₉₅[SA_x(MFe)_y]₅ series samples at any time are even lower than those of the L₉₅(Vc)₅ and L₉₅(SA)₅ specimens, respectively. Further tensile experiments show that the tensile properties of the

$L_{95}[SA_x(MFe)_y]_5$ series samples are always higher than those of the corresponding $L_{95}[Vc_x(MFe)_y]_5$ series samples with the same loadings of oxygen scavenger compounds, respectively. In order to understand these interesting thermal stability, oxygen depletion and tensile properties of these LDPE oxygen-scavenging plastics, scanning electron microscope and energy dispersive X-rays analysis of the compositions on the surfaces of $L_{95}[SA_x(MFe)_y]_5$ and $L_{95}[Vc_x(MFe)_y]_5$ series samples were performed. Possible reasons accounting for these interesting properties of these LDPE oxygen-scavenging plastics are proposed.

085

Ionic Polymer Metal Composite Actuators Employing Irradiation-Crosslinked Sulfonated Poly (Styrene-Ran-Ethylene) as Ion-Exchange Membranes

Xuan-Lun Wang, Il-Kwon Oh, Tai-Hong Cheng, Chonnam National University (Republic of Korea).

Ionic polymer metal composites (IPMC) are soft polymeric smart materials having large displacement at low voltage in moist environments or water. This type of actuators consists of an ionic membrane and noble metal electrodes plated on both surfaces. The ion-exchange membrane, Nafion, remains as the benchmark for a majority of research and development in IPMC technology. In this research, we employed sulfonated poly (styrene-ran-ethylene) (SPSE) that is crosslinked by UV irradiation as a novel ionic membrane. The crosslinking reaction between polymer matrix and crosslinking agent was proved by FTIR and TGA analysis. The sulfonic acid groups were stable during the UV irradiation crosslinking process. Water uptake, ion exchange capacity, and sulfonation degree are characterized for both pure SPSE and crosslinked SPSE membrane. Tensile tests revealed the mechanical stiffness and strength improvement after the crosslinking treatment on SPSE samples. The bending responses of SPSE actuators under both direct current (DC) and alternating current (AC) excitations were investigated. The voltage-current behaviors of the actuators under AC excitations are also measured. The blocking force for the SPSE actuators is recorded by a load cell with the help of NI-PXI system. Results showed the crosslinked SPSE actuators have better electromechanical performance such as on tip displacement and blocking force.

086

Isothermal Physical Aging of Thin Pmma Films near the Glass Transition Temperature

Jung Eun/Nam, Jong Keun/Lee, Chun Seog/Oh.

Although nanoconfinement effects have been widely investigated for polymers in the form of thin glassy polymer films, the physical aging behavior for thin films is still a matter of contention. In this study, the isothermal physical aging and the glass transition temperature (T_g) in PMMA thin films were investigated by means of differential scanning calorimetry (DSC). Freestanding thin film was obtained by spin coating onto a silicon wafer substrate and then releasing the coated film using a water floating technique for different molecular weights (MW = 120,000, 350,000, 996,000 g/mole) and film thicknesses (38~1,181 nm). The thin films were stacked in a DSC pan and isothermally aged for different aging times ($t_a = 1$ and 12 hr) and aging temperatures ($T_a = 105, 110$ and 115 °C) below but near T_g . Enthalpy relaxation (ΔH_{Relax}) due to the isothermal physical aging vs. ΔT_a ($T_g - T_a$, driving force of aging) data showed that the enthalpy value increased with increasing ΔT_a , reached maximum, and then decreased as ΔT_a increases further. As film thickness decreases, ΔH_{Relax} was reduced for larger MW samples below ~200 nm of film thickness, indicating the suppression of physical aging. The suppression of the physical

aging was discussed in this work. About 7~10 °C depression in T_g was observed for thinner films (~40 nm), compared to thicker films (~660 nm) in this study.

087

Light-driven Chiral Molecular Motors: From Materials to Applications

Quan Li, Kent State University (USA).

The elegance with which nature use performs light-driven functions is inspiring scientists to develop smart light-driven molecular motors for artificial molecular devices. An important challenge is to how to dynamically control mechanical motions of molecules by light, which is a hinge of the bottom-up nanofabrication of the molecular devices. A promising solution lies in the phototunable chiral nematic liquid crystal because its unique helical structures and physical properties can be tuned upon light irradiation. Such a phase can be achieved by doping both photosensitive molecules and chiral molecules into an achiral nematic liquid crystal host. For example, trans-Azobenzene is thermodynamically more stable than cis-azobenzene, however irradiation with ultraviolet light leads to its trans-cis isomerization. The reverse process from cis to trans isomer can occur thermally or photochemically with visible light. Since the physical and chemical properties of the azobenzene configurational isomers are different, the optically tunable switching effect has been the basis for many functional molecules and materials with applications in photonics and liquid crystal displays. In this talk, I will focus on the fascinating topics from materials to applications.

088

Load Carrying Capacity of Intact Ellipsoidal Inhomogeneity in Particle or Short-Fiber Reinforced Composite

Young Tae Cho, Choong Ho Lee, Jeonju Univ.; Kwang Hee Im, Woosuk University (Korea).

This paper deals with elastic stress distributions and load carrying capacity of intact and cracked ellipsoidal inhomogeneities. Finite element analysis has been carried out on intact and broken ellipsoidal inhomogeneities in an infinite body under uniaxial tension. For the intact inhomogeneity, as well known as Eshelby's (1957) solution, the stress distribution is uniform in the inhomogeneity and non-uniform in the surrounding matrix. On the other hand, for the cracked inhomogeneity, the stress in the region near crack surface is considerably released and the stress distribution becomes more complex. Average stress in the inhomogeneity represents its load carrying capacity, and the difference of average stresses between the intact and cracked inhomogeneities indicates the loss of load carrying capacity due to cracking damage. It is found that the cracked inhomogeneity with higher aspect ratio still maintains higher load carrying capacity.

089

Local Versus Global Buckling of Thin Films on Elastomeric Substrates

Shoudao Wang, John Rogers, Jizhou Song, Northwestern University, University of Illinois, University of Miami (USA).

Locally buckled, periodic thin films on elastomeric substrates have many important applications. For long films or relatively thin substrates, however, global (Euler) buckling has also been observed in experiments. This paper describes analytically the mechanics of local and global buckling of one-dimensional thin films or two-dimensional thin membranes on elastomeric substrates. The critical condition separating these two buckling modes is obtained analytically, and it agrees well with experiments and numerical

simulations.

090

Long Term Creep Behavior of Matrix Epoxy Resin and CFRP

Hongneng Cai, Xi'an Jiaotong University (China); Yasushi Miyano, Masayuki Nakada, Katsuya Fukushima, Kanazawa Institute of Technology(Japan).

The accelerated testing methodology (ATM) was proposed by Miyano and others to predict the long term strength of CFRP laminates using the short term strength based on time-temperature superposition principle. The micro-mechanics of failure (MMF) theory was proposed by Ha and others to predict the strength of CFRP laminates based on fiber and polymer matrix failure mechanism. Based on ATM and MMF, the new combined method MMF/ATM was proposed by Cai to construct the fatigue strength master curves for fiber and matrix in micro-level. In MMF/ATM, one important step is to get the time-temperature shift factors by measuring the creep compliance; hence the same time-temperature shift factors are applied to constant strain rate (CSR) strength, creep strength and fatigue strength.

The purpose of this paper is to present stable method to get time-temperature shift factor master curve under and over glass transition temperature by creep tests for matrix resin and transverse CFRP laminates. The viscoelastic behaviors of the matrix resin can be represented by creep compliance. A series of creep tests of matrix resin and transverse CFRP laminates under various temperatures were carried out. By shifting creep compliance curves horizontally and vertically, the creep compliance curves at various temperatures are superposed onto each other to form a master curve of creep compliance at a reference temperature against the reduced time in the horizontal time axis. The shifting algorithm to get smooth creep compliance master curve is developed. The horizontal shifting factors are expressed using Arrhenius' equation. The physical meaning of vertical shifting vector is discussed. Finally, the formulation of creep compliance master curve is carried out.

092

Martensitic Transformation of Copper Zinc Aluminum Shape Memory Alloy Prepared by Powder Metallurgy Technique

Abdul-Raheem K. AbidAli, Babylon University (Iraq).

Martensitic transformations are the main concept to obtain shape memory effects and super elasticity for most of shape memory alloys. In this paper, Martensitic transformation of porous CuZnAl shape memory alloy has been studied during direct quenching heat treatment using x-ray diffraction technique to identify phase transformations. Direct quenching heat treatment includes heating the sintered samples up to 850 °C for 1 hour and then quenching in iced water (0-2 °C). Optical microscope and scanning electron microscope have been examined for prepared specimens after grinding in 150,400,800 and 1200 silicon carbide grit paper and polishing with fine alumina for both etched and unetched specimens to reveal microstructure of formed martensite phase. Shape memory effect is calculated by measuring of hardness indentation after quenching and after shape recovery treatment using image processing and image analysis of light optical indenter image in addition to compression test. It appears that direct quenching heat treatment leads to form fully Martensitic microstructure in the system of CuZnAl alloys.

093

Martensitic Twinning in Ni-Free B-Type Ti Shape Memory Alloys

D. H. Ping, National Institute for Materials Sciences (Japan).

Since Ni is believed to be a toxic element to human body, Ni-free β -type Ti base alloys such as Ti-Nb, Ti-Mo, Ti-Ta-Nb-Zr, Ti-Zr, have attracted extensive research attentions due to the low elastic modulus and shape memory behaviours, which are potential materials in the medical applications. In such kind of alloys, a key martensitic phase transformation, which is related to their shape memory behaviour, is that the austenite (high temperature β -Ti phase with disordered bcc structure, $a \approx 3.31\text{\AA}$) transforms to an orthorhombic martensitic phase (α'' -Ti) during quenching or deformation.

Novel deformation twinning of α'' martensite in traditional β -type Ti alloys was explored and unambiguously characterized. A fully transformed α'' with stress-induced nanoscale $\{110\}$, $\{021\}$ -type compound twin or a 90° rotation twin can be formed in Ti-Nb-based alloys, which usually undergo a partial martensitic transformation (a β grain partially transformed into α'' with internal (111) twin) by quenching. The observed twinning, which matches with the prediction based on Bilby and Crocker's deformation twinning theory, will be helpful for designing advanced materials.

094

Mechanical Behaviour of Advanced Composites Enhanced with Carbon Nanotubes – Overview

Guanyan Xie, Xujin Bao, Guanyan Xie, Xujin Bao; Gang Zhou, Gang Zhou (UK).

Fibre-reinforced composite laminates have been extensively used in various sectors of industry, including aerospace, land transport and marine, to name just a few. The majority of laminated composite structures in use lack the reinforcement in the through-the-thickness direction. As a result, a damage mechanism such as delamination could occur at the relatively early stage of loading when induced local interlaminar shear (ILS) stress within the structure reaches a critical level, thereby affecting their structural performance. Delamination is thus one of most detrimental damage mechanisms and causes considerable problems to structure designer, stress and maintenance engineers. At present, load-bearing composite structures are designed such that the occurrence of delamination is minimised. This practice often leads to that composite structures are over-weight, less cost-effective and less efficient in terms of performance. Over the years, various solutions such as resin-toughening, stitching, interleaving and z-pinning have been experimented but with limited success. Some of these techniques could improve the delamination resistance of the composite structures to some extent but at the expense of substantial reduction of their basic mechanical properties. The recent advent of carbon nanotubes (CNTs) provides many exciting possibilities to engineering exploitations. One particular area of innovation is to introduce CNTs into laminated composite structures to enhance their resin-dominated mechanical properties such as delamination resistance.

CNTs can be both single-walled (SWCNTs) and multi-walled CNTs (MWCNTs). They have a nominal diameter between 2 and 100 nano-meter (nm) and a length between tens and hundreds of a micron, depending on their manufacturing techniques and their surface functional coatings. These typically result in aspect ratio of around two orders of magnitude. They have a Young's modulus of around one GPa (or five times that of steel) and a strength of around twenty GPa (or one hundred times that of steel). Their elastic and failure strains are greater than 5% and 12%, respectively. These physical features along with their mechanical properties make CNTs easily embeddable imposing no intrusion to the composite hosts and ideal for enhancing the mechanical properties of resin. They are capable of playing a vital role in creating new-generation nano-composite laminates with enhanced

mechanical performance. Because of the novelty of the field, there is little information in the public domain. In particular, those research works as discussed here reflect on many occasions results of their preliminary trials. Therefore, it is essential to have an in-depth overview of this field such that the key issues are highlighted. As a result, research efforts worldwide could be more focused on those key issues and thereby channelled into making greater progress in this emerging field.

A preliminary study has been conducted, as shown in Table 1, to summarise the results of the mechanical performance of laminated composites integrated with CNTs, including tension, in-plane compression, in-plane and interlaminar shear, flexure and mode-I and mode-II fracture toughness. This paper intends to provide a state-of-the-art overview of the published literature in this area. It aims at the establishment of a understanding of how and via what deformation mechanisms CNTs are able to influence the mechanical properties of the composite hosts. It has four specific focuses. The first one is to identify the manufacturing methods of nano-composite laminates along with the introduction techniques of CNTs. The second one is to ascertain processing and control techniques with which CNTs are subjected to before/during the manufacturing of nano-composites. During this work, attention will be exclusively paid to an orientation control of CNTs, the in-plane and through-the-thickness locations of CNTs in the nano-composite laminates and the role played by the length of and volume fraction of CNTs. The third one examines types of mechanical properties and testing methods used. Here critical discussion will be carried out as for whether or not used testing methods are suited and/or adequate to the evaluation of the mechanical performance of nano-composite laminates. It is clear after the present preliminary investigation that testing methods which have already been established for advanced composite laminates are not necessarily adequate naturally to evaluate the mechanical performance of nano-composite laminates. The final one includes a post-mortem microscopic investigation into corroborative evidence after mechanical testing. This is crucial to any conclusions drawn from the research work.

095

Membrane Wrinkling Patterns and Control with SMA and SMPC Actuators

Mingyu Lu, Limin Zhou, The Hong Kong Polytechnic University (Hong Kong, China); Yunliang Li, Harbin Institute of Technology (China); Huifeng Tan, Harbin Institute of Technology (China).

Wrinkling is a main factor affecting the performance of the membrane structures and is always considered to be a failure as it can cause dramatic decrease of shape accuracy. The study of membrane wrinkling control has the analytical and experimental meanings. In this paper, a feasible membrane shape control method is presented. The tensile wrinkles of a rectangular membrane under the pretension were analyzed firstly. An expression of relationship between the wavelength and the amplitude of the membrane wrinkles with the combination of critical shear distance were established based on the tension field theory and the Von Karman large deflection formula. The control mechanism for membrane wrinkles was developed using shape memory alloy (SMA) and shape memory polymer composite (SMPC) actuators which were attached to the boundaries of the membrane for producing contraction/expansion forces to adjust the shape of the membrane. The whole control process was monitored by photogrammetric technique. Numerical simulations were conducted using ANSYS finite element software with the nonlinear post-buckling analytical method. Both the experimental and numerical results show that the amplitudes of wrinkles are effectively controlled by SMA and

SMPC actuators. The method introduced in this paper provides the foundation for shape control of the membrane wrinkling and is important to the future work on vibration control of space membrane structures.

096

Metal Oxide Nanomaterials Based Nanosensors for Highly Sensitive and Selective Detections

Weilie Zhou, University of New Orleans (USA).

Semiconductive metal oxide nanomaterials are attractive candidates for highly sensitive and selective sensor fabrication due to their high surface to volume ratio. In this talk, I will present synthesis of nanoparticles (In_2O_3 , SnO_2 , WO_3 , etc.) and nanowire arrays (ZnO , CuO , WO_3 , MoO_3 , etc.) for highly sensitive and selective sensor applications using thermal transportation, laser ablation, chemical vapor deposition, and wet chemistry methods. Different sensor prototypes, such as individual nanowire, assembled nanowire arrays, three dimensional architecture and nanocrystals coated nanowire hierarchy structures, will be demonstrated. The nanosensors were exposed to gases, such as NH_3 , H_2S , and NO_2 , etc., for testing and the In_2O_3 nanoparticle and WO_3 three dimensional nanowire array sensors show high sensitivity to H_2S down to 20 ppb level. The selective detection nanosensor prototypes will be introduced in the talk. In addition, nanowire based back field effect transistors (FETs) for antibody detection will also be discussed.

097

Microencapsulation of Self-Healing Agents with Melamine-Urea-Formaldehyde by the Shirasu Porous Glass (SPG) Emulsification Technique

Xing Liu, Jong Keun Lee, Michael R. Kessler.

Norbornene-based healing agent candidates, ENB (5-ethylidene-2-norbornene) and ENB with a custom crosslinker, were prepared into a uniform microsphere utilizing a Shirasu Porous Glass (SPG) emulsification technique, and microencapsulated by in-situ polymerization of melamine-urea-formaldehyde (MUF). Resulting microcapsules were observed under optical and scanning electron microscopy for their morphology, outer and inner surface, and shell thickness. Particle size analysis showed more uniform size distribution with a mean diameter of 40 μm , compared to a conventional method using a mechanical impeller. The thermal and mechanical properties of microcapsules were also examined considering fabrication self-healing composites.

098

Micro-Structural Investigation of Nano-SiO₂ Effect on Production of Pozzolanic Reactions

P.Hosseini, A.Booshehrian, A.Khalifei, S.Farshchi.

Recently, nano-technology has attracted considerable scientific interest due to the new potential uses of particles in nanometer (10^9 m) scale. Regarding to this ultrafine size, nano-particles have shown unique physical and chemical properties different from those of the conventional materials. Nano technology and concrete technology are connected together by the means of nano-particles as advance materials. Also nano-silica is one of the most suitable particles for concrete matrix.

In this study, different amounts of nano-SiO₂ particles were used to obtain the optimum percent of replacement for cement. After achieving the optimum amounts based on the compressive strength, micro-structural behavior of the optimum mixes were observed for each material. In order to investigate the micro-structural properties,

different test procedures, SEM (Scanning Electron Microscopy) and XRD (X-Ray Diffraction) were done. Results indicate a better micro-structural behavior of nano- SiO₂ specimens deduced by use of XRD test as an indicator of the amount and type of productions from pozzolnic reaction and SEM which shows the matrix structure of the optimum specimens.

099

Microstructural Size and Heterogeneity: the Two Key Players at the Nano Scale

Jagannathan Rajagopalan, Taher Saif, University of Illinois at Urbana-Champaign (USA).

It is well known that mechanical properties of metals depend on size. As the microstructural and specimen size decrease, strength increases. However, the influence of heterogeneity in microstructure on strength is far less understood. Here we show that for nano grained metals, heterogeneity in grain size and texture result in apparently anomalous mechanical behavior, for example, variation in yield strengths in similar samples with similar grain size, Bauschinger effect during unloading, and recovery of plastic strain under macroscopic stress free condition. The origin of such apparently different, but fundamentally linked, behaviors is the heterogeneity in microstructures where larger or favorably oriented grains deform plastically upon loading, while relatively smaller or unfavorably oriented grains deform elastically. Depending on the degree of heterogeneity, this leads to variations in yield strengths, and strain hardening during loading. Upon unloading, the elastically deformed grains apply reverse stress on plastically deformed grains giving rise to Bauschinger effect and strain recovery. Our in situ tensile tests on aluminum and gold films in TEM confirm the above mechanism. Furthermore, TEM reveals that relatively larger grains deform plastically by dislocation mechanism both during loading and unloading, while smaller grains show no dislocation activity. Thus microstructural size and heterogeneity together determine the mechanical behavior of nanoscale metals.

101

Model-Based Simulation of the Responses of Ultrananocrystalline Diamond and Nano-hierarchical Structures

Luming Shen, University of Sydney (Australia); Zhen Chen, University of Missouri (USA), Dalian University of Technology (China).

Owing to their outstanding mechanical, tribological, electronic transport, chemical and biocompatibility properties, the ultrananocrystalline diamond (UNCD) films grown by the microwave plasma chemical vapor deposition method under hydrogen-poor conditions have become the subject of intense research interests over the past decade. In this project, a combined kinetic Monte Carlo (KMC) and molecular dynamics (MD) procedure has been developed for large-scale atomistic simulation of the responses of polycrystalline UNCD films under various kinds of loading conditions. The mechanical responses of resulting UNCD film have been investigated by applying displacement-controlled loading in the MD simulation box. By randomly adding different numbers of nitrogen atoms into the grain boundaries of these polycrystalline UNCD films, the effects of nitrogen atom number density and grain boundary width on the responses of UNCD have also been explored. Recently, a systematic study is being performed to understand the combined effects of grain size, loading rate, temperature, imperfection, loading path and history on the material strengths and failure patterns of both pure and nitrogen-doped UNCD fil In this

presentation, recent advances on multiscale (both spatial and temporal) model-based simulation of the pure and nitrogen-doped UNCD responses under various loading conditions will be discussed, which might yield an effective engineering design tool for evaluating the performance of nano-composite-based MEMS devices in an extreme working environment.

Recent MD simulation results of the size and imperfection effects on the failure mechanism of nano-scale hierarchical structures consisting of one-dimensional members arranged in parallel will also be presented to better design MEMS devices.

103

Multifunctional Performance of Cyanate Ester/Multi-Wall Carbon Nanotubes Matrix Composites

V. Kostopoulos, Mrs. E.Fiamegou, A.Baltopoulos, A.Vavouliotis, P.Karapappas, N.Athanasopoulos, I.Fotiou, University of Patras (Greece).

The incorporation of multi-wall carbon nanotubes at weight fractions of 0.5% wt. and 1% wt. in cyanate esters and toughened cyanate esters was examined. The thermo-mechanical and electrical properties of the developed nanopolymers were investigated and were compared with the neat matrix properties. An optimum preparation method was developed for each resin system. The phenomenon of re-agglomeration of nanotubes took place in the first stages of curing schedule but nevertheless according to the SEM images a good dispersion was generally achieved. DMA, DSC, TGA and thermal conductivity tests were performed for the thermal characterization. For the electrical characterization, AC and DC measurements took place. No significant change in the glass transition temperature (T_g), thermal conductivity and mass loss values was observed in comparison with the neat resin systems, in both cases the improvement of electrical conductivity was about nine orders of magnitude, indicating that percolation had been achieved. The elastic modulus in bending was examined and a slight increase was observed in direct comparison with the neat resin. Finally, the developed doped nanopolymer was used as matrix for the CFRPs manufacturing. A full manufacturing protocol was developed in order to overcome the challenging issues concerning the cyanate esters' handling and manufacturing processes. Moreover AC and DC measurements were performed along with thermal conductivity and effusivity measurements. The produced nanocomposites were also tested under monotonic tensile loading.

104

Multiscale Simulation of Nanofluidics under Confinement

N. R. Aluru, Department of Mechanical Science and Engineering, Beckman Institute for Advanced Science and Technology, University of Illinois(USA).

Fluid physics at nanometer scale can be quite different from its macroscopic counterpart. Advances in elucidating fluid phenomena at nanoscale can enable revolutionary advances in numerous applications including water purification, energy conversion and storage, nanomanufacturing, DNA sequencing, single molecule detection, biomimetic channels, membranes, cells, etc. Several experimental approaches have been used with increasing success in recent years to characterize fluid transport through nanopores of varying diameters. However, many fundamental questions concerning fluid physics still remain. For example, how does

confinement affect fluid phenomena? How does surface charge, chemical functionalization and wall structure affect fluid physics? How are rotational and translational motions coupled? How different is diffusion, mobility, osmosis and other fluid transport phenomena at nanometer scale? In this talk, we will discuss how computational approaches can provide fundamental and unique insights into fluid physics at nanoscale. The traditional continuum theory fails to take into account the effects caused by the finite size of the fluid molecules and the fluid accessible volume of the nanopore. This requires atomic scale simulations (e.g. molecular dynamics simulations) where finite size of the fluid molecules is explicitly treated. However, order of the time scales and the length scales possible in atomistic molecular dynamics (MD) simulations is far less than realistic design calculations. Further, it is known that in small diameter nanopores (~ 3nm and less) quantum-mechanical effects can influence the fluid transport. These can be computed from Density functional theory (DFT) or by semiempirical methods. In this talk, we will show that multiscale methods combining density functional theory, atomistic molecular dynamics, mesoscale particle transport and quasi-continuum theories can be used to understand the fundamental questions posed above. Computational studies on fluid transport through carbon nanotubes, boron nitride nanotubes, and solid-state nanopores will be used to demonstrate unique nanoscale fluid transport.

105

Multi-Surface-Layered Ionic Polymer-Metal Composite (IPMC)

Sang-Mun Kim, Kwang J. Kim, University of Nevada (USA).

In order to tailor the electromechanical coupling of IPMC, we attempt to utilize the field-induced re-enforcement of cation concentration by introducing a multi-surface-layer design. This type of IPMC can produce sufficient deformation under much lower actuation voltages than conventional IPMC's. In this study, a new type of IPMC encompassing a multi-surface-layer electrode within the Nafion membrane was successfully fabricated by using a unique electroless deposition technique. As the first step, the interlayer was deposited before plating the outer electrode layers in order to re-enforce electric fields and to create active mobility of cations within the Nafion. Subsequently, a newly developed interlayer deposition process, based upon the counter-current diffusion, was accomplished by diffusing a tetraammineplatinum (II) cations ($[\text{Pt}(\text{NH}_3)_4]^{2+}$) from one surface of membrane while diffusing a reducing agent from the opposite side. The resulting multi-surface-layered IPMC leads to the significant increase in both effective volume fraction of the electrode and electric conductivity of the IPMC along the thickness-direction. The conductivity prediction was conducted by the mixture rule that accounts for the geometric structure, the volume fractions and the resistivities of the each component. We found that the electromechanical coupling behaviors are strongly governed by two important parameters: volume fraction of the electrode layer and overall capacitance. In addition, we investigated the effect of microscopic structures of electrodes for the electromechanical coupling of the IPMC.

106

Nanocomposite Materials Based on Sulfonated Polyarylenethioethersulfone and Sulfonated Polybenzimidazole for Proton Exchange Membrane Fuel Cell Applications

Zongwu Bai, Narayanan Venkat, University of Dayton (USA); Shane B. Juhl, Thuy D. Dang, Wright-Patterson Air Force Base (USA); Stanley J. Rodrigues, Wright-Patterson Air Force Base (USA).

Fabrication of the nanocomposite membranes comprising a fully

sulfonated polyarylenethioether sulfone (SPTES) and sulfonated poly(p-phenylene benzobisimidazole) (SPBI) and the evaluation of the membrane properties are described. The nanocomposite membrane was obtained via a solvent cast process in a mixture of DMAc and methanol as solvents. The nanocomposite membrane proton conductivity was found to increase with increase in the SPTES content in the nanocomposite. The highest proton conductivity obtained was ~110mS/cm at 85°C and 85 % relative humidity for the SPTES/SPBI 70/30 nanocomposite membrane which was considerably less than the 300 mS/cm proton conductivity for the pure SPTES membrane, but it was found that the swelling of the nanocomposite membranes was reduced due to the reduced water uptake of the nanocomposite membrane relative to SPTES. The morphology of the SPTES/SPBI nanocomposite membranes was also examined by a combination of techniques such as X-ray diffraction (WAXD), Scanning Electron Microscopy (SEM) and tapping mode Atomic Force Microscopy (AFM) to confirm the dispersion of SPBI and study the nanocomposite structures. The MEA (Membrane Electrode Assembly) performance of the nanocomposite membranes was preliminary studied for H₂/O₂ fuel cells applications.

107

Nanoscale Electromechanical Coupling in Piezoelectric Nanowires

Xingyuan (Scott) Mao, University of Pittsburgh (USA).

We have processed piezoelectric nanowires of Li-doped ZnO ranging from 10 to 500 nm thickness and 1~10 micron long by CVD technique. When dimension of piezoelectric materials goes down to a few nanometers, the piezoelectricity still exists or not? Investigating the piezoelectric properties of low dimensional nanowire using atomic force microscopy remains, however, a challenge because the sample's displacement due to the inverse piezoelectric effect by applying an electric field is in the order of pico-meter(pm) [1-2]. Several techniques, including atomic force microscopy, have been employed to measure these small piezoelectric displacements. The AFM technique has an advantage of being able to measure the piezoelectric effect down to nanoscale on a sample, and the tip can be scanned to generate piezoelectric images. Modified AFM is used to measure the effective piezoelectric coefficient (d₃₃) of individual Li doped ZnO nanobelt lying on conductive surface. Based on references using bulk ZnO and quartz, piezoelectric constant d₃₃ of Li doped ZnO nanobelt is found to be frequency dependent and varies from 14.3pm/V to 26.7pm/V, which is much larger than that for the bulk single crystalline ZnO of 12.4pm/V. Scaling effect on piezoelectric behavior has been found. The results support the application of Li doped ZnO nanobelts as nano-scale sensors and transducers.

109

New Synthesis of High-Quality Storage Phosphors

Von Seggern H., Hesse S., Zimmermann J., Technische Universitaet Darmstadt (Germany); Meng X., Tsinghua University (China); Fasel C., Riedel R., Technische Universitaet Darmstadt (Germany).

Storage phosphors in the form of image plates are utilized in radiation detection for medical and analytical applications and have potential for space application. The talk presents a new effective method for synthesizing the alkaline-earth halide BaFBr:Eu²⁺ related photostimulable storage phosphor with high stimulation yield for use in image plates. All previously reported synthesis routes for BaFBr:Eu²⁺ are multi-step processes consisting of different sequences of grinding, sintering, washing and annealing of compounds like BaF₂, BaBr₂, NH₄Br and EuX₃ (x=F, Cl, Br). The here presented route is a one-step synthesis with starting

compounds BaCO₃, NH₄F and NH₄Br as well as EuF₃. Due to the circumstance that the ammonium compounds decompose at temperatures below 300°C into the highly volatile species of NH₃ and HBr respectively HF, the halide acids initiate the decomposition of BaCO₃ and form BaFBr efficiently. The incorporation of F-centers and europium ions occurs at temperature exceeding 550°C due to an ongoing decomposition of residual BaCO₃ and EuF₃ still remaining of the primary reaction. The individual chemical reaction steps are monitored by simultaneous thermal analysis (TG/DTA) and the gaseous reaction products are detected by in-situ mass spectroscopy. Intermediate and final products are characterized by x-ray diffraction (XRD) to determine the involved phases. Photoluminescence spectra reveal the typical Eu²⁺ emission peak accompanied by a red shifted emission band at 470 nm which will be assigned to oxygen incorporated into the BaFBr lattice signing responsible for the F-center production. It will be shown that synthesized powders exhibit a high PSL yield for grains with an average size of 5.4µm ready for direct use in image plates.

111

Novel Preparation of Carbon Nano Fiber Reinforced Sebs Gel

Deng Xu, ZhenXiu Zhang, Jin Kuk Kim, Gyeongsang National University (Korea); V. Sridhar, E'cole Polytechnique Montreal (Canada); Sung Hyo Lee, Queen's University (Canada).

Thermoplastic elastomer gels (TPEGs), molecular networks composed of a microphase-separated multiblock copolymer swollen to a large extent by a low-volatility midblock-selective solvent, are ubiquitous in a wide range of contemporary technologies, including home and office products, athletic equipment, and telecommunications devices. In this work, we investigate the effect of different loading of carbon nano fiber contain. Property and morphology development of a TPEG prepared from a microphase - ordered poly(SEBS) triblock copolymer imbibed with an aliphatic mineral oil. Dynamic rheological measurements of resultant nanocomposite TPEGs confirm that addition of these filler affects the linear viscoelastic threshold and increase, to different extent, the dynamic elastic modulus, the dynamic yield stress, and the maximum operating temperature of the parent TPEG. With the addition of CNF on TPE gels, the mechanical properties and thermal degradation temperature were also increased.

112

Observation of Diffraction Pattern in Far-Field and X⁽³⁾ Measurement of Au Nano-Particles

M.H. Majles Ara, Z. Dehghani, Z. Javadi, Tarbiat Moallem University (Iran).

Noble metal nano-particles (Ag, Au, Pt and Pd) are of continuing interest because of their unusual optical and electrical properties compared to bulk metals. In this paper the second-order nonlinear optical properties of gold nano-particles were studied using a continuous-wave (CW) He-Ne laser by z-scan technique. The nonlinear refractive indices of gold nano-particles were obtained from close aperture in order of 10⁻⁷ cm²/W with negative sign and the nonlinear absorption indices of these nano-particles were obtained from open aperture with negative sign. The real and imaginary parts of the third-order optical nonlinearity $\chi^{(3)}$ have been related with nonlinear refraction index and nonlinear absorption index respectively. Then we calculated the susceptibility $\chi^{(3)}$ for this nano-particles.

We describe another procedure for investigating nonlinear optical effects on gold nano-particles, too. It is based on observing concentric ring intensity distribution pattern in far-field; which is

due to the intensity dependent complex refractive index. This experiment is performed for different intensities and consequently we obtained nonlinear refractive index by using number of rings.

114

Optimal Design of Single and Double Link Systems Using Successive Zooming Genetic Algorithm

Young-Doo Kwon, Chang-hyun Sohn, Sang-woo Han, Kyungpook National University (Korea); Jae-gyoo Lim, R&D Center, Motonic Corporation (Korea).

Link-systems have been around for a long time and are still used to control motion in diverse applications such as automobiles, robots and industrial machinery. This study presents a procedure involving the use of a genetic algorithm for the optimal design of single four-bar link systems and a double four-bar link system used in diesel engine. We adopted the Successive Zooming Genetic Algorithm (SZGA), which has one of the most rapid convergence rates among global search algorithm. The results are verified by experiment and the Recurdyn dynamic motion analysis package.

During the optimal design of single four-bar link systems, we found in the case of identical input/output (IO) angles that the initial and final configurations show certain symmetry. For the double link system, we introduced weighting factors for the multi-objective functions, which minimize the difference between output angles, providing balanced engine performance, as well as the difference between final output angle and the desired magnitudes of final output angle. We adopted a graphical method to select a proper ratio between the weighting factors.

115

Optochemical Fiber Bragg Grating Sensors

Wolfgang Ecke, Kerstin Schroeder, Institute of Photonic Technology - IPHT Jena (Germany).

Evanescent field interaction between a guided light mode and an analyte near to the core of an optical fiber influences on the Bragg wavelength of a fiber Bragg grating in dependence on the refractive index of the surrounding analyte. Fiber etching or side-polishing technology allow for refractive index measurements basing on fiber Bragg grating sensor interrogation.

This fiber Bragg grating refractometer can be advanced to specific opto-chemical measurements by deposition of an intermediate transducer layer with specific sensor reactions. Sensor structures and measuring results are presented for pH, hydrogen, and surface plasmon resonance assisted biochemical sensing. Side-polished optical fibers with inscribed fiber Bragg gratings proved to be particularly advantageous for application of planar thin film deposition techniques and polarization selective measurements.

116

Oxidation States of Conducting Polymer Composites Pani/Pbs of Nano Crystallite Size

Upendra B. Mahatme, K.Z.S. Science College; Vilas A. Tabhane, Institute of Science; Subhash B. Kondawar, Shri Shivaji Science College (India); Sunil P. Dongre, Prashant B. Dabarase, Bhalerao Science College (India).

Polyaniline salt and its composites with lead sulphide were polymerized by chemical oxidation method in presence of ammonium persulphate [(NH₄)₂S₂O₈] as oxidant and sulfuric acid as dopant. All samples of dark green colour are found to be of salt nature. Homopolymer and its composites were characterized by UV-VIS and XRD spectroscopy. Different oxidation states (Quinoid / Benzenoid ratios) of samples were discussed by their UV-VIS analysis. XRD analysis reveals that all composites are of

polycrystalline nature and of orthorhombic crystal structure. Calculated average crystallite size from XRD spectra are found to be in the nano range. Temperature dependent electrical conductivity and activation energy of polymer and its composites has been estimated. All samples follow the Arrhenius type equation. Increment in conductivity of composites with rise in temperature (semiconductor nature) indicates that tunneling is the most prominent charge transport mechanism and also agreed with VRH model. The strong correlation between oxidation state and electrical conductivity of homopolymer and composites has been observed. All these composites follow the equation $\sigma(\omega) = A\omega^s$ for their ac conductivity [$\sigma(\omega)$] and for each of these composite value of exponent 's' found to be less than one which is independent of temperature. This is well agreement with the acceptance of quantum mechanical tunneling (QMT) of charge carriers in these composites as like PANI. The ac conductivity increases linearly with the frequency and it is the characteristics of the disordered type materials like conducting polymers.

117

Patterned Electrochromic Polymer Window

Chunye Xu, Yan Dong, University of Washington(USA).

Energy issue has become a hot spot with the development of global economy and sustainability in the 21st century. In the United States, commercial buildings account for about one-third of all the energy consumption in the U.S., a quarter of which is lost through the inefficiency of standard windows to retain heat in the winter or deflect heat in the summer; and

vehicles consume much more gasoline when using air-conditioning system to keep the car cool in hot weather. With limited energy on earth, energy efficient devices or energy saving systems are urgently required. A promising technology, developed to face this challenge, is electrochromic (EC) or "smart", switchable window.

Conjugated electrochromic polymers have drawn much attention since it was discovered. Electrochromic (EC) materials can change their optical properties reversibly for an applied potential due to electrochemical oxidation and reduction. Compared with the inorganic EC materials, EC polymers perform much faster response time and easier processing. Other unique merits of EC polymers are: they require power only during switching, have a low operation voltage and energy consumption, possess long open circuit memory, great repeatability, rich color availability; and large scale and flexible devices are easily fabricated.

Large scale EC window and lenses have been achieved in our lab based on organic EC polymer, EC devices consist of up to seven layers of materials, the central five layers, with an electrochromic active, an ion conductive and an ion storage sandwiched by two conductive transparent layers, all of which are further sandwiched between two layers of transparent substrates. Patterned EC window has been further developed to achieve different tint degree at distinct spots in the same piece of substrate. Invisible sub 50 micron gaps pattern the glass into objective pixels and each pixel can be controlled separately. This technology can be mainly applied to vehicle windows or sunroofs in order to block the sunlight from which direction it penetrates in. Additional applications of the smart window, e.g. aircraft windows and ski goggles will be discussed as well.

118

Photo-Mechanical Modeling of Photo-Activated Polymers

Kevin N. Long, Martin Dunn, H. Jerry Qi, University of Colorado (USA).

The development of photo-functional polymers, which are capable of mechanically responding to light, promises to offer exciting,

innovative, and unique material capabilities. Such materials include: photo-radical mediated cleavage and reformation of the polymer backbone in cross-linked elastomers that results in local stress relaxation; photo-switching cross-links in shape memory polymers; and photoisomerization of azobenzene groups contained in liquid crystal elastomers. This paper intends to build a theoretical constitutive framework to model photo-activated polymeric materials. This framework is applied to a cross-linked elastomeric system undergoing light-activated cleavage/reformation of the polymer backbone and photo-switching crosslinks. Modeling this photo-radical-mechanical behavior constitutes a multi-physics problem with three primary constituents: the optical penetration and attenuation throughout the material; the photo-chemistry and associated radical concentration field; and the radical concentration-coupled mechanical behavior of the material. These three processes have been implemented in a finite element code. Experimental data are used to calibrate the photo-mechanical model. Finally, model prediction simulations of novel actuators are compared with experimental results.

119

Piezoelectric Paper Speaker Using Regenerated Cellulose

Joo-Hyung Kim, Junghwan Kim, Gyu-Young Yun and Jaehwan Kim, INHA University (Korea).

The piezoelectric property and acoustic performance of regenerated cellulose electroactive paper (EAPap) were investigated for a thin flexible speaker application. It was observed that the enhancement of piezoelectric charge constant of EAPap film by simple mechanical stretching process. For the acoustic performance, the sound pressure level (SPL) as a function of distance, size and geometry of the speaker prototype was evaluated. It was revealed that the higher acoustic output from the smaller size of rectangular shape in low frequency range, while circular type seems to be better than that of rectangular shape in all frequency ranges. Therefore, we suggest that thin and flexible piezoelectric EAPap paper is a promising for acoustic application.

120

Plasma-Chemical Multilayer Structures Si(5nm)/SiO₂(15nm) with Recharging Effects in Dielectrics

S.A. Arzhannikova, M.D. Efremov, A.Kh. Antonenko, A.V. Vishnyakov, V.A. Volodin, G.N. Kamaev, D.V. Marin, S.A. Kochubei, A.A. Voschenkov, Novosibirsk State University (Russia).

Silicon based superlattices attract scientists due to combination of well known good properties of Si/SiO₂ interface and possibility for realization of quantum properties at room temperatures due to large difference in forbidden zone values. This paper is devoted to structures with several nanometers thicknesses for Si and SiO₂ layers obtained within plasma-chemical technology.

Ways were elaborated for deposition of silicon dioxide films with thickness above 50nm using hexamethyldisiloxan and hexamethyldisiloxan, as well as amorphous silicon films from mixture of monosilane and argon. Mode for manufacturing of SiO₂ films with thickness above 2nm was found owing to oxidation of amorphous and crystalline silicon in plasma of pure oxygen. Multilayered structures were manufactured with interlaced layers of amorphous silicon and its oxide with correspondent thickness 5,15nm. Electrical measurements reveal significant peculiarities connected with charge transport through prepared superlattices. At positive voltages and low frequency sharp increasing of capacitance was detected in correlation with conductivity behavior. Possibly this effect is connected with alternative current originating from charge exchanging between substrate and silicon dioxide layer. The exchanging may be the sequence of recharging of small silicon

clusters or crystallites formed in dielectric layer. Thermal treatment led to modification of Raman spectra according to phase transformation.

121

Polymer Functionalization with Manganites

V. Sandu, S. Popa, I. Ivan, C. Plapcianu, E. Sandu, N. Hurduc, and I. Nor.

We investigated the transport properties of a series of composites made of $\text{La}_{2/3}\text{Sr}_{1/3}\text{MnO}_3$ and polymethyl-methacrylate-based copolymers. The temperature dependence of the electrical resistance of the sample with polymethyl-methacrylate-co-styrene shows a wide peak that shifts to lower temperatures as the content of styrene units increases. When the matrix is made of polymethyl-methacrylate-co-butadiene, the electrical resistance displays two peaks, a high temperature peak located around room temperature and a low temperature peak located around 125 K. The transport properties are discussed in terms of spin transport through the polymer-manganite interface correlated with the magnetic properties.

122

Position Control of Ionic Polymer Metal Composite Actuator Based on Neuro-Fuzzy System

Truong-Thinh Nguyen, Young-Soo Yang, Il-Kwon Oh.

This paper describes the application of Neuro-Fuzzy techniques for controlling an IPMC cantilever configuration under water to improve tracking ability for an IPMC actuator. The controller was designed using an Adaptive Neuro-Fuzzy Controller (ANFC). The measured input data based including the tip-displacements and electrical signals have been recorded for generating the training in the ANFC. These data were used for training the ANFC to adjust the membership functions in the fuzzy control algorithm. The comparison between actual and reference values obtained from the ANFC gave satisfactory results, which showed that Adaptive Neuro-Fuzzy algorithm is reliable in controlling IPMC actuator. In addition, experimental results show that the ANFC performed better than the pure fuzzy controller (PFC). Present results show that the current adaptive neuro-fuzzy controller can be successfully applied to the real-time control of the ionic polymer metal composite actuator for which the performance degrades under long-term actuation.

123

Preparation and Characterization of Nano-Structured Proton Conductive Electrolytes

Zhigang Xu, Jag Sankar, North Carolina A&T State University (USA).

A number of recent studies have shown that nano-structured oxides have significantly enhanced ionic transport and catalytic properties compared to their micron-crystalline counterparts. This is attributed to grain boundary and interfacial effects that exhibit orders of magnitude greater diffusivity than that of the lattice.

The purpose of this study was to acquire a preliminary understanding in portion conductive electrolytes through material preparation and characterizations, as well as to measure and analyze the conductivity of the nano-structured perovskite electrolytes. This will lead to better understanding of the diffusivity in interfaces and provide the knowledge required for the design novel intermediate-temperature SOFCs. 20mol% ytterbium doped Barium cerates which is partially substituted by zirconate was chosen for study. At the first place, polymerized gel was prepared using Pechini method. Electrolyte thin films were also made by

spin-coating of the gel by repetitions of coating and annealing. Different grain sizes in the films were achieved by using different annealing temperatures and holding times. The crystallographic properties of films were determined with X-ray diffraction. The crystallite size was measure by using Scherrer method and confirmed by TEM direct observations. The morphologies of the thin films were determined on the polished and etched surfaces by SEM and TEM. The conductivity of the material was measured using ac-impedance in a temperature range from 300-800°C in the presence of 4% hydrogen in argon.

124

Preparation of $\text{Ca}_2\text{Si}_5\text{N}_8:\text{Eu}^{2+},\text{Tm}^{3+}$ Phosphor by Calcium Hydride and Their Afterglow Properties

Bingfu Lei, Ken-ichi Machida, Takashi Horikawa, Hiromasa Hanzawa, Osaka University (Japan)

Recently, Eu^{2+} -activated $\text{M}_2\text{Si}_5\text{N}_8$ phosphors with orange to red emission color for $\text{M} = \text{Ca}, \text{Sr}, \text{and Ba}$, respectively, have been proven to be a new series of excellent phosphors for lighting-emitting diodes (LEDs) conversion applications due to their nontoxicity, good chemical and physical stability, high luminescence efficiency and high quenching temperature. In the preliminary work on Eu^{2+} -activated $\text{M}_2\text{Si}_5\text{N}_8$ phosphors, the researchers mainly focused on their preparation technique and LEDs applications. $\text{M}_2\text{Si}_5\text{N}_8:\text{Eu}^{2+}$ ($\text{M}=\text{Ca},\text{Sr},\text{Ba}$) phosphors were usually prepared by the traditional solid-state reaction using corresponding metals or nitrides as starting materials, which are very sensitive to oxygen and moisture, thus leading to difficulty in powder handling, high costs, and low yields. As an alternative, the carbothermal reduction and nitridation (CRN) method and the CaCN_2 reduced method were developed to prepare $\text{Ca}_2\text{Si}_5\text{N}_8$ and $\text{CaSrSi}_5\text{N}_8:\text{Eu}^{2+}$ phosphor, respectively. However, these methods cause carbon contamination within the samples, especially for $\text{Ca}_2\text{Si}_5\text{N}_8:\text{Eu}^{2+}$, which significantly oppresses the optical properties of these phosphors. The direct reaction using oxide to prepare $\text{Sr}_2\text{Si}_5\text{N}_8:\text{Eu}^{2+}$ fails to obtain pure-phase of product but a mixture of Si_3N_4 and Sr_2SiO_4 . Consequently, developing inexpensive and efficient solid-state routes to synthesize such nitride phosphors is still urgently required.

Till now, there are few of reports on the afterglow emission phenomenon in $\text{M}_2\text{Si}_5\text{N}_8:\text{Eu}^{2+}$. In our present work, an inexpensive and efficient method has been developed to prepare $\text{Ca}_2\text{Si}_5\text{N}_8:\text{Eu}^{2+}$ phosphor using cheaper CaH_2 as raw materials. Furthermore, $\text{Ca}_2\text{Si}_5\text{N}_8:\text{Eu}^{2+}$ shows obvious afterglow properties when excited with UV or visible light compared with $\text{Sr}_2\text{Si}_5\text{N}_8:\text{Eu}^{2+}$ and $\text{Ba}_2\text{Si}_5\text{N}_8:\text{Eu}^{2+}$. The intense reddish-orange afterglow emission in $\text{Ca}_2\text{Si}_5\text{N}_8:\text{Eu}^{2+}$ phosphor can be further enhanced to some extent by codoping with Tm^{3+} . The luminescence properties of $\text{Ca}_2\text{Si}_5\text{N}_8:\text{Eu}^{2+}, \text{Tm}^{3+}$ were investigated by means of photoluminescent excitation and emission spectra, afterglow emission, and afterglow decay curve.

125

Preparation of Copper Zinc Aluminum Shape Memory Alloy by Using Powder Metallurgy Technique

Abdul-Raheem K. AbidAli, Babylon University (Iraq).

Recently, shape memory alloys have been used in wide variety of engineering applications such as biomedical, military, smart materials and communications.

In this paper, CuZnAl shape memory alloy has been prepared by powder metallurgy technique from elemental powders. Mixing of powders is done for 15 hours and cold die pressing with different compacting pressure and rate of loading. Different sintering time and sintering temperature for compacted samples are studied. X-ray

diffraction analysis for green compacts and after sintering have been achieved to identify phases and to satisfy sintering process. Particle size and its distribution of blended powders and pore size in the final products are determined by image processing and image analysis of real optical microscope image. Several physical tests such as porosity, apparent density and water absorption have been examined for prepared specimens. Vickers macrohardness is also presented as well as microstructure examination with two different etchants to reveal the internal structure of prepared alloys with different magnification resolution. It is apparent that sintering in 600° C for 3 hours followed by sintering in 900° C for 3 hours give the maximum apparent density with lower porosity and minimum percentage of water absorption . it is also apparent that rate of loading (0.2 ton/ min.) gives higher green density and finally lower porosity.

126

Principle Investigation on the Dynamics of Martensitic Transformations in Lennard-Jones Lattices

O. Kastner, Ruhr-University Bochum (Germany); G.J. Ackland, University of Edinburgh (UK).

Martensitic transformations (MT) can be simulated by molecular dynamic simulations based on Lennard-Jones potentials. In 2D, these potentials may be constructed to allow for lattice transformations between nested lattices formed by two atom species: Austenite, represented by a square lattice, may transform into variants of hexagonal-structured martensite by a shear-and-shuffle type of transformation. The lattice stability depends on the temperature. Based on this model, rectangular test assemblies were investigated. Constraints to the surface were absent (free surface) to allow for free nucleation and evolution of temperature-induced MT upon cooling. Our simulations exhibit the spatial and temporal evolution of MT in some detail. Even in 2D, the model is rich enough to reproduce the formation of complex morphologies, exemplified by the snapshot below. Observed phenomena are

- wedge-shaped plate growth,
- formation and accommodation of martensitic domains,
- propagation of traveling transformation fronts,
- dislocations and elastic precursors.

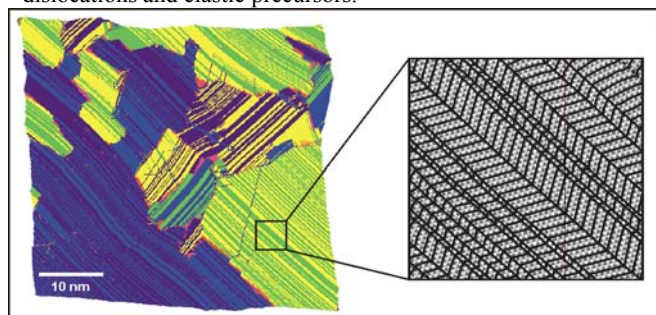


Figure 1: Martensitic domain structure formed by temperature-induced MT in a 262,000 atomic rectangle. Colours indicate four distinct variants present in the 2D model. Magnification: Finite-sized micro-twins.

The formation of micro-twin structures is of special interest: Lennard-Jones twin variants are perfectly coherent in a way that twin-twin interface energies are missing. The formation of finitesized micro-twins instead is caused by dynamic effects during MT.

Based on these 2D results, the model is presently extended to 3D. Preliminary results (Fig. 2) will be presented and related to the 2D case.

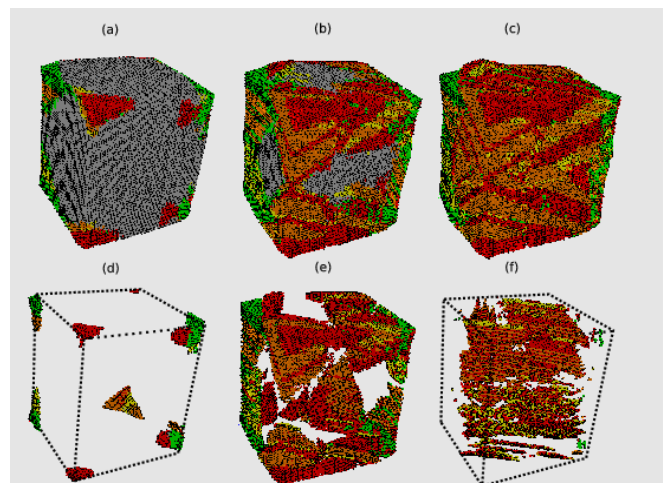


Figure 2: Structural phase transformation of a 3D quad. (a-c): Unit cell rendering at 2,000, 4,000 and 10,000 time steps. Four generic variants of the product phase coded by red, green, yellow and orange colour are produced from the B2 parent phase (gray). (d-e): Application of a potential energy threshold filters out material regions in the B2 phase during the phase transformation, thus allowing to study the evolution of habit planes. (f): A more sophisticated filter rule isolates even the planar interfaces between product variants.

128

Recent Advances on Developing Bio-Inspired Galfenol Nanowire Sensors

Patrick Downey, Alison Flatau, University of Maryland (USA); Patrick McGary, Bethanie Stadler, University of Minnesota (USA).

Galfenol ($\text{Fe}_{100-x}\text{Ga}_x$, $10 < x < 25$ at. %) nanowires have been fabricated into close packed arrays through the process of electrochemical deposition. These structures exhibit a unique combination of size, elasticity, and magnetostrictive transduction that make them well suited for use as artificial cilia in biomimetic sensor devices. The cantilevered nanowires deflect in response to excitation (acoustic, tactile, flow, etc.), and the resultant bending or compressive stresses can produce a magnetization change that can be measured using conventional magnetic field sensor technologies. This presentation will provide an overview of the fabrication nanowire process and will discuss details of strategies used to overcome some of the specific challenges in making the nanowires, e.g. maintaining uniform composition along the length of a nanowire. We also review details the complete magneto-mechanical characterization of these nanowires. Results on the mechanical properties of individual Galfenol nanowires are shown from experimental measurements taken using a custom nanomanipulator mounted inside of a scanning electron microscope (SEM). Data shows drastically improved elasticity and tensile strength in the nanowires compared with the bulk material. Magnetic force microscopy (MFM) results are shown and used to visualize the magnetic domain structure, which are in excellent agreement with micro-magnetic models. The implications of these results with regards to the influence of shape anisotropy on nanowire responses to stress and optimization of sensor design are discussed. The presentation will conclude with a summary of some of the potential applications for the proposed nanowires as critical transduction components in a sensor.

129

Residual Stress Evaluation and Fatigue Life Prediction in the Welded Joint by X-ray Diffraction

K B Yoo, J H Kim.

In the fossil power plant, the reliability of the components which consist of the many welded parts depends on the quality of welding. The residual stress is occurred by the heat flux of high temperature during weld process. This decreases the mechanical properties as the strength of fatigue and fracture. The residual stress of the welded part in the recently constructed power plants has been the cause of a variety of accidents. The objective of this study is measurement of the residual stress by X-ray diffraction method and to estimate the feasibility of this application for fatigue life assessment of the high-temperature pipeline. The materials used for the study is P92 steel for the use of high temperature pipe on super critical condition. The test results were analyzed by the distributed characteristics of residual stresses and the full width at half maximum intensity (FWHM) in x-ray diffraction intensity curve. Also, X-ray diffraction tests using specimens simulated low cycle fatigue damage were performed in order to analyze fatigue properties when fatigue damage conditions become various stages. As a result of X-ray diffraction tests for specimens simulated fatigue damages, we conformed that the ratio of the FWHM due to fatigue damage has linear relationship with fatigue life ratio algebraically. From this relationship, it was suggested that direct expectation of the life consumption rate was feasible.

130

Scale Dependence in Friction

D. Xu, K.M. Liechti, K. Ravi-Chandar, The University of Texas at Austin (USA).

Scale dependence in friction is examined using a newly developed mesoscale friction tester (MFT). A transition in frictional shear strength from several hundreds of MPa to several tens of MPa is observed over a very limited range of contact radii (20–30nm) in both ambient and dry environments. Thus, a single apparatus has been able to establish these two limits which are consistent with the values previously obtained from friction experiments using atomic force microscopes (AFM) and the surface force apparatus (SFA), respectively. Consequently, we suggest that a shear strength in the hundreds of MPa results from intimate contact (solid-solid) and a shear strength in the tens of MPa results from a monolayer lubricated contact. Furthermore, both the probe size and the normal pressure govern the interfacial conditions in the contact zone and it is these conditions, rather than the nominal environment, which in turn determine the resulting shear strengths. This quantized friction behavior (Israelachvili et al., Science 240, 189(1988)) results from the discrete separation due to the different interfacial conditions that can arise between two sliding surfaces. The consistency between the analysis and the experimental results shows that this analysis is applicable for nonwear friction with single asperity contact.

131

Silver Nanoplates: Synthesis, Structure and Functionality

X. C. Jiang, A. B. Yu, University of New South Wales (Australia).

This work reports our recent researches on the shape-controlled silver nanoplates, covering synthesis, growth mechanism, optical property and sensing application. We proposed a facile and effective self-seeding co-reduction method to prepare two-dimensional silver nanoplates with size of 2 ± 0.5 nm in thickness and 70 ± 10 nm in length at room temperature in aqueous solution. The characteristics (shape, size, and size distributions)

and functional properties (e.g., surface plasmon resonance and ionic sensing properties) were investigated in detail by various techniques such as TEM, AFM, XRD, and UV-vis spectroscopy. In particular, molecular dynamics (MD) method was applied in this study for fundamental understanding of particle growth and shape transformation at a molecule level. Furthermore, we found that the silver nanoplates show unique surface plasma resonance in UV-vis region, and they show high sensitivity and selectivity toward inorganic ions in aqueous system, such as halides, phosphates, thiocyanate and some cations. These findings will be useful for synthesis of shape-controlled metal nanoparticles with multi-functionalities.

132

Sintering Behaviour of Ti/HA and Ti/FA Composites

Xingyang Liu, National Research Council Canada/Industrial Materials Institute (Canada).

Titanium matrix composites with different concentrations of hydroxyapatite (HA) and fluoroapatite (FA) were fabricated using a powder metallurgy method. The composites were sintered at different temperatures under argon atmosphere, and the phase and microstructure changes after sintering were investigated using SEM, XRD, and FTIR. It was revealed that densification of composites samples increased with the sintering temperature until significant decomposition of HA occurred. HA in the Ti/HA composites is less stable and tends to decompose at much lower temperature as compared to pure HA, due to the interaction with Ti. In contrast, FA is more stable under the same sintering conditions. Soaking the composite samples in simulated body fluid showed that both Ti/HA and Ti/FA composites with up to 20% vol. of HA or FA were bioactive and can be potentially used as load-bearing implants.

133

Smart Materials and Devices for Solar Energy Conversions

Bin Chen, Jin Zhang, Qibing Pei, Bin Chen, Jin Zhang, Qibing Pei, University of California (USA).

Nanotechnology of composite materials has progressed to enable multifunctional devices at the unprecedented performances. We will discuss laboratory development of a solar powered catalytic converter to meet the challenges of today's diminishing energy resources and environmental sustainability. Our technology leverages on recent emerging nanotechnology to achieve both low energy cost and low material cost. The prototype device technology enables us simultaneously to reduce greenhouse gas and to convert it to hydrocarbon fuels for existing infrastructures. The result is zero carbon footprints with the sustainable energy and low cost solution processed materials. The primary objective of this proposal is to demonstrate a solar powered device that directly converts CO₂, before it emits to the atmosphere, into useful hydrocarbon fuels. One-dimensional nanostructure thin films, including TiO₂, ZnO, CdS and Cu, will be chosen to integrate a photovoltaic and photoelectrochemical (iPVEC) device. We will discuss materials applications in: 1) photovoltaic cell based on nanostructured TiO₂ nanowire array sensitized with CdS quantum dots; 2) photoelectrochemical cell (PEC) based on nanostructured TiO₂ photoanode, and Cu photocathode; 3) photoelectrochemistry measurements and iPVEC performance evaluations for CO₂ conversion. The nanostructures are fabricated using a unique robust solution-based self-assembly processes combined with CVD techniques. We take advantages of superior charge mobility and transport property; large reaction surface area and ideal exciton separation distance in nanowire thin films. Although some initial work has been performed in this area to some extent, nanowire thin films have not been thoroughly investigated in PEC. The

optimization of nanowire materials for solar conversion in PVC and CO₂ reactivity in PEC and is respectively correlated with device efficiency. The self modulated device platform could also find other applications in sensors and detectors. We will discuss device efficiency, compactness and fabrication costs, and its deployment potential to the market of either automobile industry or power plants.

134

Snap-through Dynamics of Bi-stable IPMC Actuator Considering Beam Configuration

J.H. Jeon, J. W. Park, I.K. Oh, Chonnam National University (Korea).

The snap-through dynamics of the bi-stable IPMC actuators were investigated to generate much larger displacements and periodical stable locomotion based on jumping phenomena according to boundary conditions. First, in the clamped-free BC, two curved cantilever IPMC actuators with a constant curvature and initial tip deflections of 8mm and 16mm were fabricated from flat IPMCs through thermal treatment under hot water simultaneously to reduce the residual stresses. A flat and two curved IPMC actuators were tested to evaluate the effect of initial shape in terms of step responses, harmonic responses and frequency response function tests under small and large deformation. The snap-through phenomena for the curved IPMC actuators unlike the flat IPMC actuator were observed with much larger tip displacements, low power consumption and periodical jumps of the instant velocity. Second, in case of all-clamped BC, the large and bistable responses were observed under DC and AC excitation through the end-shortening effect. These tests were conducted with various end-shortenings of 0.25, 0.5, 0.75 and 1.0 mm. The jumping phenomena of IPMC actuator was remarkably observed at 0.5mm. Present results show that the initial curved deflection and end-shortening of the IPMC actuator strongly affects the large deformation at respective boundary conditions due to the snap-through phenomena.

135

Strength of Carbon Nanotube Reinforced Nanocomposites

Ying Sun, Quanfang Chen, University of Central Florida (USA).

A study of relationship between carbon nanotube's diameter and the resultant strength of composites was conducted both analytically and experimentally. Results show that the mechanical strength of composite's strength has a parabolic relationship to the diameter and the smaller diameters of nanotubes are preferred to achieve ultrahigh mechanical strength of composites.

136

Stress Analysis of Shape Memory Alloy Composites

Yulong Wang, Limin Zhou, The Hong Kong Polytechnic University(Hong Kong,China); Yulong Wang,Zhenqing Wang, Harbin Engineering University(China); Haitao Huang The Hong Kong polytechnic University(HongKong, China).

Shape memory alloys (SMA), when in the form of wires or short fibers, can be embedded into a host material to form SMA-composite for satisfying a wide variety of engineering requirements. Recovery action of SMA inclusions induced by elevated temperature can change the modal properties and hence the mechanical responses of the whole composite structures. Due to the weak interface strength between the SMA wire and the matrix, the interface debonding often happens when the SMA composites act by external force or actuation temperature or combination of them. Thus the function of SMA inside the matrix can not be fully

utilized. It is, therefore, very important to understand the stress transfers between the SMA fibers and matrix and the distributions of internal stresses in the SMA composite in order to improve its properties. In this paper, a theoretical model incorporated with Brinson's constitutive law of SMA for the prediction of internal stresses has been successfully developed for SMA-composites based on the principle of minimum complementary energy. The typical two-cylinder model with a thin SMA fiber surrounding by epoxy matrix is employed to analyze the stress distribution in the SMA fibre, matrix and at the interface with two distinguished contributions of thermo-mechanical effect and shape memory effect. The assumed stress functions which satisfy equilibrium equations in the fiber and matrix respectively and the principle of minimum complementary energy are utilized to analyze the internal stress distributions during fiber pull-out and/or thermal loading process. The complete axisymmetric states of stresses in the SMA fibre and matrix have been developed. The results indicate substantial variation in stress distribution profiles for different activation and loading scenarios.

137

Structure Formation of Surface Modified Carbon Nanoparticles in Oligomer Material

I. Valtsifer, Y. Tselishchev, S. Astafeva, V. Valtsifer, V. Strelnikov, Institute of Technical Chemistry (Russian).

Introduction of nanosized particles into oligomer binding agent at definite process conditions promotes their structuring and formation of the continuous clusters, penetrating the bulk. Nanoparticles, including the carbon ones, have pronounced ability to structure into the chain clusters. This ability provides obtaining of materials with different rheological properties and uniform distribution of the particles in an oligomer medium at relatively low filling degrees.

The main processing factors, influencing on the formation of continuous structures of carbon-containing catalyst based on nanodispersed copper, nickel, lead and bismuth oxides within the polymer matrix have been studied. Among these are such parameters as temperature, volume filling, shear rate, structurization time; the influence of medium viscosity and surface modification of nanodispersed components on the structurization processes of nanocarbon oligomer systems has been studied too.

Experimental studies of structure formation of the superfine components in the oligomer medium were carried out using rotary viscometer Rheotest RN4.1 by the method of dynamic vibrations and retrofitted rheoconductometric installation based on viscosimeter Rheotest 2.1 for determination of electric conductivity of the composition.

Electric conductivity of the composition was shown to be the parameter for the determination of initiation of nanocarbon continuous structures. The electric conductivity of the composition, indicates the structure of carbon in the composition to be continuous. It was determined, that the current increases proportionally with the increase of the number of carbon nanoparticle chains per volume unit.

The regularities, connected with structurization and rheological properties of filled oligomer systems depending on the surface modification of carboncontaining catalysts by metal oxides have been established.

The work was carried out at the financial support of Russian fund of fundamental research (grant № 08-03-00386a, grant № 07-03-00050a).

138

Structure of a Soft Polyelectrolyte around a Rigid Electronically-Responsive Cylinder

Chongbo Sun, Tian Tang, University of Alberta (Canada).

The structure of a soft polyelectrolyte (PE) around a rigid nano-scale cylinder is studied by considering the electrostatic and van der Waals interactions between them. The PE is represented by a helix of discrete charges. The cylinder core is allowed to be conducting, dielectric, or semiconducting, and responds to the external charges electronically. Based on the Debye-Huckel theory, the electrostatic free energy of the PE-cylinder complex is obtained in closed analytical form. The effect of counterion condensation is also considered. We show that the competition between the van der Waals adhesion and the electrostatic repulsion between charges can result in an optimal wrapping geometry. The dependence of the optimal geometry on the salt concentration of the solution and the adhesion energy density is also demonstrated.

139

Study of Viscoelastic Properties of MR Elastomers

Yang Zhou, Xianzhou Zhang, Weihua Li, University of Wollongong (Australia).

As an important member of smart materials, magnetorheological elastomers (MREs) have attracted increasing interest recently as such materials exhibit characteristics that their modulus can be controlled by an external magnetic field. MREs have found applications in the development of variable stiffness devices, such as adaptive vibration absorbers. As MRE based devices usually work in a dynamic mode, the study of MRE properties under such working condition is essential to its practical applications. In this study, both experimental work and modeling approach were conducted to address this problem.

The MRE sample was prepared by mixing carbonyl iron powder, silicone rubber and silicone oil and curing under a magnetic field. Both of its steady-state and dynamic properties were measured by using a parallel-plate MR rheometer. The relationships of dynamic shear stress versus shear strain at various magnetic fields as well as different strain amplitudes and frequencies were measured. The stress-strain data form elliptical curves, which demonstrate MRE behaves linear viscoelastic properties. The slope of main axis of ellipses shows an increasing trend with magnetic field, which indicates that the MRE stiffness increases steadily with the increase of magnetic field. Also, the damping capability increases steadily with magnetic field as the elliptical loop area increases with magnetic field. Based on these experimental results, a four-parameter viscoelastic solid model was proposed to predict MRE performances. In this model, a spring element is placed in parallel with a 3 standard viscoelastic solid model. The four parameters under various working conditions (magnetic field, strain amplitude, and frequency) were identified with MATLAB optimization algorithm.

Based on the identified parameters, the stress-strain data were reconstructed. The comparisons between experimental results versus model-predictions demonstrate that the 4-parameter viscoelastic model can accurately predict MRE performances. In addition, typical viscoelastic parameters, including storage modulus, loss modulus and loss factor, were calculated and the effects of various working conditions on these parameters were summarized. It is expected that this study will make a good contribution MRE practical application.

140

Sub-Percolative Composites with High Electro-Mechanical Response for Dielectric Elastomer Actuators

H. Stoyanov, D. McCarthy, M. Kolloosche and G. Kofod.

Dielectric elastomer actuators based on Maxwell-stress induced deformation, are considered for many potential applications where high actuation strain and energy are required. However, the high electric field and voltage required to drive them, limits some of the applications. The high driving field could be lowered by developing composite materials with high-electromechanical response. In this study, a sub-percolative approach for increasing the electro-mechanical response has been investigated. Composites with conductive carbon black particles, and blends with polyaniline (PANI) introduced into a soft rubber matrix poly-(styrene-co-ethylene-co-butylene-co-styrene) (SEBS) were prepared by a drop-casting method. The resulting composites were characterized by dielectric spectroscopy, tensile mechanical analysis, and electrical breakdown strength test. The results showed a substantial increase of the dielectric constant at low volume percentages, thereby preserving the mechanical properties of the base soft polymer material. Drawback of the approach is the decrease of the composite breakdown strength, due to the local field concentrations. A proper surface treatment of the conductive particles could increase the breakdown strength of the composite without affecting the dielectric properties.

141

Superdeep Penetration-Novel Method of Nanoreinforced Composites Producing Based on Metallic, Ceramic and Polymer Matrixes

Oleg Figovsky, and Sergey Usherenko, INRC Polymate (Israel).

Qualitatively new methods of preparation and manufacture are created on the basis of new physical and chemical effects. The superdeep penetration (SDP) is poorly known physical phenomenon which is realized at a concussion of clots of cosmic dust with protective shells of flight vehicles. Feature SDP is penetration strikers in a solid body without formation of the open holes. Registration of this phenomenon meets difficulties as at SDP loss of air-tightness in a material is absent.

Dust particles are implanted in a solid body and interreact with its material within the limits of the closed system. In this system in an automodelling mode variable fields of pressures with greater gradients of pressure and temperatures operate. In a range of requirements SDP the complex of unusual physical effects which can be used for manufacture of new materials is realized. Process of a broaching of metals, ceramics and a polymeric matrix by fibrils on depths in tens and hundreds millimetres in time in shares of second is realized. These fibrils are created due to processes of synthesis at interaction of entered substance and a matrix material, and also due to bucking devices of initial structure on micro-and nano levels. Contrary to the basic models for shock in this closed system of a material the intensive energy liberation is observed: local fusion, synthesis, radiation and formation of massive composite materials.

In metal and in ceramics there are changes of structure and properties, the composite material is formed. Successful feature SDP at penetration of a clot of particles in metal fibrils that in a plastic matrix are streams of high-energy ions. These "galactic" ions (energy of individual ion ≥ 100 MeV) act on chemical bonds in plastic materials and improve properties.

Superdeep penetration well combines with other technological operations and essentially expands opportunities of modern manufacture of materials and machine components. In all-metal and big details SDP allows to create macro and micro zones with special properties, for example, with high hardenability. Such details at a thermal processing provide essentially various level of physical, mechanical and chemical properties in various macro

zones of a detail, for example various wearing capacity. Process of sintering after SDP is not required. As a result process SDP has high efficiency and can successfully be used by the small, average and large industrial enterprises.

142

Synthesis and Characterization of Halosulphate Based TLD Phosphors

K.N. Shinde, N.S. Science & Art college (India); I. M. Nagpure, S. P. Puppalwar, And S.J. Dhoble, Kamla Nehru College (India).

Sulphates are known to be good thermoluminescent materials. In recent years we have reported several phosphors which exhibits properties useful for thermoluminescence dosimetry [TLD] of ionizing radiations. High sensitivity, tissue equivalent TLD materials are important for the measurement of exposures in the field of medical physics. LiF:Mg,Cu,P is one of the such phosphor. However, limited thermal stability of this phosphor have some problem. The limited thermal stability has been attributed to the aggregation of phosphorous impurities. Lithium borate is a good tissue equivalent phosphor with $Z_{\text{eff}}=7.4$. Brunskill developed the preparation of this material to produce a useful, tissue equivalent detector but its main disadvantage was the emission at 600 nm which corresponds to the most insensitive region of the response of most photomultiplier tubes. CaSO₄:Dy is such an efficient phosphor that it is used in TLD for ionizing radiations but poor tissue equivalence. The shape of the glow curve also changes with exposures. LiF:TLD100 is tissue equivalent, but its response is poor, about 20 times less than that of CaSO₄:Dy. It also has a complicated glow curve structure.

During the course of our investigation halosulphate based materials, we have come across a phosphor showing TLD properties. As an outcome of these studies we have found a new halosulphate based TLD phosphors. In this paper, synthesis of Eu activated KZnSO₄F and K₃SO₄F phosphor by using wet chemical synthesis has been reported. The X-ray diffraction pattern shows the formation of homogeneous crystalline materials. KZnSO₄F:Eu and K₃SO₄F:Eu halosulphate based phosphors gives TLD properties. Outcome of this study has been a new halosulphate based TLD phosphors gives prominent TL glow curve with simple structure. TL sensitivity of the phosphors was compared with standard TLD- CaSO₄: Dy phosphors.

143

Synthesis and Properties of Resistive Switching Poly (aryl ether)s

Hung-Lung Tsai, Sheng-Tung Huang, Kun-Li Wang., Sheng-Chieh Wu, Tseung-Yuen Tseng, National Taipei University of Technology (Taiwan, China).

A novel bipolar aryl difluoride monomer containing electron-donor triphenylamine and electron-acceptor 1,2,4-triazole moieties was synthesized by a three-step synthesis. The 1,2,4-triazole structure formed by a facile cyclocondensation reaction from 4-aminotriphenylamine and chlorinated azine compound. The novel bipolar aryl difluoride monomer was used to prepare a series of poly(aryl ether)s via aromatic nucleophilic substitution reaction with various bisphenols. The structures of the monomer, intermediates and polymers were confirmed by NMR, IR and elementary analysis. The poly(aryl ether)s exhibited excellent solubility in organic solvents such as dimethylformamide, chloroform, toluene, dimethylacetamide and tetrahydrofuran at room temperature. The inherent viscosities were 0.28-0.35 dL/g. The poly(aryl ether)s showed high thermal stability with T_{d10} higher than 500 °C in nitrogen and glass transition temperatures (T_g) higher than 187 °C due to the rigid heterocyclic 1,2,4-triazole

groups. The memory effect of the poly(aryl ether)s was investigated by the I-V characteristics of ITO/Polymer/Al sandwich devices. The thin films of the poly(aryl ether)s indicated bistable resistive switching behavior with ON/OFF current ratios as high as 10^3 . The switching on and switching off bias voltages of the poly(aryl ether)s were affected by the bisphenol moiety. The good resistive switching behavior of the poly(aryl ether)s made them promising candidates for future nonvolatile memory applications.

144

Synthesis Pure and Rare Earth La-doped Nanocrystalline SnO₂ For Ethanol Vapour Sensing

Gaik-Tin Ang, Mohamad Zailani Abu Bakar, Ahmad Zuhairi Abdullah, Gaik-Hoon Toh, Universiti Sains Malaysia (Malaysia).

Pure and rare earth Lanthanum doped stannum oxide (SnO₂) were prepared by sol-gel method using tin tetrachloride pentahydrate lump and lanthanum nitrate hexahydrate as starting materials. The crystalline and microstructure of the powders were analyzed by X-ray diffraction (XRD) and transmission electron microscopy (TEM). The sensor fabricated from these tetragonal SnO₂ and La-doped tetragonal SnO₂ powders exhibits high sensitivity to ethanol vapour. The doped lanthanum had decreased the crystalline size and increased the sensitivity of the sensor performance to ethanol. The sensitivity of sensor pellets toward ethanol vapour was studied at different temperatures range between 150 to 350°C. The dependence of the sensitivity on the ethanol vapour concentration is observed in the range of 800 to 3000ppm. The pure SnO₂ showed the highest sensitivity to ethanol vapour at the sensing temperature 300°C. By adding the 5% and 10% atomic ratio of lanthanum, the highest sensitivity towards ethanol vapour had been decreased to 200°C sensing temperature. The enhancement of ethanol sensitivity doped by lanthanum can be explained by its increasing of surface and decreasing of crystallites sizes. The response time and recovery time had been studied in this research. The response times for the fabricated sensors are about 22-40s for pure SnO₂ and La-doped SnO₂. The results demonstrate that La-doped SnO₂ nanocrystalline can be used as the sensing material for fabricating high performance ethanol sensors.

145

The Application of Smart Materials in the Next Generation High Life Wing

Daochun Li, Shijun Guo, Cranfield University (UK).

State of the art high lift systems provide appropriate aerodynamic performance, but economical and ecological performance could further be increased by reduction of complexity, mass, power, and noise. Next generation wings will employ slim profiles to enable efficient cruise flight. High lift devices based on smart structures have the potential to significantly increase economic and ecologic performance especially for oncoming wings and constitute an enabling technology for laminar wings. A collaborative project involving many European partners is being carried on, the main objectives of which is to develop and investigate morphing smart high lift devices for the next generation wings with the reduction of system complexity and mass. In order to meet the design requirement above, smart materials have many advantages than traditional materials.

In this paper, we firstly give a discussion on the application potential of smart material in the next generation wing. Then our attention is mainly focused on the design of smart trailing edge wing.

Among the smart materials family, due to their performance and features, Shape Memory Alloy (SMA) and piezoelectric material are finding more and more applications within many engineering

fields, in particular in the aerospace field. SMA materials are generally able to transmit large force and deformations. The limitation of such materials is however represented by the working frequency range. So they could be used to adjust wing geometric structure to meet deferent flight condition. On the contrary, piezoelectric actuators exhibit a wide working frequency range, therefore may be used as control surface.

The high lift devices in the project include Smart Leading Edge (SLE) and Smart Single Slotted Flap (SSSF). In this paper, we present the design, modelling and analysis of a SSSF. A two dimensional wing section is modelled where 40 percentage of trailing edge is flexible. SMA is applied to deform the geometry of flap. The concept of design is featured with structure simplicity and practicality. The relationship between flapping angle and energy input is derived, and aerodynamic performance is evaluated to determine the optimal deformation geometry. The results show that the design is feasible and effective.

146

The Effect of Silicon Carbide Nanoparticles on the Multifunctionality of Epoxy Polymers and Cfrp

V. Kostopoulos, A. Baltopoulos, P. Karapappas, N. Athanasopoulos, E. Fiamgou, A. Vavouliotis, University of Patras (Greece); Elis. Borsella, F. Fabbri, ENEA/FIM (Italy).

In this work the effect of silicon carbide nanoparticles into an epoxy matrix was investigated. High shear mixing techniques combined with sonication methods were used to homogeneously disperse the Silicon Carbide nanoparticles (Nano-SiC) in bisphenol-A epoxy resin at 1% weight fraction. SEM was used to evaluate the Nano-SiC powder itself and the achieved dispersion in the nanocomposite. Mechanical, thermal and dynamic tests were performed to evaluate the nanopolymer and directly compared with the neat resin. On polymer level the produced materials showed improvement in the mechanical properties reaching up to 25% and 30% in Young's modulus and maximum stress respectively. The nanopolymer exhibited a more brittle behavior through the decrease of the maximum strain during loading. The thermal properties of the nanocomposite were highly affected leading to an enhancement of the thermal conductivity and thermal effusivity of the material. Meanwhile the glass transition temperature increased up to 28% as measured through DMA tests. The aforementioned material was used as the matrix material in order to produce carbon fibre reinforced panel. The improved properties of the nanopolymer is anticipated that in turn will enhance the fracture properties of the composite materials (Mode I and Mode II) as the dispersed nanospheres can work as arrestors/deflectors of the propagating cracks through the composite.

147

Fabrication of Micro Channel Employing on Hot Embossing System

Zhuqing Wang, Masato Yoshioka, Shisn-ichiro Hira.

Hot embossing method was studied for the fabrication of micro fluidic micro channels on polytetrafluoroethylene (PTFE) chip. To investigate the basic mechanism of hot embossing, a series of experiments were conducted by using male die with micro-features. With these methods, the polymer flow behavior during micro embossing was observed. A hot embossing method to achieve high replication accuracy was presented. Orthogonal experiment was used to establish the relationship between hot embossing conditions and replication accuracy. The results of the present work implied that during hot embossing cycle, the increasing temperature and pressure stage will determine the replication accuracy of micro channel in depth, and the replication accuracy of width and shape

was determined by maintaining temperature and pressure stage. The replication accuracy depends strongly on the processing conditions. By using new hot embossing method, the replication accuracy has reached over 95%.

149

The Effects of Polyaniline Additions on Structural, Optical and Gas Sensing Behaviour of Metal Oxides Nanocomposite Thin Films

M.H. Haji Jumali, I. Izzuddin, Ms N. Ramli, M.M. Salleh, M. Yahaya, Universiti Kebangsaan Malaysia (Malaysia).

The structural, optical properties and gas sensing behaviors of TiO₂ and ZnO based nanocomposite thin films were investigated. In this paper, conducting polymer Polyaniline (PANI) were directly added into two different metal oxides sol gel solutions with PANi : metal oxides weight ratios of 1:1, 2:1 and 3:1. Three layers of thin films were fabricated from each ratio using spin coating technique. Structural investigation using XRD presented that all films exhibited amorphous structure. The additions of PANi resulted in formation of porous films with metal oxides exist as agglomerated round shaped particles with the particles size varies between 50nm to 200nm. The increment of PANi resulted in formation of chains network between the particles. UV transmission measurements showed that augmentation of PANi reduced the optical energy band gap in samples from 3.8 eV to 3.5 eV. Ethanol vapor detection test conducted at room temperature showed that both ZnO and TiO₂ based films were capable to sense the vapor. The optimum ratio in sensing ethanol vapour for PANi-TiO₂ and PANi-ZnO film were 3:1 and 1:1 respectively. In term of sensitivity and stability, PANi-ZnO film with ratio 1:1 exhibited the best performance compared the other thin fil Nevertheless, other issues such as reliability, selectability and repeatability remain as the major problems.

150

The Study on Leakage Reappearance Test of High Pressure Hose for Power Steering System

Gi-Chun Lee, Jae-Hoon Kim, Hyoung-Eui Kim, Jong-Won Park, Chungnam National University (Korea).

Generally, leakage in high pressure hose assembly can be determined by that hydraulic fluid falls down through fitting which is swaged with rubber hose. The leakage which is the failure phenomenon occurred often in hydraulic system was tried to prevent. In the case of methods which verify leakage paths in power steering hydraulic system equipped with high pressure hose assembly, three types of leakage paths which can see by cutting the swaging part can be generally experienced. However, it was difficult to find out leakage paths using power steering oil. In this study, four methods which are thermal burn image method, hole drilling method of fitting metal, white paint infiltration method, and fluorescent infiltration method were tried to introduce. Thermal burn image method failed to find out the leakage path between fitting part and rubber part. Hole drilling method is the way to check leakage path on the fitting part which doesn't need to cut a hose assembly. This method succeeds to visualize the leakage path partially but it also could not check sequential path of leakage because it need to drill more closely. White paint infiltration method also could find leakage path partially by using white paint mixed with thinner, which pressurized by hand pump, instead of power steering oil. This method could check the leakage path by cutting swaging part. Fluorescent infiltration method could verify leakage path with the unaided eye simply to hold the cutting swaging part closely to the ray of light. Reappearance test methods in high pressure hose assembly, which are hole drilling, white paint

infiltration, and fluorescent infiltration method, can be applied to find failure mode and to approval test before mass production of high pressure hose.

151

Thermal Oxidation of Porous Silicon: Theory and Experiment

Chumin Wang, Rodolfo Cisneros, Universidad Nacional Autonoma de Mexico (Mexico).

The efficient photo- and electro-luminescence at room temperature observed in porous silicon has generated an increasing attention in the last decade, due to its compatibility with the microelectronics. It is well known that the crystalline silicon has an indirect gap which avoids an efficient radiative recombination. In addition, porous silicon possesses a very high surface to volume ratio of $500 \text{ m}^2/\text{cm}^3$, which could lead to a new generation of gas and biological molecule sensors. At the same time, the oxidation process of this huge surface area should be investigated in detail for almost every application. In this work, we report an ab-initio study within the Density Functional Theory by starting from a crystalline silicon supercell of 32 atoms, where a column of 9 atoms is removed along the [001] direction, dangling bonds are firstly saturated with hydrogen atoms, and a clear enlargement of both the lattice parameter and the electronic band gap is observed. When these hydrogen atoms on the surface of porous silicon are partially replaced by oxygen atoms, a reduction of the band gap is found. However, when oxygen atoms are additionally introduced into the bulk of porous silicon, the electronic band gap grows towards that of quartz. This two-stage thermal oxidation process has recently been observed and the experimental results will be presented in detail.

152

Thermo-mechanical Behaviour of Copper Based Shape Memory Alloys

O. Adiguzel.

The behaviour of many materials is evaluated by the structural changes in microscopic scale.

Shape memory alloys take place in a class of functional materials by exhibiting a peculiar property called shape memory effect, and they are one particular class of smart materials.

A series of alloy systems exhibit this property which involves the repeated recovery of macroscopic shape of material, at different conditions. This property is characterized by the recoverability of desired shape on the material at different conditions. Shape memory materials can be plastically deformed under a stress and then are able to recover their original shape on removing the stress just by thermal means upon heating. Due to this property, these alloys can be called smart materials.

On the other hand, the shape memory materials are very important and useful in many interdisciplinary fields such as the medicine, bioengineering and many engineering fields. The choice of material as well as actuator and sensor to combine it with the host structure is very essential to develop main materials and structures.

Thermo-elastic martensitic transformation is essential on the occurrence of this important property. Shape memory materials can be permanently deformed under a stress and then are able to recover their original shape just by thermal means.

Shape memory alloys are attractive materials as sensors or actuators for some adaptive structures. Design and improvement of these smart structures requires a better understanding of the basic and fundamental mechanisms of thermoelastic or stress-induced martensitic transformation.

Martensitic transformations in shape memory alloys occur by two or more lattice invariant shears on a $\{110\}$ -plane of austenite

matrix which is basal plane of martensite. The order of martensite structure is closely related to the order of parent phase due to the diffusionless character of the transformation, and the martensite exhibits the order of parent existing prior to the transformation. Martensite phase has the unusual layered structures which consist of an array of close-packed planes with complicated stacking sequences called as 3R, 9R or 18R martensites depending on the stacking sequences on the close-packed planes of the ordered lattice. On the basis of austenite-martensite relation, it is experimentally determined that the basal plane of 9R (or 18R) martensites originates from one of the $\{110\}$ - planes of the parent phase.

Martensitic transformation and the associated mechanical shape reversibility in copper-based shape memory alloys is strongly influenced by cycling and ageing effects, due to the metastable character. These materials can be plastically deformed by variant transformations, in case they are stressed in the martensitic condition. The effects of thermal cycling (repetition of the temperature induced martensitic transformation) on the transformation characteristics of Copper-based shape memory alloys have been investigated on two shape memory alloys.

153

Three Dimensional Fabric Sensor Assemblies for Monitoring Foot Pressure

Qiao LI, Yangyong Wang, Hua Tao, Xiaoming Tao.

Knitted fabric sensor has a large electrical response to the strain deformation. However, purely knitted conductive fabric could not function as a pressure sensor. In this study, a three dimensional knitted fabric sensor assembly were created for sensing pressure from foot motions. The intelligent insole comprised two conversion layers: the Top Conversion Layer was made by knitted fabric containing seven sensing units and textile-based circuit; the Bottom Conversion Layer was the silicone insole with seven holes for the location of the sensing units. The sensing units was realised via coating conductive composites to the knitted fabric. Textile-based circuit was created by sewing silver coated nylon yarn (70D*2) to knitted fabric. The insole size and the portion of the sensing units were decided by the footmarks of the subject. And the sensing units were designed with different shape and size for monitoring pressure distribution accurately. The sensitivity and repeatability of the pressure sensing insole were evaluated. The three dimensional knitted fabric sensor assemblies open the way for the application of pressure sensing field.

154

TWSME Improvement by Thermal Cycling at Zero Stress in NiTi Shape Memory Alloys

C. Urbina, S. De la Flor, F. Ferrando, Rovira i Virgili University(Spain).

Phase transformation behaviour plays an important role in the development of the two-way shape memory effect (TWSME) in NiTi shape memory alloys (SMAs). Most of the TWSME training methods published consider that the transformation between martensite and austenite phases must take place in one step in order to obtain a substantial two-way memory strain (ϵ_{tw}). However, other papers suggest that the intermediate R-phase may have an advantageous influence on the development of the TWSME. Given that the R-phase can be developed in the alloy by repeated thermal cycles at zero stress (TC), this paper studies experimentally how the TC and the R-phase influence two different training procedures for developing the TWSME in NiTi SMAs. Two different sets of NiTi wire are used in the study: one set has been heat treated to ensure a transformation path with no R-phase, whereas the other set

has had the same heat treatment which is then followed by repeated TC in order to develop the R-phase. After this, two different TWSME trainings, that is, thermal cycling under constant load and isothermal tensile deformation under martensite state, are performed on each set of samples. The study then analyzes how both the TC and the associated R-phase affect the training procedures, the training parameters, the ϵ_{tw} , the transformation temperatures and the hardness evolution for each training procedure and each sample. The results show that 1) after 30 TC cycles, the SMA not only develops the R-phase, but also becomes considerably harder; 2) the presence of the R-phase did not prevent substantial ϵ_{tw} in either of the training procedures (5% for isothermal and 4% for constant load); 3) the ϵ_{tw} is similar in both the thermally cycled sample and the non-thermally cycled sample; and 4) prior TC leads to lower permanent strain in both the training procedures.

155

Use of Optically Transparent Lead Lanthanum Zirconate Titanate (PLZT) as Actuators and Sensors

Quantian Luo, Liyong Tong, The University of Sydney (Australia).

Optically transparent lead lanthanum zirconate titanate (PLZT) ceramics recently developed has the potential of being used to store high resolution, high contrast, high density and nonvolatile optical information. For this intrinsic photo-ferroelectric effect, optical storage is based on using near ultra violet light at the PLZT band gap energy to switch the ferroelectric remnant polarization. PLZT ceramics can also be used as actuators and sensors in micro-optomechanical systems, in which, photo induced strains are due to superposition of photovoltaic and converse piezoelectric effects when ultra violet light illuminates on PLZT materials.

As light absorption in PLZT materials, significant photo responsive effects are only observed within 10-100 μm near the irradiating surface. To efficiently utilize PLZT materials with light illumination, thin layer PLZT ceramic is normally deposited or bonded a substrate.

When light illuminates on PLZT ceramics, complicated processes of energy transformation occurs: photovoltaics, optothermics, pyroelectrics, piezoelectrics and thermal expansion. To achieve ferroelectric domain switching or large photo induced strain, strong light illumination is required to obtain high electrical field strength. Due to incompatible deformations induced by light illumination and large strain caused by intensive light, interfacial fracture is a common failure mode in this type of PLZT device.

This paper first presents a basic constitutive model for PLZT that relates light intensity to induced strain. Thence, for a bi-layered PLZT beam, distinctive features of photo induced strains in PLZT wafers poling along thickness is discussed and then the energy release rates for interfacial fracture of bi-layered PLZT beams are presented based the Timoshenko beam theory.

157

Wrinkling Atop Shape Memory Polymer with Patterned Surface

W.M. Huang, Y. Zhao, N.N. Ei, Nanyang Technological University (Singapore).

We have previously demonstrated that various types of patterns at different scales can be easily realized atop shape memory polymers through a procedure including three major steps, i.e., indentation, polishing and heating. In addition, by coating a thin metallic layer (e.g., a few nanometers thick of gold) atop shape memory polymers with or without pre-straining, different types of wrinkles could be generated. In this paper, we investigate the wrinkling patterns formed on the top of shape memory polymers with patterned

surface. As the wrinkles are resulted simultaneously by two phenomena upon heating, namely the shape recovery in the shape memory polymer substrate and buckling of the elastic metallic layer, the wrinkling pattern varies from one location to another depending on the local strain. Utilizing this technique, we are able to produce a surface with complicate patterns at two levels (protrusion and wrinkle).

158

Carbon Nanopapers and Nanocomposites: Processing, Characterization, and Applications

Jihua Gou, Yong Tang, Haibao Lu, Fei Liang, Jinfeng Zhuge, University of Central Florida (USA); Haibao Lu, Jingsong Leng, Shanyi Du, Harbin Institute of Technology (China).

The research and development of nanocomposite materials has gained significant attention in recent years due to their potential applications in the engineering, medical, and defense fields. We recently explored a unique concept of manufacturing nanocomposites with carbon nanotube/nanofiber based nanopapers for structural and multifunctional applications. This approach involves making carbon nanopaper by the filtration of well-dispersed carbon nanotubes and carbon nanofibers under controlled processing conditions. The carbon nanopaper has excellent mechanical, electrical, and thermal transport properties close to the component individual carbon nanotubes and nanofibers. Therefore, the carbon nanopaper offers numerous potential applications including conductive and high strength composites, electronics, heat sinks, fuel cells, supercapacitors, sensors and actuators, and artificial muscles. In this study, carbon nanopapers are integrated into composite laminates using modified liquid composite molding processes such as Resin Transfer Molding (RTM) and Vacuum Assisted Resin Transfer Molding (VARTM). Several applications of carbon nanopaper based nanocomposites are illustrated; in particular, structural and acoustic damping, lightning strike protection, electromagnetic interference shielding, fire retardancy, and shape memory polymer (SMP) nanocomposites are discussed. This interdisciplinary research combines manufacturing methodologies, nanomaterials science and engineering, process and property analysis to enhance our understanding of nanocomposites development. The future directions for process development and property analysis are also presented.

159

Carbon Nanotube Composites and Their Energy Storage and Conversion Applications

B. Q. Wei, University of Delaware (USA).

Research in the development of new materials for energy storage and conversion applications is an ongoing pursuit in the development of high energy and power density power sources. Carbon nanotubes (CNTs) have been full of surprises since their discovery and this trend continues. Utilizing CNTs and their composites for various energy storage and conversion applications such as electrodes in lithium ion batteries and supercapacitors and as catalyst supports in fuel cells are under close scrutiny because of the promising electrochemical performance of such materials. In this presentation, I will report our research efforts in assembling CNT composites using chemical vapor deposition and wet chemistry methods. A simple method for forming a homogenous composite of $\alpha\text{-MnO}_2$ and SWNTs has been demonstrated and a long cycle performance study at a high current for the composites has been studied. An in-situ formation of a sandwich composite structure involving copper oxide, CNTs and copper, lead to an improved electrochemical performance with a reversible capacity

of 220 mAh/g at high cycling rate of 50 C. The improvement in electrochemical performance has been addressed with a model involving a sandwiched composite structure, which can be extended to other metal oxides/CNT composites. I will also discuss their electrochemical properties as electrode materials for energy conversion devices.

164

Distributed Fiber-Optic Sensing System with OFDR and Its Applications to Structural Health Monitoring

H. Murayama, K. Kageyama, K. Uzawa, the University of Tokyo; H. Igawa, Japan Aerospace Exploration Agency (Japan); K. Omichi, Fujikura Ltd.; Y. Machijima, Lazoc Inc. (Japan).

In the field of optical fiber sensors, fiber-optic distributed sensors that return a value of the measurand as a function of linear position along an optical fiber are regarded as a promising sensing technology which can be applied to structural health monitoring (SHM). In recent years various techniques for distributed strain measurements have been proposed and applied to structural monitoring. Among them, the techniques based on Brillouin scattering have been developed by many researchers and have drawn attention in the SHM field. Although in the early stages the spatial resolution was more than 1 m and not enough to assess the structural integrity on the basis of the strain distribution, it has been dramatically improved up to several cm by the recent works. The size of defect or damage which can be detected by a distributed sensor is depending on its spatial resolution.

We have developed a distributed strain measurement technique using long gauge fiber Bragg grating (FBG) sensors based on optical frequency domain reflectometry (OFDR) system. FBGs functioning as mirrors with wavelength-selective reflectivities have been used as strain or temperature sensors. OFDR is a technique designed to measure backreflections from optical fiber networks and components. With our system, we use a longer gauge FBG whose length is ordinarily more than 100 mm and we can measure a strain distribution at an arbitrary position along the FBG. Therefore, we can obtain continuous strain data along the optical fiber. Furthermore, since the spatial resolution is less than 1 mm beyond the ability of other distributed sensing systems, it enables us to measure the strain distribution of stress concentrated area such as welded and bonded joints precisely. In this paper, we describe the principle of the distributed sensing technique and show applications of the system to structural health monitoring.

165

Intelligent multi-reactive textiles in integrating nano-filler based CPC-fibres

Hua Deng, Nanocyl S.A., R&D department (Belgium)

This paper covers some of the most important and revolutionary advances being brought to the aerospace industry by adaptive aerostructures. These shape and property changing structures are helping improve the performance of full-scale aircraft, enhance mission performance and even enable new forms of missiles, munitions and uninhabited aerial vehicles (UAVs). The paper begins with the now 20 year-old underpinnings of the industry when the first adaptive aerostructures patent was filed, described shape-changing missile and mortar fins, helicopter blades and airplane wings. A brief historical overview follows the technology through the mid '90's when the first early adaptive hard-launched munitions were developed. The paper tracks these programs to the Steerable Adaptive Bullet (StAB) program of today, the first MAVs and morphing fixed-wing UAVs, ultra-high performance convertible UAVs and the latest classes of advanced hovering

missiles. Developed specifically for adaptive missiles and munitions, Post-Buckled Precompressed (PBP) piezoceramic actuators expand adaptive materials performance by an order of magnitude beyond what conventional techniques and materials can offer for just a few percent in weight and cost growth. PBP actuators have been shown to increase aircraft C_{Lmax} by as much as 28% with weight, drag and cost penalties of fractions of a percent. The paper includes photos and the presentation will integrate videos of several high-performance aircraft which use these PBP techniques to lend astounding performance levels and methodical improvements to aircraft as small as 5mm to widebody transports. Flight videos of the first morphing-wing UAV will be shown along with videos of the world's first post-stall maneuvering, convertible UAV which hovers like a helicopter then dashes like a missile. The presentation concludes with an unclassified, unlimited distribution airing of the fundamentals of airborne visual stealth, adaptive munitions technologies and an assessment of the important intellectual property landscape, patents issued and pending.

166

Adaptive Materials and Aerostructures: Revolutionizing Uninhabited Aerospace Systems

Ron Barrett, The University of Kansas (USA).

This paper covers some of the most important and revolutionary advances being brought to the aerospace industry by adaptive aerostructures. These shape and property changing structures are helping improve the performance of full-scale aircraft, enhance mission performance and even enable new forms of missiles, munitions and uninhabited aerial vehicles (UAVs). The paper begins with the now 20 year-old underpinnings of the industry when the first adaptive aerostructures patent was filed, described shape-changing missile and mortar fins, helicopter blades and airplane wings. A brief historical overview follows the technology through the mid '90's when the first early adaptive hard-launched munitions were developed. The paper tracks these programs to the Steerable Adaptive Bullet (StAB) program of today, the first MAVs and morphing fixed-wing UAVs, ultra-high performance convertible UAVs and the latest classes of advanced hovering missiles. Developed specifically for adaptive missiles and munitions, Post-Buckled Precompressed (PBP) piezoceramic actuators expand adaptive materials performance by an order of magnitude beyond what conventional techniques and materials can offer for just a few percent in weight and cost growth. PBP actuators have been shown to increase aircraft CL_{max} by as much as 28% with weight, drag and cost penalties of fractions of a percent. The paper includes photos and the presentation will integrate videos of several high-performance aircraft which use these PBP techniques to lend astounding performance levels and methodical improvements to aircraft as small as 5mm to widebody transports. Flight videos of the first morphing-wing UAV will be shown along with videos of the world's first post-stall maneuvering, convertible UAV which hovers like a helicopter then dashes like a missile. The presentation concludes with an unclassified, unlimited distribution airing of the fundamentals of airborne visual stealth, adaptive munitions technologies and an assessment of the important intellectual property landscape, patents issued and pending.

167

Evaluation of Vibration Control Performance of Smart Hull Structure Featuring Piezoelectric Composite Actuators

J. W. Sohn, O. C. Kwon, S. B. Choi, Smart Structures and Systems Laboratory, Department of Mechanical Engineering, Inha University (Korea).

Active vibration control of hull structure is very important for structural stability and has a wide range of applications in engineering science and technology. Therefore many research works on active vibration control of hull structure have been conducted by the use of smart materials such as piezoelectric materials. In the present paper, modal characteristics and vibration control performance of smart hull structure are investigated and compared between in the air and under the water conditions. Macro Fiber Composite (MFC), advanced anisotropic piezoelectric composite actuator, is used as actuator and sensor. It is noted that MFC has been recently developed in NASA in order to mitigate disadvantages of traditional piezoceramics and has great flexibility, large induced strain and directional actuating force. In this work, finite element models are constructed and modal analysis is carried out under each environmental condition and natural frequency and mode shapes are investigated. For the verification of the finite element analysis, numerical results of modal analysis are compared with modal test results. Optimal controller is designed and then experimentally implemented for vibration control of hull structure. Vibration control performances are evaluated both in the air and underwater conditions

168

Dynamic Modeling and Vibration Control of Wheeled Military Vehicle Featured by MR Suspension System

S. H. Ha, Q. H. Nguyen, S. B. Choi, E. J. Rhee and P. S. Kang.

This paper proposes a new type of semi-active suspension system and applies it to military vehicle for vibration control. The proposed suspension system consists of gas spring and magnetorheological (MR) damper. After describing the configuration and operating principle of the MR damper, a quasi-static modeling of the damper is conducted on the basis of Bingham model of MR fluid. And then the lumped parameter models of MR fluid flows in the damper are established and the integrated lumped model of the whole damper system is obtained by taking into account for dynamic motions of annular duct and gas chamber. Subsequently, a military vehicle of 6WD is adopted for the integration of the MR suspension system and its nonlinear dynamic model is established by considering vertical, pitch and roll motion. Then, a sky-hook controller associated with semi-active actuating condition is designed to reduce the imposed vibration. In order to demonstrate the effectiveness of the proposed MR suspension system associated with the lumped parameter model, computer simulation is undertaken showing vibration control performances such as roll angle and pitch angle which are evaluated under bump and random road profiles.

169

Design and Vibration Control of Vehicle Engine Mount Activated by MR Fluid and Piezoelectric Actuator

D. Y. Lee, Y. K. Park, S.B. Choi, H. G. Lee.

An engine is one of the most dominant noise and vibration sources in vehicle system. Therefore, in order to resolve noise and vibration problems due to engine, various types of engine mounts have been proposed. This work presents a new type of active engine mount system featuring a magneto-rheological (MR) fluid and a piezostack actuator. As a first step, six degrees-of freedom dynamic

model of an in-line four-cylinder engine which has three points mounting system is derived by considering the dynamic behaviors of MR mount and piezostack mount. In the configuration of engine mount system, two MR mounts are installed for vibration control of roll mode motion whose energy is very high in low frequency range, while one piezostack mount is installed for vibration control of bounce and pitch mode motion whose energy is relatively high in high frequency range. As a second step, linear quadratic regulator (LQR) controller is synthesized to actively control the imposed vibration. In order to demonstrate the effectiveness of the proposed active engine mount, vibration control performances are evaluated under various engine operating speeds (wide frequency range) and presented in time domain.

200

Study on Interface Behavior of 3d Composites Reinforced by Chemically Connected Cnts by Molecular Dynamics

Lin Yang, Liyong Tong, The University of Sydney (Australia); Lin Yang, Xiaodong He, Harbin Institute of Technology (China).

Fiber-reinforced polymeric materials have excellent in-plane properties but poor through-the-thickness properties, such as delamination resistance. Recently, attempts have been made to place the vertically aligned carbon nanotubes (CNTs) between two adjacent fibre-reinforced laminas, namely, to toughen the resin-rich layer and to strengthen the connection between fibres on the two adjacent plies, hence to enhance the out-of-plane mechanical properties. Chemical vapor deposition and chemical decoration have been used successfully to grow and connect CNTs to fiber cloth. Tests have been done to examine the mechanical properties of CNT-connected-fiber reinforced 3D composite materials. These experiments show that the vertically aligned carbon nanotubes can effectively reinforce the interlaminar fracture toughness. However, the mechanism of CNTs' reinforcement to the interface area is still unclear. In this study, we used several molecular dynamic models to simulate the pull-out process of a CNT that has been chemically connected to a fiber, and calculated the CNTs' geometry variation, displacement, energy, and stress change in this process. We also simulated the CNTs' outer layer, inner layer's pull-out, oblique direction pull-out and shear process. In our simulation, the CNTs' elongation and necking phenomena have been noted before the CNT's end inside resin moves. Our simulation yields a CNT's plastic constitutive model in the pull-out process. Chemically connected CNTs' fracture resistance capability is then discussed. In the simulation of shearing, the prediction of the CNTs' capability of shear resistance has been made. Finally, multi-bond connected CNTs' pull-out process has been studied and shows better effectiveness.

201

Study on Preparation of Nanoporous Silica Aerogels Derived from Silica Sol

Pan Liu, Gangqiang Geng, Yangjun Wany, Yanqiang Zhao, Chang'an University (China).

Research on preparation of nanoporous silica aerogels that using cheap silica sol as silica source, undering atmospheric drying. Using orthogonal test method study the different components how to influence the gel time and the aerogel density and obtaining the best ratio. Also study the different PH value how to influence the gel time, aerogel density and the micro-structure. The results showed that: in Silica Sol, ethanol and water system, the ratio of silica sol and alcohol has significantly affected on gel time and aerogel density, the best

volume ratio is 1:3, PH from 2 to 5 aerogel density is about 0.32g/cm³ but the gel time decreases rapidly, PH from 5 to 7 aerogel density increases to 0.4g/cm³ quickly, and gel time changes a little, SEM

showed that the micro-structure of aerogel is the best when the PH is 5. The non-critical drying method of cheap preparation comes true.

202

Effects of Nanoparticles on Hygrothermal Property of Epoxy Resin Composites

Xinying Lv, Rongguo Wang, Wenbo Liu, Harbin Institute of Technology (China).

Polymer composites are widely used in aerospace field, especially carbon fiber reinforced epoxy resin composites, because of the outstanding performance, became the most popular polymer matrix composites. However, the hygrothermal property of epoxy resin, as the matrix of the structure composite, is crucial to the whole composites. In this paper, the main focus is to modify the epoxy resin with nano-SiO₂, nano-TiO₂ and nano-CaCO₃ to enhance the hygrothermal property. Ultrasonic dispersion technology was used to prepare the nano-TiO₂, nano-SiO₂ and nano-CaCO₃ epoxy resin composites. The three kinds of composites were disposed in the climatic chamber for constant conditions. The effect of nano-particles on the hygrothermal property of epoxy resin composites were investigated by dynamic mechanics analysis (DMA), thermo-analysis and mechanical properties testing. TEM images were taken to characterize the decentralization of the nano-particles in the composites. It is shown that nano-particles can be dispersed in the epoxy resin by ultrasonic dispersion. Thermo-analysis and mechanical testing results were presented that the epoxy nanocomposites has the excellent hygrothermal property under the same aging condition. Accordingly, the modified epoxy resin matrix can be used to prepare carbon fiber reinforced composites with remarkable hygrothermal property.

203

A Comparative Study on Vibration Analysis of Beams Treated with Active Constrained Layer Damping Using Different Assumed Modes Methods

Miao Wang, Guang Meng, Shanghai JiaoTong University (China).

In present study, two different assumed modes methods are used for vibration analysis of beams treated with active constrained layer damping based on the traditional Mead-Markus model. In the first case, the assumed modes are chosen for the axial displacement of the active constraining layer, the axial displacement of the host beam, and the flexural displacement of the whole structure. However, the assumed modes are selected for the axial displacement of the host beam and the flexural displacement in the second case. And detailed comparisons are made on the predictions of natural frequencies, modal loss factors, mode shapes and so on, in which the results from the references are used as a benchmark. It seems that the two different assumed modes methods have their own aspects on the analysis of ACLD/beam structures.

204

Active Structural Acoustic Control Based on Distributed Structural Volume Velocity Sensor

Guoyong Jin, Zhigang Liu, Harbin Engineering University(China).

Using a simply supported rectangular plate as analytical model, firstly the relationship between structural surface volume velocity and sound power radiated by the plate is analyzed in the wave-number domain; the mathematical formula which indicates the contributions of structural modes to the volume velocity is derived. Based on this expression, combined with charge output equation of the PVDF piezoelectric film and orthogonal property of trigonometric function, a new design approach for volume velocity sensor is presented. An experiment for measuring structural volume

velocity is conducted, and good accuracy is obtained. On the basis, experiments for active structural acoustic radiation control are carried on for single frequency and band-limited excitations. Excellent control effects are obtained, and so the validity of this design approach of the distributed volume velocity sensor and the effectiveness of active structural acoustic control using the designed sensor are further verified.

205

An Ionic Polymer-Metal Composite Actuator Based on PSMI-Incorporated PVDF with Chemical Stability and Performance Durability

Il-Kwon Oh, Chonnam National University (Korea);Sang-Gyun Kim, Korea Research Institute of Chemical Technology (Korea);Sunwoo Lee, Chonnam National University (Korea); Jun Lu, Southwest Jiaotong University (China).

To develop artificial muscles with improved performance, a novel ionic polymer-metal composite (IPMC) actuator was developed by employing the newly-synthesized ionic networking film of poly (styrene-alt-maleimide) (PSMI)-incorporated poly (vinylidene fluoride) (PVDF). Scanning electron microscope and transmission electron microscopy revealed that much smaller and more uniform nano-sized platinum particles were formed on the surfaces of the film as well as within its polymer matrix after the electroless-plating process. Fourier transform infrared results suggested that no hydrolysis occurred for the as-prepared film actuator before and after the exposure to the elevated PH solutions at 25°C for 48h. The new actuator showed much larger tip displacement than that of a Nafion-based counterpart under the applied electrical stimulus, and overcame the back relaxation of the traditional IPMC actuator under the constant voltage. The current actuator was operated over 6.5h at high-frequency sinusoidal excitation, and its tip displacement was still comparable to that of the referenced Nafion actuator when the test was terminated. The excellent electromechanical performance is due to the inherent large ionic-exchange capacity and the unique hydrophilic nano-channels of the ionic networking film. Furthermore, the working principle of the developed IPMC actuator is thought to be based on a combination of piezoelectricity and ionic transport. The film of PSMI-incorporated PVDF has some advantages over the most widely-used Nafion-based one by diversifying niche applications in biomimetic motion, and the present study is believed to open a new avenue for the design and fabrication of the electro-active polymer film with unique functional properties.

206

Color-Forming Property of Optical Sensitive Polyurea Microcapsule Synthesized with Interfacial Polycondensation Method

Weidong Lai, Xiaowei Li, Shuangshuang Meng, Guangsheng Fu, Hebei University (China).

The nano- or sub-micrometre core-shell structured microspheres arising from microencapsulation technique have made strong progress during the last decades. The microcapsules usually act as smart polymer composites to achieve various functions such as slow-release of core ingredients, energy-storage by core phase-change material, structure crack self-healing based on microcapsule shell rupture, artificial organ to encapsulate insulin etc. The driving-forces for microcapsule applied so far are mostly ascribed to the similitude between natural macromolecule and such artificial core-shell structured microsphere. Both of them have continuous and semipermeable films or coatings, and applied as micro-carriers or micro-reactors to manipulate physical, chemical or biological response in confined space, based on external stimuli of PH, temperature, or pressure etc. Function control of these

microcapsules lays either in variation of shell chemical structures, or in modification of surface properties. With latter method, the distinctive negative temperature-sensitive release function have been realized by grafted poly N-isopropylacrylamide(PNIPAM) chains into microcapsule surface pores. Recently, microcapsules acted as micro-reactors have been extended such as electric ink (E-ink) technique, which is based on electrophoresis of electrically charged granules to transform reflected color of microcapsules controlled by the external electric field, or photo-sensitive microcapsules, which have been reported by Lu et. al. that the acrylamide derivatives in layer-by-layer(LBL) assembled microcapsules are UV-exposed to form medical slow-release composites.

Since highly selective regulation can be conveniently achieved by selecting the exposure wavelength and photo-reactive core compounds, the optical functional microcapsules have potential application in pharmacy, cosmetic, or in environment protection. But compared with the fast development of temperature-sensitive microcapsules, the optical-sensitive microcapsules have drawn few attentions which are restrained by lack of information about synthesis technique and optical responding behavior of such materials when irradiation exposure is applied.

In this paper, interfacial polycondensation method combined with O/W (oil/water phase) emulsification is applied to encapsulate the optical sensitive compounds. The diameter distribution of the microcapsules in O/W emulsion after TEPA added is shown in Fig. 1. With dispersion time increase from 1min to 90min, the distribution width is narrowed slightly, though a shoulder form distribution around 3 μ m appears after 10min, which may be due to the microcapsule agglomeration during shell formation process.

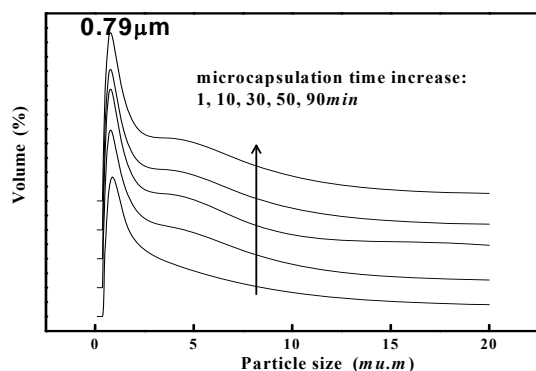


Fig. 1. Diameter distribution of microcapsules during interfacial polycondensation reaction.

The morphology of the functional microcapsules is shown in Fig. 2. Most of the microcapsules are regular core-shell structured microsphere. The shell thickness is approximately 60nm. Part of the microcapsules are agglomerated together with the shell adhered with each other to form interconnecting structure, which is accorded with the microcapsule size distribution variance in Fig. 1 presented as the shoulder form distribution. It implies that the microcapsule shell has been formed in interfacial polycondensation reaction after TEPA is added, and the microcapsules can act as basic functional cell to respond the outside stimuli at sub-micrometre space. The obtained microcapsules are mixed thoroughly with D-8 (4-Hydroxy-4'- Isopropoxydiphenylsulfone, C₁₅H₁₆O₄S, melting point at 130°C) dispersion, which can react with the ODB-2 ((C₃H₃N₂O₃, melting point at 182°C) molecules encapsulated in microcapsules to perform color-forming reaction.

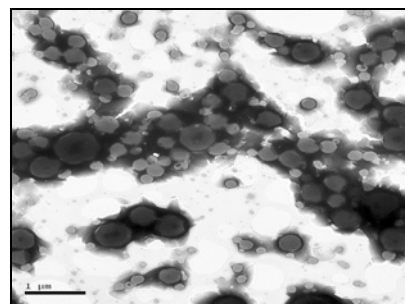


Fig. 2. TEM micrograph of the microcapsules.

To apply as micro-reactors, the microcapsule thermal property is important. In Fig. 3a, the thermal decomposability (TG) of microcapsules is analyzed as a function of temperature.

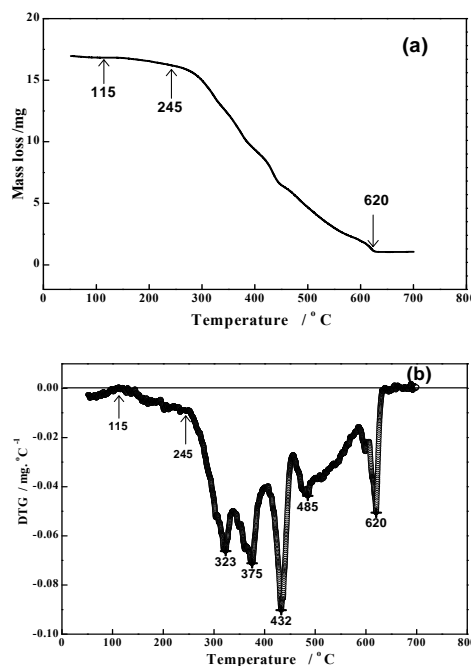


Fig. 3. (a)TG, (b) DTG analysis of the microcapsules at heating rate of 10°C/min.

The microcapsule presents decomposing trend after 115°C, and a sudden increase after 245°C. Before complete decomposition, there also have remarkable mass loss variance at 323, 375, 432, 485°C as presented in DTG curve in Fig. 3b. These may be ascribed to the diffusion of core reagents and weight loss of wall material. Above 620°C, the residual materials are decomposed completely. From the TG and DTG result, it can be concluded that the microcapsule shell membrane are thermal stable in room temperature, and the phase change point of the microcapsule shell is started from 115°C. Thermal analysis result shows that the microcapsule can be controlled by thermal technique, which is the basis for practical usage of the temperature-sensitive microcapsules.

On the basis of high thermal stability at room temperature, the microcapsules are exposed with UV irradiation at different time. To detect optical reaction in the microcapsules, the color-forming image density variance when heating developed at 135°C for 10s is obtained as shown in Fig. 4. With exposure time increase, image density has a fast decrease trend before 30s; after 30s, the image density is almost unchanged with further exposure. The maximum decrease variance of image density is 0.22, compared between 0.62 at 0s and 0.4 after exposed for 30s. UV irradiation has changed the microcapsule core state and affects the image-forming reaction between the D-8 and ODB-2 molecules.

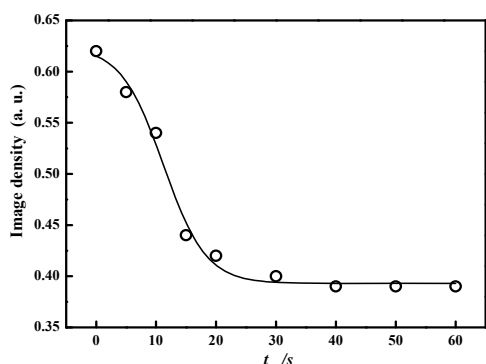


Fig. 4. Relationship between color-forming image density and exposure time with heating developed at 135°C for 10s.

To illustrate the optical-response generated in microcapsules, FT-IR spectra of the ingredient monomers acted as microcapsule core material are detected as shown in Fig.5.

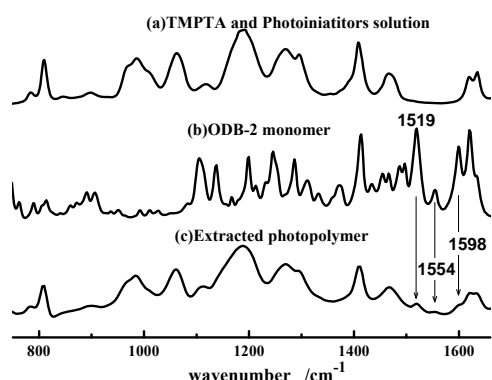


Fig. 5. FT-IR spectra of (a) the photosensitive solution of TMPTA and photoinitiator TPO, ITX; (b) the colorless dye-precursor ODB-2; (c) the extracted solid composites from the mixture of ODB-2 and photosensitive solution after UV exposure.

With UV exposed, the photosensitive solution comprised with TMPTA, photoinitiator TPO and ITX as well as the colorless dye-precursor ODB-2, which is acted as microcapsule core material, are photo-solidified. The solid composites is extracted by acetone from the remnant solution and detected with FT-IR technique. The characteristic absorption at 1519, 1554, 1598 cm^{-1} of ODB-2 monomer has appeared in the IR spectra of the extracted photo-solidified composites as shown in Fig. 5c. It implies the TMPTA monomers have performed C=C bond cleavage reaction initiated by the ITX and TPO free-radicals, and cross-linking polymer network are formed when exposed by UV irradiation. Since the optical sensitive reagents have been mixed with ODB-2 molecules as blending solution, ODB-2 molecules are confined in the polymer networks. As a result, the color-forming image density degree of microcapsules is decreased by reducing ODB-2 concentration in the reaction, which is confined in the cross-linking C=C polymer networks in microcapsule core. The color-forming functions of the core ingredients have directly manipulated by UV response function of the microcapsules.

In this article, the core-shell structured microcapsules with micrometre size are synthesized by interfacial polycondensation method. The interfacial polycondensation reaction takes completion after TEPA added, and the microcapsule shell membranes are with thickness of about 60nm. With high thermal stability at room temperature, the microcapsules are optically sensitive due to C=C bonds cleavage of TMPTA monomers to form network polymers in microcapsule core. In microcapsules, the C=C cross-linked polymer network have encapsulated ODB-2 blending

solution to decrease reaction concentration of ODB-2 in color-forming process. As a result, the optical function of the microcapsules is presented as the decreasing variance of color-forming image density after UV irradiation.

207

Effects of Self-healing Microcapsules on Bending Performance in Composite Brake Pads

Li Zhang, Hui Wang, Xiuping Dong, Beijing Technology and Business University (China).

For the purpose of reducing self-weight, friction noise and cost, improving shock absorption, enhancing corrosion and wear resistance, brake pads made of composite materials with self-healing function are prepared to substitute metal ones by designing ingredients and applying optimized production technology. As self-healing capsules are chosen, new method with technology of self-healing microcapsules, dicyclopentadiene (DCPD) microcapsules coated with poly (urea-formaldehyde), is put forward in this paper. In the crack's extending process, the stress is concentrated at the crack end, where the microcapsule is designed to be located. When the stress goes through the microcapsules and causes them to break, the self-healing liquid runs out to fill the crack by the capillary and it will poly-react with catalyst in the composite. As a result, the crack is healed.

In this paper, polymer matrix composite brake pads with 6 prescriptions are prepared and studied. Three-spot bending tests are carried out according to standards in GB/T 3356—1999 and the elastic constants of these polymer matrix composites are obtained by experiments. In accordance with the law of the continuous fiber composite, elastic constants of the short-fiber composite can be calculated by proportions of each ingredient. Results show that the theoretical expected results and the experimental values are consistent. 0.3-1.2 % mass proportion of microcapsules has little effects on the composite's bending intensity and modulus of elasticity. These studies also show that self-healing microcapsules used in composite brake pads is feasible.

208

DNA Biosensors Based on Layer-by-Layer Self-Assembled Multilayer Films of Carbon Nanotubes and Goldnanoparticles

Yiyun Xiao, Zhao Dai, Jiechun Pang, Jimei Zhang, Shichao Xu, Guo Zheng, Tianjin Polytechnic University(China).

A novel DNA biosensor based on layer-by-layer self-assembled multi-walled carbon nanotubes (MWNTs) and nanogold particles(GNPs) was presented in this paper, in which the probe HS-ssDNA oligonucleotides, MWNTs and GNPs were all covalently immobilized through chemical Au-Sulphide bonding. Firstly, the super short MWNTs were prepared and modified with thio groups which could be self-assembled onto the surface of Au electrode by Au-sulphide bonding, then the GNPs were chemically adhered to the surfaces of MWNTs by forming Au-sulphide bonding again, at last the self-assamble of probe DNA oligonucleotides were also covalently immobilized via Au-sulphide bonding between thio groups at the ends of the DNA oligonucleotides and GNPs. Hybridization between the probe HS-ssDNA oligonucleotides and target DNA oligonucleotides was confirmed by the changes in the voltammetric peak of an anionic intercalator, anthraquinone-2,6-disulfonic acid (AQDS).The cyclic voltammetric (CV) response demonstrate that the DNA biosensors based on Layer-by-layer self-assembled multilayer films of MWNTs and GNPs offer an much higher hybridization efficiency and selectivity compared to those based on only random MWNTs or GNPs. The cathodic peak current of Layer-by-layer self-assembled Au electrode system with the AQDS as indicator

increased significantly after the hybridization program even the target was a single base-pair mismatch DNA sequence. There was an excellent linearity of 0.01~10 nmol/L for the concentration of complementary DNA with the cathodic peak current of the layer-by-layer self-assembled modified electrode. The limit of detection of 7.5×10^{-11} mol/L was also achieved.

209

In-Situ Formation of Gold Nanoparticles on Self-Assembly Monolayer Modified Silicon Substrate

Lei Qi, Shantang Liu, Wuhan Institute of Technology (China).

Gold Nanoparticles have been the subject of high interest in the past decade due to their unique optical, electronic and catalytic properties. Here we demonstrate an effective route for the in-situ chemical synthesis of gold nanoparticles on monolayer modified silicon substrate. The formation of gold nanoparticles is based on the ability of the amino groups of the monolayer to bind AuCl_4^- ions, followed by the reduction of AuCl_4^- to Au^0 with NaBH_4 . Thus, by repeating the ion binding and reducing cycle, densely packed arrays of gold nanoparticles can be generated on the monolayer. The particles size can be controlled by the cycles of the deposition-reduction process. UV visible spectroscopy and scanning electron microscope (SEM) confirm that the well-dispersed gold nanoparticles are formed on the substrate. From AFM images, we find the particles with characteristic size of 2-10nm are generated on the monolayer in one cycle deposition-reduction process. Therefore, this facile procedure can give a new approach to the formation of gold nanoparticles on the self-assembly monolayer modified silicon substrate.

210

Experimental Study of Gas Discharge Using Aligned Multi-Walled Carbon Nanotube Electrode

Guohua Hui, Xiaoling Wu, Nanjing Medical University; Lili Wu, Henan Agricultural University (China); Min Pan, Yuquan Chen, Zhejiang University (China).

The results of an experimental study of corona discharge on aligned multi-walled carbon nanotubes electrode in air at atmospheric pressure are presented in this paper. The breakdown voltage and corona pulses on nanotubes electrode are discussed compared with aluminum electrodes. It is found that the breakdown voltage reduced largely by using nanotubes electrode, and the repetition rate of nanotube pulses is much higher than that of metal pulses. The mechanisms of positive and negative corona pulse and the field emission of CNTs are all also discussed in detail. The results of our experimental study provide a basic preparation for the next research on CNTs gas sensor by dc corona with multi-walled carbon nanotubes electrode.

211

Multi-Walled Carbon Nanotubes under Protons Beam Irradiation

Ahmad Ishaq, A. R. Sobia, Long Yan, Xingtai Zhou, Dezhong Zhu Chinese Academy of Sciences (China).

Since the protons are the most abundant type of particle in deep space and have large flux with energy less than 200 keV. Therefore it becomes important to understand the effects of low energy proton irradiation on carbon nanotubes (CNTs) for future application of CNTs as some components of various space applications, such as coating layers, radiation shields, and electronic devices in space shuttles and space stations. In this letter we report effects of proton irradiation on structure of multi-walled carbon nanotubes (MWCNTs) at different temperatures. Protons 70-keV was used to

irradiate samples at temperatures ranging from 600 to 1000 K at various irradiation doses. It was found that at the temperature of 600K, graphite phase of MWCNTs structure could be transformed to amorphous phase in a highly controlled fashion under proton irradiation. In addition to future high technology application, graphite phase encapsulated amorphous phase at nanoscale regime may open new application of CNTs. Nevertheless, with increasing the temperature, the radiation damage in MWCNTs that could destroy the structure could be minimized. Moreover, at the temperature of 800K, the interconnection of adjacent parallel could be realized at an irradiation dose of 5×10^{17} ions/cm². This interconnection is ascribed to the fact that two adjacent MWCNTs share a common graphene.

With a further increase of the temperature of specimen from 800K to upward during proton irradiation, the MWCNTs structure remained stable even at higher doses. At critical temperature of 950K for proton irradiation on MWCNTs, the mobility of carbon interstitials is high enough to promote annealing with vacancies. No more clustering of interstitials can take place, and the graphite lattice remains free of extended defects. Structural changes in MWCNTs upon bombardment with 70-keV protons were monitored by transmission electron microscopy in a wide range of irradiation doses and temperatures.

213

Fabrication, Structures and Properties of Functionalized Fiber-Reinforced Composites

Ronghui Liu, Zhongfu Zhao, Dalian University of Technology (China).

Thermoset composites, especially fiber-reinforced composites, have become attractive engineering materials to replace conventional metallic materials in many important sectors of industry such as aircraft, naval constructions, ships, building and offshore structures. But, their non-conductive property greatly limits their application in industries. In order to increase their market penetration, their functionalization becomes one hot research subject in both industry and academy society. In this work, a high-pressure filtering system and vacuum-assisted resin transfer molding can be utilized to concentrate some expanded graphite, carbon nanotube and other nanoparticles onto the skin surfaces of fiber-reinforced polyester/epoxy composites. Thus, these nanoparticles can functionalize the skin surfaces of composites with excellent electric conductivity, which imparts good anti-lightning strike properties and shielding effect of electromagnetic interference to the composites. The emphases of this study are to optimize the fabrication, structures and properties of functionalized composites and to build their relationship with electric conductivity of composites. This method can avoid the big issues arising in the directly-dispersing nanoparticles in polyester/epoxy resin, greatly reduce the fabrication cost of functionalized composites through decreasing the loading level of nanoparticles and displacing carbon nanotubes with expanded graphites.

214

Synthesis of Iron-Filled Carbon Nanotube Arrays by Floating Catalytic Chemical Vapor Deposition

Jin Cheng, Xiaoping Zou, Guang Zhu, Maofa Wang, Yi Su, Gangqiang Yang, XueMing Lü, Beijing Information Science and Technology University, Education Ministry Key Laboratory for Modern Measurement and Control (China).

Iron-filled carbon nanotubes have been attracted many attentions for their potential applications in magnetic force microscopy,

biochemical nano-sensors, nanocomposites and electromagnetic wave-absorbing materials.

Ethanol as carbon source not only possesses low toxicity, easier storage and transportation, but also does not tend to form amorphous carbon on dissociation. So in our experiments, we use ethanol as carbon source to synthesize carbon nanotubes.

In this paper, we report floating catalyst chemical vapor deposition (FCCVD) for synthesizing iron-filled carbon nanotubes arrays. We utilized ferrocene as catalyst precursor to synthesize carbon nanotubes by FCCVD. The FCCVD setup consists of two-stage furnace fitted with independent temperature controllers, carbon source supply system, carrier gas supply system and pump system. The ethanol was introduced into furnace tube by bubbling liquid ethanol under carrier gas flow of 100sccm 3% H_2 /Ar and 100sccm N_2 . Catalyst precursor ferrocene was placed at low temperature (300°C) region. Then ferrocene gas was introduced into high temperature (higher than 850°C) region by carrier gas. Ferrocene was decomposed to form iron nano-particles as catalysts. These catalysts catalyzed the growth of carbon nanotubes which were deposited on substrates and the wall of furnace tube. After about 3h synthesis time, we obtained mass production of carbon nanotubes.

The deposits were characterized by employed scanning electron microscopy, transmission electron microscopy, and Raman spectroscopy.

The iron-filled CNTs have a relatively good graphitization and the filled iron has no significant effects on the graphitization of the CNTs. The key factors for growing iron-filled CNTs are excessive ferrocene and synthesis temperature. For synthesizing iron-filled CNT arrays, excessive ferrocene and relatively higher synthesis temperature (about more than 850 °C) are needed.

215

Effects of Synthesis Parameters on the Preparation of Carbon Nanofibers by Ethanol Catalytic Combustion

Jin Cheng, Xiaoping Zou, Guang Zhu, Maofa Wang, Yi Su, Gangqiang Yang, XueMing Lü, Beijing Information Science and Technology University, Education Ministry Key Laboratory for Modern Measurement and Control (China).

Combustion method is a simple method for synthesizing carbon nanotubes (CNTs) and carbon nanofibers (CNFs), which employs flames of carbon-contained reactant to synthesize CNTs and CNFs. It has been proved that combustion method is an effective method for synthesizing CNTs and CNFs. Up to now, various nanostructures have been produced by combustion method, such as single-walled CNTs, multi-walled CNTs, bamboo-like CNTs, Y-junction CNFs, etc. However, different carbon products, such as CNs, nanocoils, non-coiled CNFs, Y-shaped CNFs, etc., are symbiotic in deposits synthesized by flames. It is difficult to obtain single-type products, such as non-coiled CNFs, or nanocoils, because there are many factors that could influence on carbon products prepared by combustion method. It has been reported that flame temperature, catalyst, carbon source and additive have some influence on carbon products prepared by flames.

In this paper, The effects of position of substrates in flames, preparation time and stability of flames on carbon nanofibers are investigated in ethanol catalytic combustion. For investigating the effects of these influence factors on carbon nanofibers, several sets of controlled experiments are performed, such as different position of substrates and different preparation time. The as-synthesized products are characterized by scanning electron microscopy. Our results show that the optimal position of substrates in flames is more than 1cm and less than 2.5cm for massive yield, the optimal preparation time is more than 5min and less than 30min for massive yield.

216

Study on a New Semi-active Vibration Isolation System

Kexiang Wei, Yingchun Liu, Liwei Ning, Hunan Institute of Engineering (China); Kexiang Wei, Guang Meng, Shanghai Jiao Tong University (China).

Magnetorheological (MR) elastomers are a new class of magnetorheological materials. They are interesting candidates for active-passive hybrid vibration control of structural systems because they have both advantages of magnetorheological materials and elastomer materials. In this paper, a squeeze mode MR elastomers isolator is designed. A new active-passive hybrid vibration isolation system using the designed MR elastomers isolator is developed. The performance of the system is experimentally evaluated. Results demonstrate that the MR elastomers isolator has good vibration isolation effect and controllable property.

217

The Active Damping and Vibration Control in Engineering Structures

FengMing Li, Harbin Institute of Technology (China); Feng-Ming Li, Kikuo Kishimoto, Tokyo Institute of Technology (Japan); Yue-Sheng Wang, Beijing Jiaotong University (China); Zhao-Bo Chen, Harbin Institute of Technology (China).

The active damping and vibration control of beams, plates and shells have been studied using a velocity feedback method and reviewed in this paper. Based on the traditional theory of structural dynamics, a theoretical method is employed. This method is easy to understand and verified by numerical simulations. Hamilton's principle with the Rayleigh-Ritz method has been used to derive the equations of motion of the complex electromechanical coupling system. The equations of motion for these kinds of structures can be easily solved and effectively used for the structural active vibration control. The forced vibration responses of the electromechanical coupling systems are computed to study the active vibration control. From the numerical results it can be seen that the control gain and the size of the piezoelectric patches have significant effects on the vibration control of the base structures. The larger the control gain is, the better the active damping characteristic is. With the increase of the size of the piezoelectric patches, the active damping properties of the base structures are improved and lower control voltages are needed to control the structural resonant responses.

218

Study on Damping Property of Epoxy Resin with PZT Piezoelectric Film Improvement

Yan Qin, Wei Mao, Zhixiong Huang, Dongyun Guo, Wuhan University of Technology (China).

Damping property of epoxy resin is improved by adopting lead zirconate titanate (PZT) piezoelectric film. The PZT piezoelectric film has been prepared by sol-gel method on Pt/Ti/SiO₂/Si substrates. The XRD results show that the PZT film which mainly with the orientation of (1 0 0) has been prepared on Pt/Ti/SiO₂/Si substrates. The produced film and the substrates have been joined into epoxy resin as constrained layer, and then the damping property of composites has been studied. Through improving the annealing process when preparing film, the optimum filming technology which can improve the damping property of composites has been obtained. The film was heated up to 650°C with 10°C/min and holding time for 30min, then cooling with furnace. By this way, the piezoelectric strain constant (d_{33}) of piezoelectric film has reached maximum, and the damping property of composites achieves best. The peak of the damping $\tan\delta$ has reached 1.075, the

temperature range of the damping ΔT has reached 45.2°C ($\tan\delta > 0.3$). The results show that the damping property of epoxy resin has been improved with the addition of PZT piezoelectric film.

219

Nonlinear Parameter Estimations for Hysteretic Dynamics of Smart Materials and Structures Using Hybrid Optimization Methods

Linxiang Wang, Benny Lassen.

Benny Lassen, Smart materials, structures, and devices have been extensively employed in many engineering applications, due to their unique properties of converting energy between different physical fields. Among various related researches and application deployments, it is the dynamical modelling and control of the smart structures and devices in some systematic manner that is really the focus of much attention of the “smart structure” community. For the purpose, an essential element is the modelling and parameter estimation for the hysteretic dynamics of smart structures and devices.

In the current presentation, the hysteretic dynamics of smart materials and structures are modelled by a bifurcate dynamic system based on the Landau theory for phase transitions. Due to the bifurcation nature of the dynamical system, the system states will switching among different stable equilibrium branches. This fact make the parameter estimation a very challenging task, because it is always problematic to deal with the un-stability of the system in the numerical simulations, particularly at the beginning of the estimation procedure when the initial parameters are not very close to the its final values. To cope with the difficulty, a hybrid optimization method is employed together with a least-square approximation strategy. With given experimental data, the initial values of the parameters are first estimated by using very few measurements. The genetic algorithm is applied to roughly estimate the parameter values, the estimated values are then refined by using a direct search strategy with all the measurements.

In order to validate the current parameter estimated methods, the numerical results with the estimated parameter values are compared with experimental counterparts. It is shown that accurate fitting is achieved. Both the hysteresis loops and the nonlinear coupling between different physical fields are successfully modelled.

220

Hierarchical Fuzzy Identification of MR Damper

Hao Wang; Haiyan Hu.

MR dampers, recently, have found many successful applications to civil engineering and numerous developments for mechanical engineering. When an MR damper is to be used for vibration suppression, an inevitable problem is to determine the input voltage so as to gain the desired restoring force determined from the control law. This is the so-called inverse problem of MR dampers and is always an obstacle in the application of MR dampers to vibration control. A rough, but reasonable, solution of this problem is to adjust the input voltage according to the on-off control law.

The neural network can be used to establish the inverse model of an MR damper in principle. However, the neural network is extremely complicated and not easy to be realized on line. As some fuzzy system has the universal ability of approximation, it can be implemented to adjust the input voltage of an MR damper according to the desired restoring force, that is to say, to identify the inverse model of MR damper.

Considering a MR damper with three inputs, if a single fuzzy system consisting of three inputs is used to model the inverse dynamics of MR damper, ‘Curse of dimension’, which will be

time-consuming, will occur when a much higher accuracy is demanded. As a comparison, this work presents, firstly, a new way of system identification, that is, a two-layer hierarchical fuzzy system to approximate the inverse model of MR damper. It will simply consider less parameters than those of a single fuzzy system. The numerical simulation demonstrates that the hierarchical fuzzy system using to give the inverse model of MR damper can acquire a faster approximation than a single fuzzy system under the same conditions for the accuracy of modeling. Such hierarchical fuzzy identification can also be applied in system identification and system control for the complicated system.

221

No Direction High-frequency Underwater Transducer

G.Wang, L.K.Wang, L.Qin, Beijing Information Science & Technology University (China).

A no direction high-frequency acoustic transducer has been designed and prepared with PZT-5 type piezoelectric ceramic cylinder. When the piezoelectric ceramic cylinder vibrates on its thickness mode, the resonant frequency is higher than that of other modes. The affiliation of the resonant frequency and the size of piezoelectric ceramic cylinder transducer is obtained by finite element analysis. The resonant frequency of transducer increase when its thickness decreases. The resonant frequency of transducer is liner with its thickness. The resonant frequency of piezoelectric ceramic cylinder transducer increases lightly when its height decreases. The diameter of piezoelectric ceramic cylinder has nothing to do with its resonant frequency. The actual samples are produced for verifying the accuracy of the simulation results. The affiliation of the resonant frequency and the size of actual transducer is the same as the simulation results. So we have produced high-frequency acoustic transducers whose resonant frequency is 290 kHz by the simulation results. Transmit voltage response for the product is 143dB. Compare the products and the traditional cylindrical transducers, the products haven’t only a good no direction circle directional, but it also has a high resonant frequency (290 kHz).

222

Investigation on Modeling and Controllability of a Magnetorheological Gun Recoil Damper

Hongsheng Hu, Jiaying University (China); Hongsheng Hu, Jiong Wang, Yancheng Li, Xuezheng Jiang, Nanjing University of Science & Technology (China).

Its primary purpose of this study is to provide a comprehensive investigation on modeling and controllability of a Magnetorheological (MR) gun recoil damper. Performances of MR damper under random load, mainly in the transportation applications, seismic protection in civil engineering and wind-rain-induced load in Cable Bridge, have been well investigated by many researchers. The application of MR damper under impact and impulsive load is of great value for shock vibration reduction. For example, MR dampers can be desired to provide optimal damping force to control the recoil mechanisms dynamics for gun or other weapon systems, so that large peak of recoil forces can be avoided with a certain limited stroke, and the firing stillness and stability are ensured. However, little research has been focused on its dynamic modeling and its controllability of MR damper under high impact load. At present, a systematic architecture has still not been formed, including its structure design, dynamic-modeling and controlling method of a MR damper subjected to high impact load.

In this paper, the research is developed and aims at the MR gun recoil damper. To evaluate its controllability of a MR gun recoil

damper, a test rig which uses a closed bump to produce an impact load is developed. A novel large-scale single-ended MR damper without the accumulator is used as the specimen. To provide the optimal damping force, fast response time is required so that good force tracking can be obtained. First, impact tests were done to evaluate the response time of the special designed long-stroke MR gun recoil damper, corresponding to the step signal of the operating current. It's followed that, modeling of the damping force control system of the MR damper was presented, and three revised control strategies, including on-off control, PID control, adaptive fuzzy control method, was investigated to improve the performance of the MR damper under high impact load. Finally numerical simulation and experimental verifications were provided. It is indicated that this developed MR gun damper has a good controllability compared with small double-ended MR damper under impact load. Some detailed investigations have also been done on the difference of time duration and control principle.

223

Design Method of Spring Accumulator of Single-Ended Mr Damper

Xinchun Guan, Harbin Institute of Technology (China), Yonghu Huang, Shaohua Hu, Jinping Ou, Dalian University of Technology (China).

Compared with double-ended MR damper, single-ended MR damper possesses larger stroke, and is more suitable to be used in the mechanical fields which only have limited installation space. For the single-ended MR damper one accumulator is needed to compensate the volume change of fluid caused by the moving in and out of rod from the cylinder. In this paper, according to the structure of single-ended MR damper, the formulas that used to calculate the damping force of MR damper were built. Based on those formulas, the influence of the stiffness of spring on the characteristics of single-ended MR dampers was studied. And the results show that, if the stiffness of spring is too small, the effect of compensation would lose; if the stiffness of spring is too big, huge pressure would create in cylinder which would damage seal ring. Consequently, for traditional spring, it is difficult to satisfy the requirement of spring accumulator. Based on above analysis, a new spring accumulator which is manufactured by shape memory alloy was put forward, and the design method of this new spring accumulator was also built.

224

Study of the Response Time of Mr Damper

Xinchun Guan, Pengfei Guo, Jinping Ou, Harbin Institute of Technology (China).

Response time is an important parameter which determines the applied field and effect of the damper. However, up to now, only a few papers discuss the test and analysis of response times. In this paper, the response time of a large-scale magnetorheological fluid (MRF) damper at different velocities and currents was firstly tested. Then, the variation of the magnetic field inducted by changed electric current was simulated by finite element analysis (FEA). Based on the variation of the shear yield stress of the MRF at the gap between the cylinder and piston, the response time of MRF damper was calculated. Finally, the tested and calculated response time was compared, and the influence of an eddy current and electric current response time on the damper's response were also investigated. The research shows that using history-curve of average effective shear stress of MRF at gap which calculated by FEA to study response time of MRF damper is valid. The results also show that electromagnetic response time is the most important factor to influence the response time of MRF dampers, and

reducing eddy current is the key method to reduce the response time of an MRF damper. Moreover, the influence degree of an eddy current is much higher at a condition of current decrease than at a condition of increase, and with the same skipping current, whether the current increases or decreases, the smaller the initial current is, the greater the eddy current affects the damper's magnetic circuit and the longer response time of damping force. A shortened response of the electric current may induce a higher eddy current, and not reduce response time of damping force.

225

Multi-Modal Vibration Control Using a Synchronized Switch Based on a Displacement Switching Threshold

Hongli Ji, Jinhao Qiu, Kongjun Zhu, Yuansheng Chen, Nanjing University of Aeronautics and Astronautics (China).

A new semi-active method using the nonlinear synchronized switch damping (SSD) approach based on a displacement switching threshold was proposed in this paper for multi-mode vibration control. Several extensions of the SSD approach including the SSDI (SSD on inductance), SSDV (SSD on a voltage source), enhanced SSDV, and adaptive SSDV have been developed to improve the control of the single-mode vibration, but the weakness of the SSD approach for the multi-modal vibration control has not been solved. In all these extensions of the SSD approach, the switch is controlled by the same algorithm, that is, it reverses the voltage of the piezoelectric element at all extrema of displacement. This switching algorithm is effective in single-mode control, but it leads to over-frequent switching in multi-mode control. In the method proposed in this study, an improved switching algorithm based on a displacement threshold, which prevents the switch in the shunt circuit from over-frequent on-and-off and accordingly increase the converted energy to improve the control performance, is proposed. The switching algorithm is applied to a SSDI system and used in the vibration damping of a beam with two excited modes. Compared to the classical SSDI, the control performance of the first mode is improved from 3.7 dB to 18.2 dB, but that of the second mode is slightly worse from 3.46 to 2.6.

226

Aspect Ratio Dependence of 1-3 Polymer/Cement Based Piezoelectric Composite Properties

Lili Guo, Shifeng Huang, Dongyu Xu.

Piezoelectric ceramic (lead niobium lithium zirconate titanate, P(LN)ZT), sulphoaluminate cement and polymer were used to fabricate 1-3 polymer/cement based piezoelectric composites by cut-filling technique. The influence of P(LN)ZT aspect ratio on the piezoelectric and dielectric properties of composites was investigated. The results show that as the P(LN)ZT aspect ratio increases, the piezoelectric strain factor d_{33} and relative dielectric factor ϵ_r decrease evidently, while the piezoelectric voltage factor g_{33} initially decreases evidently and then levels off. The acoustic impedance Z and the dielectric loss $\tan\delta$ are hardly influenced by the aspect ratio. At the same time, the influence of temperature on the dielectric properties of the composites was studied. The result shows that with increasing the temperature at the frequency of 1kHz and 150kHz, the dielectric factor ϵ_r all exhibit the trend of increase. In the range of -40°C - 110°C , the dielectric loss $\tan\delta$ first increase slowly, but increases evidently when exceeding the temperature of 80°C . Comparing with P(LN)ZT piezoelectric ceramic, the vibration at thickness mode of 1-3 type piezoelectric composite is strengthened. Although the electromechanical quality factor is reduced, the band width of composites is increased greatly.

Preparation and Electricity Performance Research of IPMC

Guifen Gong, Danyu Liu, Yujun Zhang, Harbin University of Science and Technology (China).

EVOH-based Comb Ionic polymer (EVOH-g-nSPEG) was prepared by the direct sulfonation reaction of poly(ethylene-co-vinyl alcohol) (EVOH) and 1,3-sulfonic acid propiolactone. The thin film of EVOH-g-nSPEG and its composites based on EVOH-g-nSPEG containing different counter ions and metal (IPMC-0-M) were prepared through the method of solution casting and penetration-reduction method (chemical deposition). The micro-morphology of IPMC-0-Na was determined by scanning electron microscope (SEM). The maximum tip displacement was determined by electrode formation equipment, and the relationship between input voltage and electrochemical activity was evaluated by cyclic voltammetry. The results showed that the smoothness and compactness of IPMC surface electrode were improved when using secondary penetration-reduction technology. The tip displacement of IPMC-0-M (H, Li, Na, K) increased with the input voltage increasing and reached to its maximum value when the input voltage being 4.2V~4.4. The relationship of the tip response time was $T_{Li} > T_{Na} > T_K > T_H$ under the same input voltage. The tip response time of IPMC containing the same counter ion decreased with the input voltage increased.

229

Solid Biopolymer Electrolytes Came from Renewable Biopolymer

Ning Wang, Xingxiang Zhang, Tianjin Polytechnic University (China).

Solid polymer electrolytes (SPEs) have attracted many attentions as solid state ionic conductors, because of their advantages such as high energy density, electrochemical stability, and easy processing. SPEs obtained from starch have attracted attention in recent years because of its abundant, renewable, low price, biodegradable and biocompatible. It can be processed to thermoplastic starch (TPS) by melt extrusion or casting. In addition, the efficient utilization of biodegradable polymers came from renewable sources is becoming increasingly important due to diminishing resources of fossil fuels as well as white pollution caused by ungradable plastics based on petroleum. So corn starch plasticized by DMAc containing different LiCl concentration is studied as solid biopolymer electrolytes in this paper. Li^+ can complexes with the carbonyl atoms of DMAc molecules to produce a macro-cation and leave the Cl⁻ free to hydrogen bond with the hydroxyl or carbonyl of starch. This competitive hydrogen bond formation serves to disrupt the intra- and intermolecular hydrogen bonding existed in starch. So a conductive TPS can be achieved during melting extrusion. Moreover, the improvement of LiCl content can increase the water absorption of TPS and improve the conductance of TPS. The conductance of TPS with 18 wt% LiCl content can achieve to $10^{-0.5} S cm^{-1}$ at 18 wt% water content.

230

Bioelectrochemical Activity of an Electroactive Macromolecular Weight Coenzyme Derivative

Pu Liu, Haitao Zheng, Tao Sun, Tianjin Polytechnic University (China).

As coenzyme utilized by more than hundreds of dehydrogenases, the efficient immobilization and regeneration of nicotinamide adenine dinucleotide (NAD^+) are of great important and have practical applications in industrial, analytical and biomedical field. In this paper, an electroactive macromolecular weight coenzyme

derivative (PEI-DHB-NAD) was prepared by attaching both NAD^+ and 3,4-dihydroxybenzaldehyde (3,4-DHB) to a water-soluble polyelectrolyte, polyethylenimine (PEI). The functional polymer exhibited both electrochemical properties of catechol unites and coenzymatic activity of NAD moieties. The macromolecular NAD analogue showed a substantial degree of efficiency relative to free NAD^+ with alcohol dehydrogenase (ADH) and glucose-6-phosphate dehydrogenase (G6PDH), and a litter higher Michaelis-Menton constant (K_m) was obtained for the coenzyme derivative than free NAD^+ . The bioelectrochemical properties of PEI-DHB-NAD was investigated by using G6PDH as the model enzyme, and both of them were retained on electrode surface by ultrafiltration membrane. The modified electrode showed typical response to substrate without the addition of free coenzyme, which indicated that PEI-DHB-NAD can carry out the electron transfer between electrode and NAD-dependent dehydrogenase. The utilization of polymer-based PEI-DHB-NAD is convenient for the immobilization of both electron mediator and coenzyme, and offers a practical approach for the construction of reagentless dehydrogenase biosensors.

232

Insertion of Intelligent Hydrogel into Silicone Resin for Thermal Control Applications

Hua Wei, Dengteng Ge, Zeng Fan, Feng Liu, Yao Li, Harbin Institute of Technology (China).

The poly(N-isopropylacrylamide) (PNIPA) hydrogel, which is a kind of intelligent temperature-sensitive polymer, has its lower critical solution temperature(LCST) at 33°C. Below and above the LCST, the PNIPA could change from transparent to opacification due to its phase separation. The reversible thermal chromic property of PNIPA is useful in intellectual thermal control field. Herein, silicon coatings were doped with PNIPA particles, which were obtained by rotary cutting after N-isopropylacrylamide cross linked between N-isopropylacrylamide and N, N -methylenebisacrylamide in the aqueous solution below 20°C. The reflectance of the PNIPA/silicon at 20°C and 40°C are obtained from UV-Vis-NIR spectral photometer. Furthermore, reflectance, interface and morphology were characterized by means of UV-Vis-NIR, FTIR, and SEM, respectively. Based on the results, the coating shows quick reflectance tenability with temperature and a best proportion was obtained.

233

Preparation and Characterization of High Contrast Electrophoretic Display Suspension Containing Charged Black-and-White Nanoparticles

XiaoNan Yao, JianPing Wang, XingXiang Zhang, XueChen Wang, Tianjin Polytechnic University (China).

Electrophoretic image displays (EPIDs) have attracted a great deal of interest because of their attributes of good brightness and contrast, wide viewing angles, state bistability and low power consumption compared with liquid crystal display. Nevertheless, preparation of the electrophoretic display suspension containing two kinds of display particles with opposite charges for high-contrast black-and-white display has been rare reported in the present literatures. In this study, TiO_2 nanoparticles with sizes ranging from 300 to 400 of nanometers were modified by two-step dispersion polymerization using poly (styrene-co-divinylbenzene) -methyl methacrylate [P (St-co-DVB)-MMA]] as shell. And core, carbon black (CB) nanoparticles with size ranging from 30-50nm and polymer shell poly (methacrylic acid) [PMAA] were prepared by grafting polymerization, too. Modified nanoparticles were characterized on structure, mean particle size and size distribution,

morphology with FT-IR, TEM, and image analyzer. Furthermore, modified TiO₂ as negatively charged electrophoretic particles and CB nanoparticles as cationically charged electrophoretic particles were homodispersed in tetrachloroethylene (TCE) to make the electrophoretic display suspension with Span-80 as dispersant and OLOA 1200 as charge control agent. The zeta potential and mobility of white (TiO₂) and black (CB) charged particles were measured to be -61.4 mV, 9.50×10^{-6} cm² /V s and 12.8 mV, 1.98×10^{-6} cm² /V s by using an electrophoresis test device, respectively. Final, the electric response behaviors of the electrophoretic display suspension were studied under electrostatic field. The black-and-white particles moved quickly and reversibly inside ITO electrodes while the electric field alternated.

234

Preparation, Microstructure Characterization and Dielectric Properties of Relaxor Ferroelectric Thick films

Huiqing Fan, Jin Chen, Northwestern Polytechnical University (China).

The phase structure and the microstructure of pyrochlor-free (1-x)PMN-xPT (x=0.2~0.4) relaxor ferroelectric thick films prepared by an electrophoretic deposition on Pt substrate were investigated by XRD and SEM. The dielectric properties of PMN-PT thick films was studied in terms of diffused phase transition along with frequency dispersion of the temperature of dielectric permittivity maximum (T_m). The dielectric permittivity maximum ϵ_m (at 1 kHz) were in the range of 18000~26500, which are comparable to the reported values for bulk relaxors. Vögel-Fulcher relationship was used to analyze the frequency dependence of T_m. Deviations from Curie-Weiss behavior and temperature evolutions of the local order parameter were observed in PMN-PT film. The degree of relaxation obtained from the modified Curie-Weiss law strongly suggests the relaxor behavior. Above the transition temperature, the temperature dependence of the dielectric permittivity also can be well described by a Lorenz-type law; even it fails at the low temperature side of the dielectric maximum of a first-order ferroelectric phase transition. Therefore, the evolution and dynamic behavior of polar nano-regions (PNRs) was discussed in detail to elucidate the diffuse phase transition in relaxor ferroelectric films.

235

A Hybrid Elements Model of the Stress-Strain Hysteresis in Shape Memory Alloys

Yongzhong Huo, Fudan University (China).

Shape memory alloys (SMAs) show strong hysteresis in stress-strain-temperature relations. The hysteretic behavior is mainly caused by the thermodynamic irreversibility during the thermo elastic martensitic transformation. The various types of stress-strain hysteresis observed for SMAs at different temperatures have been attributed to the martensitic reorientation (MR) and the stress-induced martensitic transformation (SIMT) processes occurred under loading. Based on such observations, a model is proposed to consist of two types of elements: MR elements and SIMT elements. The MR elements show only martensitic reorientation and the SIMT elements can behavior only according to the stress-induced martensitic transformation. A SMA sample is a proper combination, determined by two temperature dependent distribution functions, of these two types of elements in series, i.e. the stresses on the elements are identical and the strains sum up. Experiments are designed to determine the distribution functions and numerical simulations are performed to show the capability of the model in reproducing the stress-strain hysteresis of SMAs in the whole temperature range of applications.

237

An Biosensing of Toxoplasma Gondii DNA with CdTe/Fe₃O₄ Dual Functional Quantum Dot as Reporter Group

Shichao Xu, Juan Yang, Jimei Zhang, Zhao Dai, Tielin Feng, Yan Zi, Jingwei Liu, Chu Liang, Hao Luo, Tianjin Polytechnic University (China); Bo Sun, Nankai University; SUN Shu-qing, Tianjin University (China).

Toxoplasma gondii is an intestinal coccidium that parasitizes members of the cat family as definitive hosts and has a wide range of intermediate hosts. Infection is common in many warm-blooded animals, including humans, the early detection of Toxoplasma gondii was concerned in recent years. In the current research, we presented a fast, specific, and sensitive sensing probe to detect Toxoplasma gondii DNA based on mechanism of fluorescence energy transfer (FRET), and a magnetic-fluorescent CdTe/Fe₃O₄ core-shell quantum dots (mQDs) was utilized as energy donor, and BHQ-2 was used as energy acceptor, respectively. The CdTe/Fe₃O₄ mQDs with average size of 15nm were prepared by layer-by-layer (LBL) process at ambient temperature. The sensing probe was fabricated through labeling a stem-loop Toxoplasma Gondii DNA oligonucleotide with mQDs at the 5' end and BHQ-2 at 3' end, respectively, and the resulting sensing probe can be simply isolated and purified from the reactant with a common magnet. Properties of mQDs and sensing probe were determined by transmission electron microscopy (TEM) and fluorescence spectrum (FS). The TEM data demonstrated that the size of mQDs was 15nm, and the FS data indicated 50% of fluorescence recovery (FR) was observed when the complete complimentary target Toxoplasma Gondii DNA was introduced, however, only weak FR was observed when the target DNA with one-mismatch base pair was added, this result revealed the sensing probe has high sensitivity and specificity. The current sensing probe will has great potential applications in the life science and related research.

238

The Effect of Humidity on Indentation Crack Growth in Lead-Free Ferroelectric Ceramics

H. J. Zhang, J. X. Li, L. J. Qiao, W. Y. Chu, University of Science and Technology Beijing (China).

Ferroelectric ceramics are operated in atmosphere environment under electric field when they are used in smart structures, such as actuator, micro-positioner and sensor. Our previous investigations indicated that humid air could cause delayed cracking of PZT ferroelectric ceramics under sustained electric field, sustained stress and mechanical-electrical coupling. The effect of humidity on subcritical crack growth of unloaded indentation crack in KNN free-lead ferroelectric ceramics has been investigated in this work. The results show that subcritical crack growth of unloaded indentation in lead-free ferroelectric ceramics can occur in humid air of 70% and 90%RH without electric field and mechanical stresses but does not in air with RH≤30%. The subcritical crack growth of indentation crack can occur in dry air when the field is larger than the threshold field $E_{th}(y)=0.01E_C$ (normal to the poling direction) or $E_{th}(z)=0.05E_C$ (parallel to the poling direction) and the larger the field, the shorter the incubation time. The increment of subcritical crack growth in humid air under sustained field, Δc , is composed of three parts, i.e., $\Delta c = \Delta c_1 + \Delta c_2 + \Delta c_3$, where Δc_1 is the increment in humid air without field, Δc_2 that in dry air under sustained field and Δc_3 that induced by combined effect of electric field and humidity because of humidity promoting domain switching.

241

Surrounding Rock Mass Stability Monitoring of Underground Caverns in a Geomechanical Model Test Using FBG Sensors

Yong Li, Weishen Zhu, Xiaojing Li, Qianbing Zhang, Shandong University (China); Xiaojing Li, Shandong Jianzu University (China).

Fiber Bragg Gratings (FBG) sensor is widely accepted as a structural stability device for all kinds of geomaterials by either embedding into or bonding onto the structures. The physical model in geotechnical engineering, which can accurately simulate the construction processes and the effects on the stability of underground caverns on basis of satisfying the similarity principles, is an actual physical entity. Due to a large number of restrained factors, a series of experiments are difficult to be carried out, in particular for how to obtain physical parameters during the experiments. Using the geo-mechanical model test of underground caverns in Shuangjiangkou Hydropower Station as a research object, the FBG sensors were mainly focused on and adopted to figure out the problem how to achieve the small displacements in the large-scale model test. The final experimental results show that the FBG sensor has higher measuring accuracy than other traditional sensors like strain gages and mini-extensometers. The experimental results agree well with the numerical simulation results. In the process of building the model, it's successful to embed the FBG sensors in the physical model through making a reserved pore and adding some special glue. In conclusion, FBG sensors can effectively measure the small displacement of monitoring points in the whole process of the geomechanical model test. The experimental results reveal the deformation and failure characteristics of the surrounding rock mass and make some guidance for the in-situ engineering construction.

242

Research on the Optical fiber's Photosensitivity Influenced by the Doping Process

Feng Tu, Deming Liu, Xinwei Qian, Huazhong University of Science & Technology (China); Jie Luo, Tao Deng, Chen Yang, Yangtze Optical Fibre and Cable Co (China).

Fiber gratings written into photosensitive fiber by UV holographic techniques are attracting considerable attention due to their broad range of potential application in photonic devices and optical communications such as dispersion compensation, and sensors. Being an optical filter, the fiber grating can also be applied to a demultiplexer in OFDM high-speed communication system. The feasibility of this approach is contingent on the possibility of a wide range of wavelength tuning and the abstention of filter bandwidths in the order of those corresponding to the transmitted channels.

Photosensitive fibers are based material for writing optical fiber grating. However, the normal communication optical fiber's photosensitivity is inadequate to write high quality fiber grating. Unless adopt the H₂ load technology to increase the fiber's photosensitivity, but this process need many time and bring risk to fiber splice process. So the high quality photosensitive fiber used in UV light writing fiber grating without H₂ load procedure is needed to be studied. Germanosilicate glass fibers have a well known photoinduced refractive index change initiated by UV light at wavelengths near 240nm and this phenomenon has been used to form reflection gratings at telecommunication wavelengths.

Based on the plasma chemical vapor deposition (PCVD) process, the Ge/F (Germanium/Fluorine) and Ge/B (Germanium/Boron) co-doped photosensitive fiber was developed. Through analyze the fiber's photosensitivity, study the fiber's photosensitivity influenced by the doping process. The fiber's data indicate that the

high F doped (5%) Ge/F photosensitive fiber's grating has the 80% reflectivity, much lower than the low F doped (1%) Ge/F photosensitive fiber's 94% reflectivity. Then the Boron doped would increase the fibre's photosensitivity distinctly just when the dope content reach about 5%. Then the Boron content would get the saturation to increase the fiber's photosensitivity about 30%.

243

One Kind of Fiber Bragg Grating Displacement Sensor Using Micro-Elastic Spring

Xuefeng Zhao, Jinping Ou, Dalian University of Technology, Dalian, Harbin Institute of Technology (China); Michael Fernandez, Gangbing Song, University of Houston, Houston (USA).

A novel micro fiber Bragg grating displacement sensor is proposed and studied in this paper. A type of micro-elastic spring was used as a displacement-wavelength conversion component. According to the sensor package design established, one micro FBG displacement sensor with outer diameter of 1.3mm was constructed. Tests were designed and conducted to study the displacement and temperature sensitivity of the sensor. Results show that there are good linear relationships between wavelength and displacement, as well as between wavelength and temperature. The displacement coefficient and temperature coefficient are 10.97pm/mm, and 21.38pm/°C, respectively.

244

Structural Shape Monitoring Using Fbg Strain Sensing for Morphing Structures

Kun Yang, Weicheng Gao, Wei Liu, Harbin Institute of technology (China).

The accurate shape monitoring is expected to be useful for full-scaled structural monitoring of a wide variety of morphing structures such as morphing aircraft, large antennas, and solar sails. In this paper, the shape algorithm reconstruction is constructed for the deflection in the deformation of composite laminates based on the modal superposition theory only using the high-resolution distributed strain data, which is obtained by the optical fiber bragg grating (FBG) sensors. According to the modal superposition theory the deflection in the deformation of a structure is taken as the superposition of its modeshapes in which both the modeshapes of displacement and strain are used. The strain modeshapes can be obtained by analyzing the strain measurements using FBG sensors with eigensystem realization algorithm (ERA). However, the displacement modeshapes in most cases cannot be measured directly. Hereon, the displacements modeshapes are derived from the strain modeshapes using elastic plate theory. Hence the structural shape simultaneous on-line monitoring for morphing structures could be realized only with the FBG sensing network.

The algorithm is validated experimentally using a prototype of a variable cantilevered plate provided with a network of distributed FBG sensors whose locations are optimized by a genetic algorithm (GA). The deflection of the plate is successfully predicted with the constructed algorithm by using obtained distributed strain data. And a scanning laser vibrometer (SLV) is used to determine displacement modeshapes to comparison with the predicted results. Furthermore, to illustrate the problem completely the numerical simulation is investigated, and the results comparison between theoretical prediction and experiment and numerical simulation are given as well, which shows an acceptable agreement between each other. From the result, it is shown that the deformation of plate-like composite structures is able to be reconstructed with a few percents of the prediction error using the developed algorithm.

High Birefringence Photonic Crystal Fiber Design

F.F. Shi, Y. Zhao, M.C. Li, L.C.Zhao.

Photonic crystal fibers (PCFs)—fibers with a periodic transverse microstructure—have been in practical existence as low-loss waveguides since early 1996. Based on Maxwell equations and use of the finite element method (FEM), the effective refractive indexes of fundamental mode were investigated.

A novel high birefringence photonic crystal fiber (PCF) was proposed (Fig1). An octagonal photonic crystal fiber (O-PCF) structure with thirty two air-holes on the fourth ring is proposed. And the first three rings are the standard hexagonal PCF (H-PCF) structure with specified revolving. These helped the mode field focus on the core (Fig2).

There are many methods to induce birefringence in PCFs. The key point is to destroy the symmetry of the structure, and make the effective index difference between the two orthogonal polarization states (Fig3). The birefringence is found to be largely dependent on the variation of the free-space wavelength, diameter of the air holes and space between the air holes. Our suggested structures can considerably enhance the birefringence in PCFs and show that the birefringence can be as high as the order of 10^{-3} at the wavelength of 1550 nm.

The results show that high birefringence can be obtained by changing the number of air holes along orthogonal direction in inner cladding. It is also proved that enlarged air holes of inner cladding reduce the confinement loss, and increase the dispersion, but the impact of diminished air holes is reversed; the fewer the air holes in inner cladding are, the flatter the dispersion is.

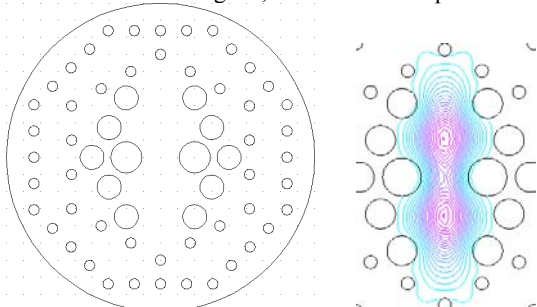


Fig 1. Cross section of PCFs Fig2. Mode field pattern

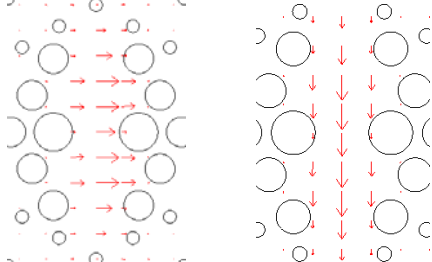


Fig. 3. Transverse electric-field vector distributions of the HE11x and HE11y modes

Newly Development in Damage Monitoring of Composite Structures with Fiber Bragg Grating Sensors

Shaowei Lu, Shenyang Institute of Aeronautical Engineering; Shaowei Lu, Jinsong Leng, Harbin Institute of Technology (China).

Structural health monitoring techniques have recently been developed for composite structures. Among various sensors for intelligent structure systems, Fiber Bragg Grating sensors have the greatest advantages such as high-accuracy and multiplexing capability, moreover FBG sensors are very sensitively to

non-uniform strain distributions due to internal damage in composite structures. Based on this principle, the damage in composite structures can be estimation from the reflection spectrum shape of fiber Bragg grating sensors. In this article, the recent research and development in composite structure damage monitoring using FBG sensors, such as transverse cracks detection, delamination detection, damage pattern monitoring and estimation, residual stress/strain measurement, disband monitoring in composite single-lap joints etc, have been reviewed and discussed.

Simulation of Fiber Bragg Grating Sensor for Rebar Corrosion

Geng Jiang, Wu Jin, Zhao Xinming, Nanjing University of Aeronautics and Astronautics(China).

It is world widely concerned in the durability of reinforced concrete structures. Corrosion of rebar is one of the most important factors which can affect the durability of the concrete structures, which may result in damage to the structures in the form of expansion, cracking and eventually spalling of the cover concrete. In addition, the structural damage may be due to loss of bond between reinforcement and concrete and loss of reinforcement cross-sectional area, and finally it may cause structure failure. With the advantage of linear reaction, small volume, high anti-erosion capability and automatic signal transmission, the smart sensors made of fiber bragg grating (FBG) to monitor strain, stress, temperature and local crack have got wide application in civil buildings, bridges and tunnels. FBG can be adhered to the surface of the structure, and also can be embedded into the inner of the structures when the project is being under construction to realize the real-time health monitoring. Based on volume expansion, the fiber bragg grating sensor for rebar corrosion was designed. The corrosion status of the structure can be obtained from the information of sensors. With the aid of the finite element software ANSYS, the simulation of the corrosion sensor was also carried in this paper. The relationship between corrosion ratio and the change of wave length was established. According to the results of the simulation, there were differences between simulated results and measured results. The reason of the differences was also studied in this paper.

Application of Fiber Bragg Grating Sensor for Rebar Corrosion

Jiang Geng, Jin Wu, Xinming Zhao, Nanjing University of Aeronautics and Astronautics (China).

Corrosion of rebar is one of the most important factors which can affect the durability of concrete structure, so in the service of these structures, measuring the degree of corrosion, and then evaluating the reliability of these structures are very important. The most significant characteristic of the rebar corrosion is the volume expansion of the rebar. By the principle and characteristic of FBG, a sensor is designed, and it is called the fiber bragg grating sensor for rebar corrosion. In this paper, based upon laboratory studies, the fiber bragg grating sensor was applied in No.58 Berth of Lianyungang Port. According to the filed condition, a proper embedding scheme was proposed. Considering the optimal sensor placement, the monitoring points were determined and five sensor groups were applied in the structure. Based on the results of the calibration experiment, the relationship between corrosion ratio and the change of wave length was established. So the corrosion status of the structure can be obtained by measuring wave length. The study showed that the fiber bragg grating sensor was feasible to monitor the status of rebar in concrete structures.

An Analytical Model for Surface Stress of a Microcantilever-DNA Chip

ZouQing Tan, Shanghai Institute of Applied Mathematics and Mechanics (China); JingJing Li, NengHui Zhang, Shanghai University (China).

The paper is devoted to formulating an analytical relation between various biomolecular interactions during the process of label-free DNA-detection and change of surface stress, which is widely accepted as the origin of nanomechanical motion of a microcantilever-DNA chip. First, considering electrostatic interactions between neighboring strands, hydration forces between DNA molecules and hydrogen bonding networks in water, conformational entropy of DNA chains, and mechanical energy of non-bilayers, the energy potential of a DNA chip and its first-order approximate expression are formulated. Second, the analytical expression for surface stress of a DNA chip is given by the minimum principle of energy. Third, the effects of grafting density and salt concentration on surface stress are investigated. Numerical results show that surface stress is a strong function of grafting density, which is in agreement with Stachowiak's experimental results.

251

Studies of Preparation of Poly (acrylic acid)-Titanium Oxide (PAA-TiO₂) and Its Self-assembly Thin Films

Xuefeng Li, Shaoxian Peng, Yuan Sun, Hubei University of Technology (China).

Here, we describe the preparation of poly (acrylic acid)-titanium oxide (PAA-TiO₂), and the fabrication of multilayer thin films constructed from PAA-TiO₂ and DR via a layer-by-layer technique and the conversion of the linkage bonds under UV irradiation.

Tetrabutyl titanate in the acidic medium reacted to be the hydrolysis product of the TiO₂ Sol. TEM was consistent with the results of the particle size distribution analyzer, TiO₂ sol was the size of the standard normal distribution, the average size of 64 nm. Diazoresin (DR) as a cationic polyelectrolyte deposits on the quartz glass surface easily, then PAA-TiO₂ deposits on the DR layer, to form a DR and PAA-TiO₂ bilayer on both sides of the quartz glass in each fabrication cycle. The absorbance of DR on quartz glass after each cyclic deposition was recorded using a UV-vis scanning spectrometer to monitor the self-assembly process (Fig.1). The peak at 383 nm is assigned to the absorption of the diazonium group of DR and increase linearly with increasing bilayer number. It can be seen that the absorbance increases by ca. 0.03 every two bilayers indicating smooth step-by-step deposition. The five bilayers film was then irradiated with UV light and the resulting absorbance determined. The UV-vis spectra of the DR and PAA-TiO₂ films before and after irradiation and decomposition of the diazonium groups of the film are shown in the experiment. The absorbance at 383 nm (diazonium group absorption) decreased with irradiation, which indicates that the ionic bonds of DR and PAA-TiO₂ convert partially to ester bonds. The diazonium group of the DR and PAA-TiO₂ film decomposes easily under irradiation with UV light because it is sensitive towards UV light. The conversion of the ionic bonds to covalent bonds is shown in scheme 1.

The films consisting of both cationic and anionic groups exhibit an extremely high tendency to aggregate by the ionic attractive force. The conversion of ionic bonds into covalent bonds makes the multilayer self-assembled films more stably packed. The unirradiated films keep the original ionic structure and are much more unstable in polar solvents, such as DMF, and can be washed away. The solubility of the films was changed dramatically after

irradiation. The irradiated films do not dissolve in DMF, because of the formation of the covalently crosslinked structure. This shows that the stability of the films towards polar solvents increases significantly after UV irradiation.

The surface roughness of one layer DR film and five bilayers DR / PAA-TiO₂ films on mica were visualized using AFM in tapping mode. The images revealed the films are rather flat and uniform though the step-by-step technique. The particles of TiO₂ are dispersed well in the thin film and no apparent aggregation can be seen. Our experimental results demonstrated films were in regularity, but we believe the intrinsic molecular chains were locally disordered due to long chains tangled in the films of polymers.

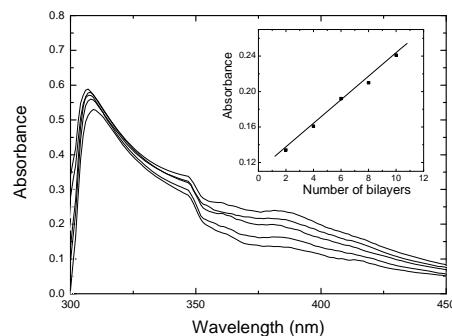
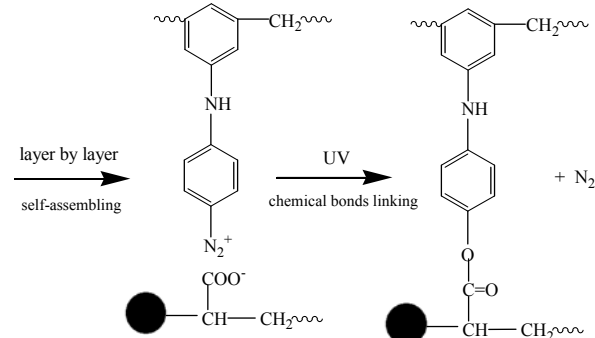


Fig. 1 The UV-vis spectra of the multilayer films at 383 nm with difference numbers of bilayer
Bilayer number (bottom to top): 1, 2, 3, 4, 5 Insert: Relationship between the absorbance at 383nm and the bilayer number.



Scheme 1 The bond conversion taken place in PAA-TiO₂/DR multilayer film under UV irradiation

252

Microwave Heating of Lead Zirconate Titanate Thin Films

Z. J. Wang, Chinese Academy of Sciences (China).

Lead zirconate titanate (Pb (Zr_xTi_{1-x}) O₃: PZT) have excellent ferroelectric, pyroelectric and piezoelectric properties. Techniques for the deposition of PZT thin films have been developed rapidly in recent years because of the large number of potential applications of PZT thin films in nonvolatile ferroelectric random-access memories (FeRAMs) and micro-electromechanical systems (MEMS) such as micro-scanning mirror devices and atomic force microscopy (AFM) cantilevers. It is imperative to decrease the thermal processing temperature and time to prevent interdiffusion between the elements of the films and the substrate and to prevent the evaporation of lead and lead oxide from the surface of the film. In this study, PZT thin films were coated on Pt/Ti/SiO₂/Si substrates by a sol-gel method and then crystallized by single-mode 2.45 GHz microwave heating. The crystalline phases and microstructures as well as the electrical properties of the microwave-heated PZT films were investigated as a function of the elevated temperature generated by microwave heating. Experimental results indicated

that microwave heating is effective for obtaining well-crystallized PZT thin films with good properties at low temperatures or in a short process time.

253

Preparation of Visible Light-Responsive TiO₂ Photocatalyst by Codoping with Lanthanum and Iodine and Its Catalytic Performance under Sunlight Irradiation

Chen Wen, Jing Y. Xu, Li M. Jia, Hai Y. Wu, Institute of Material & Chemical Engineering (China); Chang F. Xiao, Tianjin Polytechnic University (China).

In this paper, sunlight-responsive TiO₂ photocatalysts with a mixed structure of anatase/rutile phase were successfully prepared by a sol-gel process through lanthanum (La) and iodine (I)-codoping. Brunauer-Emmett-Teller method, X-ray diffraction, X-ray photoelectron spectroscopy, and UV-visible diffuse reflectance spectra demonstrated that the TiO₂ framework was modified by La and I-species incorporated into crystal lattices by the adsorbed La₂O₃ and by arising from I⁵⁺ substituting for Ti⁴⁺, which would be likely to give new states as molecularly chemical site originated from the I of the IO₃ group, and where it is indispensable for the electron transfer efficiency. The La-I-TiO₂ indicates stronger absorption in the 200-800 nm range and serves as a sunlight induced photocatalyst; it shows remarkably higher photocatalytic activity than pure, I-TiO₂, and La-TiO₂ prepared by the same procedure toward the phenol degradation under sunlight and visible light (> 420 nm) irradiations, respectively. The La 0.3-I-TiO₂ with 75 % anatase and 25 % rutile phases (calcined at 700°C) was found to exhibit the highest photocatalytic activity under sunlight irradiation, implying a possibility for in situ photocatalytic oxidation of industrial wastewater. The promoting effects of La-I-TiO₂ on the photocatalytic capacity were considered by relating to the higher surface area, full coexistence of anatase/rutile phase, excellent thermal stability, and the cooperative action of I and La₂O₃. The photochemical reactions of I species as new states regenerated TiO₂ which gave an appropriate explanation for the enhanced photocatalytic efficacy, together with important mixed phase-dependent behavior.

254

Experiment and Simulation on Responses of Polymer Induced by Laser Irradiation

Haiming Huang, Xiaoliang Xu, Beijing Jiaotong University (China).

With the development of MEMS technology, the limitations of machining technology for silicon-based materials become more and more distinct. With its abilities on sub-micron structure machining, the pulsed laser micro-fabrication technology has an extensive application prospect in MEMS and many other materials. The thermal interaction process of polymer under laser irradiation is very complex, regularities on polymer plates under laser irradiation between displacement and laser energy density can only be obtained through experiments. Based on finite element method (FEM), simulations have been done with the same conditions in experiments. Relational expressions among pulsed laser intensity, actuation duration and thermal impact loads were obtained with the comparison between numerical results and experimental data. This study provides theoretical basis to the pulsed laser micro-fabrication technology's application in the fields of ME

255

Investigation of Luminescence Property in Seawater on Long-Life Afterglow Fluorescent Coatings Modified by Nano-TiO₂

Zhanping Zhang, Yuhong Qi, Dalian Maritime University (China).

For developing new marine non-toxic antifouling coating, it was investigated the luminescence property in seawater on long-life afterglow fluorescent coatings modified by nano-TiO₂. The influences of the content and crystalline microstructure of fluorescent powder, of different coating resins were studied on the luminescence characteristic of the coating. The luminescence characteristic tests were carried out as following. Each panel was put in an 800ml beaker (Φ100mm), add 200ml sterile filtered (0.45 μm) sea water. All beakers were put in container with light at different photometer illumination. After some period exposure of the panels under artificial illumination, lamp-house was turned off and the fluorescences of coatings were measured with luminometer at regular intervals. The results showed that fluorescent coatings modified by nano-TiO₂ represent the good luminescence characteristic in seawater. With the increase of the content of fluorescent and nano-TiO₂ powders in coating, the luminescence property of coating increases. As light afterglow time increases, the illuminance of both fluorescent powder and luminous coating decays exponentially. Compared with long-life afterglow fluorescent coatings not modified by nano-TiO₂, the afterglow illuminance of the coatings modified by nano-TiO₂ was remarkably improved. The luminescence property in seawater of the coating based on fluorocarbon resin is much more than that of the coating based on acrylic resin.

257

Luminescent Quantum Dots Assembled With Mesoporous Template Al₂O₃ As A Kind of Labeling Smart Materials or Devices

Benwei Yu, Yue Shen, Hao Yan, Jiancheng Zhang, School of Materials Science and Engineering, Shanghai University (China); Xiaofeng Zhang, Shanghai Chinese Traditional Medicine Hospital (China).

CdTe QDs were directly synthesized in the aqueous solution with mercapto- succinic acid (MSA), including one thiol and two carboxyl functional groups, as a stabilizing agent. The effects on luminescent or optical properties of CdTe QDs and its size distribution under a variety of amount of MSA added and different pH value were studied by Vis-UV, PL (photoluminescence), TEM, HRTEM and SEM etc. The best relative reaction conditions were found in the synthesis of CdTe QDs. The quantum dots capped with this chelating reagent, involving double carboxyl, show to be water- soluble and biocompatible. Their first excited absorption peaks in the VIS-UV spectra from 480nm to 510nm can be measured and then calculated by Brus equation, leading to the obtaining QDs' varied sizes with 2-5nm which are consistent with the results observed by HRTEM. And the PL peaks are tunable about 530-600nm respectively, and PL quantum yield (PLQY) of the QDs with better mono-dispersing property likely achieve to above 50%.

After that, meso-porous Al₂O₃ thinner film prepared from our lab could be used as a template and followed to assemble in the tunnels of the Al₂O₃ with CdTe QDs capped with MSA as mentioned-above, and at last to form two kinds of the emitting PL peaks, in general, being inclusive of the QDs PL peaks as mentioned-above 530-600nm, and of another PL peak with about 450nm of the meso-porous Al₂O₃ emitted from UV wavelength 330nm. A series of bio-conjugation was investigated as the prototype basis of immuno-ship with porous matrix. In order to probe into this kind of assembled Al₂O₃ template with QDs as a so-called labeling smart material or into another kind of simulating bio-molecular labeling device, the sheep anti-rabbit IgG was

conjugated with the QDs based on the Al_2O_3 carrier by some coupling agents, such as EDC or NHS (in water), DCC or DIC (in organic) etc. In this work, the protein (this IgG) combined on the template with CdTe QDs according to the different sizes is observed PL varied from 530 nm to 600nm by the UV microscope.

258

Study on the Bifurcation and Chaos of Giant Magnetostrictive Actuators

Haiquan Zeng, Changzheng Chen, Shenyang University of Technology (China).

Nonlinearity between exciting current and output displacement spoils magnetostrictive actuators' performance. Chaotic and Quasi-periodic motions are important aspects of nonlinear character for magnetostrictive actuators. To explore the erratic behaviors of the actuators, a nonlinear dynamic model was established. The bifurcation diagrams, phase portrait, Poincaré mapping diagrams, amplitude spectrum, Lyapunov exponent, etc. which demonstrate dynamical characteristics of the system were obtained by numerical integration. Analysis indicates: Nonlinearity of response could be improved by increasing of damping coefficient. Chaos would appear when stiffness of the system is relatively low. At frequencies below 10Hz, exciting current also brings chaos.

260

Study on Magneto-Mechanical Coupling Model for Giant Magnetostrictive Actuator

Guoping Li, Tongpeng Han, Jie Shen, Ningbo University (China).

Based upon an analysis of the motion law of giant magnetostrictive material magnetic domain under magnetic field, a hysteresis model of magnetization-based for giant magnetostrictive actuator is established. The model incorporates operating conditions of the actuator and fully considers nonlinear and hysteresis characteristics of the material. It includes two sub-models: magnetostriction and magnetization. The relationship between the strain and the magnetization M is illustrated in the magnetostriction model. The magnetization model describes the relationships amongst the effective field H_{eff} , the anhysteretic magnetization M_{an} , the reversible magnetization M_{rev} , the irreversible magnetization M_{irr} and the total magnetization M . The full set of parameters was estimated through a least square fit with experimental data. The model is proved to be able to describe the relation accurately between the input current I and the output strain λ by analyzing the experimental result. The magneto-mechanical coupling model provides the reference for the giant magnetostrictive actuator's application in the turning vibration control system.

261

Preparation and Microwave Absorption Property of the Core-Nanoshell Composite Absorbers with Magnetic Fly-Ash Hollow Cenosphere as Nuclear

RuXin Che, YingJuan Ni, ChunXia Wang, Dalian Jiaotong University (China).

The core-nanoshell composite absorbers with magnetic fly-ash hollow cenosphere as nuclear were prepared by sol-gel and liquid-phase coating technology. The results of X-ray diffraction analysis (XRD), scanning electron microscope (SEM), transmission electron microscope (TEM), energy dispersive spectroscopy (EDX), vibrating sample magnetometer (VSM) and vector network analyzer (VNA) analysis indicate that the hollow cenosphere is dielectric loss; the exchange-coupling interaction happens between ferrite of hollow cenosphere and nanocrystalline magnetic material

coating. The exchange-coupling interaction enhance magnetic loss of composite absorbers. They have a perfect electromagnetic parameters in the frequency between 2 GHz and 18 GHz, The biggest absorptivity is -50dB, the lowest reflectivity is -18dB; density is 0.2-0.6 g / cm^3 , intensity is 2-4 Mpa, and they could be dispersed uniformly in phenolic cement. The microwave absorptivity of the core-nanoshell composite absorbers is better than single material.

262

External Characteristics Detection and Analysis of Magnetically Controlled Shape Memory Alloy

Chengwu Lin, Shenyang University of Technology (China); Yongzhi Cai, Liao Ning Institute of Science and Technology (China).

Magnetically controlled shape memory alloy (MSMA) is a kind of new magnetically material which was found in the 1990s. It's Martensitic transformation temperature is often lower than Curie transition temperature. MSMA is a unique martensite phase transition material that has both ferromagnetism and thermo-elastic property in the Heusler alloys. The advantages of MSMA are not only large strain, quick response, high thrust, but also the feature of shape memory. MSMA is of a bright future of its applications in military, precision control and smart sensors and actuators.

The external characteristics detection of MSMA is the basis of application. However, the research on the external characteristics of MSMA is still in the stage of beginning. In order to built a base for the application of MSMA material, it is necessary to study the detection technique and testing method of MSMA external characteristics much deeper, from that, we could find out the impact and strain effect of temperature, force and magnetic field on external characteristics, and observe the strain behavior of the material in multi- environment .

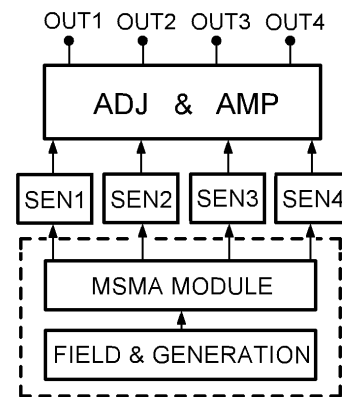


Fig.1 Experiment equipment of MSMA

An external characteristic detection equipment of MSMA is designed and manufactured successfully to realize the intention mentioned above. Basic structure is shown in Fig.1.

Based on MSMA's multi-sensitivity, the experimental equipment of 4-channel-measurement is designed. It is not only able to finish the high precision and independent detection of temperature, displacement, magnetic induction intension and force, but also finish the interdependency detection of multi-parameter. The structural design is of four independent output terminals, it helps to compose to be a signal acquisition and analysis system with other equipments. The seamless technique is introduced in the dynamic detection. LabVIEW SignalExpress TE is used to increase of experiment efficiency, and it achieves the combination software and hardware in data processing

Fig.2 shows the dynamic strain curve of MSMA on the pre-stress of

0.7MPa. From the curve, we can see the static state deformation rate is 1.7% and dynamic state deformation rate is 0.73%. With the increase of pre-stress, the static state deformation rate decreases, but the change of the dynamic state deformation rate is complicated, it only reaches the maximum if the pre-stress is appropriate

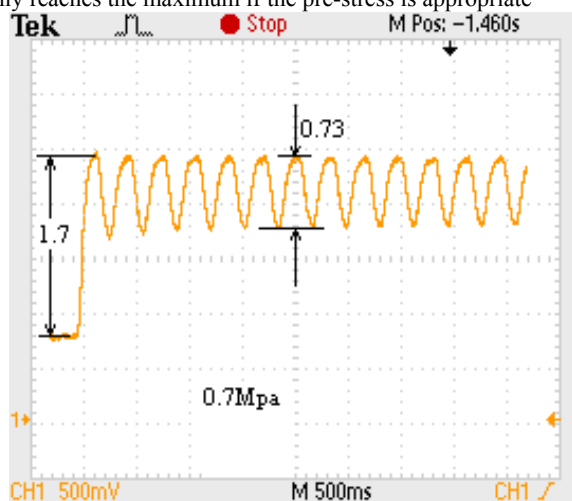


Fig.2 The dynamic strain curve of MSMA

The experimental results show that the equipment structure is reasonable, easy to use and able to realize multi-parameter interdependency and coupling detection. Based on the external characteristic analysis, MSMA can be not only used as sensors and actuators design, but also designed as intelligent detection system such as self-sensing actuator (SSA) based on its interdependency and anti-characteristic. Combining the theoretical analysis and experimental study results, it proves that, definitely, MSMA has the value for both science research and application.

263 Fabrication, Characterization and In-vitro Cytotoxicity of Magnetic Nanoparticles Composite Sustainable Polymeric Film for Multi-functional Medical Application

Lingyun Zhao, Xiaowen Wang, Jiantian Tang, Tsinghua University (China); Xiaoyu Xu, Xiaochen Dai, Beijing University of Chinese Medicine (China).

Cancer comprehensive treatment has been fully acknowledged as it can provide an effective multimodality approach for fighting cancers. In this study, various innovative technologies for cancer treatment including cancer nanotechnology, chemotherapy by controlled release, as well as magnetic-mediated hyperthermia (MMH) have been integrated for the purpose of cancer comprehensive treatment. Briefly, such kind of treatment can be realized by application of the tailored magnetic nanoparticles composite sustainable polymeric film. Such a hybrid film could be fabricated by solvent evaporation method. Both Fe_3O_4 magnetic nanoparticles acting as the agent for MMH, and anti-cancer drug paclitaxle as chemotherapeutic agent had been incorporated within the biodegradable polymeric film. Physio-chemical characterizations on the film have been systematically carried out by various instrumental analyses, such as TEM, SEM, XRD, FTIR etc. HPLC analysis has been applied for in-vitro drug release investigation. Hyperthermia could be induced by stimulating the composite film under an alternative magnetic field. The synergetic effect of the drug-loaded Fe_3O_4 magnetic nanoparticles film on human cervical carcinoma cells was assessed in vitro by using the colorimetric MTT assay and compared with the drug free film. Our results demonstrate that the composite film has been successfully

prepared by solvent evaporation method. Film composite, such as nanoparticle content, drug loading ratio and polymer type have effect on the film properties, such as drug-release profile, heating effect and cytotoxicity. The in-vitro cytotoxicity results indicate there existing synergetic effect between the hyperthermia and chemotherapy. The magnetic nanoparticles composite sustainable polymeric film can realize cancer comprehensive treatment thus has great potential in clinical application.

264 Design and Test of a Micro-Displacement Actuator Based on Giant Magnetostrictive Material

Liang Shao, Dehua Yang, Kunxin Chen, Chinese Academy of Sciences (China); Liang Shao, Graduate School of the Chinese Academy of Sciences (China); Bintang Yang, Shanghai Jiao Tong University (China).

To meet the performance requirements of co-focusing and co-phasing of segmented mirror active optics in modern astronomical telescope, micro-displacement actuators with nanometer resolution and millimeter stroke are necessary. A design and test of a micro-displacement actuator based on giant magnetostrictive material is presented in this paper. The actuator's main components such as giant magnetostrictive drive core, displacement pantograph mechanism, output guide mechanism and output connection hinge mechanism are discussed in detailed. The giant magnetostrictive drive mechanism based on inchworm creep principle basically offers nanometer resolution and micron stroke. A displacement/stroke pantograph mechanism is designed with flexible and absolutely sealed hydraulic cylinder structure to enlarge the stroke. And a secondary giant magnetostrictive drive mechanism is integrated to serve final resolution of final displacement output. In view of flexure exhibiting excellent mechanical properties free of friction, clearance and lubrication, a flexure guide mechanism with the capacity of lateral load is designed to fulfill linear displacement output steadily. In addition, a flexible hinge is introduced to the displacement output connection of two free rotary degrees and two minor linear degrees of motion. The sub-systems like the giant magnetostrictive drive core and displacement pantograph mechanism has tested before assembly of the whole integrated actuator. The final test of the actuator is carried out with dual frequency laser interferometer at lab. Besides, to meet technical requirements of application in future extremely large telescope, further development issues mainly related to practicality of the actuator is discussed at the end.

265 Molecular Mechanics Simulation to the Deformation Behaviors and the Mechanical Properties of Nano Composite of Polyethylene and POSS

Enlai Hu, Yi Sun, Fanlin Zeng, Harbin Institute of Technology (China).

The influences of the polyhedral oligomeric silsesquioxane (POSS) on nano hybrid materials have caused widespread attention. In the current work, the mechanical properties of the polyethylene (PE) copolymerized with POSS were studied using the molecular mechanics simulations. First, the nano scale atomistic models of the pure PE and the polyethylene incorporated with 25 wt% vinyl-POSS (v-POSS-PE), were built. Then the mechanical behaviors of the two kinds of polymers under different tensile strains were simulated. By using the COMPASS force field, the deformations of structures and the stress-strain curves were obtained. As a result, the structure deformations indicate that, when the tensile strain of PE reaches 0.11 the micro voids appear. The stress-strain c

tensile stresses of PE approximately keep linear increasing with the increasing strain before this strain, which shows a elastic region. And the corresponding tensile modulus of PE is 2.02GPa, which is in good agreement with the experimental result. On the other hand, when the tensile strain of v-POSS-PE reaches 0.074 the micro voids appear, the tensile stresses of v-POSS-PE are almost keeping linear increasing before the strain of 0.025, and the corresponding tensile modulus is 3.21GPa. In conclusion, owing to the incorporation of POSS, the deformation of PE has been restrained locally, the elastic modulus and the tensile strength of PE have been observably improved, and the toughness of PE had been decreased. This work is significant to understand the reinforcement mechanism of POSS and provides important referential message to the applications of POSS.

266 Sensing Performance of Magnetic Shape Memory Alloy Actuator with Self-Sensing

Baiqing Sun, Yu Ding, Fengxiang Wang, Shenyang University of Technology (China).

As further studies of active materials, possibilities of developing the self-sensing actuator using the active material are enhanced increasingly. In this paper, for developing self-sensing actuators based on magnetic shape memory alloy (MSMA), the sensing properties of MSMA actuator are studied. An testing set shown as in Fig.1 is developed to measure and analyze relationships among the strain, stress, temperature and magnetization of the MSMA actuator.

The developed testing set is compose of magnetic induction unit, pre-stressing unit, mechanical shock, and measuring unit, etc., In which the pendulum is used to produce controllable and reproduceable mechanical shock that is perpendicular to the direction of magnetic field and acted on the pre-stressed MSMA actuator being in stationary magnetic field. This field is produced by an electromagnet with a permanent magnet embedded in its magnetic circuit. In this paper, as the MSMA actuator is impacted, the corresponding responses of strain, magnetization, and temperature are measured, and relationships between impacting force or acceleration and them are analyzed.

As shown in Fig.2, it is a voltage inducing from deformation of the actuator caused by mechanical shock, which influences magnetization of the actuator. The result of experiment shows that in stationary magnetic field, mechanical shock can produce deformation of the MSMA actuator in a certain range, thereby influence its magnetization, and obtain induced voltage in the coil consequently. There are coincidence relations between impacting force or acceleration and parameters mentioned above in a certain range. It is an aid to research and develop MSMA Actuators with self-sensing.

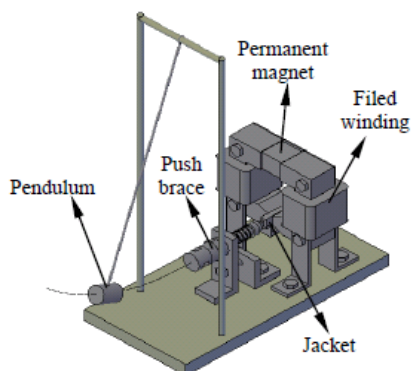


Fig. 1 Host structure illustration of the testing set

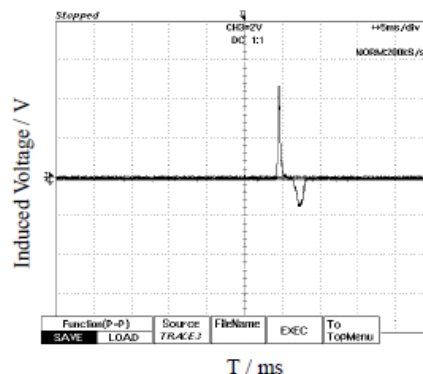


Fig. 2 Induced voltages caused by a mechanical shock

267 An Investigation of Magnetic and Fluorescent Core-Shell CdTe/Fe₃O₄ Nano-Composites

Juan Yang, Jimei Zhang, Shichao Xu, Zhao Dai, Tielin Feng, Yan Zi, Jingwei Liu, Chu Liang, Hao Luo, Tianjin Polytechnic University (China); Bo Sun, Nankai University; Shu-qing Sun, Tianjin University (China).

The magnetic nanoparticles with luminescent properties make the marker and separation work further convenient in the biological fields, such as bio-imaging, bio-labeling, bio-medicine, bio-treatment, etc. In the current research, a multifunctional nanoparticles with a magnetic Fe₃O₄ core and a CdTe quantum dots (QDs) shell of was prepared via self-assembling method and characterized via transmission electron microscopy (TEM), ultraviolet spectrum (UV), and fluorescence spectrum (FS). Magnetic Fe₃O₄ nanoparticles were firstly prepared by chemical precipitation method with sodium hydroxide as precipitant at 50°C, well dispersed Fe₃O₄ nanoparticles in size of 10 nm were observed via TEM and were use as core. The synthesized CdTe QDs were surface modified with 2-mercaptopropionic acid and the magnetic core-shell CdTe/Fe₃O₄ nanoparticles were constructed by the formation of electrovalent bond between -NH₃⁺ and -COO⁻. The prepared core-shell CdTe/Fe₃O₄ nanoparticles can be simply separated or precipitated from the reactant solution. The factors influencing the properties of nanoparticles were investigated, including mol ratio of Fe₃O₄:CdTe, refluxing time, reacting temperature, and pH value etc. The results indicated the core-shell CdTe/Fe₃O₄ nanoparticles with excellent magnetic and fluorescent properties can be achieved when the mol ratio of Fe₃O₄:CdTe is 1:3, and pH was set at 6.0, refluxed for 0.5h at 30 °C. 15nm of average size of the CdTe/Fe₃O₄ nanoparticles was confirmed with TEM. The red shift of maximum emission wavelength from 530 nm to 570 nm and maximum absorbance wavelength from 530 nm to 535 nm were determined via FS and UV, respectively, these data inferred the formation of CdTe shells. The core-shell magnetic and fluorescent CdTe/Fe₃O₄ nano-composites will be an useful tools in biological, genetics, and bio-pharmic applications.

268 Effect of Orientation and Pre-Stress on the Magnetostriction in FeGa Alloy

Zhibin Wang, Jinghua Liu, Chengbao Jiang, Huibin Xu, Beijing University of Aeronautics and Astronautics(China).

The orientation and pre-stress are proved to be very important in determining the performance of magnetostrictive alloys. This paper first investigates the influence of the orientation on the magnetostriction behavior of FeGa alloy theoretically by

simulation based on the phenomenological theory. Besides, the effect of compressive pre-stress on the magnetostriction behavior of <001> oriented FeGa crystal is studied from the experiment and theoretical analysis.

For simulation, the domain rotation path in the applied magnetic field is determined and the resultant magnetostriction is calculated under different compressive pre-stress. The simulated results show that the <001> oriented single crystal has better magnetostrictive property than <110> oriented single crystal in FeGa alloy. The critical pre-stress necessary for the magnetostriction jump effect is also revealed and well explained in this work.

The effect of compressive pre-stress on the magnetostriction behavior is systematically studied in the <001> oriented FeGa alloy from the experiment and theoretical analysis. Three important parameters, including saturation magnetostriction coefficient λ_s , magnetostriction saturation field H_s and piezomagnetic coefficient d_{33} are investigated under a large range of compressive pre-stress. The measured saturation magnetostriction in the <001> oriented $\text{Fe}_{81}\text{Ga}_{19}$ rod increases when increasing the compressive pre-stress and its maximum gets as high as about 300ppm. Two-stage phenomenon on the curves of H_s and d_{33} against compressive pre-stress σ are observed with the cross point at around 52 MPa in the $\text{Fe}_{81}\text{Ga}_{19}$ alloy. H_s increases with increasing σ by the 2/3 th power function at the first stage, while, linearly increases at the second stage. d_{33} increases first and decreases at the second stage with a reciprocal function under high compressive pre-stress. By simulation, it is found that the magnetostriction behavior under different compressive pre-stress is according to two different mechanisms. The equations of H_s - σ and d_{33} - σ are also established based on the two mechanisms, which match well with the fitted functions of the experimental data.

270

Synthesis Of A Novel Phosphorylcholine Functional Biomimetic Polymer As A Non-Adhesive Antifouling Coating

Shijun Feng, Yu Gao, FengLing Qing, Donghua University (China); Feng-Ling Qing, Chinese Academy of Science (China).

A biomimetic polymer containing a phosphorylcholine (PC)-substituted acrylate unit was synthesised by copolymerization with hydroxyethyl acrylate and perfluoropolyether (PFPE) substituted styrene. Bulk and surface properties were assessed through ^{31}P NMR spectra, TG and XPS. The biomimicking polymer was rationally designed for use as coatings to prevent biofouling, especially for marine biofouling. By incorporation cell membrane constituents---phosphorylcholine or phospholipid analogues into the polymer, one would expect PC groups strongly reduces cell attachment at the surface even in polar marine environment. Another advantage is the presence of perfluoropolyether (PFPE) substituted styrene in designed polymer. As is reported, PFPE graft terpolymers are a unique class of materials which have incredibly low surface energy (12-20 mN/m). As a result, fouling organisms such as marine bacteria, protein, cell et al. are hard to adhere and settle on substrates. Besides, the functional -OH in the hydroxyethyl acrylate monomer makes designed biomimetic polymer capable of adhering to many materials including glass and metal devices. Finally, the antifouling potential of the biomimetic polymer surface was evaluated employing serum proteins, ubiquitous *Staphylococcus aureus*, *Escherichia coli*. and the green fouling diatoms in our laboratory. Experimental results indicated the combination of the low surface energy group (PFPE) and natural antifouling lipid headgroup (PC) allowed the biomimetic polymer surface possessing better antifouling properties than did a standard poly(dimethyl siloxane) (PDMS) coating.

271

Upconversion Emission of $\text{Er}^{3+}/\text{Yb}^{3+}$ -Codoped Silicate Glass Micro-Particle under High Excitation Intensity

Jiyou Wang, Nanzheng Li, Ping Duan, Beijing University of technology; Lipu Wang, Xingtai medical college(China).

The upconversion luminescence is a well-known phenomenon in rare earth doped crystalline and glass. In many papers, the emission spectra of the upconversion were studied under the excitation intensities about $10\text{W}/\text{cm}^2$, and only a small part of the sample were irradiated. In this paper, the upconversion emission of the micro-particles [about $40\mu\text{m}$ in diameter] of the SiB glass co-doped with Er^{3+} and Yb^{3+} were measured. The excitation intensity was up to above $3000\text{W}/\text{cm}^2$, and meanwhile, the all part of the material was irradiated.

The upconversion emissions at 522nm and 547nm have been obtained by exciting the silicate glass micro-particle at 976nm. It was observed that the intensity ratio of the 522-nm emission to the 547-nm emission ($I_{522\text{nm}}/I_{547\text{nm}}$) in SiB glass co-doped with Er^{3+} and Yb^{3+} increased when increasing the excitation intensity, and $I_{522\text{nm}}$ became larger than $I_{547\text{nm}}$ when the excitation intensity was above about 18mW [about $300\text{W}/\text{cm}^2$]. It is proposed that the phenomenon resulted from the rise of the temperature of the sample measured because the whole sample was irradiated by the excitation light. Yb^{3+} ions strongly absorbed the excitation light. The rise of the temperature of sample resulted in the increase of the intensity ratio of $I_{522\text{nm}}/I_{547\text{nm}}$.

273

Research on the Corrugated Composites for the Skin of Morphing Wing

Changwei Mou, Bangfeng Wang, Nanjing University of Aeronautics & Astronautics (China).

Morphing wings are able to adaptively change aerodynamic characteristics in various flight conditions to improve the vehicle's comprehensive performances. But large deformation of morphing wings challenges the features of skins greatly. Conventional skins usually play two roles. One is to maintain the aerodynamic wing shape. The other is to withstand (especially withstand bending loads) and transfer aerodynamic loads. However, high flexibility in deformation direction, which the conventional skins do not possess, is essential for the skins of morphing wings. Corrugated composites are very flexible in the corrugation (longitudinal) direction and highly resistant against bending loads in the direction (transverse) perpendicular to the corrugation. And corrugated composites are applicable to the skins of morphing wings. In this investigation, corrugated fiberboard (basal body) was studied. Based on the energy method, analytical model for corrugated composites basal body was established to solve the tension deformation capability. The relationship between the force and elongation amount of the basal body in the longitudinal direction was researched. The transverse bending deformation capability of the basal body was also computed by analytical model of flexural rigidity. To verify the correctness of the analytical models, corrugated skin specimens were manufactured. The skin was made of a basal body and elastic rubber. The basal body was composed of composite materials enhanced by glass fibers. The tensile test and bending test were carried out, and the experiment results showed a great accordance with the computation results. And the optimization of the corrugated structure was done to obtain a basal body that had the best mechanical properties by both analytical and experimental methods.

274

Effects of Bias Force on the Transformation Characteristics of Prestrained NiTi/NiTi Alloy

Zhu Yan, Lishan Cui, Yanjun Zheng, China University of Petroleum (China).

This study was a first attempt to prepare bulk NiTi/NiTi shape memory alloy (SMA) laminates with a macroscopic heterogeneous composition by explosive welding. Differential scanning calorimeter (DSC) was used to study the reverse martensitic transformation characteristics of the deformed NiTi-1/NiTi-2 alloy. Results showed that variation of the thickness of NiTi-1 or NiTi-2 changed the internal bias forces significantly between the NiTi plates, and the different constraint between NiTi-1 and NiTi-2 strongly affected the reverse martensitic transformation behavior of the NiTi/NiTi SMAs. DSC measurements showed that after deformation, the reverse martensitic transformation temperatures of the composite decreased with the decreasing thickness of NiTi-2 and increased with decreasing thickness of NiTi-1.

276

Fabrication and Optical Properties of the Germanium/Polystyrene Sphere Photonic Crystal Composites

Xiangdong Meng, Liu Xin, Wuhong Xin, Li Yao, Harbin Institute of Technology (China); Xiangdong Meng, College of Physics Jilin Normal University (China).

In this paper, the photonic crystal of germanium/polystyrene sphere (PS) composites were prepared by magnetron sputtering method through the interstitial spaces between PS assembled colloidal crystal on glass substrates. The different PS diameters (320nm, 368nm, 560nm) and sputtering times had important effects on the formation and optical properties of the photonic crystal (PC) composites. The morphologies of surface and cross section of the PC composites were characterized by scanning electron microscopy (SEM). The position and width of the photonic band gap (PBG) of PS composites were investigated by UV-VIS infrared spectrophotometer. Our result shown that germanium clusters do not penetrate deep into the colloidal crystal template, resulting in a continuous dense thin film along the surface of the top layer. But interesting phenomena is found that in-situ growth of germanium on PS surface and keep same morphologies with PS colloidal crystal. For the different PS diameters, the different growth rate of germanium was investigated. With an increase of the sputtering times, PBG of the Ge/PS composites have red shift phenomena for same PS diameter.

277

Vibration Characteristics of Ni-Ti Pseudo-Elastic Wire Inter-Weaved Fabric Composites

Lei Xu, Rui Wang, Qihong Yang, Dong Li, Tianjin Polytechnic University (China).

For the actuator and damper use, Ni-Ti alloy is commonly considered to have the best driving force and stiffness among many shape memory alloys (SMA). Recently, Ni-Ti SMA can be commercially extruded into fine wires, and be easily embedded into composite panel or shell structures to enhance the damping (with its pseudo-elasticity), or to design smart composite structures that can change certain property to meet external stimuli (with its shape memory effects).

In this paper, vibration characteristics of Ni-Ti wire in-weaved glass yarn woven fabric/epoxy composite are investigated. Two types of woven structure are adopted ---- include the laminated plain weaved and the interlocked. First, the Ni-Ti pseudo-elastic wire energy dissipation behaviors are obtained by static and

dynamic mechanical tensile test. Then, three $\Phi 0.2\text{mm}$ Ni-Ti pseudo-elastic wires, adopted as warp yarns, fabricated with glass yarns to form composite preform. After the composites manufactured by molding and tested by a dynamic mechanical analyzer (DMA) instrument, they are cut into a $80\text{mm}\times 20\text{mm}\times 1.2\text{mm}$ shaped cantilever plate samples for the free vibration test.

The experimental results indicate two following issues:

(I) The energy dissipation capacity of the wire can be significantly improved by increasing the strain and strain speed, but slightly affected by loading frequency;

(II) Although the Ni-Ti volume fractions are less than 2% in the composites, the in-weaved wires result in the increment of the storage modulus and the change of the loss factor. In the buckling vibration of the composites cantilever plates, the damping effects of Ni-Ti pseudo-elastic wires also vary with the woven structures: compact woven structure, big undulation and suitable location of the in-weaved wire would cause a good passive control of certain vibration.

278

Functional Materials for Lithium-Ion Battery

Huisheng Zhou, Xinghua Xie, Minhui Yang, Anhui University of Science and Technology (China).

Nanoproducts spherical spinel lithium manganese oxide (LiMnO_2) with about 20nm in diameter was synthesized by explosive method. The growth of lithium manganate via detonation reaction was investigated with respect to the presence of an energetic precursor, such as the metallic nitrate and the degree of confinement of the explosive charge. The detonation products were characterized by scanning electron microscopy. Powder X-ray diffraction and transmission electron microscopy were used to characterize the products. Lithium manganate with spherical morphology and more uniform secondary particles, with smaller primary particles of diameters from 10 to 30 nm and a variety of morphologies were found. Lithium manganate with a fine spherical morphology different from that of the normal spinel is formed after detonation wave treatment due to the very high quenching rate. It might also provide a cheap large-scale synthesis method. Explosive detonation is strongly nonequilibrium processes, generating a short duration of high pressure and high temperature. Free metal atoms are first released with the decomposition of explosives, and then these metal and oxygen atoms are rearranged, coagulated and finally crystallized into lithium manganate during the expansion of detonation process.

280

Electro-Mechanical Analysis of a Dielectric Elastomer Membrane Undergoing Large Deformation

Tianhu He, Cheng Chen, Leilei Cui, Lanzhou University of Technology (China).

In the family of smart material transducers, muscle-like transducers, i.e., dielectric elastomer transducers, have attracted much interest in recent years due to their many fascinating attributes such as large strain, fast response, high efficiency, simple, potentially low cost and lightweight. The essential part of dielectric elastomer transducers is a dielectric membrane sandwiched between two compliant electrodes. Subject to a voltage, the dielectric membrane reduces its thickness and expands its area, converting electrical energy into mechanical energy. Due to large deformation, nonlinear equations of state, and diverse modes of failure, modeling the electro-mechanical response for dielectric elastomer transducers has been challenging. In this paper, the electro-mechanical behavior of a dielectric membrane deformed by the application of voltage and weight into an out-of-plane, axisymmetric shape is

investigated. Ogden model is adopted to formulate the state equations by combining kinematics and thermodynamics. A set of ordinary differential equations characterizing the large out-of-plane deformation of the dielectric membrane are derived, and shooting method is applied to solving the equations numerically. The obtained results show that the field in the membrane is very inhomogeneous, which leads to most part of the membrane functioning inefficiently. Several potential modes of failure, including electrical breakdown, loss of tension, and rupture by stretch, are illustrated. This can be used to optimize the design of electromechanical transducers for specific applications.

281

Large Deformation Analysis of a Dielectric Elastomer Membrane-Spring System

Tianhu He, Leilei Cui, Cheng Chen, Lanzhou University of Technology (China).

Due to the capability of high strain, dielectric elastomers are promising for applications as transducers in cameras, robots, valves, pumps, energy harvesters and so on. The dielectric elastomer transducers are based on the deformation of a soft polymer membrane contracting in thickness and expanding in area, which is induced by the application of a voltage across the two compliant electrodes coated on both sides of the membrane. This paper focuses on the large deformation analysis of a dielectric elastomer membrane-spring system. The system is constructed from attaching a disk in the middle of a circular dielectric membrane and then connecting the disk with a spring. This configuration can be potentially used as a key part in valves. The basic governing equations describing the large out-of-plane deformations are formulated, and the obtained equations are solved numerically. The relations related to the displacement of the disk, the spring force, the applied voltage, and the parameters of spring including stiffness and initial length are illustrated. The results show the expected displacement of the disk can be achieved by adjusting the spring and the applied voltage individually or simultaneously, and the parameters of the spring, that is, stiffness and initial length, play an important role in the performance of the membrane-spring system.

282

Bi A-SPAES/TiO₂ Hybrid Membranes for Direct Methanol Fuel Cell

Ni Zhang, Huiling Liu, Zhi Xia, Junjing Li, Harbin Institute of Technology (China).

A series of bisphenol A-based sulfonated poly(arylene ether sulfone) (bi A-SPAES, $D_s=0.4$)/TiO₂ hybrid membranes with various contents of nano-sized TiO₂ particles were prepared and characterized through sol-gel reactions. Scanning electron microscopy (SEM) images indicated the TiO₂ particles were well dispersed within polymer matrix. These composite membranes were evaluated for proton exchange membranes (PEM) in direct methanol fuel cell (DMFC). These membranes showed good thermal stability and mechanical property. It was found that the water uptake of these membranes increased with the increase of the TiO₂ contents in the hybrid membranes. Meanwhile, the introduction of inorganic particles increased the proton conductivity and reduced the methanol permeability of the hybrid membranes. The proton conductivities of these membranes were improved with the increase of TiO₂ particles content and temperature. The proton conductivity of bi A-SPAES/TiO₂ hybrid membranes with 8 % TiO₂ is elevated from 0.054 S/cm to 0.067 S/cm at 100 °C. Moreover, the methanol diffusion coefficients (5.8×10^{-9} cm²/s) of bi A-SPAES/TiO₂ hybrid membranes with 8 % TiO₂ are much lower than that of pure bi A-SPAES membrane

(4.2×10^{-8} cm²/s). Bi A-SPAES/TiO₂ hybrid membranes were therefore proposed as a candidate of material for PEM in DMFC.

283

The Performance Study of Electrospun Membrane IPMC and Cast Membrane IPMC

Guifen Gong, Danyu Liu, Yujun Zhang, Harbin Univ. Sci. & Tech. (China).

The cast and electrospun membranes of EVOH-g-nSPEG were prepared respectively by solution cast method and electrospun method. The cast membrane IPMC and electrospun membrane IPMC were prepared by penetration-reduction process. The micro-morphology of these two IPMCs was studied by scanning electron microscope (SEM). The surface resistance (R_s) and critical response voltage (U_R) of IPMC electrode were tested and calculated by four electrode method and intercept method. And the bending stress of IPMC was tested by electrodeformation experiment. The results indicated that the surface of cast membrane IPMC had better smoothness and compactness than that of electrospun one. The electrospun membrane possessed compact surface while loose inside. The U_R for electrospun membrane IPMC was lower than that of cast one. And the U_R for both IPMCs increased with the R_s increase when testing under the same membrane structure and metal electrode. The cast membrane IPMC had higher bending stress with the maximum value being 4.75MPa while being only 0.66MPa for electrospun membranes.

284

A Method of Calculating Residual Stresses through Elastic Modulus Measured by Nanoindentation

Yanshen Wang, Yuxian Gai, Harbin Institute of Technology at Weihai (China); Yanshen Wang, Shiliang Qu, Harbin Institute of Technology at Weihai (China); Shen Dong, Yingchun Liang, Harbin Institute of Technology (China).

Residual stress is a very important effect that influence the performance of ultra-precision micromachined devices, especially in the filed of aeronautics and astronautics. Nanoindentation is a good method for characterizing residual stresses with large gradient that distributed in a very confined area. Many researchers do a lot of works in such scope. In our previous work, a formula was brought out to correlate residual stresses with elastic modulus measured by nanoindentation method. In this paper, the formula will be validated through X-ray diffraction (XRD) method.

In this paper, aluminum bulks with about 15mm×15mm squared shape with a thickness of about 3.5mm were used as samples. They were machined to be mirror surface on one side with the roughness of $R_a=3.76$ nm through ultra-precision diamond turning. Samples were compressed and stretched by load instruments. Nanomechanical properties such as elastic modulus in the areas on the mirror surface of the compressed and stretched samples were both measured by a commercial nanomechanical test system (TriboIndenter, Hysitron Inc.). For comparison, the elastic modulus of the origin samples were also tested. Using the formula, then, residual stresses in such area can be got. After that, the samples above were all tested by the XRD instrument (X'Pert, Philips Inc.). The mean values of residual stresses on the mirror surface were calculated through the acquired experimental data. Comparing the residual stresses that obtained through nanoindentation and XRD methods, their difference was no more than 10%, which showed that the formula is suitable for characterizing residual stresses of materials even it has high plasticity.

Through the paper, the formula correlating residual stresses with elastic modulus values measured by nanoindentation method was

validated by XRD method. Experimental results also showed that there are no direct relations between hardness values got from nanoindentation experiments and residual stresses. More details on the nature about the relation between elastic modulus and residual stresses are under investigation in our group.

285

Plane Magneto-Electro-Elastic Moduli of Fiber Composites with Interphase

R. Guinovart-Díaz, R. Rodríguez-Ramos, J. Bravo-Castillero, Universidad de La Habana. Facultad de Matemática y Computación. Vedado (Cuba); F. J. Sabina Universidad Nacional Autónoma de México (México); H. Camacho Montes, Universidad Autónoma de Ciudad Juárez (México); Yue-Sheng Wang, Beijing Jiaotong University (China).

Combining two or more distinct piezoelectric and piezomagnetic (magnetostrictive) constituents, piezoelectric/piezomagnetic composite materials can take the advantages of each constituent and consequently have superior coupling magnetoelectric effect as compared to conventional piezoelectric or piezomagnetic materials. In the present paper, by using the asymptotic homogenization method, the derivation of the plane effective properties for three-phase magneto-electroelastic fiber unidirectional reinforced composite with hexagonal and square cell symmetry is reported. Closed analytical expressions and universal relations for the effective coefficients are given. Matrix and inclusions materials belong to symmetry class 6mm. Numerical calculations for all plane effective properties are done. Some comparisons with other theoretical models are presented. It is remarkable that the analytical formulae derived for all effective properties have a simple form. The computational implementation is easy. Besides its theoretical importance, they can be used for checking the implementation of experimental, numerical and analytical models.

287

Capillary Adhesion Analysis in the MEMS/NEMS

Shiqiao Gao, Xinjian Liang, Lei Jin, Beijing Institute of Technology (China).

Capillary action exists in all scales, but is particularly important in the micro-nano scale. With the rapid development and in-depth study of the MEMS/NEMS technology, the MEMS/NEMS devices have been used widely. In the processing and use of the MEMS/NEMS devices, due to the capillary force, the devices will occur adhesion failure in different degrees, which affects the reliability and commercialization of the MEMS/NEMS devices. In view of the capillary adhesion to the important impact on the performance of MEMS/NEMS device, this article investigated the law of capillary adhesion mechanics in micro/nano scale, the results of adhesion failure to the MEMS/NEMS device performance, as well as capillary adhesion control technology.

288

Research on Piezoelectricity Materials Films of MEMS Surface Acoustic Wave Gas Sensor

Chengjun Qiu, Dan Bu, Hongmei Liu, Yafei Feng, Heilongjiang University (China).

The velocity and frequency of surface acoustic wave (SAW) gas sensor can be varied with the component of detecting atmosphere, the high qualitative analysis implemented for different gases is determined by property of piezoelectricity materials films and the selectivity of gas sensing film. Thus, one important problem is to fabricate the sensing films for the gas sensor, and the other one is to develop piezoelectricity materials films for SAW device. Through

investigating the sensing principle of SAW device, a novel structure for the SAW gas sensor based on the PZT film is provided. The improved Sol-Gel process method of PZT piezoelectric thick film manufacture on the structure of Au/Cr/SiO₂/Si multilayer membrane and the quality of PZT piezoelectric thick film is influenced with density of PVP has been discussed, the relationships of dielectric, ferroelectric and piezoelectric properties between the thicknesses of films were also given systematically. The MEMS process technique was also used in the structure base on the silicon which including thermal oxidation, optical lithography and hydro-etching etc. Thus the fabrication problem of compatibility between piezoelectric thick films and MEMS processes was resolved. The maximal piezoelectric constant d_{33} of the thick films was 201pC/N that obtained by the loading method, the maximal volume density was 4.31g/cm³ tested by buoyancy method, and the maximal dielectric constant was 808. The remanent polarization and the coercive field of PZT thick films were up to 60 μ C/cm² and 23kV/cm at 25V respectively. The results demonstrate that the silicon-based PZT thick films possess well property in piezoelectric, ferroelectric and dielectric capacities which suitable for SAW device for farther application.

289

Protein Absorption and Fouling on Poly(Acrylic Acid)-Graft-Polypropylene Microfiltration Membrane

Yanjun Liu, Chunying Lv, Jia Yang, Huiying Ma, Tianjin Polytechnic University (China); Xueqi Fu, NanKai University (China).

A pH-sensitive membrane, poly (acrylic acid)-graft-polypropylene hollow fiber microfiltration membrane was prepared by UV-photo-initiation. The zeta potential of grafted membranes was calculated by streaming potential which was measured by internal and external Electrodes. Bovine serum albumin (BSA) was chosen as the model protein to investigate the BSA absorption and fouling behaviors on membranes. The results show that the hydrophilicity of grafted membrane surface was improved by poly (acrylic acid) chains, but part of membrane pores were blocked shown by SEM photos. The grafted membranes have markedly pH-dependence on the water permeability as pH was altered from 1 to 11, so that the membrane pores seem to be closed in acid solution but be open in alkaline solution. The zeta potential of grafted membranes indicates the membrane surface is negatively charged in most pH range. Electrostatic interaction energy calculated by DLVO theory shows the electric interaction force between grafted membrane and BSA is attractive. With the rise of grafting degree, the electric attractive force between grafted membrane and BSA increases at pH 3 and decreases at pH 8, while it keeps basically unchanged at pH 4.7. As a result, the grafted membrane have a lower BSA absorption and lower flux decrease and better antifouling behavior at pH 8 than pH 3 by compared with the ungrafted membrane. In conclusion, the absorption and fouling behavior of BSA on membranes are pH-dependent, due to the pH-dependence of membrane charge, and the conformation and charge status alternation of the of BSA and grafting chains.

290

A New Digital Silicon MEMS Gyroscope

L.F Wu, Beijing University of Posts and Telecommunications (China); F.X Zhang, Beijing Information Science and Technology University (China).

This paper presents a new, digital silicon MEMS gyroscope, which consists of micro-sensor, signal processing circuit and micro-processor (MSC1214). The gyroscope structure allows it to achieve roat rate and yaw rate of rotating carrier. That is, it can

detect the attitude of a rotating carrier. The non-linearity of the gyroscope is measured to be better than 0.5% and sensitivity of the gyroscope is 20mV/(°/s) at atmospheric pressure, measuring range of yaw rate and roat rate of rotating carrier is ± 500 °/s and 40 Hz, respectively. The key techniques of MEMS gyroscope are presented.

291

Nitrogen Dioxide Sensing Properties and Mechanism of Nickel Phthalocyanine Film

Chengjun Qiu, Yanwei Dou, Wei Qu, Yanmei Sun, Heilongjiang University (China).

A Nitrogen Dioxide gas sensor on silicon substrate was fabricated by MEMS technology; the principle, configuration and process of sensor were described. The Nickel Phthalocyanine (NiPc) films and their derivatives, as typical organic multifunctional films, possess special properties, including optic, electric, acoustic, gas sensitive, magnetic and chemical etc. Furthermore, they are p-type semiconductors with rather high thermal and chemical stabilities; thus, the fabrication of Nickel Phthalocyanine film can be obtained by vacuum evaporation. The sensitive characteristics of the gas sensor were studied and the experiment results were confirmed by the nitrogen dioxide sensitive mechanism of the sensor. When NO₂ gas concentration changes from 0ppm to 100ppm at room temperature, the resistance decreases obviously from 60k to 5k. The reason is that NO₂ is an oxidizing gas and NiPc is a p-type semiconductor, in which the carrier's hole will be increased when the NiPc adsorbed NO₂, and thereby the conductivity is enhanced. The sensitivity of NiPc films were affected by different temperature, serials temperature experiment results show that the highest sensitivity of NiPc films is 110°C which is the optimizing working temperature. The sensitivity of NiPc films were also affected by annealing process. The heat treatment results indicate that the sensitivity of NiPc films increase from 0.08 to 0.36 when NO₂ concentration is 20ppm. The response and recover time of NiPc thin film gas sensor is 13s and 16s respectively at 65ppm of NO₂ concentration. After annealing at 300°C for one hour, the response and recovery time increase to 1.8 minute.

292

Effect of Structure on the Optical Properties of Ni-Mn-Ga Alloy

Z.Y. Gao, C.L. Tan, C. Liu, J.H. Sui, W. Cai, Harbin Institute of Technology (China); C.L. Tan, Harbin University of Science and Technology (China).

Ni-Mn-Ga ferromagnetic shape memory alloy (FSMA) is a kind of novel material which possesses thermoelastic martensitic transformation and ferromagnetic transition. Despite the giant magnetic-field-induced strain developed in Ni-Mn-Ga alloys, however, little information is obtained about optical properties of Ni-Mn-Ga alloys as candidate materials in digital information storage. In this letter, the optical reflectivity of Ni-Mn-Ga alloys in martensite and austenite states has been investigated. The results reveal that the martensitic transformation causes significant changes of the optical properties for Ni-Mn-Ga alloys. The maximum reflectivity difference between martensite and parent phase is about 24%, indicating the promising application of the Ni-Mn-Ga alloys as phase-transition information storage materials. The calculated DOS shows that the remarkable effect of martensitic transformation on the optical properties is attributed to the change of the Ni 3d partial DOS between austenite and martensite.

293

Structural and Mechanical Characterization of Zinc Oxide Nano-Films on Glass Substrates

Zhansheng Guo, Shanghai University (China); Yanping Liao, Shenzhen Tianma Micro-Electronics Co. (China); Jie Li, Shanghai University (China).

Mechanical properties of zinc oxide (ZnO) nano-films on glass substrates grown by rf magnetron sputtering were studied by nanoindentation. Surface morphologies and crystalline structural characteristics were examined using atomic force microscopy (AFM) and X-ray diffraction (XRD), respectively. The crystalline structures of the ZnO nano-films are well ordered with a high c-axis (002) orientation at 34.78 degree. The surface morphologies of ZnO thin films are smooth and grains grow and distribute uniformly. The hardness and Young's modulus of ZnO nano-films were ranged from 8.2 to 10.4GPa and 105 to 120GPa, respectively.

294

A Novel Strategy to Design Bipolar Molecules for Highly Efficient OLEDs

Ziyi Ge, Zhong Xin, College of Chemical Engineering, East China University of Science and Technology (China); Masa-aki Kakimoto, Tokyo Institute of Technology (Japan); Toshiyuki Akiike, Display Research Laboratories, JSR Corporation (Japan).

In the past decade, considerable efforts have been made to develop phosphorescent organic light-emitting diodes (OLEDs), in which the significant point to emphasize is to prevent the back excitation transfer from the guest molecules of heavy metal complexes to the host materials. Bipolar molecules bearing the suitable electron-rich and -deficient moieties in the molecular structures have attracted much attention, since a balanced density of charge and high efficiency could be attained by simultaneously supplying the electron and hole to electroluminescent (EL) materials sandwiched between two electrodes. To date, there is a great limitation to illustrate the structure-performance relationship in molecular design for OLEDs.

Herin, we will first present a new strategy to design bipolar molecules for highly efficient OLEDs, which encompasses theoretical modeling, synthesis, spectroscopy and device fabrication/characterization based on 5 bipolar benzimidazole-triphenylamine and 8 bathophenanthroline-carbazole-triphenylamine derivatives.

First, 5 star-shaped bipolar benzimidazole-triphenylamine derivatives, TIBN, Me-TIBN and DM-TIBN, m-TIBN and Me-TIBN containing hole-transporting triphenylamine and electron-transporting benzimidazole moieties are designed based on the theoretical calculation of DFT, and then successfully prepared. The theoretical calculation on energy levels of TIBN derivatives affords helpful ideas to molecular design with the favorable localization of HOMO and LUMO and pre-defined enhancement of triplet energy gap. TIBN derivatives were employed as the hosts to fabricate phosphorescent OLEDs by two methods of spin-coating and vacuum deposition. Notably, the spin-coated Me-TIBN and DM-TIBN devices exhibit much better performance than respective vacuum-deposited ones, in which the spin-coated DM-TIBN device (47500 cd·m⁻², 27.3 cd·A⁻¹, 7.3 lmW⁻¹) is outstanding with respect to other seminar work for solution-processed OLEDs.

To further demonstrate our theory, we designed 8 bathophenanthroline-carbazole/triphenylamine derivatives, the electronic structures of eight bathophenanthroline derivatives were elucidated by DFT calculations, and four representatives of which, CZBP, m-CZBP, m-TPAP and BPAP were synthesized and employed as the hosts to afford highly efficient phosphorescent OLEDs. The calculated molecular orbital energies agree well with the experimental results, which further demonstrates that the localization of HOMO and LUMO at the respective hole- and

electron-transporting moieties is desirable in bipolar molecular designs.

296

A Nonlinear Magneto-Mechanical Coupling Constitutive Model for Soft Ferromagnetic Materials

Haomiao Zhou, China Jiliang University (China); Haomiao Zhou, Youhe Zhou, Lanzhou University (China).

To better utilize soft ferromagnetic materials in engineering application, their constitutive relations are essential for predicting the magneto-mechanical characteristics of soft ferromagnetic materials subjected to pre-stress and magnetic field. However, it is usually difficult to develop a good and complete phenomenological constitutive model for soft ferromagnetic materials because their elastic and magnetic behavior is coupled and nonlinear. In this paper, a nonlinear and coupled model is suggested to describe the constitutive relations for a soft ferromagnetic materials rod subjected to an axial pre-stress and then located in an axial magnetic field. The new model uses a Taylor series expansion of independent variables of stress and magnetization to obtain a polynomial relation in terms of elastic Gibbs free energy, and then substitutes appropriate transcendental function for some polynomial terms to achieve a more compact representation based on magnetoelastic coupling mechanism. In detail, from the viewpoint of magnetic domains, a nonlinear part of the elastic strain produced by the pre-stress is related to the domain wall motion and is responsible for the change of the maximum magnetostrictive strain with the pre-stress, and the reduction of magnetostrictive strain under the maximum magnetostrictive strain is related to the domain rotation. The numerical simulation exhibits that the predicted magnetostrictive strain and magnetization curves for various pre-stresses (compressive and tension) are in good agreement with the experimental data given by Kuruzar et al and Jiles et al, respectively. In comparison with the previous models, the new model can more effectively describe not only the effect of the pre-stress on the magnetostrictive strain and the magnetization but also the effect of the stress and the magnetic field on the Young's modulus, i.e. the ΔE effect. Additionally, the model can be simplified to Zheng-Liu model for giant magnetostrictive materials.

297

Calculation of Hysteresis Losses for Terfenol-D Ultrasonic Transducer

Jianbin Zeng, Baodong Bai, Haiquan Zeng, Shenyang University of Technology (China).

Hysteresis losses are the main source for heating the Terfenol-D ultrasonic power transducer. A new method of calculation for hysteresis losses, which based on Jiles-Atherton hysteresis model and electro-magnetic field finite element analysis, is proposed in this paper. The hysteresis losses obtained by this method can be used as thermal sources in electro-thermal finite element analysis.

298

Research on a Distributed Measuring System for the Deformation Survey of Corrugated Composites

Jintao Zhao, Bangfeng Wang, Ruijun Ge, Changwei Mou, Nanjing University of Aero. and Astron (China).

The corrugated composites skin has large deformation capability in transverse direction and huge bending stiffness in longitudinal direction. So it can satisfy the deformation and load requirements of the morphing wings skin. Yet an efficient measuring method is needed to obtain real-time perception of the skin for the control of

the deformation of the morphing wings. In this paper, a measuring system for corrugated composites skin was studied. A kind of distributed strain gauges array and its signal conditioning circuit were designed for measuring the deformation of the corrugated composites. The strain gauges array was pasted on the wave peak and wave trough of the corrugations where the deformation is the most significant. The relation between the global deformation of the skin and the local strains at the wave peak and wave trough positions of the corrugation was established. The calibration of this kind of distributed measuring system is made as well. A corrugated composites skin was manufactured and the local strains of the corrugations were measured under a series of tensile forces with the measuring system. And the deformation of the whole corrugated composites skin was obtained according to the relationship established in the paper. The results from the measuring system and the deformation of the corrugated composites measured by the LDS (Laser Displacement Sensor) were compared. The comparison results showed that the measuring system was able to provide quite accurate deformation of the corrugated composites skin. It could serve as an efficient real-time detecting method for the research of corrugated composites and morphing wings.

299

FRP Debonding Monitoring Using OTDR Techniques

Shuang Hou, Jinping Ou, Dalian University of Technology (China); Shuang Hou, C.S. Cai, Louisiana State University (USA).

Debonding failure has been reported as the dominant failure mode for FRP strengthening in flexure. This paper explores a novel debonding monitoring method for FRP strengthened structures by means of OTDR-based fiber optic technology. Interface slip as a key factor in debonding failures will be measured through sensing optic fibers, which is instrumented in the interface between FRP and concrete in the direction perpendicular to the FRP filaments. Slip in the interface will induce power losses in the optic fiber signals at the intersection point of the FRP strip and the sensing optic fiber and the signal change will be detected through OTDR device. The FRP pulling tests and four-point bending tests were conducted to verify the proposed monitoring method. It is found that the early debonding can be detected before it causes the interface failure. The sensing optic fiber shows signal changes in the slip value at about 0.08-0.2 micrometer which is beyond sensing capacity of the conventional sensors. The tests results show that the proposed method is feasible in slip measurement with high sensitivity, and would be cost effective because of the low price of sensors used, which shows its potential of large-scale applications in civil infrastructures, especially for bridges.

300

Marine Biofouling on the Fluorocarbon Coatings Comprising PTFE Powder

Zhan-ping Zhang, Yu-hong Qi, Dalian Maritime University (China).

An International Convention held on 5 October 2001 required to ban the application of TBT-based antifouling paints from 1 January 2003, and the presence of such paints on the surface of the vessel from 1 January 2008. Thus, the paint industry has been urged to develop TBT-free products able to replace the TBT-based ones, but they should yield the same economic benefits and cause less harmful effects on the environment.

One of the strategies is to utilize low-surface-energy coatings, also known as fouling-release coatings. The significance of such coatings becomes apparent when the lack of universally applicable and environmentally friendly protection against biological and other fouling is appreciated. Low-surface-energy coatings are an

attempt to prevent the adhesion of fouling organisms by providing a low-friction, ultra-smooth surface, on which organisms have great difficulties in settling. PTFE is one of polymers with lowest surface energy and is used for low-surface-energy coatings. However, except surface energy, morphology and roughness of coatings can influence the settlement of marine organisms. Many investigations indicate that diatom play very important role during biofouling. Ectocarpus is one of main fouling macro-algae which are found on ship's hull.

In this work, three fluorocarbon coatings were developed with respectively 10%, 20% and 30% PTFE powder. Influence of content of PTFE on microstructures and roughness of coatings was investigated using SEM and roughometer. It was studied that the effect of coating roughness on settlement of benthic diatom and Ectocarpus with biological microscope, stereo microscope, image processing and spectrophotometer. Results indicated that the surface roughness of coatings decreases and the quantity of benthic diatom and Ectocarpus reduces attaching onto the coating with the increase of content of PTFE in paint studied. Benthic diatoms attached much more on horizontal specimen than on vertical one; they prefer to settle onto the coatings that there are lots of micro-cracks in it. These results are helpful for developing new non-toxic antifouling paints.

301

Investigation on Anti-corrosion Property of Nano-TiO₂ Fluoro-carbon Coatings

Zhanping Zhang, Yuhong Qi, Xuepeng Du, Dalian Maritime University (China).

To meet the need of long-term anticorrosive protection of steel, a heavy-duty anticorrosive coatings system was developed with Fluorocarbon top paint which was modified by Nano-TiO₂. The corrosive characteristic in seawater of low carbon steel coated with the system was investigated by the exposition tests and Electrochemical Impedance Spectroscopy (EIS). The exposition tests include salt fog test for 180 days, exposition in natural seawater for 180 days at 70°C to simulate boundary plating between heated bunker tank and ballast tank in double bottom, and cycle test for 180 days as simulating the condition of actual ballast tank runs for two weeks with natural seawater and one week empty. The temperature of the seawater is to be kept at 35°C. EIS tests were carried out for initial specimen and the specimen after exposure test for 180 days with IM6eX Electrochemical Workstation with COating & Laminate Tester (COLT). Test data were treated with Thales software package.

The results show that the protective system with fluorocarbon top coating modified by Nano-TiO₂ has much better endurance than the reference system with fluorocarbon top coating not modified by Nano-TiO₂. There isn't any rusting and blistering on the surface of former coating, the coating system remains in "GOOD" condition. But some rusting and blistering were found on the surface of reference coating. EIS results indicated that the impedance of the Nano-coating system decreases much less than that of the reference one. The Nano-coating system is hopeful to meet the need of new coatings standard and to provide a target useful coating life of 15 years for ship's ballast.

303

The Study of Molecularly Imprinted Polymers on Thymidine

Zhenhe Chen, Liquan Sun, Aiqin Luo, Beijing Institute of Technology (China).

Molecularly imprinted polymers (MIPs) are synthesized macromolecular polymers with tailor-made receptor sites. MIPs, with perfect physical and chemical stability and high selectivity based on molecular recognition, can bear high temperature, high

pressure, strong acids and alkali and organic solvents. MIPs, therefore, have been widely used in column separation and analysis, drug delivery, chemical sensors and catalysts.

3'-fluoro-3'-deoxythymidine (FLT) is a very useful drug of tumor diagnosis in positron emission tomography. In terms of bulk polymerizing method, molecularly imprinted polymers were prepared using thymidine as template which is quite a similar analogue of FLT. Unfortunately, the synthesized polymers show poor adsorption capacity to thymidine in spite of every efforts. Therefore, we perform another strategy to synthesize MIPs, that is, using 5'-tosylthymidine as the template to increase solubility of thymidine part in non-proton solvent.

Through adsorption experiments, the polymers were evaluated by adsorption rate and adsorption capacity, the optimum molar ratio of template, functional monomer and cross linker is 1:6:30. The adsorption experiment indicated that using trimethylolpropane trimethacrylate (TRIM) as the cross linker, the imprinted polymer's adsorption capacity for thymidine is 0.120mg·g⁻¹; the non-imprinted polymer's adsorption capacity is 0.103mg·g⁻¹; polymers suitable for HPLC solid phase were synthesized using ethylene glycol dimethacrylate (EDMA) as the cross linker, retention time of the imprinted polymer for thymidine is 8.532min, while non-imprinted polymer is 7.112min. The results show that the imprinted polymers are able to bind thymidine selectively.

304

The Micro Mechanical Environment on the Comb Capacitive Micro-Machined Gyroscope

Haipeng Liu, Shiqiao Gao, Shaohua Niu, Lei Jin, Beijing Institute of Technology (China).

As a kind of typical micro-electro-mechanical sensor, the characteristics of comb capacitive micro-machined gyroscope are lower cost, small size, lower power, high capability on overloading and high adaptability, which make it widely applied in military and civilian fields. The typical working mode of capacitive micro-machined gyroscope is electrostatic driving and comb capacitive detection.

With the in-depth researches on the micro-electro-mechanical sensors, a lot of mechanical problems are encountered inevitably. Especially for the comb capacitive micro-machined gyroscope, the particularity of its structure and micro size determines the characteristics of the mechanical environment. The reduction in the structural size of the comb capacitive micro-machined gyroscope, not only leads to changes in scale, but also results in changes in the system mechanical environment, mechanical properties, mechanical behaviors and mechanical laws. These changes will lead to special characteristics and laws in mechanics of the comb capacitive micro-machined gyroscope. In the world of micro scale, the mechanical environment of the comb capacitive micro-machined gyroscope has changed dramatically.

With the reduction of structural size, the ratio of surface force and body force has increased clearly. Comparing with the roles of body forces, the roles of surface forces in the micro-electro-mechanical sensors become more and more important. In this micro scale condition, some micro forces which have been neglected in macro state, such as electrostatic force, Van de Waals force, Lorentz-force, and capillary force, may not be neglected. For example, the electrostatic force which is often neglected in macro state has become a familiar actuating mode in the comb capacitive micro-machined gyroscope. During the vibration of micro comb, the air-damping force has become a main factor influencing the dynamic properties of micro-gyroscope. The micro forces in the comb capacitive micro-machined gyroscope will influence its operation and working performance.

The micro forces, such as electrostatic force, Van de Waals force,

Lorentz-force, capillary force and air-damping force were analyzed, and the action ranges of these micro forces were obtained. The influences of these micro forces on the working performance of the comb capacitive micro-machined gyroscope were discussed.

305

The Electromagnetic Design of Magneto-Rheological Mount and Its Open-Loop Semi-Active Control

Ling Zheng, Yinong Li, Yong Hu, Chongqing University (China).

Magneto-Rheological mount is a new type of semi-active and intelligent vibration isolator. It can adjust damping to reduce unwanted vibration from engine by supplying required input currents. The performance of the MR (Magneto-Rheological) mount is much better than the conventional rubber mount or the hydraulic mount due to its controllable and flexible. In this paper, a novel MR engine mount with the fluid mode-type for a sedan is devised, manufactured and characterized. Some important parameters are optimized to meet the requirements of electromagnetic design so that the magnetic flux density distribution in different areas is more reasonable and no magnetic saturation occurs in these areas. Electromagnetic finite element analysis verifies the effectiveness of the magnetic circuit design. The dynamic performances of the MR engine mount in frequency domain are investigated experimentally. The results show that the dynamic stiffness and the retardation angle of the MR engine mount can change continuously according to different input current, a wide dynamic range is demonstrated to reach an effective vibration isolation for engine. In addition, an open-loop control strategy based on engine rotation speed measurement is presented and the control system is performed in hardware and software. The experimental and theoretical results identified the effectiveness of such a semi-active vibration isolation system.

306

Design and Fabrication of a Microfluidic Chip Driven and Adhered by Dielectric Elastomers

Bo Li, Hualing Chen, Jiuhui Wu, Zicai Zhu, Xi'an Jiaotong University (China).

This paper presents the design and fabrication of a microfluidic chip which is driven and adhered by dielectric elastomers (DEs). DE is a kind of Electroactive Polymers (EAPs) which is soft, flexible and known as "Artificial Muscles" for EAP could transfer electric energy into mechanical energy. During the past several years they are explored in applications ranging from worm robot and vibration control to switchable optics and haptic interface. So far, however, little research has been reported on DE application in micro/nano devices.

This microfluidic chip was mainly composed of three layers. The bottom layer was SU-8 photoresist, on which a pump chamber of 5mm diameter and a pair of nozzle/diffuser were patterned to UV exposure under a mask. The middle diaphragm layer was made of two pieces of acrylic dielectric elastomers, VHB 4910 and VHB F9473 (3M company), which served as the vibration membrane and conglomerating film. The top layer was PMMA, which had an opening for the out-of-plane displacement. The overall size of the pump was approximately 16mm×10mm×3mm. Since both of the diaphragm and the sealing layer were VHB elastomer, great compatibility was achieved and no more mechanical part was required. After testing on several microfluidic chips, the maximum flow rate value of 50 μ l was observed at a working condition of 3500V and 10Hz.

Since both of SU-8 and DEs are polymers, this micro chip may have a better compatibility with biologic structure which offers a wider application in bioengineering and medical implantology. And

this feature may lead to a new development for EAPs used as "artificial muscle" devices which would completely replace the damaged biologic muscles in the future.

307

Bio-Inspired, Smart, Multiscale Interfacial Materials

Lei Jiang, Chinese Academy of Sciences (China).

Bio-inspired smart materials should be a "live" material with various functions like organism in nature, they must have three essential elements as sense, drive and control. Our recent studies are focused on the design and fabrication of bio-inspired surfaces with special wettability based on these ideas. The studies on lotus and rice leaves reveal that a super-hydrophobic surface with both a large CA and small sliding angle needs the cooperation of micro- and nanostructures, and the arrangement of the microstructures on this surface can influence the way a water droplet tends to move. Considering the arrangement of the micro- and nanostructures, the surface structures of the water-strider's legs were studied in detail. These results from the natural world provide a guide for constructing artificial super-hydrophobic surfaces and designing surfaces with controllable wettability. Accordingly, super-hydrophobic surfaces of aligned carbon nanotube films, aligned polymer nanofibers and differently patterned aligned carbon nanotube films have been fabricated. The large scale fabrications of super-hydrophobic polymer surfaces have been developed by modification of the traditional template method, the adoption of one-step coating and electrohydrodynamic processes respectively. Many of the methods had been applied in making superhydrophobic films with multi-functional properties, such as structural colored, transparent and/or conductive superhydrophobic film. Under certain circumstances, a surface wettability can switch between superhydrophilicity and superhydrophobicity, just like in Chinese ancient Taiji philosophy that "Yin" and "Yang", the two opposing fundamental properties of nature, are switchable. The cooperation between surface micro- and nanostructures and surface modification of poly (N-isopropylacrylamide) gave reversible switching between superhydrophilicity and superhydrophobicity in a narrow temperature range of about 10 °C. By grafting the copolymer of temperature-sensitive and pH-sensitive components on the surface, a dual-responsive surface that can be controlled by either or both of temperature and pH was fabricated. Besides the organic surfaces, a series of inorganic switchers were also made in our lab. UV light stimulated transition between superhydrophobic and superhydrophilic by aligned ZnO, TiO₂, and SnO₂ films are successfully prepared respectively. In addition, a dual-responsive WO₃ film with controlled wetting and Photochromism was obtained by an inexpensive and simple electrochemical deposition process. These studies have great application potentials in the fields of integrated micro-electronic devices, microfluidic control, trace bioanalysis and smart functional windows, etc.

308

DNA Electrochemical Biosensor Based on Au Nanoparticles Self-Assembled Au Electrode

Zhao Dai, Yiyun Xiao, Jimei Zhang, Shichao Xu, Weixia Zhang, Guo Zheng, Tianjin Polytechnic University (China).

A novel electrochemical DNA biosensor system based on Au nanoparticles (AuNPs) modified Au electrode and anthraquinone-2,6-disulfonic acid (AQDS) as hybridization indicator was presented in this paper. AuNPs with different particle sizes were prepared from gold chloride by reduction, and self-assembled on Au electrode (AuNPs/Au electrode) by cysteamine as linker. Then, 5' end -SH modified DNA (HS-DNA) as nucleotide probes were self-assembled onto the surface of

AuNPs modified Au electrode (HS-DNA/AuNPs/Au electrode), and the HS-DNA/AuNPs/Au electrode could detect target DNA (completely complementary with HS-DNA). Because AuNPs were on Au electrode, the surface of Au electrode was increased. Therefore, this would result in the increase of electrochemical signal and increase the sensitivity of biosensor. If a completely complementary single stranded DNA (ssDNA) as target existed in the detection system, the cathodic peak current (ΔI_p) of AuNPs modified Au electrode was increased about 3 times than the HS-DNA/AuNPs/Au electrode because of the hybridization between HS-DNA and complementary DNA target and the formation of double stranded DNA (dsDNA), and if the target was a mismatching base-pair with HS-DNA, the electrochemical signal of electrode would have no obviously change. These results showed that this DNA biosensor system based on AuNPs self-assembled Au electrode had an excellent sensitivity with a complete complementary DNA sequence.

309

Effect of Nano BaCO₃ on Pyrolytic Reaction of Phenol-Formaldehyde Resin

Qingzhi Ma, Wanxi Peng, Yiqiang Wu, Central South University of Forestry and Technology (China); Yunyun Peng, Shubin Wu, South China University of Technology (China).

Phenol-formaldehyde resin is used as the most adhesive to produce waterproof plant-based composite. However, this product contains phenol and formaldehyde which can be easily released to pollute air. Based on the single-factor method, the effect of nano BaCO₃ on situ BaCO₃ of pyrolytic reaction of UF resin was studied by Py-GC/MS. There were components including carbon dioxide, D, α -tocopherol, 1,3-bis(trimethylsilyl) benzene, phenol from UF resin in 590°C He gas. However, the 20 compounds including phenol, 2,4,6-trimethyl-, phenol, 2-methyl-, phenol, 2,4-dimethyl-, benzene, 1,3-dimethyl-, 9-anthracenamine, 9,10-dihydro-, phenol, 2-ethyl-, benzene, 1,2,3-trimethyl-, phenol were identified by Py-GC/MS after UF/BaCO₃ composite was pyrolyzed in 590°C He gas, and phenol and phenol derivants were found in the compounds. The result showed that nano BaCO₃ could effectively delay the pyrolysis of UF resin.

310

Fabrication and Characterization of Carbon Nanofibers by Ethanol Catalytic Chemical Vapor Deposition

Yi Su, Xiaoping Zou, Jin Cheng, Zhu Guang, Maofa Wang, Beijing Information Science and Technology University (China).

Carbon nanofibers have been attracted many attentions for their potential applications in nanocomposites and electromagnetic wave-absorbing materials due to their remarkable mechanical, electrical and other properties. Ethanol as carbon source not only possesses low toxicity, easier storage and transportation, but also does not tend to form amorphous carbon on dissociation. So in our experiments, we use ethanol as carbon source to synthesize carbon nanofibers. In this paper, we report ethanol catalytic chemical vapor deposition (ECCVD) for synthesizing carbon nanofibers. We utilized ferrocene as catalyst precursor to synthesize carbon nanofibers by ethanol chemical vapor deposition. The ECCVD setup consists of two-stage furnace fitted with independent temperature controllers, carbon source supply system, carrier gas supply system and pump system. The ethanol was introduced into furnace tube by bubbling liquid ethanol under carrier gas flow of 100sccm 3% H₂/Ar and 100sccm N₂. Catalyst precursor ferrocene was placed at low temperature (300°C) region. Then ferrocene gas was introduced into high temperature (800°C) region by carrier gas. Ferrocene was decomposed to form iron nano-particles as catalysts.

These catalysts catalyzed the growth of carbon nanotubes which were deposited on substrates and the wall of furnace tube. After about 1h synthesis time, we obtained mass production of carbon nanofibers. The deposits were characterized by employed scanning electron microscopy, transmission electron microscopy, and Raman spectroscopy.

According to experimental results, we can find that the synthesis temperature of 650°C is a transition temperature. The CNFs synthesized at 650°C have a relatively low graphitization and large diameters, whereas, if the synthesis temperature is higher than 650°C, the CNFs turn to have thinner diameters and higher graphitization. Another phenomenon that we can observe from our results is that the synthesis temperature has few effects on the diameters and graphitization of CNFs when the synthesis temperature is higher than 700°C.

311

Flower-Like ZnO Nanostructures with Different Morphologies Synthesized by Hydrothermal Reaction

Yi Su, Xiaoping Zou, Jin Cheng, Guang Zhu, Maofa Wang, Beijing Information Science and Technology University (China).

Flower-like ZnO nanostructures with various morphologies were synthesized in aqueous solutions by hydrothermal reaction. It enable easily obtained flower-like ZnO nanostructures on various substrates from an aqueous solution of zinc salt. The method is inexpensive and fast fabrication for ZnO nanostructures in moderate temperatures. We can get various morphologies of flower-like ZnO nanostructures by control the pH levels. We also study the effects of other critical process parameters such as concentration, temperature and time, type of substrate.

In our experiment, an aqueous solution containing zinc nitrate and methenamine (C₆H₁₂N₄). And we use strong aqua ammonia to control the pH levels of the mixed solution. This transparent solution was transferred to a laboratory glass bottle with screw cap. We could use various substrates, such as, a bare piece of glass, Si wafers, or copper plate. The substrates were ultrasonically washed by deionized water and absolute ethanol, and were placed in the bottles and heated at a constant temperature of 95°C for 1 day in a regular laboratory oven. Then the bottle was removed, after the bottle had cooled to room temperature, white material was found on the surface of the substrates (indicating the deposition of material). Subsequently, the thin films are thoroughly washed with deionized water and absolute ethanol to remove any residual salt or amino complex, and dry in air at room temperature.

We use X-ray diffraction, scanning electron microscopy and transmission electron microscopy to characterize the morphology and nanostructure of flower-like ZnO nanostructures.

312

Optical Properties of ZnO Nanowires Grown by Thermal Evaporation

Zhi Zhao, Yue Lin, Jian Zuo, Zejun Ding, University of Science and Technology of China (China).

The mass production of ZnO nanowires were synthesized by a simple and rapid method based on the thermal evaporation of metal zinc pellets without the use of noble metal catalyst. The PL spectrum at room temperature shows a strong near band gap emission (NBE) peak and a weak deep-level emission (DL) peak, which implies its good crystallinity and high optical quality. The DL and NBE emission are considered to come from the singly ionized oxygen vacancy and the overlap of free exciton and free-to-band emission respectively by electron paramagnetic resonance (EPR) spectroscopy and low temperature photoluminescence. The coupling parameters of exciton-acoustic

phonon and of exciton–longitudinal-optical phonon were determined as 63.44 $\mu\text{eV/K}$ and 898 meV, and 251 K for Einstein temperature according to the temperature dependence of free exciton emission spectra.

314

Study on the Microwave Absorbing Properties of Nano-Carbon Black/SiC/Epoxy resin Composites

Youpeng Wu, Xiangxuan Liu, Bin Mo, Xi'an Institute of High Technology (China).

Epoxy (EP) was filled with nano-carbon black (CB) and micron-SiC. The effects of CB and SiC fraction on the absorbing properties of the EP composites were studied. The structure and morphology of the samples were characterized by scanning electron microscopy (SEM). The spectroanalysis indicates that the absorbent particles are dispersed uniformly in the coating. At 8~12GHz, the composite coating, as its thickness is 1.05mm, the absorbing bandwidth less than -5dB is 7.7GHz and less than -8dB is 4.6GHz, and the most reflection loss can reach -19.27dB. The wave absorbing peak values of composite increase with the increasing of the thickness. The bandwidth and the wave absorbing peak values increase with the increasing of the content of CB filling fraction. And the absorbing mechanism of the composite was also discussed.

315

A Study on Ductility of High Strength Concrete Containing Nanophase Particles

Chengming Lan, Hui Li, Harbin Institute of Technology (China).

Ceramics and ceramic composites are promising materials having rather high strength characteristics but quite low ductility properties at the same time. This is one of the major factors hindering the wide-scale application of these materials in various fields of human activities. Recent years many methods and materials were used to improve the fracture toughness of ceramics and ceramic composites. Among these nanophase materials and nanocomposites used became one of the most important methods to improve the various properties of ceramics and ceramic composites, in particular the ductility.

Similarly, it is well known that the high brittleness is the biggest disadvantage of concrete, especially of high strength concrete. Many methods, such as the incorporation of all kinds of fibers into concrete, have been applied to attempt to upgrade the toughness for a long time. As mentioned above, nanophase materials mixed were expected to improve the ductility of high strength concrete, and it has been proved to be feasible that nanophase materials could be mixed in mortar to achieve good mechanical properties.

Concrete mixed with nano-TiO₂ in amount of 5% and 10% by weight of binder was proposed and fabricated, and their mechanical and deformation properties were experimentally studied in this paper. In order to demonstrate improvements on mechanical and deformation of nano-concrete, specimens of plain concrete and concrete containing silica fume were also made. The results indicated that the compressive strengths of concrete containing nanoparticles were higher than that of plain concrete, however, little lower than that of concrete containing silica fume, with the same water-binder ratio at the 28th day. Especially the peak strains and ultimate strains measured at the 28th day of concrete containing nano-TiO₂ were much larger than that of plain concrete and concrete containing silica fume, and the peak strains and ultimate strains measured at the 90th day of concrete containing nano-TiO₂ were still much larger than that of plain concrete. The results indicated that mixing nanophase materials into high concrete was an available and potential way to improve both of

ductility and strength of high strength concrete.

316

Field Emission Properties and Fabrication of CdS Nanotube Arrays

Xuemin Qian, Yinglin Song, Huibiao Liu, Yuliang Li, Harbin Institute of Technology (China).

Large area of CdS nanotube arrays are fabricated using ZnO nanorod arrays as templates. The ZnO nanorod arrays are fabricated by a two-step hydrothermal process. In the first step, ZnO nanocrystals were spin-cast several times onto a silicon wafer to form a thick film of crystal seeds, and the silicon wafer would be annealed at 400°C for two hours. Then the wafer was putted into the solution which was composed of zinc nitrate hexahydrate and methenamine, and heated at a constant temperature of 75°C for 10 hours in a regular laboratory oven. Subsequently, the thin films were washed by deionized water, and dried in air at room temperature. CdS layer is successively deposited on the surface of ZnO nanorod by alternately dipping into the aqueous solutions of 0.05 M cadmium nitrite and 0.05 M sodium sulfide for 5 minutes, respectively. After the wafer with ZnO nanorod arrays are immersed in the solution Cd²⁺ and Cd²⁺ is adhere to the lattice site on the surface of ZnO nanorods. Then, the wafer is immersed in the aqueous solution of 1 M sodium hydroxide for removing the ZnO nanorod. The arrays of CdS nanotube are obtained after removed the ZnO nanorods. Three CdS nanotubes with different wall thickness are prepared by above-mentioned process for 12 (sample A), 9 (sample B), and 6 (sample C) deposition cycles, respectively. XRD pattern shows three CdS characteristic peaks. The room PL measurement shows a red emission band around 750 nm which can be explained as a trapped emission of CdS. The radius of three samples are 70 nm, 85 nm, and 101 nm. The CdS wall thicknesses of three samples are 9 nm, 16 nm, and 22 nm. The length of nanotube is about 1.5 μm . The field emission properties of three samples are investigated by a homemade vacuum chamber. The turn-on fields of three samples are 11.33 V/ μm , 9.99 V/ μm , and 7.99 V/ μm , respectively. The threshold fields of three samples are 14.92 V/ μm , 13.44 V/ μm , and 11.27 V/ μm , respectively.

317

Novel Way to Synthesize Mn₃O₄ Nanobelts via Oriented Attachment

Jinquan Sun, Zifeng Yan, Hongzhi Cui, University of Petroleum (China); Jinquan Sun, Hongzhi Cui, Jisen Wang, Yunbo Chen, Shandong University of Science and Technology (China).

Manganese oxide is important electronic material, useful catalysts for oxidation and reduction reactions, and has superior character in oxygen absorption and desorption. Here, the paper reported a new way to synthesize Mn₃O₄ nanobelts by the oriented attachment. The growth phenomena have been observed by transmission electron microscopy (TEM) and their composition were analyzed by X-ray diffraction. The method applied to synthesize the Mn₃O₄ nanorods is based on our work.

Microemulsions is a effectively way to prepare suitable nanoprecursors by a microheterogeneous medium. The surfactant stabilizing microcavities provides a cage-like effect that limits particles nucleation, growth and agglomeration. The precursors were characterized by TEM shown in Figure 1. It shows that the shape of individual particles is uniform and their size is in range of few nanometers. The initial particles took on floss-like structure because of the high surface energy.

The growth process was discussed and the growth modal has been built up, which can be described as Figure 2. Firstly, the precursors used as nano-unites were synthesized by microemulsion technique.

Secondly, NaCl is used as salt-assisted additive. Under the high temperature and the salt conditions, the adjoining nano-unites can easily move to find low energy plane to attach, which can adsorb in certain plane of particles that restrict growth along this axis. Experiments indicate that Cl⁻ ion plays an important role to control size of precursors and to change crystalline growth during oriented growth process.

The primary nanoparticles have been prepared by microemulsion technique, and then take place oriented aggregation forming Mn₃O₄ nanobelts in the presence of NaCl. Importantly, salt-assisted heat treatment is critical for both controlling size of precursors in heat treatment and for accelerating oriented aggregation and recrystallization.

318

Ag/WO₃-codoped TiO₂ nanoparticles: Relation between Structure, Sorption and Photocatalytic Activity

J.Y. Xu, C. Wen, L.M. Jia, Institute of Material & Chemical Engineering (China); C.F. Xiao, Tianjin Polytechnic University (China).

Nanostructured Ag/WO₃-TiO₂ particles responding to sunlight were synthesized by dissolving silver nitrate, sodium tungstate and tetrabutyl titanate precursors in a suitable solvent. The obtained powders were characterized by a series of analytical methods including X-ray diffraction (XRD), Brunauer–Emmett–Teller (BET) surface area analysis, Zeta potential measurements and UV–vis diffuse reflectance spectra (UV–vis DRS) to demonstrate their physicochemical properties. The as-prepared Ag/WO₃-TiO₂ samples were evaluated for their photocatalytic activity towards the degradation of methylene blue (MB) under sunlight irradiations. Both silver (Ag) and tungsten (W) species were well dispersed over TiO₂ surface with less than 6.0 mol % Ag and 3.0 mol % W to Ti element and contributed to a formation of crystalline WO₃. XRD analysis particularly demonstrates the existence of mixed-phase TiO₂ materials, to which the improvement in photocatalytic activity is attributed. Besides, the light absorption of doped samples is prominent red shifted relative to the pure TiO₂ due to the synergetic effect among the components of Ag, WO₃ and TiO₂ in the codoped-TiO₂. The particle size of the Ag/WO₃-TiO₂ powders was found to be a decrease which is accompanied with the increase of the surface area. The excellent stability and dispersity of the Ag/WO₃-TiO₂ powders in aqueous solution could be attributed to the enhanced zeta potential. On the other hand, the adsorption performances of different samples were tested in the removal of two dyes from aqueous solution (congo red and methylene blue). The first-order adsorption rate constants were determined and the results obtained were fitted by Langmuir monolayer formation. Thus, the Langmuir adsorption isotherm parameters were estimated from the experimental data.

319

Alignment and Construction of Electrospun Nanofibers and Cables

Hao Yan, Luqi Liu, Zhong Zhang, National Center for Nanoscience and Technology (China).

Morphology control of electrospun nanofibers is a major task to facilitate their wide applications. In this work, various dielectric materials were employed as collectors to prepare electrospun fiber mesh based on polyvinyl alcohol (PVA) and polyvinyl pyrrolidone (PVP) polymers. Experimental showed the nanofiber alignment is strongly depended on the collectors' relative static permittivity. Theoretical simulations revealed that the electric field can be tuned by different dielectric collectors. The horizontal electric field strength is the major factor to stretch electrospinning jet across the

gap, and to eventually achieve the aligned fiber-mesh. Moreover, new methodology for constructing twist cables using electrospun nanofibers has been further developed. The length of the cable could reach up to several meters and the diameter about 20 to 50 microns constructed by single fibers with the diameter of several hundred nanometers. Mechanical properties of nanofiber twist cables were systemically investigated. This work is believed to be of help to the design of more complicate structures based on the electrospinning technique.

320

Fabrication and Characterization of Nanoclay Modified Pmr Type Polyimide Composites Reinforced with Three-Dimensional Woven Basalt Fabric

Jianfei Xie, Yiping Qiu, Donghua University (China).

Nanoclay modified PMR type polyimide composites were prepared from 3D orthogonal woven basalt fiber preforms and nanoclay modified polyimide matrix resin, which derived from 4,4'-methylenediamine (MDA), diethyl ester of 3,3',4,4'-oxydiphthalic acid (ODPE), monoethyl ester of cis-5-norbornene-endo-2,3-dicarboxylic acid (NE) and nanoclay. In this study, a series of modified polyimide resins with different nanoclay loading and molecule weight were obtained, and the rheological properties of these PMR polyimide matrix resins were investigated. From the results of analysis, a two step compression molding process can be established for the composites. In the first step, the 3D fabric preforms were impregnated with polyimide resin in a vacuum oven and heated up for degassing the volatiles and by-products. In the second step, composites were compressed. The resulting composites exhibited high thermal stability and good mechanical properties. The scanning electron microscopic analyses for the composites revealed that the matrix was bonded to the fibers very well and the void content was relatively low.

321

Lead Hydroxide Nanorods Structure Precipitates from Lead Nitrate Solution

Jin Cheng, Xiaoping Zou, Guang Zhu, Maofa Wang, Yi Su, Gangqiang Yang, XueMing Lv, Beijing Information Science and Technology University (China); Jin Cheng, Beijing University of Posts and Telecommunications (China).

In this paper, we report the synthesis of lead hydroxide nanorods by solution-phase reaction of Pb (II) ions and hydroxide ions.

The typical precipitation procedure to obtain lead oxide nanorods is as follows. A 50ml of 0.01M lead nitrate aqueous solution precursor (0.166g of lead nitrate hydrate with a purity 99.5% dissolved in 50ml distilled water in a 50ml glass beaker) was heated to about 80°C. For synthesizing rod-like lead hydroxide nanostructures, a little sodium chloride (about 0.06g) was added into lead nitrate aqueous solution precursor. When about 0.084g of KOH pellets was added at the same time with vigorously magnetic stirring, white (but not pure white) flocculent precipitate separated out in less than a minute. The precipitate was washed many times (more than 8 times) with distilled water, filtered and dried naturally for overnight. The concentration ratio of Pb²⁺ : Cl⁻ : OH⁻ is 1:2:3.

We have characterized the precipitate by employing scanning electron microscopy, transmission electron microscopy, high-resolution transmission electron microscopy, energy dispersive X-ray spectroscopy and XRD.

Our results indicate that, by adding chloride ions into lead nitrates aqueous solution, the lead hydroxide nanorods can be obtained when an alkali is put into the precursor solution. The chloride ions are the key factor for the formation of rod-like morphology. The

as-prepared lead hydroxide nanorods are single crystals with hexagonally crystalline structure.

322

Nanometer Functional Materials from Explosives

Huisheng Zhou, Xinghua Xie, Jing Zhu, Minhui Yang, Jinying Zhang, Anhui University of Science and Technology (China).

The growth of $\text{Li}_{1+x}\text{Mn}_2\text{O}_4$ via detonation reaction was investigated with respect to the presence of an energetic precursor, such as the metallic nitrate and the degree of confinement of the explosive charge. The detonation products were characterized by scanning electron microscopy. Powder X-ray diffraction and transmission electron microscopy were used to characterize the products. $\text{Li}_{1+x}\text{Mn}_2\text{O}_4$ with 1~2 μm spherical morphology and more uniform secondary particles, but with smaller primary particles of diameters from 20 to 60 nm and a variety of morphologies were found. The oxides produced by this method affirmed the validity of detonation synthesis of nano-powders.

325

Preparation of Magnetic Fluorescent Hollow Nanoparticles with Multi-Layer

Xiuxue Sun, Jimei Zhang, Zhao Dai, Ping Li, Shichao Xu, Wen Zhou. Guo Zheng, Tianjin Polytechnic University (China).

A kind of novel magnetic fluorescent hollow nanoparticles with multi-layer shells by layer-by-layer self-assembly process was presented in this paper. Non-crosslinking poly(acrylic acid) (PAA) nanoparticles as core with 250 nm in diameters were prepared by distillation-precipitation polymerization in acetonitrile with 2, 2-Azobisisobutyronitrile (AIBN) as initiator and without any stabilizer and crosslinker. Then 4-vinylpyridine (4VPy) as monomer was self-assembled on the surface of PAA nanoparticles because of hydrogen-bonding effect between the surface carboxyl of PAA nanoparticles and pyridine of 4VPy. The 4VPy as first shell layer were crosslinked by ethylene glycol dimethacrylate (EGDMA) by seeds distillation-precipitation polymerization in acetonitrile. The core/shell structure of this kind of nanoparticles was investigated by FTIR and TEM. We can find that the products had an absorption peak at 1641 cm^{-1} from the FT-IR, which showed that the vinyl groups had been connected in the polyAA microspheres. After that, the non-crosslinking PAA core was removed under a solution of sodium hydroxide in ethanol-water. On the other hand, CdTe quantum dots (QDs) with about 3 nm in diameters as shell were prepared in aqueous solution with 3-mercaptopropionic acid (MPA) as stabilizer and 1, 6-hexylenediamine modified Fe_3O_4 nanoparticles with about 11 nm in diameters as core were synthesized in water respectively. Because of the hydrogen-bonding between the surface carboxyl of MPA on CdTe QDs and the amino on Fe_3O_4 nanoparticles, the core/shell magnetic-fluorescent nanoparticles were obtained. Then, the magnetic-fluorescent nanoparticles as second shell layer were self-assembled on the hollow 4VPy nanoparticles.

326

Preparation of Nano-TiO₂ Powder by Polyacrylamide Gel Method

Xiaowei Fan, Xiaoping Liang, Rongtao Wang, Jianxin Li (China).

Polyacrylamide gel method is a new successful technique for preparing nanometer metallic oxide materials, such as $\alpha\text{-Al}_2\text{O}_3$, ZnO and MgAl_2O_4 . And TiO_2 has high electro-catalytic activity, especially the anatase- TiO_2 , but has not been made by polyacrylamide gel method. In this study, the nano- TiO_2 powder was prepared using the novel method with TiCl_3 as raw materials,

and with acrylamide and N,N'-methylene diacrylamide as crosslinking agent. The nano- TiO_2 was examined by scanning electron microscopy, and X-ray diffraction. The results show that grain size of the TiO_2 particles is smaller than 25 nm by the polyacrylamide gel method. Those particles are regular in shape and have good distribution. Adding SO_4^{2-} in the network gel process can enhance the content of anatase- TiO_2 phase, and can decrease the sintering temperature. This may be explained in terms of the SO_4^{2-} can be formed coordination compound with Ti^{4+} , which has the lower symmetry. The coordination compound is prone to generate anatase- TiO_2 at lower temperature.

327

Study on Synthesis, Structure and Photochromic Property of Nanometer Amino Acid Polyoxometalate Compounds

Dehui Sun, Changchun Institute of Technology (China); Jilin Zhang, Hongjie Zhang, State Key Lab of Rare Earth Resource Utilization (China).

In recent years, nanosized polyoxometalate (denoted as POM) exhibit exotic physical and chemical properties different from conventional bulk materials because of diverse topological and the size effect and present a wide potential application in information displays, chemical sensors, and holographic storage device, therefore, design and synthesis of nanometer POM compounds is a frontier problem in materials field. As one of synthesis methods for nanomaterials, low-heating solid-state chemical reaction has advantage of free of solvent, lack of pollution, high efficiency, good selectivity and convenient operation, so it shows enormous potential on the preparation of nano-sized POM compounds. To the best of our knowledge, the preparation of nano-sized amino acid POM compounds is still scarce.

In this paper, a series of amino acid-polyoxometalate compound nanomaterials were successfully synthesized from Silverton-type polyoxometalate and amino acids by solid-state chemical reaction at room temperature. Elemental analysis results indicate that the actual measurement values are consistent with the calculated values, so the rationality of composition for the samples is confirmed. Fourier transform infrared absorption spectra data of the as-synthesized samples and the reactants show that the characteristic peaks of samples are similar to those of the corresponding Silverton-type POM, which indicates that the POM anions in the sample molecules still remain in their Silverton-type structure. Scanning electron microscopy images show that morphologies of $(\text{HThr})_7\text{PMo}_{12}\text{O}_{42}\cdot 4\text{H}_2\text{O}$ and $(\text{HTyr})_7\text{PMo}_{12}\text{O}_{42}\cdot 5\text{H}_2\text{O}$ are 2 D nanoplates and 1 D nanorods, respectively, while morphologies of $(\text{HSer})_7\text{PMo}_{12}\text{O}_{42}\cdot 5\text{H}_2\text{O}$ and $(\text{HGlU})_7\text{PMo}_{12}\text{O}_{42}\cdot 4\text{H}_2\text{O}$ are 0 D nanoparticles. Structures of amino acids can play a template agent role in synthesis of the Silverton-type polyoxometalate compounds and result in the difference in their morphologies. Irradiated with ultraviolet light, color of these samples changed from white into blue. Synthesis of nanometer amino acid POM compounds would provide more information in further to explore POM photochromic properties.

328

The Application of Conductive Polymer Nano Emulsion in Printing Ink

Luhai Li, Yi Fang, Zhiqing Xin, Xiaojun Tang, Beijing Institute of Graphic Communication (China); Mo Linxing, Graduate School of Tianjin University (China); Bin Li, Yatushi Printing Co. Ltd (China).

In order to achieve the acquirement of flexible displayer, such as e-paper and touch screen, and to reduce the cost of conductive printing ink, the application of conductive polymer in printing ink

is studied, and conductive flexible layer is acquired. The effect of N,N-dimethylformamide, glycerol, deionized water, and pH value on the performance of water-based nano conductive polymer ink is studied by secondary doping of Polythiophene conductive polymer nano emulsion. The effect of various polymers on the conductivity of printing ink is researched by adding various polymer resins. At last, printing performance of the conductive polymer ink is tested by some printing methods, such as flexo, screen, and offset printing. Conductive printing layer which can be compared with the traditional conductive ink in the conductivity is acquired and the conductive layer is water-proof.

329

Image-Based Meshing for Computational Simulation of Micro and Nano Structures

P.G. Young, B. Notarberardino, A. Abdul-Aziz, Exeter University (UK); L. Yang, Shanghai Gaitech Scientific Instruments Co. Ltd. (China).

Computational simulation is a very effective and valuable tool in investigating materials behavior at the micro and nano-scale level and in assessing its influence on the overall macro-scale properties. Well established computational techniques can now be used to simulate mechanical, fluid dynamics, thermal or any combined (multi-physics) phenomena at the micro and nano-scale level. Crucial to the success of such a simulation is the ability to represent the 'micro-architecture' accurately and efficiently - which has proved to be a very challenging task so far. This paper will present an innovative image-based mesh generation technique that converts 3D images of micro and nano-structures (as provided by typical Micro/NanoCT scanners) directly into high fidelity computational models. The approach provides a deeper understanding than experimental tests, and achieves more realistic model results than via analytical approaches. Real-life applications will be presented, including the densification analysis of open celled foam.

Open celled foams are used in an increasing number of industrial applications, (e.g. seating, helmets, space vehicles) due to their interesting mechanical properties, in particular their light weight and high energy absorption. However, the material properties of foams are a result of complex relationships involving different aspects of the micro-architecture and properties of the parent material. A wide range of studies have been carried out using analytical, experimental and computational approaches to increase our understanding of the physical behavior of foams. In the present study, for the first time, a new image-based meshing approach is used for characterizing the mechanical properties of foams based on high resolution computed tomography data. The new meshing tool generates geometrically and topologically accurate finite element meshes of open celled foams based on 3D imaging data.

331

Enhancement of Retention and Antifouling Capability for PVDF UF Membrane Modified By Nano-TiO₂ Sol

M.J. Li, W. Chen, Y.X. Jing, Institute of Material & Chemical Engineering (China); F.X. Chang, Tianjin Polytechnic University (China).

Novel PVDF/TiO₂ hybrid membranes were prepared by phase inversion process from a PVDF/DMAc/PVP/tetrabutyltitanate/water system. The membrane characteristics such as morphology, thermal properties, porosity, water contact angle, tensile strength and separability were investigated by a series of analytical methods including atomic force microscope (AFM), X-ray diffraction (XRD), thermogravimetric analysis (TGA) and zeta potential measurements. The performances and surface properties of hybrid and PVDF membranes were tested by the removal of bovine serum

albumin (BSA) from aqueous solution, evaluated by using two dyes with different charge (congo red and methylene blue). Based on the experimental results, TiO₂ nanoparticles of a quantum size (~8 nm or less) in anatase crystal structure were obtained from the controlled hydrolysis of tetrabutyltitanate. Besides, TiO₂ sol was introduced into polymer molecule for the hybrid membrane with less than 12 vol % TiO₂ sol to PVDF and contributed to a smooth surface and more apertures due to both the interaction and compatibility between polymer and TiO₂ sol, to which the improvement in hydrophilicity, thermal stability, mechanical strength and antifouling ability is attributed. The observed rejections were optimized for PVDF/TiO₂ hybrid membrane with respect to PVDF membrane. In particular, the pure water permeation flux was increased from 126.6 to 166.7 L/m²·h for hybrid membrane with a relative flux of 80 % compared to 50 % of relative flux observed for PVDF membrane.

332

Evolution of Surface Structure of Bilayer Oleic Acid-Coated Fe₃O₄ Nanoparticles During Ethanol Washing

H.B. Peng, K. Yang, Y.H. Wen, Sichuan University (China).

Compared with single layer oleic acid-coated Fe₃O₄ nanoparticles, bilayer oleic acid-coated ones can be well dispersed in not only nonpolar but also polar carrier liquids. Thus bilayer oleic acid-coated Fe₃O₄ nanoparticles can be applied in more areas. The studies revealed that the primary layer in the bilayer oleic acid-coated structure was chemically absorbed on the surface of nanoparticles, and the secondary layer is physically absorbed on the primary layer through the interpenetration of the tails of the primary and secondary surfactants at their interface. The bilayer oleic acid-coated Fe₃O₄ nanoparticles was mainly prepared by the excess addition of oleic acid and the residual oleic acid on the surface of bilayer oleic acid-coated Fe₃O₄ nanoparticles is usually removed by ethanol washing. Because the ethanol has a strong penetration and low surface tension, it may permeate into the interpenetration layer and separate the secondary layer from the primary layer. As a result of the separation, the secondary layer may be washed away by the ethanol, thus the bilayer coated structure may evolve into the single layer coated structure. To know the evolution of surface structure, the surface structure of oleic acid-coated Fe₃O₄ nanoparticles was studied using TEM and FT-IR together with TGA as a function of washing times. The results showed that after five times washing, the bilayer oleic acid-coated structure was attained, while after twenty times washing, the bilayer oleic acid-coated structure evolve into the single layer because the secondary layer was washed away by the ethanol.

334

Fibers Effect on Elytra Cuticle of Dung Beetle (*Copris Ochus Motschulsky*) Investigated by Nanoindenter

Jiyu Sun; Jin Tong; Zhijun Zhang; Jinabin Lin.

Natural biomaterials have some special structures and functions because of their evolution through the exchanges of energy, matter and information with their surroundings over millions of years. The cuticle represents 25% of the dry weight of the entire insect body. It is tenacity, waterproof and lightweight which is an excellent crude composite material. The surface materials and structures of insect cuticle can provide useful information for designing anti-adhesion components material. Quantitative measurement of mechanical properties of insect cuticle will help to develop biomimetic materials suitable for industrial products. Field emission scanning electron microscopy (FESEM) was used to investigate the detail structure of elytra cross-section in transverse direction and longitudinal direction. Shown in transverse direction, the fibers of

the deeper layers of the endocuticle are orientated in rotation angle and neighbor fibers are rotated in relation to the each other in the same direction. While the fibers in longitudinal direction show the epicuticle, exocuticle and endocuticle clearly multilayer in parallel. In this work, the mechanical properties of the elytra cuticle of dung beetle *Copris ochus* Motschulsky, reduced modulus and hardness in nano-scale, were investigated by using a nanoindenter. The reduced modulus (E_v) and hardness (H_v) of surface cuticle in the vertical direction obtained by nanoindentation was 3.54 ± 0.12 GPa and 0.20 ± 0.01 GPa, respectively. The nanoindentation result was shown that the reduced modulus (E_t , E_l) and hardness (H_t , H_l) of each layer was gradually reduced from the outer layer to the inner layer in the transverse direction and the longitudinal direction, respectively. E_v was less than the largest E_t presented at outer layer (7.06 ± 0.54 GPa) and was larger than that of E_l (1.92 ± 0.54 GPa). It was supposedly formed as a result of the composite effect of the multilayer. Considering the anisotropy of chitin, an experimental model was proposed to describe the nanomechanical properties of elytra cuticle.

335

Improving the Aging Properties of Silicone-Acrylate Copolymers Nanocomposites for Encapsulation of Outdoor Exposed Stone Substrates

Yuan Liao, Shuhua Qi, Donghong Wang, Northwestern Polytechnical University (China); Qiaomei Fu, Graduate University of Chinese Academy of Sciences (China); Liyu Yan, Xi'an Leo Technological Co.Ltd (China).

Nanocomposite systems based on silicone-acrylate copolymers and different amounts of the modified nano-silicon dioxide (nano-SiO₂) (1, 2 and 4 wt %) were tested as protective and encapsulating agents for the outdoor exposed stone substrates. The conservation and encapsulation efficiency of these treatments was evaluated through physical investigations (resistance to ultra violet, freeze-thaw aging resistance and accelerated ageing resistance to artificial climate). The results have evidenced that the nano-scale dispersion of low amounts of the modified nano-SiO₂ into the polymeric matrix enhances the encapsulating and protective action of the outdoor exposed stone substrates. In fact, the outdoor exposed stone substrates treated with the nanocomposite systems exhibits a more marked reduction in resistance to ultra violet, freeze-thaw aging resistance and accelerated ageing resistance to artificial climate with respect to stone treated with the neat silicone-acrylate copolymers and B72 polymer, a commercial copolymer ethyl methacrylate/methyl acrylate (EM/MA).

336

Improving the Damping Ability by the Addition of Nano SiO₂ to the Concrete Materials

Dujian Zou, Tiejun Liu, Jun Teng, Harbin Institute of Technology (China).

Damping in structures is commonly provided by viscoelastic nonstructural materials. Due to the large volume of structural materials in a structure, the contribution of a structural material to damping can be substantial. In this paper, the experimental investigation on damping ability of concrete materials and its members with Nano SiO₂ is carried out by the method of 3-point bending beam damping measurement and cantilever beam free vibration respectively. The microstructure of concrete mix with nano SiO₂ was observed by XRD, and SEM, then damping mechanism was discussed. The experimental results show that: the damping reinforced effect achieved best with the 4% mixture ratio of Nano SiO₂, but the optimal adulteration quantity of nano SiO₂ was 3% of cement weight by the comprehensive consideration of

cost, workability, strength and dynamic properties. Nano materials as a mixture increase contact interfaces, and the non-uniform stress distribution under external force improves frictional damping energy consumption ability of concrete. The experiment results on the damping ratio and the loss tangent of the concrete materials with nano materials are consistent.

337

Microwave Hydrothermal Synthesis and Characterizations of NiS Nano-Needle

Bai Bo, Xuemei Hou, Chang'an University (China).

NiS with needle-like nanostructure was successfully prepared via a facile and rapid microwave-hydrothermal method. The as-prepared products were characterized by X-ray diffraction (XRD), X-ray fluorescence spectroscopy (XRF), transmission electron microscopy (TEM), Brunauer-Emmett-Teller (BET) measurements, Raman spectroscopy, thermo-gravimetric analysis (TGA) and differential thermal analysis (DTA), respectively. The experimental results showed that NiS was needle-like, and the product possessed a uniform size with the diameter in a range of 20 nm to 35 nm and the length of about 100-200 nm. The structure belonged to α -NiS crystal phase. The specific area exceeded 45.0 m²/g. Moreover, the possible growth mechanisms were discussed. It was proposed that with the presence of surfactant of polyethylene glycol-400, the formative micelle in aqueous solution had acted as templates for the formation of these kinds of α -NiS crystal with typical morphologies due to the orientated aggregation effect. Comparing with the conventional hydrothermal method, microwave hydrothermal technique could not only accelerate the reaction but also make the formed NiS precursors well crystallized.

339

Preparation and Electrorheological Properties of TiO₂/ZnC₂O₄ Nanocomposites

Fenghua Liu, Gaojie Xu, Yichuang Chen, Jinghua Wu, Jianjun Guo, Ping Cui, Chinese Academy of Sciences (China).

TiO₂/ZnC₂O₄ nanocomposites were synthesized by means of co-precipitation method. The X-ray diffraction analyses, Fourier transform infrared spectrometry, scanning electron microscopy, etc., were used to determine the structure of the nanocomposites. The electrorheological (ER) activity was studied by the rheological curve and yield stress under an electric field. An excellent ER effect is found with the suspension of TiO₂/ZnC₂O₄ nanocomposites dispersed in silicone oil. Under 5 kV/mm external electric field, the yield stress can reach up to 80 kPa, and the leaking electric current density is lower than 15 μ A/cm². Furthermore good sedimentation property of its electrorheological suspension is observed.

340

Structure and Property of Nano-SiO₂-PMMA/Wood Composite

Yongfeng Li, Yixing Liu, Fenghua Wang, Xiangming Wang, Northeast Forestry University (China); Xiangming Wang, FPInnovations-Forintek Division (Canada).

A nano-SiO₂-PMMA/wood composite, combining a high mechanical and physical property and a multifunctional property including decay resistance, dimensional stability, and fire retardant, was prepared by impregnating a vinyl monomer, MMA, and AIBN as an initiator, and nano-SiO₂ with unsaturated double bonds (C=C) into the special honeycomb-shaped vesicular structures of wood material; and further initiating them to copolymerize in situ through a heat process. Its structure was characterized with SEM, FTIR and XRD. And the performances of the composite were also

determined. The analyzing results with SEM, FTIR and XRD showed that MMA polymerized by its double bonds, and also copolymerized with modified nano-SiO₂ as a free radical form by their double bonds in the porous structure of the composite, and the resultant polymer chemically bonded wood cell walls, which mainly existed as an amorphous form. The testing results of comprehensive performance indicated that the modulus of rupture (MOR), modulus of elasticity (MOE), compression strength and hardness of nano-SiO₂-polymer/wood composite increased by 75%, 102%, 131% and 190% than untreated wood, respectively; and the dimensional stability of the nano-SiO₂-polymer/wood composite improved 2.1 times; and the decay resistance of the nano-SiO₂-polymer/wood composite increased by 12.56 times than untreated one; and the initial pyrolysis temperature improved near 40°C than untreated one. The excellent performance of the composite could endow it with a wide application in the area of architecture and traffic.

341

Bio-Nanocomposites Reinforced by Reactive Nanocrystalline Cellulose and Hydrophobic-Modified Cellulose Microfibrils

C. Wang, S. Sun, B. He, H. Xiao, South China University of Technology (China); S. Li, H. Xiao, University of New Brunswick (Canada).

The work presented herein has been focused on two biocomposites or nanocomposite systems: 1) polypropylene (PP)-based biocomposites; 2) Bio-nanocomposites originating from furfural resins reinforced by nanocrystalline cellulose (NCC). To reinforce PP-based biocomposites, hydrophobic-modified cellulose microfibril (CMF) grafted by poly (butyl acrylate) (CMF-g-PBA) was prepared via an atom transfer radical polymerization (ATRP) of butyl acrylate. The CMF-g-PBA obtained was analyzed using FT-IR, TG, contact angle and SEM. The results from FT-IR and SEM indicated that PBA was indeed grafted onto the surface of CMF. TGA measurements further confirmed that the amount of grafted PBA on CMF was approximately 55% (wt); whereas the contact angle results demonstrated that the hydrophobicity of CMF was increased substantially after the grafting. As a result, the compatibility between CMF-g-PBA and polypropylene (PP) was improved, thus allowing CMF-g-PBA as an effective reinforcement for biocomposites. To further extend our work on biocomposites, furfuryl alcohol (FA) resin was reinforced by NCC which was prepared via an innovative process in an attempt to create a bio-nanocomposite completely based on natural resources. FA prepolymers was synthesized with an acid catalyst, and NCC was rendered reactive via the grafting of maleic anhydride (MAH). The resulting NCC and nanocomposites were characterized using TEM, SEM and FT-IR. It was found that NCC appeared to be spherical in shape with diameters under 100 nm. FT-IR confirmed that there were hydrogen and esterification bonding between MAH and NCC or FA prepolymer. After solidified with paratoluenesulfonic acid, NCC-reinforced FA resin composites showed granular cross-section while FA resin with layered. Mechanical Property tests indicated that NCC-reinforced FA resin composites possessed the improved tensile and flexural strengths, in comparison with FA resin.

342

Investigation of Nanometer Chitin Fiber of Chafer Cuticle

B. Chen, X. Peng, L. J, Chongqing University (China).

Most natural biomaterials take the form of composites. After many centuries' evolution, these natural biomaterials gain the current optimized nanometer-scale microstructures, which endow these natural biomaterials with excellent mechanical properties. It can

explain why biotechnology can be recognized as a potential contributor to the design of many key nanometer engineering materials or composites. In this work, the microstructures of a kind of natural biocomposite, chafer cuticle, was observed with a scanning electron microscope (SEM) and a transmission electron microscope (TEM). The observed results showed that the chafer cuticle is a kind of nanometer biocomposite. The composite consists of many nanometer-scale chitin-fiber layers and collagen protein matrix. The nano-chitin-fiber layers are arranged in several particular patterns, which include a kind of dual-helical structure. The observed result also showed that the chitin-fiber layers consist of many nanometer chitin fibers. The diameter of the chitin fibers is 5-10 nm and the chitin fibers are of several particular shapes, which include a kind of branched one. The branched fibers thrill through the protein matrix and connect with the fibers in their adjacent fiber layers, which compose a kind of particular nanometer fiber-reinforced microstructure. The fracture toughness of the biocomposite with the nanometer fiber-reinforced microstructure was analyzed based on its representative model. It showed that the nanometer fiber-reinforced microstructure can markedly improve the fracture toughness of the composite, which was verified with comparative experiments.

343

Optical Behavior of Pr³⁺-Doped Barium Titanate-Calcium Titanate Nano-Crystallites Prepared by Sol-Gel Method

Xiaoyan Wang, Yanxue Tang, Qizhuang He, Zifei Peng, Dazhi Sun, Shanghai Normal University (China).

Barium titanate is a classical example of ferroelectric material with perovskite structure. The related devices are widely used as infrared detectors, transducers and high permittivity capacitors. Additives or binary systems improve the physical properties significantly. Here, we reported that nanocrystalline powders of Barium titanate-Calcium titanate doped with Pr³⁺ were obtained by the sol-gel method. The sintering temperature was between 900 – 1200 °C. It was observed that the material exhibited luminescence within wavelength of 550-650 nm. The concentration of Pr³⁺ played an important role in the luminescence. The concentration of one percentage was an optional amount for luminescence. The intensity was also dependent upon the grain size that was controlled by the annealing temperature. We observed that the aging behavior of the luminescence, as well. The intensity of luminescence decreased with aging time. It was an evidence of the movement of ions. Then, the phenomenon was explained in terms of shift of defect during aging. The (Ba,Ca)TiO₃ is a ferroelectric material when the concentration of calcium is less than 20 atom%. The Curie temperature is about 100 °C. Therefore, it is a potential system that controls the luminescence performance by modifying ferroelectric domains at room temperature.

344

Preparation and Photocatalysis Properties of La-doped Nano-NiO Novel Photocatalyst

Peng Liu, Zhi yuan Yang, Xi'an University of Science and Technology (China).

The novel photocatalyst, La-doped Nano-NiO, was prepared by Sol-Gel with nickel nitrate hexahydrate and lanthanum chloride and characterized by means of XRD and SEM. The photocatalytic activities of prepared nano-NiO photocatalysts were evaluated by degradation direct bordeaux solution as model compound to photocatalytic degradation under irradiation of UV lamp. The results show that the pure NiO powder is uniform sized with a mean size of about 37.38 nm and its crystal phase is cubic syngony wholly. The grain size of NiO powder decreases whereas the crystal

plane spacing of NiO increases with the doping content of La in NiO increasing. Under optimal addition amount of LaCl₃ into NiO 0.16(mole fraction), the average grain size of NiO powder is about 12.52 nm. Meanwhile, the degradation rate of direct bordeaux solution after irradiation for 90min by the Nano-NiO powder doping La under optimal doping content approaches approximately 100%. The XRD results show that trace amounts of perovskite-like structure of La₂NiO₄ exists in composite structure of La-NiO, which contributes to the increase of photo-catalytic activities.

345

Quantitative Analyses of Extrudate Swell for Polymer nanocomposites

Kejian Wang, Chongxiao Sun, Daming Wu, Beijing University of Chemical and Technology (China).

Extrudate swell is often observed to be weakened in nanocomposite compared to the pure polymer matrix. Its quantitative theory is significant either for optimum processing or for understanding their viscoelasticity. By generalizing one die swell theory for entangled polymers in long capillary extrusion and other empirical formula for die swell in short capillary, one unified extrudate swell correlation with material properties and capillary parameters was developed for polymer melt and their nanocomposites when considering reservoir entry effect. More importantly, it was the first to find that the composite swell ratio can be the matrix swell ratio multiplied by the concentration shift factor, which is similar to that for dynamic moduli of composites. The factor is the functions of the shear field (stress or shear rate), filler content, filler internal structure and the surface state as well as the matrix properties. The swell data for organobentonite-filled polypropylene nanocomposites, calcium carbonate nanoparticle-filled isotactic polypropylene, clay filled fluoroelastomer nanocomposites, quasi-nanogel particles filled natural rubber and electron beam-cross-linked gels-natural rubber compound were chosen from publications to test the new theories. The quantitative model was well fitful for the five kinds of nanocomposites, which verified the certain rationality of the swell theory for the nanocomposites.

346

Microstructure-Property Correlation for the Tunneling Percolation Behavior in Metal/Insulator Nanocomposites

Liujuan Zhu, Wenzhong Cai, Shandong Tu.

Metal/insulator composite systems are usually found in cermets and functionally graded materials (FGMs). Understanding the relationship between their microstructures and macroscopic properties is important for the design and application of these materials. A microstructure-property correlation for the electrical conduction in the metal/insulator nanocomposites is still an unresolved issue while it has been established for the counterparts of microcomposites. The electrical conduction in the nanocomposites is determined by two mechanisms: geometrically continuous network of conducting phase and/or electrically tunneling network between isolated conducting particles. The tunneling distance is typically a few nanometers and comparable to the nanoparticle size. The tunneling regions around nanoparticles generally act as the interfacial shells. The tunneling network is attributed to the interacting tunneling shells. The classical percolation theory, regardless of universal or nonuniversal exponents, fails to account for the whole transition process from the electrically tunneling conduction to geometrically percolating conduction in the nanocomposites. Therefore, a tunneling percolation model is developed for the peculiar conduction behavior in the nanocomposites. In this model, each conducting particle and its tunneling shell may be mapped into an equivalent

particle. In this manner, the interparticle tunneling network in the nanocomposites is considered as a random network of the equivalent-particle system. The model provides a clear microstructure-property correlation by combining many-particle statistics, effective-medium theory, and classical percolation theory. Its availability is assessed by experimental data. Furthermore, the effect of the nanoparticle size and interparticle tunneling on the tunneling percolation thresholds and the nanocomposite conductivity is studied. The origin of nonuniversality in the continuum percolation systems is explained. The unique nonlinearity of exponent in the classical percolation theory is discussed by considering the tunneling percolation transition process in the nanocomposites.

348

Experimental Study on the Output Characteristics of Piezoelectric Micro-Displacement Actuator

Guoping Li, Tongpeng Han, Luwei Wang, Ningbo (China).

Piezoelectric micro-displacement actuator has been widely used in the precision positioning system because of its high-resolution, fast response, large output power and so on. In this paper, the characteristics and the applications of piezoelectric micro-displacement actuator are introduced, and the actuation principle of the actuator is elaborated. Necessary experimental researches on the WTYD0808042 type piezoelectric micro-displacement actuator have been made with self-designed output characteristics test system. The displacement of actuator together with static and dynamic output characteristics of force have been tested respectively under the conditions of free output of displacement, free output of force, and output of force-displacement coupling, in addition, the frequency response characteristics of the actuator have also been tested. Based on the tests, the output displacement of actuator shows the very good linearity with the drive voltage in the 60V-120V area, a satisfied static response characteristic was obtained. Moreover, it can be concluded that the actuator with the ideal characteristics of the transient output in displacement and force within dynamic curve output coincidence good precision. The researches provide the reference for the actuator's application in the turning vibration control system and the noncircular turning system.

349

Circumferential SH Waves in Functionally Graded Piezoelectric Hollow Cylinders

Jiangong Yu, Xiaoming Zhang, Henan Polytechnic University (China).

Based on linear three-dimensional piezoelectricity, the Legendre polynomial series expansion approach is used for determining the characteristics of circumferential SH waves in orthotropic hollow cylinders composed of functionally graded piezoelectric materials (FGPM) with axial polarization and open circuit. Circumferential SH wave dispersion curves, displacement and electric potential distributions in FGPM hollow cylinders under different gradient fields and different ratios of outer radius to thickness are calculated. The effect of the gradient fields and the piezoelectricity on dispersion curves and displacement distributions is shown. The changing of the gradient fields can influence the dispersion and the piezoelectric effect of the FGPM pipes. The piezoelectricity can change the extent of the dispersion of the circumferential SH waves. The influence of the ratio of radius to thickness on the circumferential SH wave characteristics is discussed. The changing extent of the dispersion is influenced by the ratios of radius to thickness. For a large ratio, the piezoelectricity weaken the dispersion of the SH wave. As the decrease of the ratio, the

weakening extent becomes light. When the ratio is very little, the piezoelectricity even strengthens the dispersion of the SH wave. The ratio has also a significantly influence on the electric potential distribution. For a large ratio, the electric potential distributes mostly near the side of the stronger piezoelectricity material; for a small ratio, the electric potential always distributes mostly near the outside of the FGPM pipe.

351

A Piezoelectric Sensor Array and Wavelet Analysis Based Damage Imaging Technology for Structures of Carbon Fiber Composite Materials

Lei Qiu, Shenfang Yuan, Qiang Wang, Xiaoyue Zhang, Nanjing University of Aeronautics and Astronautics (China).

Permanently attached piezoelectric sensors (PZT) array are adopted for damage imaging of structural health monitoring (SHM) incorporating active Lamb wave methods. These kinds of damage imaging methods are proved to be effect on plate structures of aluminum. In recent years, carbon fiber composite (CF) materials are used widely in aircraft structures. Compared to the aluminum, these kinds of multiple-scattering and isotropic media have more complicated damage mechanisms and make the scattered Lamb wave signals more complicated to be analyzed. This paper proposes a PZT array and wavelet analysis (WT) based damage imaging method for damage localization on structures of CF materials. Group velocity of Lamb wave signals calculating by continuous WT method is discussed first. Then, this damage imaging method also uses continuous WT method to extract signals (called imaging signals) of different scales from the scattered Lamb wave signals. Thirdly, a delay and sum imaging algorithm which is based on the imaging signals of one scale is discussed. Each imaging signals of a special scale can

give out a damage imaging result, averaging these results can obtain a more accuracy result. Adopting this damage imaging method, a validating experiment is applied on a plate structure of CF materials. The experimental result shows that this method can localize the artificial damage effectively and the error of damage localization is less than 20mm comparing the monitoring area of 300mm×300mm.

352

Analyze the Vibration Mode of 1-3-2 Piezoelectric Composite

L Qin, L.K. Wang, G. Wang, B.S. Sun, Beijing Information Science & Technology University (China); L Qin, B.S. Sun, Beijing University of Posts & Telecommunications (China).

Based on finite element analysis (FEA) method, the variations of thickness resonance frequencies with the changing of volume fractions of PZT rods in 1-3-2 piezoelectric composite has been calculated. This method has been checked by the experimental data of 1-3-2 PZT5A/Polymer-618 piezoelectric composites. It shows some matches between experimental results and the calculation, but also has limitation. To avoid non-considering periodicity and boundary condition in conventional FEA method, much more elements have been used in FEA model to simulate periodicity and boundary condition. Some kinds of vibration modes occurred in 1-3-2 piezoelectric composite have been identified. The minimum numbers of elements, which can provide precision calculation results using in FEA, has also been given. The vibration displacement of sample has also been calculated in FEA method. It shows a good math between the simulation results and the test results, which is tested by using laser scanning vibrometer.

353

Thermal Analysis of Piezoelectric Langevin Transducers

Bo Fu, Fei Chen

The overall performance of piezoelectric Langevin transducers may be substantially degraded due to heating. It is necessary to evaluate the temperature field of piezoelectric transducers before they are driven continuously. Based on the heat conduction equation and the FEM, the finite-element thermal analysis model of piezoelectric Langevin transducers was established. The temperature fields of the transducers with various end block materials (steel, titanium, aluminum magnesium, aluminum and brass) as well as piezoelectric rings were simulated and analyzed. According to the analysis result, the preferred end block material and structure of piezoelectric transducers are proposed. This work provides a foundation for the thermal analysis and optimization of large power piezoelectric Langevin transducers.

354

Three-Dimension Finite Element Analysis on Coupling Effect of Piezoelectric Ceramic Inside the Concrete Slab Under the Concentrated Load

Chen Qu, Zhe Jiang University of Science and Technology (China).

In recent years, the piezoelectric ceramic has been one of the mostly extensively applied concrete structures. Due to the complexity of piezoelectric ceramics boundary condition and its stress state as a concrete structure, it will be less efficient and limited in result if the relevant research on it is carried out in the way of the traditional experiments. In view of this, the paper studies the piezoelectric ceramic's boundary condition and its stress state by setting up the three dimension finite model of piezoelectric ceramic in the concrete and using finite element technique through computer simulation. In the simulation, varied concentrated loads are applied and different positions where the piezoelectric ceramic lies inside the concreted structure are adopted. And the three-dimension block element is adopted to simulate the concrete slab, while the plane element is adopted for the piezoelectric ceramic. Firstly, the stress distribution of the concrete slab and that of the piezoelectric ceramic inside the slab are derived from the computer nonlinear solver. Then by using the computer model and simulating the piezoelectric properties of the piezoelectric ceramic shown in the stress field, the equivalent circuit parameters of the piezoelectric ceramic are obtained when the varied concentrated loads are applied. The results of the analysis show that three-dimension finite element technique is a convenient and reliable tool for the studies on the coupling problems of the piezoelectric ceramic inside the concrete slab. The study offers references for the further three-dimension finite analysis on concrete structure stress monitoring with the use of the piezoelectric ceramic inside the concrete slab.

355

High Piezoelectric Activity in Tetragonal $K_{0.95}Li_{0.05}Ta_xNb_{1-x}O_3$ Lead-Free Single Crystals

H. Tian, J. Li, Z. Zhou, Y. Li, R. Zhang, Harbin Institute of Technology (China).

In the past several years, significant attention has been paid to the lead-free piezoelectric ceramics for the environmental problem, especially to the potassium sodium niobate (KNN) ceramics. Single crystals provide the opportunity to conveniently investigate the physical properties as a function of crystallographic orientations, and always have the better piezoelectric properties than the same composition ceramics. In this work, tetragonal $K_{0.95}Li_{0.05}Ta_xNb_{1-x}O_3$ lead-free single crystals have been grown by top-seeded solution growth technique and high quality as-grown crystals without striations were obtained. Dielectric and

piezoelectric properties of $\langle 001 \rangle$ poled crystals were measured as a function of temperature and dc bias using the LCR Meter and impedance analyzer, respectively. Both orthorhombic-tetragonal and tetragonal-cubic phase transition temperatures of $K_{0.95}Li_{0.05}Ta_xNb_{1-x}O_3$ shift to lower temperatures as the Ta content is increased. High piezoelectric activity ($d_{31} > -150$ pC/N, $k_{31} > 30\%$) was found to the crystals in their tetragonal phase, especially to the crystals in their tetragonal-cubic phase transition boundary, which due to phase transition as well as domain instability. For $K_{0.95}Li_{0.05}Ta_{0.59}Nb_{0.41}O_3$ single crystal, piezoelectric coefficient (d_{31}) and electromechanical coupling factor (k_{31}) achieved -340 pC/N and -40% at 19 °C, respectively, which were much larger than those of lead-free piezoelectric ceramics and even conventional lead piezoelectric ceramics Pb (Zr,Ti)O₃.

356

Point-by-Point Scanning Piezoelectric Phased Array for Detecting Damage for SHM

Xingang Li, Zhenqing Wang, Harbin Engineering University (China).

The aim of the present work is to develop a system of smart devices that could be permanently attached on the surface of the structure for monitoring cracks in most aerospace structures in isolated environments. It is shown that temporal and spatial focusing can be achieved through synthetic time-reversal array method for a linear phase array of sensors and actuators. Numerical simulation verifies the convergence of piezoelectric phased array. Near-field and far-field radiation pattern are also investigated to get the ultrasound field convergence plot. The scanning precision can be adjusted by changing the size of the focus patch. A Piezoelectric phased array system performs a point-by-point scanning in which focusing allow the inspection of large areas. Damage to the structure can be inferred if there is a significant change in the transient response of the structure using the analysis of the amplitude of the received signal. The location of this damaged area can be determined using the analysis of the time it reaches the transducer. By the method of synthesis of received signal time delay from multiple sensors, we can considerably enhance the signal strength, thus reducing the negative effects of noises to solve the tough problem of processing the echo signal. The results suggest an accuracy better than 1 mm in finding the location of crack tips.

357

Repeatable Piezoresistance of Conductive Rubber and Pressure-Sensitive Device

Qingwen Zhu, Long Ba, Chengxi Zhou, Enrong Li, Wei Dong, Southeast University (China); Juying Wu, Yuhong Huang, Jun Mei, China Academy of Engineering Physics (China).

A new conductive rubber composite was fabricated by mixing the ruthenium oxide nanoparticles with silicone rubber. The temperature dependent electrical conductivity of composite shows that the electron transportation is quite different beyond and below the glass transition temperature. The electron transmission microscopy reviews that there are polymer gaps between most nanoparticles. The conductivity of composites exhibits percolative behavior as the volume fraction of conductor phase increases across critical point. It was found that the composite filled with surface grafted ruthenium oxide presents stable piezoresistant recurrence. Based on the random resistor network model and transfer matrix approach, a Monte-Carlo numerical calculation was conducted to simulate the percolative and piezoresistant behavior of the composite. Experimental study also shows that the longitude piezoresistant factor was changed from negative to positive at large compressive strain (>20%), which was caused by transverse

poisson's expansion. A tactile sensor arrays using piezoresistant rubber and its drive electronics have been fabricated. The quantitative pressure measurement and 3D distribution visualization of flexible materials can be realized based on calibration and position creation. The research shows that the macroscopic recurrence of strain dependent electric conductivity can be improved by molecular scale tuning, and provides wide application potential in the fields of flexible strain or load sensors, smart structure, and tactile sensors.

358

Structure Evolution and Phase Development of NKN-BNT Piezoelectric Ceramics

Huiqing Fan, Laijun Liu, Northwestern Polytechnical University (China).

$Na_{0.5}K_{0.5}NbO_3$ (NKN) and $Bi_{0.5}Na_{0.5}TiO_3$ (BNT) are the most potential candidates of lead-base piezoelectric materials. The microstructure and phase transition behavior as well as dielectric and piezoelectric properties of NKN-BNT solid solution fabricated by mechanical alloying method were investigated. Nanopowder (~35 nm) could be obtained after calcining at a relative low temperature. A coexistence region of tetragonal and orthorhombic was found in pure NKN, and the region shifted to low temperature ranges with the introduction of impurities or the second phase. The crystal structure and microstructure of NKN-BNT solid solution changed dramatically with the increasing of BNT, and all phase transition temperatures deduced. The coexistence region shifted to room temperature while the amount of BNT is at 6 mol %. The morphotropic phase boundary (MPB) as well as the polymorphism behavior (PPB) of NKN-BNT solid solution is discussed in detail.

359

Multi-Sub-Layer Joint Model and Their Application to Piezoelectric Smart Beams Analysis

Ruixiang Bai, Liang Wang, Dalian University of Technology (China).

With increasing use of smart materials in engineering, the analysis of interface bond between conventional materials and PZT becomes an important topic. When a PZT patch is bonded on the surface of a beam, both shear and peel stresses exist in the adhesive between the PZT patch and the host beam. This paper presents exact static solutions to smart beams with perfectly bonded piezoelectric (PZT) actuators including shear and peel stresses, a multi-sub-layer shear deformable beam theory and multi-sub-layer joint model are developed to account for the adhesive between the PZT patch and the host beam. Then the ordinary differential equation (ODE) of the coupled shear and peel stresses are completely solved analytically. The exact solutions are applicable to smart beams with PZT actuators, the solutions give the shear and peel stresses in the adhesive actuated by the applied voltages, and for the actuated stress resultants and displacements in the host beam. The actuated stress distributions in the adhesive and the adhesive edge stresses varying with the thickness ratios are obtained. The ANSYS results to compared with the predicted by using this model.

360

Finite Element Simulation of Lamb Wave with Piezoelectric Transducers for Plasticity-Driven Damage Detection

Wenzhong Qu, Li Xiao, Yanguo Zhou, Wuhan University (China).

Structural health monitoring (SHM) is an emerging research area with multiple applications. There is a large number of non-destructive evaluation (NDE), non-destructive testing (NDT),

and non-destructive inspection (NDI) techniques for identifying local damage and detect incipient failure in critical structures. Lamb waves, or plate waves, are ultrasonic elastic waves that travel inside and along thin plates and is frequently used as diagnostic tools to detect damage in plate-like structures. In non-destructive evaluation, non-linear elastic wave spectroscopy (NEWS) methods represent powerful tools to explore damaged zones in a sample. In this paper, finite element simulation of Lamb wave with piezoelectric transducers for plasticity-driven damage detection in an aluminum plate is carried out. The aluminum plate shaped at 681 mm*720 mm*1.6 mm and twelve rectangular piezoelectric disks are surface bonded. The embedded two-dimensional piezoelectric wafer active sensors were used to generate and receive guided Lamb waves propagating in the plate structure. The plasticity damage zone is 24 mm*27 mm and produced by reducing the thickness of the plate. The material of this zone takes into plasticity when the plate is tensioned, but other area is in elastic. A full-scale FEM model for the aluminum plate was created using 8-node three-dimensional brick elements and piezoelectric wafer active sensors were created using coupled field elements on the commercial finite element code ANSYS 9.0 platform. The FEM mesh was particularly densified in the plate, where more than 6 FEM nodes per Lamb wavelength were guaranteed to exist, and ensuring simulation precision. A numerical experimental study of parametric interaction between two incident signals ($f_1=100$ KHz and $f_2=5000$ Hz) is led. Measurements of components at $f_2 - f_1$ and $f_2 + f_1$ around the plasticity-driven damage zone are performed and discussed. The nonlinear components of received Lamb waves are obtained using empirical mode decomposition (EMD). A virtual beam steering method with special nonlinear component delay was implemented as a signal post-processing procedure. The results of the numerical simulation demonstrate that the approach can detect the structural plasticity-driven damage.

361

Properties of 1-3 Connectivity Piezoelectric Ceramic/ Polymer Composites

Shuangshuang Liao, Shifeng Huang, Dongyu Xu, Xin Cheng.

In this paper, the main characteristics of the 1-3 connectivity piezoelectric composites were described, 1-3 connectivity piezoelectric composites were fabricated by the dice and fill method using epoxy resin as matrix and PZT-41 ceramic as functional phase. The fabricated composites have different numbers of ceramic elements whose cross-sectional area is 2mm×2mm and 1mm×1mm respectively. The interface bonding condition between matrix and piezoelectric functional phase was investigated by using SEM. Piezoelectric properties, dielectric properties, electromechanical properties and acoustic impedance of the 1-3 connectivity piezoelectric composites were also studied. The results show that interface bonding of the two-phase materials is compact, and d_{33} value of the composites is almost independent of the cross-sectional area and numbers of ceramic elements. The 1-3 connectivity piezoelectric composite with 33 ceramic elements and 1mm² cross-sectional area exhibits much larger g_{33} than that of PZT-41, and the largest value is up to 60.5(mv)mN⁻¹. Comparing with PZT-41, the vibration in the thickness direction is strengthened, thickness electromechanical coupling coefficient K_t of 1-3 connectivity piezoelectric composites with 33 ceramic elements and 1mm² cross-sectional area is up to 64.63%. The mechanical quality factor Q_m of the composites is significantly reduced. Its acoustic impedance Z is also lower than that of PZT-41.

362

Experimental Analysis of Carbon Nanotube Strain Sensor

Wei Qiu, Yi-Lan Kang, Qiu Li, Tianjin University (China); Zhen-kun Lei, Quan Wang, Dalian University of Technology (China); Qing-Hua Qin, Australian National University (Australia).

Strain is expected to have an important role in future devices based on micro-syste Different methods have been used to engineer strain in devices, leading to complex strain distributions. However, it has proved elusive in practice to measure the strain, especially the normal and shear components, directly and wireless with micro/submicro solutions. Owing to the investigating progresses of carbon nanotube (CNT) recently, it is well known that CNT has outstanding mechanical characteristics, its Raman shift is very sensitive to axial deformation, and its polarized resonant Raman behaves as the antenna effect. All these properties make carbon nanotube a potentially robust and wireless sensor applicable for the measurement of strain components. Some of research woke has been done in CNT strain sensor in application, but, it is lack in theoretical and modeling study for CNT strain sensor by Raman.

In this work, a theoretical study of the CNT strain sensor is presented by applying the CNT polarized Raman properties. Based on this work, the model of the planar strain components with the Raman shift is erected and a new technique of strain measurement named as Raman Strain Rosette is developed.

363

High-Sensitivity Humidity Sensor Based on a Single Sb-doped SnO₂ Whisker

Jiarui Huang, Junhai Wang, Anna A. Zhukova, Marina N. Rumyantseva, Alexandre M. Gaskov, Kun Yu, Cuiping Gu, Jinhuai Liu

Sb-doped SnO₂ whiskers were prepared by thermal evaporation of mixture of SnO and Sb₂O₃ powders. These were characterized by scanning electron microscopy (SEM), Transmission electron microscope (TEM), X-ray diffraction (XRD), X-ray photoelectron spectroscopy (XPS) and Auger electron spectroscopy (AES). FE-SEM observations reveal that the synthesized products consist of a large number of whiskers. Some of them are more than 2.0 mm in length. XPS result indicates that no other elements can be detected except for Sn, O and Sb, and the elemental composition of Sb in Sb-doped whiskers is 14.77 at%. Auger measurements demonstrate antimony is predominantly distributed on the surface of the whiskers.

The humidity sensitive characteristics of single SnO₂ whisker-based sensors also have been investigated. These sensors show high humidity sensitivity, rapid response and recovery, small hysteresis, and good stability. It is found that the impedance of the sensor decreases by about five orders of magnitude with increasing relative humidity (RH) from 43.2 to 84.3%. The response and recovery time of the sensor is about 12 and 8 s, respectively. The sensor showed a logarithmic dependence on the relative humidity in the range of 43.2-84.3% RH. No obvious drift was observed after aging the sensor in different RH at 25 °C for 7 days. The sensitivity of the Sb-doped SnO₂ whiskers-based sensor has been improved one order compared with pure SnO₂ whiskers-based sensor. These results indicate that the Sb-doped SnO₂ whiskers can be used in fabricating high-performance humidity sensors.

364

Ultrasonic Damage Detection in Concrete Structures by Using Pulse-Echo Sensor Arrays and SAFT

Lihua Shi, Zhixue Shao, PLA University of Science and Technology (China).

In Nondestructive Testing (NDT) of concrete structures, ultrasonic pulse-echo method is usually used to evaluate the inner structure.

Ultrasonic B-scan can be realized by moving the probe along one direction on the surface of the structure and then a cross-section image of concrete structure can be given. To improve the detection speed, a pulse-echo sensor array is designed for quick B-scan and easy operation; and to improve the detection resolution, Synthetic Aperture Focusing Technique (SAFT) is adopted. SAFT uses the multi-channel pulse-echo measurement records to synthesize a large aperture and thus improve the transverse localization accuracy. Design of the sensor array and the instrument that control the synthesizing process are introduced in this paper. The new detection system is then used to detect a test specimen with multiple embedded targets. The test results are also provided and analyzed in this paper.

366

Frequency Shift of Piezoelectric Microcantilever Humidity Sensors

Fei Wang, Jun Liang, Xuezheng Zhao.

Piezoelectric microcantilever sensors (PEMS), consisting of a highly piezoelectric layer bonded to a nonpiezoelectric layer, are used for humidity detection recently. Desorption of the water molecules increases the sensor's mass, which in turn decreases their flexural resonance frequency. Detection of humidity is achieved by monitoring the resonance frequency shifts of the sensors. However, recent experiments indicated that PEMS' flexural resonance frequency shifts during detection were more than two orders of magnitude larger than could be accounted for by the mass change alone, which limits the application of PEMS as humidity sensors with high sensitivity effectively. Therefore, it is still unclear what physical change is responsible for the observed large resonance frequency shifts. Recent research on dynamic behavior of micro cantilevers showed that the PEMS flexural resonance frequency could be influenced by air in which it immersed as a result of viscous damping effect. It is possible that a PEMS larger than the expected resonance frequency shift is also a result of the decrease of viscous damping during the humidity decreasing, and a detailed theoretical analysis of the frequency response of a PEM immersed in air and excited by an arbitrary driving force is presented in this paper to prove the possibility. In the modeling, the couple stress theory (Cosserat theory) is also introduced to the dynamic deflection function of a PEM to explain the size effect. Numerical results based on the presented theory have shown a great agreement with the experiments, which indicates that the viscous damping effect of air could be taken as a good explanation for the frequency shift of piezoelectric microcantilever humidity sensors. Methods for prediction of dynamic characteristics of long beam-like micro components could be easily derived based on the presented theory, which is of great value to users and designers of micro-electro-mechanical systems (MEMS).

367

Synthesis, Surface Modification and Ethanol Sensing Properties of Sb-doped SnO₂ Whisker

Jiarui Huang, Junhai Wang, Anna A. Zhukova, Marina N. Rumyantseva, Alexandre M. Gaskov, Kun Yu, Cuiping Gu, Jinhui Liu

Sb-doped SnO₂ whiskers were prepared by thermal evaporation of mixture of SnO and Sb₂O₃ powders. And then the surface of the whisker was modified with the Au nanoparticles by in situ

reduction method. These were characterized by scanning electron microscopy (SEM), Transmission electron microscope (TEM), X-ray diffraction (XRD), X-ray photoelectron spectroscopy (XPS) and Auger electron spectroscopy (AES). FE-SEM observations reveal that the synthesized products consist of a large number of whiskers. The Au nanoparticles were homogeneously distributed on the surface of the whisker. EDS result indicates that no other elements can be detected except for Au, Sn, O and Sb, and the elemental composition of Au on Sb-doped whiskers is 3.44 at%.

The ethanol sensitive characteristics of single SnO₂ whisker-based sensors also have been investigated. These sensors show good sensitivity, rapid response and recovery. The response and recovery time of the sensor is about 10 and 12 s, respectively. It is found that the working temperature of the sensor decreases from 280 °C to 160 °C after the surface of Sb-doped whiskers modified with Au nanoparticles. The sensitivity of the Au modifying the surface of Sb-doped SnO₂ whiskers-based sensor to ethanol has been improved 2.5 times compared with unmodified Sb-doped SnO₂ whiskers-based sensor. These results indicate that the Au modifying the surface of SnO₂ whiskers is important for improving its sensitivity and lowering working temperature.

368

Preparation, Modification, Morphology Tailor and Application of Conjugated Conductive Polymer in Chemical Sensors

Xingfa Ma, Mingjun Gao, Huizhong Xu, Yantai University (China); Guang Li, Zhejiang University (China).

In order to obtain a chemical sensor with high-sensitivity, rapid response, reversible at room temperature operating, it is necessary to develop the new sensitive materials with high sensitivities and good preparation technology. So far, the materials in these areas have been emphasized on the metal oxides semiconductor, SWNTs, MWNTs, conductive polymers, metal organic compounds, and so on. And among the so many above-mentioned advanced functional materials, the conductive polymer is one kind of sensitive materials at or near room temperature operating. The electrically conducting polymers have received considerable attention in the recent decades for chemical sensors and biosensors. Based on our previous reports in this field, progress of conductive polymer as sensitive film for sensor to chemical vapors is reviewed in this paper. Especially, the feature of conjugated polymer, the processing technology, doping characteristics and some factors affecting gas responses are discussed. Otherwise, the construction of conductive polymer with different morphology via a assembly process, the developments of nanostructured conductive polymer and organic-inorganic hybrid film sensor with high sensitivity and rapid response to vapors are also described, and some suggestions are proposed for further investigation.

370

Investigation of Thermal Distortion and Control of Spacecraft Based on Shape Memory Materials

Hongwei Sun, Xingwen Du, Huifeng Tan, Harbin Institute of Technology (China).

Gossamer space structures are relatively large, flimsy, and lightweight. As a result, they are more easily affected or distortion by space thermal environments compared to other space structures. This study examines the structural integrity of a Five-Meter Ka-Band Inflatable/Self-Rigidizable Reflect Antenna under space thermal environments. To maintain the required accuracy of the reflector under orbital temperature changes, the Gossamer space structures will utilize an active control system, consisting of boundary control actuators and an electrostatic figure control system with a real time closed loop feedback. An experimental

system is established to verify the control mechanism with photogrammetric measurement technique and Bragg fiber grating (FBG) sensor technique. The shape control experiments are finished by measuring and analyzing small amplitude distortion of Five-Meter Ka-Band Inflatable/Self-Rigidizable Reflect Antenna based on the active components made of shape memory alloy (SMA) and shape memory polymer composite (SMPC) material. Then, simulations are finished by NASTRAN finite element software with active effect which is considered to be deformation applied on the analytical model. The amplitude of distortion are obtained by the simulations. Both the experimental and numerical solution show that the amplitude of accuracy are developed which proves the feasibility of shape control using shape memory materials and this investigation explores the feasibility of utilizing an active cable based control system of shape memory materials to reduce global distortion due to thermal loading. It is found that through proper assemble of cable lengths and attachment points, significant thermal distortion reduction is achieved. Specifically, radial distortion due to on-orbit thermal loading .

371

Enhanced Mechanical and Shape Memory Properties of Poly(L-lactide-co-ε-caprolactone) Biodegradable Copolymers by Functionalized Carbon Nanotubes

Ali Nabipour Chakoli, Wei Cai, Jie He Sui, Maryam Amirian, Jiang Tao Feng, Harbin Institute of Technology (China).

Effect of pristine and functionalized multiwalled carbon nanotubes as reinforcement materials on the shape memory and mechanical properties of poly(L-lactide-co-ε-caprolactone) (PCLA) biodegradable shape memory copolymers was investigated. PCLA has not enough sufficient characters for hard tissue engineering. To improve the shape memory effect and mechanical properties of PCLA, we considered the fabrication of PCLA polymer composites. Functionalized multiwalled carbon nanotubes with PCLA (MWCNT-OH-g-PCLA)s are synthesized by in-situ ring opening polymerization of L-lactide (LA) and ε-caprolactone (CL) using stannous octanoate and hydroxylated MWCNTs (MWCNT-OHs) as the initiating system. The prepared MWCNT-OH-g-PCLA was used as a master batch to blend with neat PCLAR80 (80% LA, 20% CL) to obtain composites of varying MWCNT-OH-g-PCLA content. To compare the MWCNT-OH-g-PCLA with pristine MWCNT as reinforcement materials, MWCNT/PCLAR80 composites were prepared by the same way. The prepared composites were characterized with DSC, SEM, XRD and Tensile test device. In comparison between the MWCNT-OH-g-PCLAs and pristine MWCNTs as reinforcement materials for PCLA, the MWCNT-OH-g-PCLAs are more effective reinforcement materials than pristine MWCNTs. The tensile strength of (1 wt%)MWCNT-OH-g-PCLA/PCLAR80 composite is 28 % more than the tensile strength of neat PCLAR80 and the elongation at failure of this composite is 49 % more than the neat PCLAR80. SEM micrographs of the fracture surface of tensile test samples show that the tensile loading in composite can be completely transferred to the MWCNT-OH-g-PCLA. The shape memory effect analysis, strain deformation using tensile tests, show that both of pristine CNTs and MWCNT-OH-g-PCLAs increase the shape recovery of PCLAR80. but increasing in shape recovery using MWCNT-OH-g-PCLAs is more than using pristine CNTs.

373

Stress Self-Accommodation Characteristic of Fe-Mn-Si Shape Memory Alloy

Chengxin Lin, Deping Sun, Linlin Liu, Yizhuo Wang, Dalian Maritime University (China).

As we all known, the $\gamma \rightarrow \epsilon$ martensitic transformation in Fe-Mn-Si shape memory alloy is implemented by the movement of a $a/6 \langle 112 \rangle$ Shockley imperfect dislocation which exists in every other layer austenite surface (111) in turn, Three possible shear transformation directions which exist in every (111) γ surface, that are equative, formed HCP crystals of the same orientation. Similarly, the $\gamma \rightarrow \epsilon$ reverse martensitic transformation is implemented in manner of analogous positive transformation by the Shockley imperfect dislocation of three equivalence shear transformation directions in the (0001) ϵ surface.

It is confirmed ϵ martensitic of the thermo-induction or the spontaneity transformation commonly all presents self-synergism shape, then makes the shape strain of every anamorphosis canceling one another and the macroscopical shape transformation approaching zero. The stress induction martensitic transformation is a shape change which preferential formed by a single martensitic anamorphosis, produced a bigger transformation and effectively contributed to shape memory effect by the Shockley imperfect dislocation of a single type chooses the movement, when Fe-Mn-Si shape memory alloy subjects to external force then produces strain, When the external force is cancelled and the temperature is enough high (greater than A_f), ϵ martensitic anamorphosis of the preferential orientation in Fe-Mn-Si shape memory alloy can reversely transform to austenite by the original place and make the distortion sample approximately resuming the original shape, namely implement $\epsilon \rightarrow \gamma$ reverse transformation by the reverse movement of Shockley imperfect dislocation, simultaneity resume due to shape change arose by transformation, it is the mechanics of Fe-Mn-Si shape memory effect.

Based on the martensitic transformation shear theory and thermodynamics basic principle, if the stress induction martensitic transformation is forced about T_1 temperature, the critical machine driving force $\Delta G_{T_1}^S$ will be described as follows:

$$\Delta G_{T_1}^S = \Delta G_{M_s}^{\gamma \rightarrow \alpha'} - \Delta G_{T_1}^{\gamma \rightarrow \alpha'}$$

Where $\Delta G_{M_s}^{\gamma \rightarrow \alpha'}$ is the chemistry driving force of M_s ; $\Delta G_{T_1}^{\gamma \rightarrow \alpha'}$

is the chemistry driving force about T_1 temperature; Then we known the driving force offered by stress and temperature react to martensitic transformation is equivalent in the theory. Fe-Mn-Si shape memory alloy occurred transformation distortion by stress induced martensitic above M_s point (below M_d), also occurred reverse martensitic transformation which made the shape resuming and produce shape memory effect, when canceling the stress and heightening the temperature to the some one. It is concluded that the FCC/HCP interface of the alloy will reversely transform the austenite along the reverse of position transformation when applied to the reverse stress again, after the stress induced martensitic transformation and the reverse transformation under outside stress, due to the FCC/HCP interface of the Fe-Mn-Si shape memory alloy is reversible in the crystallogeny, namely the alloy occurred the stress induced martensitic reverse transformation then produced shape recovery. The recovery shape which produced by the reverse stress included the transformation distortion as well as the eldstoplasticity distortion which produced by the reverse stress unlike the shape memory effect; Fe-Mn-Si would preferential tropistically occur the stress induced martensitic and offer reverse transformation distortion along one of the three equivalence shear directions again, if it continue the reverse stress; similarly, the alloy would occur the martensitic reverse transformation and make the transformation distortion resuming again, if it applied the break-in stress to the sample.

The paper studied the characteristic of distortion and transformation of Fe-Mn-Si with position and reverse stress by XRD、SEM and TEM, then illuminated the stress self-

accommodation characteristic of the alloy.

375

Thermoelectric Module Driving Flexible Shape Memory Alloy Actuator

Baiqing Sun, Chao Zhang, Fengxiang Wang, Shenyang University of Technology(China).

In this paper, a flexible Shape Memory Alloy (SMA) actuator driving by thermoelectric module (TEM) is presented. The proposed actuator is consisted of a pre-shaped SMA wire at several located positions, and a many couples of Thermoelectric Modules, and some temperature and straining sensors.

Fig.1 shows the host structure illustration of a driving/actuating unit of the proposed actuator which compose of a couple of TEM affixed on the SMA wire by flexible thermal conductor, and thermal insulating materials wrapped up outside the thermal conductor and the wire. The sides of thermoelectric module couple (TMC) connected with the SMA wire can cool/heat synchronously or asynchronously any location only by alternating the current polarity of the TEM located at that point. Moreover, the actuator can be driven accurately through controlling the temperature of the pre-shaped location by modulating the main current value of the TMC. In order to improve control precision of the actuator, a thermistor sensor is embedded in the thermal conductor nearby the pre-shaped point, and two pieces of strain gauges are stuck on the surface of thermal insulating materials being perpendicular to the direction of moving.

Since the TMC is being used as driving devices, any extra cooling device is unessential. Therefore, the structures of the actuator are simplified further. The actuator with the proposed structure uninvolving transmission mechanism, it not only can improve response speed of the system, but also increases energy density and the control accuracy of the actuator. The detailed design principle, the structure and the fabrication method of the proposed actuator are introduced in this paper. Experiments show that the proposed actuator can bend or extend smoothly and rapidly following instructions. It suggests that the system have good dynamic response.

376

Synthesis of Shape Memory Polyurethane Using Bulk Polymerization

Ziming Yang, qiongling Jiang, wuyi Zhou, Zhuohong Yang, South China Agriculture University (China).

Shape memory polymers (SMPs), a novel class of functional materials, were developed quickly over the last decades. Polyurethane SMPs have been attracting a great deal of attention recently, due to their unique properties such as the wide range of shape recovery temperatures (from -30 to 70°C), high shape recoverability, good processing ability, and excellent biocompatibility.

While, up to the present, all SMPUs were prepared using solution polymerization. However, these SMPUs cannot endure repeated changes in shape memory, and the retention and recovery of shape memory will decrease after several cycles of shape memory recovery; Some studies have even found that the shape retention and shape recovery of SMPUs decrease dramatically after first cycle.

In our previous studies, some SMPUs were synthesized and studied. Although some SMPUs showed good shape memory effect according to chemical crosslinking, the mechanic property still is not satisfied. As bulk polymerization can effectively enhance the properties of polyurethanes, save cost and improve efficiency compared with solution polymerization. Besides, we also wish to

develop one kind of preparing method of shape memory fiber from SMPU.

In this paper, we introduced one series of shape memory polyurethane, which were synthesized using bulk polymerization. Their properties were analyzed by DSC and DMA, and the shape memory effect was also investigated. Of these prepared SMPUs, One kind of shape memory polyurethane fiber was spun by melting method and its shape memory properties were also investigated.

377

Study on Wrinkling Deformation Control of Inflatable Boom Based on Shape Memory Alloy

Zhenhui Tian, Zheng Guo, Hui Feng Tan, Changguo Wang (China)

As a new space structure, the space inflatable structure has received increasing attention in recent years. Inflatable boom is the fundamental structural part of space inflatable structures maintaining the expected configuration of the whole system, supporting external loads and guaranteeing the efficiency of the membrane surface. However the structures can be easily distorted and even collapsed by local wrinkling. In this study, the behavior of an inflatable boom is investigated numerically and experimentally, the methodology to control the wrinkling growth and the deformed configuration of the inflatable boom structure with a shape memory alloy (SMA) wire actuator is developed to achieve a better bending strength. The experimental equipment has been established to delay the growth of wrinkling that rapidly deteriorates the bending strength of the inflatable boom. The inflatable boom made of Kapton film is arranged as a cantilever and SMA wires are attached on the wrinkling edge of the boom as actuators, some parameters of the wrinkling deformation have been measured before and after using the SMA actuator with various internal pressures, such as wavelength and amplitude to compare and analysis the effect of the SAM wires. To understand the behavior of an inflatable boom due to wrinkling, the structure is numerically modeled using the ANSYS FE program with the equivalent nodal force method developed based on the thermal performance of SMA wire. The recovery force generated by the SMA wires could remove wrinkling and restore the deformation of the inflatable boom. The results from the experiment and numerical analysis show that SMA wires can eliminate the wrinkling deformation of inflatable boom effectively; the fundamental work for the pointing accuracy control of inflatable boom and the following study on the wrinkling behavior of large space membrane structures in space environment has been made.

379

The Theoretical Model and Application of the Double-N SMA Bundles Cooperating with Rubber Bearing

Guangping Zou, Jie Lu, Zhiqiang Shen, Harbin Engineering University (China).

Extensive attention has been paid to researches and applications of shape memory alloy(SMA) as a remarkable smart material for structural vibration control in recent years. The SMA-rubber bearing with hysteretic damping is initially developed by incorporating SMA wires and laminated rubber pad. A novel isolation seismic bearing model named the double-N SMA-rubber bearing is proposed and designed in this paper. The basic design idea is to add SMA wire bundles closed around the rubber bearing to improve the whole mechanical properties of the isolation seismic bearing. The corresponding theories equations and the working mechanism of this new isolation device are deduced. Also the application of this isolation model which is used in the vertical storage tank is presented. The shaking table test of the 1000m³

storage tank model is carried out. Different test working conditions and seismic excitations are given to analyze the structure response of the storage tank and the presented bearing properties. The presented bearing model is used in the first working condition. The displacement and acceleration responses of vertical tank model are obtained. Only the rubber bearing without SMA bundles is applied in another working condition. Also the structure response results are gained and contrasted with the former results. The experiments indicate that the movement of above structure is similar to translational movement and the comparative displacement is small in an effect shock absorption stiffness. Also the experimental results show the presented isolation seismic model is effective in absorbing energy and can be used in the isolation seismic design of the vertical storage tanks.

380 Characteristic of TiNi(Cu) Shape Memory Thin Film Based on Micropump

Huijun Zhang, Chengjun Qiu, Heilongjiang University (China).

In recent years, thin films of TiNi-based shape memory alloys are of increasing interest as actuating elements in silicon-based micro-electromechanical systems (MEMS), which have the potential to become a primary actuating mechanism for micro-actuators, medical fields, and biomedical applications. TiNi-based thin films provide a large energy density, higher frequency response and long working life time at the microscale. Also they can be engineered into structures of micro-size dimensions, patterned with standard lithographic techniques and fabricated in batch. However, the martensitic transformation temperatures are very sensitive to their compositions and metallurgical factors. Compared with the commonly studied binary TiNi thin films, the ternary TiNiCu thin films show less composition sensitivity to martensitic transformation temperature, a narrower temperature hysteresis (thus quick actuation response), stabilization of shape memory effects, superior fatigue property, etc., which makes them more suitable for micro-actuator application. In this study, a micropump driven by TiNiCu shape memory thin film is fabricated. TiNiCu thin film on silicon-based micropump has been prepared by magnetron co-sputtering of TiNi targets and Cu target. TiNiCu/Si film microstructure and phase transformation behavior have been characterized, the actuation property of TiNiCu thin film of micropumps has been analyzed. The film surface shows a smooth and featureless morphology without any cracks, and the hysteresis width ΔT of TiNiCu film is about 9 °C. By using the recoverable force of TiNiCu thin film and biasing force of silicon membrane, the actuation diaphragm realizes reciprocating motion effectively. Experimental results show that the micropump driving by TiNiCu film has good performance, such as high pumping yield, high working frequency, stable driving capacity, and long fatigue life time.

381 Synthesis and Characterization of Shape-Memory Polyurethane Films with Blood Compatibility

Cunxia Liang, Ying Wang, Nanjing Normal University (China); Li Li, Ninglin Zhou, Jun Zhang, Jian Shen, Nanjing Normal University, Nanjing University (China).

A number of thermal-responsive shape-memory polymers (SMPs) have been investigated as a potential family of special biological or medical devices. Among various SMPs, shape memory polyurethanes (PUs) are receiving much attention for their easy control of glass transition temperature (T_g) around the room temperature and excellent shape memory effect even at the room temperature. A family of crosslinked polyurethanes was

synthesized and characterized with 4,4-methylene bis(phenyl isocyanate) as hard segments and with either polytetrahydrofuran with different molar mass or polyethylene glycol as soft segments. Three-arm network junctions were provided by 1,1,1-trimethylol propane with an isocyanate group on each arm. Shape-memory effect of the PU were displayed at room temperature. Then the surface of the PU was modified by monomers of 2-(methacryloyloxy) ethyl-2-(trimethylammonium) ethyl phosphate (MPC), the phosphorylcholine groups. The grafted films were characterized by ATR-FTIR, XPS and contact angle measurement. The blood compatibility of the grafted films was evaluated by platelet adhesion in platelet rich plasma and scanning electron microscopy observation using PU film as the reference. Thermorheological response of each polymer was characterized by tensile creep tests through the glass transition of the soft segments. The purpose of this work is to synthesis PUs that exhibit a wide range of shape-memory and thermomechanical responses at body temperature to adapt and meet specific needs of minimally invasive cardiovascular devices. And no platelet adhesion is observed for the grafted films for 24h.

383 Effective thermo-Mechanical Properties and Shape Memory Effect of CNT/SMP Composites

Qingsheng Yang, Xia Liu, Fangfang Leng, Beijing University of Technology (China).

Shape Memory Polymer (SMP) is a kind of smart material with ability of shape memory. A micromechanical model and thermo-mechanical properties of CNT/SMP composites were studied in this paper. The thermo-mechanical constitutive relation of smart composites with isotropic and transversely isotropic CNT was obtained. Moreover, the shape memory effect of CNT/SMP composites was investigated and the effect of temperature and the volume fraction of CNT was discussed. The work shows that CNT/SMP composites exhibit excellent macroscopical thermo-mechanical properties and shape memory effect, while both of them can be affected remarkably by temperature and microstructure parameters.

Contributions of this paper are listed as follows:

- (1) CNT/SMP composite is of good mechanical properties and shape memory effect. But both of them are evidently affected by temperature and microstructure parameter.
- (2) The volume fraction of CNT has a remarkable effect on stress-strain curves of composites. The effect of reinforcement of CNT improves as the increase of volume fraction of CNT. The stress level of composites improves as the increase of aspect ratio of CNT, which implies better mechanical properties.
- (3) Effect of the temperature on mechanical properties of CNT/SMP is remarkable. Total stress level of stress-strain curve is low at a high temperature. The composites can exhibit good shape memory effect at high temperature for the same volume fraction of CNT.
- (4) The reinforcement of CNT enhances the mechanical properties of SMP but weaken the shape memory effect. In order to get enhanced properties and good shape memory effect, there is an optimal value of volume fraction of CNT.

384 Scaling Analysis for Hardness of Shape Memory Alloys in Sharp Conical Indentation

Guozheng Kang, Qianhua Kan, Southwest Jiaotong University (China); Wenyi Yan, Monash University (Australia).

Based on the dimensional analysis approach and finite element calculations, several scaling relationships in the indentation of

super-elastic shape memory alloys with sharp conical indenter were obtained. These scaling relationships illustrate the dependence of the indentation response and the hardness on the material properties of shape memory alloys, such as the phase transformation and plastic deformation. In the finite element calculation, a newly developed constitutive model of super-elastic shape memory alloy including the plasticity of induced martensite phase was employed. It is shown that the yield stress and strain-hardening parameter of induced-martensite plays an important role in the indentation response besides the phase transition properties. Additionally, the general relationships between the indentation hardness and the phase transformation stress, maximum transformation strain, martensite yield stress, and strain-hardening parameter of shape memory alloys were obtained. The results show that the indentation hardness of shape memory alloys is not proportional to the phase transformation stress and martensite yield stress, and cannot be used directly to measure the phase transformation stress and yield stress of super-elastic shape memory alloys.

386

Preparation of Single Crystal of TiNi Alloy and Its Shape Memory Performance

Ziming Guo, Ming Zhu, Chonghe Li, Xionggang Lu, Xiaosu Ye, Qijie Zhai, Shanghai University (China); Panxin Zhang, Ming Zhu, Nonferrous Metals Processing center(China).

Abstract: One unidirectional solidification equipment based on Bridgman method with high temperature gradient was designed, and the single crystal of Ti-50.0at%Ni NiTi alloy was successfully fabricated by this equipment as well as a selective growing zigzag-shaped crystallizer and a steady growth container that were made of electro graphite. The microstructure of single crystal sample was studied by means of OM, SEM and EDS; the orientation of single crystal was measured by X-ray technology; the phase transformation points were determined by DSC; the maximal recoverable deformations, the tensile strength and the elongation percentage were measured. The following conclusions are obtained:

1. By means of the designed unidirectional solidification equipment as well as a selective growing zigzag-shaped crystallizer and a steady growth container which made of electron graphite, NiTi single crystals were fabricated successfully with the following parameters: Molten temperature (1773K), Temperature gradient (140K/mm), and Pull velocity of rod (0.5~0.8mm/min).
2. Compared to polycrystalline NiTi alloy, the single crystal possesses excellent shape memory properties. Its maximum recoverable strain reaches 10%. Its fatigue life is also improved.
3. The microstructure of the cross- and vertical-sections of sample is dendritic, there exists Ti_2Ni intermetallic between the dendrites, the angle between the orientation of single crystal and [111] plane is about 15 degree.

387

Structural, Magnetic and Mechanical Properties of NiMnGaCu Shape Memory Alloys

Huibin Xu, Jingmin Wang, Chengbao Jiang, Beihang University (China).

NiMnGa ferromagnetic shape memory alloys (FSMAs) has been an intensively studied subject in recent decade, due to the interesting ferromagnetic shape memory effect, large magnetocalory and magnetoresistance. In this paper, the structural, magnetic and mechanical properties of Cu-doped NiMnGa alloys are studied. For $Ni_{50}Mn_{25}Ga_{25-x}Cu_x$ ($x=0-5$) and $Ni_{50}Mn_{30}Ga_{20-y}Cu_y$ ($x=0.2-5$) systems, while the Cu atom substitution for Ga greatly increases the martensitic transformation temperature, it is found that the

magnetic transition temperature T_C^M of the martensite is significantly decreased but no obvious variation in T_C^A for the austenite. Based on this, the mathematic equations are deduced to quantitatively reflect the relationship between T_M , T_C^M and T_C^A . By analyzing the effect of the element content variation on them a $Ni_{45}Mn_{37}Ga_{18-x}Cu_x$ system is obtained, in which some certain compositions exhibit $T_C^M < T_M < T_C^A$. The compositions can transform from paramagnetic martensite to ferromagnetic austenite at T_M , exhibiting large magnetization variation. Combining the very small entropy change during the transformation of NiMnGaCu alloys, a magnetic field induced martensitic transformation would be expected in these alloys.

The $Ni_{50}Mn_{25}Ga_{25-x}Cu_x$ ($x=3-20$) alloys are clarified into three groups according to their microstructure, martensitic transformation temperature and mechanical properties, i.e. $x=3-8$ with single martensite phase of body-centered tetragonal structure, $x=10-14$ with martensite phase and the second γ phase, and $x=16-20$ with single martensite phase of face-centered tetragonal structure. 7.2% shape memory effect is obtained. Compared with previously reported shape memory alloys that are generally compressed in mechanical tests but are difficult to be tensed, Cu doping significantly improves the mechanical properties of NiMnGa alloys. Especially, $Ni_{50}Mn_{25}Cu_{18}Ga_7$ alloy is developed a new high-temperature shape memory alloy with high plasticity, martensitic transformation at 616 °C, and face-centered tetragonal martensitic structure. The tensile stress and strain of the as-cast polycrystalline $Ni_{50}Mn_{25}Cu_{18}Ga_7$ are achieved to be 488.7 MPa and 11.7%, respectively; and a compressive true stress and true strain of 785.6 MPa and 70% are obtained without fracture.

388

Highway Bridge Unseating and Reduction Analysis Using Sma Restrainers under Near-Fault Earthquakes

Anxin Guo, Hui Li, Harbin Institute of Technology (China).

Ground motion records from recent strong earthquakes reveal the near-fault ground motions are different from far-field ground motions. The unique characteristics of near-fault ground motions impose large demands on the highway bridge and induce the unseating of the bridge. The aim of the current study is to investigate the effect of the near-fault ground motions on the unseating of the highway bridges, and the unseating reduction of the highway bridge by using the shape memory alloy (SMA) restrainers. A finite element model of a highway bridge is established, and the dynamic characteristics of the highway bridge are analyzed subjected to three near-fault ground motions. To mitigate the unseating of the highway bridge, a SMA restrainer is developed and the performance of the SMA restrainer for eliminating the bridge unseating of the highway bridge is analyzed. Numerical simulation results indicate that the near-fault ground motions strongly increase the structural responses, and the SMA restrainer can be effectively used to mitigate the bridge unseating subjected to the near-fault ground motions.

391

A New Diagnostic Method for Detection of Bolt Loosening in Thermal Protection Panels

Weihua Xie, Shanyi Du, Boming Zhang, Songhe Meng, Fuhong Dai, Dong Yu, Harbin Institute of Technology (China).

Research and development efforts are underway to provide structural health monitoring systems to ensure the integrity of thermal protection system (TPS). An improved analytical method was proposed to assess the fastener integrity of a bolted structure in this paper. A new unsymmetrical washer was designed and fabricated, taking full advantage of piezoelectric ceramics (PZT) to

play both roles as actuators and sensors, and using energy as the only extracted feature. This method doesn't restricted by the materials of the bracket, panel and base structure. A series of experiments on metallic honeycomb sandwich panel TPS were completed to detect the bolt loosening. Studies show this method can be used not only to identify the location of loosening bolts rapidly, but also to estimate the torque levels of loosening bolts. It has been found that energy is the only extracted feature in this method, which making the computation process become very simple, so the operation speed rises greatly without impacting the accuracy of the results.

392

A New Type Wireless Smart Sensor and Sensor Network for Structural Health Monitoring

Y. Lei, Y. L. Tan, J. X. Wang, Xiamen University (China).

Traditionally, structural health monitoring employs wire-based monitoring system which requires vast amount of labor and cost for installation and maintenance of wires. In recent years, some innovative wireless monitoring systems have been proposed. However, more exploration and developments on the new wireless sensing systems are required before wireless monitoring systems can substitute for the traditional wire-based system. In this paper, a new type wireless sensor and sensor network is proposed for the health monitoring of structures. The new wireless sensor module mainly consists of three functional modules: 1) sensing interface with a 4-channel, 16bit ADC; 2) computational core with a 8-bit Atmel128 microcontroller, and wireless communication module with a IEEE 802.15.4 compliant wireless modem module Chipcon CC2430. The sensor network has a two-level cluster-tree architecture with Zigbee communication protocol. The communication of sensor nodes in a cluster with the cluster head forms the lower level while the communication between the cluster heads forms the upper level. Important issues such as power saving and fault tolerance are considered in the design of the sensor network. Each cluster head in the network is characterized by its computational capabilities that can be used to implement the computational methodology of structural health monitoring, making the Wireless Sensor and Sensor Network to be a smart one. Performance of the new type wireless sensor and sensor network is validated by the ambient vibration study of the Wuyuan steel arch bridge in Xiamen, China. Measurement data collected by the wireless system are compared with those obtained by the tethered system. The local computational capacity of the smart sensor units is also tested. It is shown that the new type wireless smart sensor and sensor network provides a efficient tool for structural health monitoring.

394

Application of Cement-Based Piezoelectric Composites in Acoustic Emission Detection for Concrete

Lei Qin, Jinan University (China); Zongjin Li, Hong Kong University of Science and Technology (Hong Kong, China).

1-3 cement-based piezoelectric composites that have good compatibility with concrete material have been developed for health monitoring of concrete structures. Transducers made of this type of composites have been especially designed to meet the requirement of being embedded into concrete materials. In the property calibration, the transducers show broadband frequency response which is the basic requirement of acoustic emission (AE) transducers. The frequency response of the transducers made of 1-3 cement-based composites and piezoelectric ceramic are compared. Plain concrete beams with embedded 1-3 cement-based piezoelectric transducers are prepared and tested. During loading,

AE events are recorded. The accumulated AE event number was analyzed with the loading history. The damage evolution of concrete beam could be evaluated using the system including embedded transducers and software to record and analyze the data.

395

Corrosion Monitoring of Reinforcing Steel in RC Beam by an Intelligent Corrosion Sensor

Guofu Qiao, Jinping Ou, Harbin Institute of Technology (China); Jinping Ou, Dalian University of Technology (China).

Health degradation by corrosion of steel in civil engineering, especially in rough environment, is a persistent problem. Structural health monitoring (SHM) techniques, including embedded corrosion rate sensors, can greatly improve the quantification of the steel corrosion rate, which can lead to improved estimates of structural safety and serviceability. The reinforcing concrete (RC) beams immersed in 3.5%NaCl solution have been studied. Firstly, an intelligent five-electrode corrosion sensor has been developed to provide the platform for corrosion monitoring of the steel bar in concrete beam by electrochemical method. Secondly, half-cell potential of the RC beam has been measured. Thirdly, galvanostatic step method has been used to excite the steel-concrete system and the transient response of the system has been obtained. The data of the transient response has been analyzed by segmented method. It has been certified that the time constant could be used to determine the corrosion state of the steel bar qualitatively. Finally, wavelet transform method has been used to analyze the electrochemical noise (EN) of the steel bars in RC beam. The results show the corrosion sensor can provide a good platform for many electrochemical methods. The half-cell potential changes greatly before and after corrosion and it is effectively to analyze the data of the transient response by segmented method. The energy distribution plot (EDP) of EN can be used as a benchmark method to determine the present of the pitting corrosion.

396

Experimental Research of New Cement-Based Piezoelectric Sensor System for Structural Health Monitoring

Xiaoming Yang, Haiqing Liu, Liaoning Technical University (China); Zongjin Li, The Hong Kong University of Science and Technology (Hong Kong, China).

A new cement-based piezoelectric sensing system has been designed, fabricated and tested for the application of structural health monitoring. The sensing system was composed of sensing element, small scale home made amplifier, and a home made (Analog-digital) conditioner. The experiments, including the frequency response in the general frequency range of civil engineering structure from 0.01Hz to 40 Hz and the relationship between output and input of sensing system, were adopted to test the basic performance of the sensing system. Moreover, the performance of the system subjected to a complex load, random load and square load were measured. The sensing system showed a good phase independency that met the basic requirement of dynamic measurement. It was found from the amplitude sweep test that the output of sensor was linearly corresponding to the input of sensor. Similar phenomenon was observed in the experiments with complex load and random load. The sensing system has been applied in a prism and a two story model frame structure. The column was compressed by Material Test System with harmonic load and the frame was shaken on a shaking table with sine wave, Northridge earthquake wave, Kobe earthquake wave and Taiwan earthquake wave. The results showed that the sensing system worked properly and reflected the real stress condition in the structure. Thus, the sensing system had a good potential to be used

in civil engineering structural health monitoring.

397

Experimental Research on Stable Fretting Wear of Stainless Steel Wires in Transformable Component

Xiuping Dong, Li Zhang, Beijing Technology and Business University (China); Guoquan Liu, Jianchun Yang, University of Science and Technology Beijing (China); Hongbai Bai, Jianchun Yang, Ordnance Engineering College (China).

Cool-drawn 1Cr18Ni9 stainless steel wires of ϕ 0.1~0.5 mm can be woven and punched to prepare transformable component which has loose, reticulate structures. When it is uploaded with vibrating force, the displacement will cause intense frictions between wires' surfaces which will dissipate abundant energy and thus it can serve as dampers like natural rubbers. Since such new type of material has double characteristics of both rubbers and metals, it is commonly called "Metal Rubber".

There is certain amount of contact point/surface on wires in the transformable component and the displacements between wires are at micron levels. Previous experiments showed that wear course of 'fretting cell' could be plotted as four phases: polish, adherence, forming of the third bed and stabilization. The stabilization phase, in which the friction coefficients are comparatively stable, dominates the whole course. Based on data of Metal Rubber vibration fatigue experiment, ϕ 0.3 mm cool-drawn 1Cr18Ni9 stainless steel wires' dry fretting experiments at different load are made on SRV high temperature wear tester, friction coefficients are collected and fret traces are studied by laser scanning confocal microscope (LSCM). Results indicate that wire's stabilization wear phase is the circulation process of grindings' forming, concentrating to blocks of ϕ 10 μ m, busting and discharging. Deformation induced martensite transit in wire's cool drawing has significant effects on grinding blocks' bursting performances.

398

Health Monitoring of a Continuous Rigid Frame Bridge Based on PZT Impedance And Strain Measurements

Zhe Liu, Huaqiang Zhou, Huazhong University of Science and Technology (China).

Critical civil infrastructures such as bridges, dams, and pipelines present a major investment and their safety and security affect the life of the citizens and national economic development. So monitoring their health status on board is a greatly important mission for engineers and researchers. PZT is one of piezoelectric smart materials, which has direct and converse piezoelectric effects and can serve as an active sensor. A health monitoring technique based on PZT impedance and strain measurements is addressed in this paper, which use the electromechanical coupling property of PZT. The main features of the technique are that it is not based on any physical models and sensitive to tiny damage for its high frequency characteristics. An engineering application on health monitoring of a continuous rigid frame bridge is implemented based on the PZT impedance and strain measurements. In this application, some PZT active sensors are embedded into the box-sectional girders and the electrical admittances (inverse of impedance) of distributed PZT active sensors and strains of concrete are measured when the bridge is constructing or suffering from operational loads. Based on the obtained PZT admittance and strain measurements the health status of the continuous rigid frame bridge in construction and operation process is monitored and evaluated successfully.

399

Health Monitoring of Reinforced Concrete Structures Based on

PZT Admittance Signals

Dansheng Wang, Hongping Zhu, Huazhong University of Science and Technology (China).

Reinforced concrete (RC) structure is one of most familiar engineering structure styles in the civil engineering community, which often suffer crack damage during their service life because of some factors such as overloading, excessive use, and bad environmental conditions. Thus early detection of crack damage is of special concern for Reinforced concrete structures. Piezoelectric materials have direct and converse piezoelectric effects and can serve as actuators or sensors. A health monitoring method based on PZT admittance signals is addressed in this paper, which use the electromechanical coupling property of piezoelectric materials. The basic principle of the technique is that by measuring the electrical admittance of PZT bonded to the surface of host structure, the changes in structural mechanical impedance resulted from the presence of crack damage are monitored because the electrical admittance of PZT is directly related to the mechanical impedance of host structure. The main features of the technique are that it is not based on any physical models and its high frequency characteristics. An experimental study on health monitoring of a reinforced concrete beam is implemented based on the PZT admittance signals. In this experiment, the electrical admittances of distributed PZT sheets are measured when the host beams are suffering from variable loads. From the obtained PZT admittance curves one can find that the presence of incipient crack can be captured and the cracking and fracture load of the RC beam can also generally determined. By the experimental study it is concluded that the health monitoring technique is quite effective and sensitive for reinforced concrete structures, which indicates its favorable application foreground in civil engineering field.

400

Immune System Based Approach to Fault Diagnosis for Wireless Sensor Networks

Yongjun Chen, Shenfang Yuan, Jian Wu, Yingjie Zhang, Nanjing University of Aeronautics and Astronautics (China).

Wireless sensor networks are a complete distributed system. The reliability and robustness have been recognized early as one of the key issues. Considering distribution features of sensor nodes, however, the faults happened in wireless sensor networks are usually random and unpredictable. The conventional diagnosis methods become increasingly difficult to deal with. As a result, the applications in different conditions are seriously limited. To solve the problem, an approach inspired by artificial immune system is presented and discussed to diagnose the faults in wireless sensor networks. Firstly, the feature signals of sensor nodes consisted of data packet, energy cost and monitored object value are gained in normal and known-fault situations, which are reckoned respectively in self and known-fault patterns of artificial immune system. Secondly, the signals are normalized and constructed in a phase space between 0 and 1. The cluster centers of self patterns are obtained by fuzzy clustering algorithm and the detector centers with genetic algorithm are generated to improve the spatial distribution and speed up the training stage. Finally, the paper regards unknown-fault patterns as antigens and detectors as antibodies. Using the mechanism of evolution learning of artificial immune theory and the distributions zones of antibody, an immune calculation is executed. The corresponding zones of different faults were distinguished and marked on the phase space. The simulation result has demonstrated that the approach to fault diagnosis is feasible for wireless sensor networks. Compared with generated detectors of negative selection algorithm, the efficiency is raised approximately 10%.

401

Investigation and Detection on Corrosion of Concrete Structure in Marine Environment

Dandan Zhang, Jin Wu, Jun Li, Jiang Geng, Nanjing University of Aeronautics and Astronautics (China).

Due to the effect of marine environment, the corrosion of steel reinforcement in concrete structure is a very serious issue, so the field detection of steel reinforcement corrosion is a very important. The corrosion rate of the sampled steel reinforcement was obtained according to the field investigation of Lianyungang Port and the experiment of the sampled steel reinforcement. The chloride concentration in the concrete of different position and the sampled concrete powder at different depths in the splash zone was measured in the laboratory. Moreover, the corrosive parameter of concrete structure was obtained by statistical analysis. The tests results indicate that the reinforcement corrosion is very serious. The corrosion rate of the sampled steel reinforcement and the concentration of chloride in concrete fragments are both very high, which shows that Berth 14# in Lianyungang Port has been deteriorated badly. The chloride content at splash zone of Berth 57# and Berth 58# are also very high, which indicates that the chloride penetration for reinforcement concrete structures is very serious. The bearing capacity and the reliability of members can be calculated by experiment data. The bearing capacity and the reliability of members decreased obviously and members need to be maintained and strengthened in time.

402

Life Assessment of Marine High Performance Concrete Based on Reliability in Cross-Sea Bridges

Qingling Wu, Hongfa Yu, Nanjing University of Aeronautics and Astronautics (China); Jiachun Wang, Xiamen University of Technology (China).

Probability analysis on the durability life of marine high performance concrete in Cross-sea bridges is little known. Using the probability method on the basis of the second Fick's law, research work was carried out to investigate the distribution factors that may influence the durability life of marine high performance concrete. Due to the deficiency of the decisive method for prediction of durability life, a method based on reliability is proposed. The relationship between the durable reliability index and the corrosion time is established. The present paper takes the time when the durable reliability index falls below a stipulated index as the end of durable life. The proposed predictive method of durability life for marine high performance concrete in Cross-sea bridges is therefore improved.

403

Monitoring Forces in Bridge Steel Cables Based on EM Sensor and a Wireless Monitoring System

C. Liu, Y. Lei, Xiamen University (China); J. P. Lynch, University of Michigan (USA); K.H. Law, Stanford University (USA).

Bridge cable forces are important parameters for the safety of bridges. Some techniques have been developed for the measurement of bridge steel cable forces. For bridges in service, steel cable forces are usually monitored by the technique based on the vibration frequencies of cables. In recent years, a useful alternative technique based on the magnetoelastic sensors (ME or EM sensors) has been proposed. However, all the systems current available for monitoring bridge cable forces are wired-based. Installation and maintenance of such wired-based monitoring systems for large span bridges is time consuming and expensive.

With recent developments of wireless sensing, wireless monitoring systems have been developed to eradicate the extensive lengths of wires in the tethered system. In this paper, the wireless monitoring system developed by researchers at Stanford University and Michigan University is employed to measure steel cable forces using the method based on the approach of EM sensor. A novel by-pass type EM sensor with temperature compensation is developed and it is incorporated as the sensing interface of the wireless sensing system. To validate the performance of the wireless sensing system for monitoring bridge cable forces, experimental test for measuring cable force in laboratory is conducted. Measurement results of cable forces based on the wireless sensing system are compared with those obtained by the wire-based system. It is shown that the wireless sensing system can provide a low-installation cost and efficient technique for monitoring bridge steel cable forces.

404

Monitoring the Cracks in Concrete Frame-Shear Wall Structure Model Using FBG Sensors

Li Sun, Hongnan Li, Dalian University of Technology (China); Li Sun, Hong Kong Polytechnic University (Hong Kong, China).

Civil structures have to meet the application requirements. Among others, the structures have to work properly during ordinary conditions without, e.g., over-deformation, vibration and large crack, which the users may feel uncomfortable with. Hence, it is required to monitor the occurrence of cracks and track the growth of them, and subsequently the width of cracks can be obtained. This is a long time unsolved issue in civil engineering. In this paper, we use fiber Bragg grating (FBG) sensors to investigate a reinforced concrete frame-shear wall structure during vibration test. FBG sensors are able to monitor the occurrence and growth of cracks till the failure of the structure. It is thus demonstrated the capability of this technique as an effective and reliable approach for structure monitoring.

405

Photo-Damage Resistant and Phase Matching Properties of Double-Doped In:Zn:LiNbO₃ Crystals

Yiran Nie, Yudong Huang, Yuanjun Song, Rui Wang, Biao Wang

In:Zn:LiNbO₃ crystals have been grown by Czochralski technique. The infrared transmission spectra of the samples showed that the OH⁻ absorption peak of In(3mol.%):Zn(3mol.%):LiNbO₃ located at about 3508cm⁻¹, while those of In(1mol.%):Zn(3mol.%):LiNbO₃ and In(2mol.%):Zn(3mol.%):LiNbO₃ located at about 3485cm⁻¹. The photo-damage resistant ability of the crystals was measured with the directly facula-distort observing method. The results showed that, when doped In³⁺ and Zn²⁺ concentrations reached their threshold concentrations, the photo-damage resistant ability of In(3mol.%):Zn(3mol.%):LiNbO₃ was two orders of magnitude higher than that of pure LiNbO₃. Second harmonic generation (SHG) experimental results showed that the phase matching temperature of In(3mol.%):Zn(3mol.%):LiNbO₃ was almost at room temperature, and their SHG efficiency was higher than that of Zn(7mol.%):LiNbO₃ and pure LiNbO₃.

406

Prediction of Impact Damage on Stitched Sandwich Composite Panels

Xitao Zheng, Linhu Gou, Jianfeng Zhang, Northwestern Polytechnical University (China).

Sandwich structures are extensively employed in the aerospace and automobile industries. The understanding of their behaviour under

impact conditions is extremely important for the design and manufacturing of these engineering structures since impact problems are directly related to structural integrity and safety requirements. One of the main drawbacks of sandwich structures is the loss of load carrying capacity due to through-thickness (out-of-plane) properties. One method to enhance the out-of-plane properties is the stitching of dry semi-finished fiber products in the thickness direction prior to the infusion of the resin. On the other hand, the insertion of stitching yarns in the thickness direction may affect the mechanical properties in the laminate plane such as stiffness and strength.

To quantify the effect of structural through-thickness reinforcement in foam core sandwich composite panels, a finite element based unit-cell model was developed to estimate the elastic constants of structurally stitched foam core sandwich composite panels taking into consideration the yarn diameter, the stitching pattern and direction as well as the load direction. A numerical simulation is performed to predict the effects of stitching on the low-velocity impact response of stitched sandwich composite panels. The load/displacement relations during the impact are assumed to be the same as in the corresponding static problem. Hence a solution to the problem of a stitched delaminated beam under a static contact force is developed. The effects of stitches are modeled as a constant shear traction in the stitch bridging zone to account for the shear resistance offered by the unbroken stitches. From the static simulation the load/displacement and displacement/crack-extension relations are obtained. From the area under the load/deflection diagram the apparent fracture toughness due to the stitching is also estimated. The impact simulations provide information on the load at which the crack propagation initiates, the maximum contact force, and the extent of crack propagation at the end of the impact event. The results indicate that stitching does not increase the load at which delamination begins to propagate, but greatly reduces the extent of delamination growth at the end of the impact event.

407

Research on BOTDR Sensing Technique in Structural Health Monitoring

Xuefeng Zhao, Jie Lu, Jinping Ou, Dalian University of Technology (China); Jinping Ou, Harbin Institute of Technology (China).

Feasibility study on application of BOTDR (Brillouin Optical Time-Domain Reflectometer) to structural health monitoring for civil structures was conducted in this paper. According to the features of civil engineering structures, one novel kind of fiber optical strain sensors (sensing gauge: 10m~100m) based on BOTDR sensing technique was proposed and developed. Strain calibration and temperature calibration test were conducted to study the feasibility of the sensor. Also the temperature compensation technique was studied and validated by comparison test. Test results show that the sensor can measure the strain and temperature correctly, and the temperature compensation technique can compensate the signal noise caused by environmental temperature variation. Fiber optical sensor based on BOTDR sensing technique can be applied to large gauge distributed strain sensing field.

408

Strain Properties Analysis and Wireless Collection System of PVDF for Structural Local Health Monitoring of Civil Engineering

Yan Yu, Weijie Dong, Yajing Jin, Yang Wang, Dalian University of Technology (China); Jinping Ou, Harbin Institute of Technology (China).

For large civil engineering structures and base establishments, for example, bridges, super-high buildings, long-span space structures, offshore platforms and pipe systems of water & gas supply, their lives are up to a few decades or centuries. Destroyed by environmental load, fatigue effect, corrosion effect and material aging, these structures produce inevitably such side effects as damage accumulation, resistance reduction and even accidents. And the traditional civil structure is a kind of passive one, whose performance and status are unpredictable to a great extent, but the informatics' introduction breaks a new path to obtain status messages of structure, thus it is an important research direction to evaluate and design reliability of civil structure by the use of monitoring and health diagnosis technique, and this also assures the security of service for civil engineering structures.

Smart material structure, originated from aerospace area, has been a research hotspot in the application of civil engineering, medicine, shipping, and so on. For structural health monitoring of civil engineering, the research about high-performance sensing unit of smart material structure is very important, and this will possibly push further the development and application of monitoring and health diagnosis technique. At present, piezoelectricity material is one of the most widely used sensing materials among the research of smart material systems (structures). As one of the piezoelectricity materials, PVDF (Polyvinylidene Fluoride) film is widely concerned for its property advantages of low cost, good mechanical ability, high sensibility, ability of being easily placed and resistance of corrosion, but there exist a few researches about building a mature monitoring system using PVDF.

In this paper, for the sake of using PVDF for sensing unit for structural local monitoring of civil engineering, the strain sensing properties of PVDF are studied in detail. Firstly, the operating mechanism of PVDF is analyzed. Secondly, wireless collection system of PVDF is integrated with PVDF sensor, charge amplifier, wireless transceiver and the corresponding software of signal collecting. Then, with strain gauge as a reference, experiments have also been done to study the quasi-static and dynamic strain responding of PVDF sensing element respectively, such as sensitivity, linearity and frequency responding, etc. The experimental results show that, PVDF is sensitive to the impact response of civil engineering structures, and can finish absolutely the local monitoring in different frequency response cooperating with strain gauge; the developed wireless collection system has the characteristics of no lines, saving cost and installation time, and thus further pushed the practical application of PVDF for civil engineering structures.

410

The Application of Carbon Fiber Resistance in Monitoring of Curing

B.M Zhang, X.Y. Sun, Harbin Institute of Technology (China).

Thermal residual stress in resin matrix composite due to the different coefficient of thermal expansion (CTE). The CTE of carbon fiber is lower than resin matrix. Based on mechanics, rising temperature will cause tensile stress, cooling down will cause compress in fiber. There exists expanding and shrinkage during curing process of epoxy. In single fiber composite system, they play different roles, present with tensile and compress stress on fiber. This paper deals with the relationship of the carbon fiber resistance with strain and temperature. The effect of expanding and shrinkage on residual stress is got by the fiber resistant measurement. Compared with the numerical method, the resistant experiment has a good precision. Resistance variety curve of the experiment shows the chemical process during resin solidification. The shear stress between fiber and matrix existing during temperature load can also be measured by the same method. The

carbon fiber's resistant can be used as sensor to monitor and control the curing process. This is a simple and effective method to research the curing process.

411

The Flaw-Detected Coating and Its Applications in R&M of Aircrafts

Feng Hu, Mabao Liu, Zhigang Lv, Xi'an Jiao-tong University, Xi'an Jiaotong University (China).

The accumulation of fatigue damage in critical structural members of the aging aircrafts is an increasingly complex and continuing high priority problem. There is growing evidence that (i) multiple site damage or multiple element damage may compromise fail safety in older aircrafts, and (ii) significant fatigue damage, with subsequent formation of cracks, may occur at locations not considered in original fatigue failure evaluations. Thus, there is now a critical need for: (i) a wide area scanning technology capable of detecting microcrack clusters over wide areas of complex shaped components, with the objective of identifying potential problem areas; and (ii) a reliable permanently mounted monitoring tool for fatigue damage detection at identified fatigue critical locations, particularly at locations that are difficult to access for inspection.

A new monitoring method called ICM (Intelligent Coating Monitoring), which is based mainly on the intelligent coating sensors has the capability to monitor crack initiation and growth in fatigue test coupons has been suggested in this study. The intelligent coating sensor is normally consisted of three layers: driving layer, sensing layer and protective layer where necessary. The sensing layer is made of conductive materials and the surface cracks in substrate can be represented by the variation of the resistance of the sensing layer. Fatigue tests with ICM on the surface inside a 8.00mm hole in an TC4 tension-tension fatigue specimen, demonstrated the capability to detect cracks with $l < 300\mu\text{m}$, corresponding to the increment of the sensing layer's resistance at the level of 0.05 Ω . Also, ICM resistance measurements correlate with crack length, permitting crack length monitoring. Numerous applications are under evaluation for ICM in difficult-to-access locations on commercial and military aircrafts. The motivation for permanently flaw-detected coating monitoring is either (i) to replace an existing inspection that requires substantial disassembly and surface preparation (e.g. inside the fuel tank of an aircraft), or (ii) to take advantage of early detection and apply less invasive life-extension repairs, as well as reduce interruption of service when flaws are detected. Implementation of ICM is expected to improve fleet management practices and modify damage tolerance assumptions.

412

Ultra Thin Fiber Laser Accelerometer for Structure Vibration Detection

Wentao Zhang, Xuecheng Li, Faxiang Zhang, Fang Li, Yuliang Liu, Chinese Academy of Sciences(China).

Accelerometers are often used in structural health monitoring, smart structures, and aircraft damage detection. In this paper, an ultra thin fiber laser accelerometer (FLA) for structure vibration detection based on a flat diaphragm is presented. This accelerometer uses an flat diaphragm to transfer the acceleration-induced displacement of the mass to the axial elongation of the fiber laser. The flat diaphragm is clamped by the sensor shell to reduce the transverse sensitivity (Fig.1). The interrogation of the fiber laser accelerometer is achieved by using phase generated carrier (PGC) demodulation (Fig.2). A piezo-electric fiber stretcher in one of the unbalanced Mach-Zehnder interferometer (MZI) arms in the demodulator

induces a phase-shift carrier signal on the sensor output signals that enables passive recovery of dynamic phase-shift information. This set-up uses a commercially available Dense Wavelength Division Multiplexer (DWDM) as a wavelength filter at the output of the MZI to interrogate multiple sensors. Both theoretical and experimental investigations are presented in this paper. The result shows that the proposed accelerometer has a high sensitivity and a flat frequency response. Owing to the greater deformation of the diaphragm with a mass at its center, ultra thin dimensions have been achieved.

413

Synthesis and Properties of Pbo/Swnt Composite Fibres

Feng Wang, Yudong Huang, Harbin Institute of Technology (China).

The PBO/SWNT composites have been successfully synthesized by the in-situ polymerization method, and have been spun into fibres using dry-jet wet spinning. The single-walled carbon nanotubes were treated with strong oxidizability acids to form the carboxylic single-walled carbon nanotubes. SWNT and PBO/SWNT fibres have been analyzed using Raman spectroscopy and X-ray photoelectron spectroscopy. The thermal resistance and the tensile strength of have been characterized. The results show that the surface of SWNT after treatment contains many carboxyl groups and hydroxyl groups and PBO/SWNT fibres have super thermal resistance like PBO and the tensile strength of PBO/SWNT fibres is about 50% higher than that of the PBO fibres containing no SWNT.

414

Thermo-Sensitive Hybrid Microcapsules Prepared with Pickering Suspension Polymerization

Chaoyang Wang, Quanxing Gao, Hongxia Liu, Zhen Tong.

When solid particles instead of surfactant molecules are used to stabilize the emulsion, such emulsion is referred to as Pickering emulsion. In the past few years, the Pickering emulsions droplets have been used as templates to prepare highly controlled elastic membranes and shells with the supracolloidal structures (Dinsmore et al. Science 2002;298:1006; our paper ChemPhysChem 2007;8:1157). Most recently, Pickering emulsion droplets are used as polymerization vessels to fabricate hybrid polymer particles with supracolloidal structures (Chen et al. Polymer 2008;49:2650; Yang et al. J Mater Chem 2008;18:998; our paper J Polym Sci Polym Chem in press). The solid particles first self-assemble at the liquid-liquid interface and act as the effective stabilizers during the polymerization process without the need for any conventional stabilizers. After the polymerization completion, the particles are captured at the surface of the resultant polymer beads where they can be most effective for subsequent applications. Such surfactant-free emulsion polymerization, called Pickering emulsion polymerization is more attractive in preparation of hybrid beads than the convention emulsion polymerization. Sometimes, this kind of polymerization is called as Pickering miniemulsion polymerization, suspension polymerization and dispersion polymerization. Polymerization based on Pickering emulsion droplets can also be used to fabricate inorganic/polymer hybrid hollow microcapsules (Chen et al. Adv Mater 2007;19:2286). Herein, thermo-sensitive nanocomposite poly (N-isopropylacrylamide)(PNIPAm)microcapsules with supracolloidal structures were prepared from SiO₂-stabilized suspension polymerization based on inverse Pickering emulsion droplets. PNIPAm is temperature-responsive polymers having the lower critical solution temperature (LCST) around 32 °C. When polymerization was carried out at 50 °C above LCST, the hybrid microcapsules with

SiO₂/PNIPAm shell and liquid core were obtained. Thermo-sensitive microcapsules with aqueous cores are ideally suited for biological encapsulation due to no contact with harsh solvents. The permeability of the obtained microcapsules could be double controlled due to the present of the supracolloidal structures and thermo-sensitivity.

416

A Three-Phase Confocal Elliptical Cylinder Model for Predicting Thermal Conductivity of Composites

Fuli Chen, Chiping Jiang, Beijing University of Aeronautics and Astronautics (China).

Composites are extensively used in aerospace engineering for their several advantages, including high-modulus, high-strength, high-temperature resistance, designability, and so on. Thermal conductivity is an important property of composites. Prediction of the effective thermal properties of composites is essential for a successful design of manufacturing of such materials.

The former theoretical studies show that the generalized self-consistent method seems to be a more appropriate tool for analyzing heterogeneous materials. However, the most three-phase models for predicting thermal conductivity of composites can only accommodate circular and spherical inclusions, and the studies are still insufficient on the generalized self-consistent method accounting for inclusion shape variations.

In this paper, a three-phase confocal elliptical cylinder model with any section orientation is developed for predicting the thermal conductivity of composite material. The represent volume element consisting of a fiber and a matrix elliptical ring is embedded in an infinite homogenous composite. Using the conformal mapping technique and the Laurent series expansions approach, the analytical solutions for the thermal conductivities of composites are obtained. A comparison with other micromechanics methods such as the dilute, self-consistent and Mori-Tanaka models shows that the present method provides convergent and reasonable results for a full range of variations in fiber section shapes (from circular fibers to ribbons), for a complete spectrum of the fiber volume fraction (from 0 to 1). Numerical results give some interesting variations of the effective conductivities of composites with fiber conductivity and aspect ratio. The present solutions are helpful to analysis and design such thermal insulation composites.

417

Thermal Stress Reduction of Bilayered Systems by Means of Linearly Graded Interlayer

Binglian Wang, Yizeng Li, Shurong Ding and Yongzhong Huo, Fudan University (China).

Multilayered structure is the main configuration in microsystem. One major factor affecting the system failure and reliability is the thermal stress due to the thermomechanical mismatch among dissimilar layers. It has been well known that these stresses depend not only on the differences between the preparation and service temperatures of the multilayered systems made by materials with different thermal expansion coefficients, but also on the different elastic modulus and geometrical parameters, e.g. thicknesses, of all the layers.

To keep the maximal thermal stress in a reasonable range is one of the key concerns in preparation of such multilayered microsystem. Suitable interlayers are often introduced between two layers to reduce the otherwise too large thermal stresses. Since the concept of graded materials was proposed, it has been believed that such a graded interlayer would be the best choice for thermal stress reductions. Large amounts of numerical case-by-case studies have indeed confirmed this conjecture. However, certain studies have

also indicated that a successful stress reduction might require a graded interlayer with its thickness even much larger than the original system, thus not practicable. A general understanding of the applicability of the graded interlayer in thermal stress reduction of multilayered systems is still lacking.

In this work, thermal stress reductions of bilayered systems with linear graded interlayers are considered with analytical approaches. It has been found that the maximal stress in the system will always be lowered with a thick enough interlayer. However, if the interlayer thickness is restricted, a critical range of the elastic modulus and layer thicknesses of the original bilayer system can be identified only in which the maximal stress can be reduced. An even smaller range is further found within which the maximal stress always decreases with the increase of the interlayer thicknesses.

419

Study of the Thermal Property of CuO Nanowires

C. F. Dee, B. Y. Majlis, Universiti Kebangsaan Malaysia (Malaysia)

As a high potential candidate for field-emission emitters, gas sensors, high-critical temperature superconductors, CuO nanowires have been intensively studied in the synthesized methods, electrical properties and chemical properties. However, there are not many literature reports on the thermal property. It is important for one to understand the thermal behaviour in order to justify the failure limit of the material. In this paper, CuO nanowires synthesized through direct heating in atmospheric ambient were heated up in nitrogen ambient to different temperature to check the critical thermal failure point where the free standing CuO nanowires start to collapse. It is found that CuO nanowires with diameter around 100 nm start to collapse after dozens of minutes of heating in the nitrogen ambient. Increase in temperature will cause the nanowires with bigger diameters start to fail one after the other. Nanowires in same diameter range will be able to withstand the temperature up to few hours if they don't collapse in the initial dozens of minutes of heating. This result is important for CuO nanowires which incorporated into the other heat sensitive device. The aging effect and durability in high temperature are also studied under prolonged heating. The results are important for justifying the failure behaviour for devices based on CuO nanowires.

420

Finite Element Analysis of the Role of Phase Transformation in Micro-Wear of Super-Elastic NiTi alloy

Qianhua Kan, Guozheng Kang, Southwest Jiaotong University (China).

Shape memory alloys (SMAs) are used in many applications such as smart structures, biomedical stents, and micro-electro-mechanical systems (MEMS) due to their well-known super-elastic behavior and shape memory effect. Recently, several experimental studies of SMAs indicated that the wear property of superelastic NiTi alloy is superior to many traditional wear-resistant metals. It is necessary to realize why the NiTi alloy possesses such high wear-resistance. In this work, based on a new developed temperature-dependent constitutive model considering plasticity of superelastic NiTi alloy, the contribution of the stress-induced martensite transformation and plastic yield of martensite to the high wear-resistance of NiTi alloy is investigated by numerical contact analysis. The effects of elastic modulus, transformation stress, transformation strain and plastic yield stress of martensite on the wear-resistance of NiTi alloys are discussed from the finite element calculations. In the meantime, the partition of the elastic, transformation and plastic areas within the contact zone is also revealed from the calculated results. The numerical

simulation shows that the low elastic modulus, the low transformation stress, the large transformation strain and the high plastic yield stress of martensite result in excellent wear-resistance. Additionally the high wear-resistance is linked to the increased in the environment temperature.

421

Nonlinear Differential Equation Approach for the Two way Memory Effects of One-dimensional Shape Memory Alloy Structures

Linxiang Wang, Changquan Zhou, Changshui Feng, Institute of Mechatronic Engineering, Hangzhou Dianzi University (China)

Shape Memory Alloys (SMA) has been wide deployed in many applications due to their capability of converting energy between the thermal and mechanical types automatically. But it also exhibit fairly complicated nonlinear (hysteretic) behaviors in both the mechanical and thermal fields. In order to model and control the SMA structures and devices, it is essential to construct a suitable model for its hysteretic dynamics. On the other side, it is always beneficial if the hysteretic dynamics can be described accurately by Ordinary Differential Equations (ODE) since theories for system analysis and control were well established for ODE.

In the current paper, a macroscopic differential model is constructed for one-dimensional SMA structures on the basis of a phenomenological theory for the martensitic transformations. The hysteresis loops in both the mechanical and thermal fields are treated as macroscopic illustrations of the martensitic transformations and variant re-orientations induced in the SMAs. A non-convex free energy function is constructed such that each of its local equilibriums can be used to characterize one of the martensite variants involved. System states (strain) can be transformed upon external loadings (mechanical or thermal) from one stable equilibrium to another, thus the dynamics of martensitic transformations can be modelled by investigating the transition dynamics of the system states from one equilibrium states to another. The Rayleigh relaxation effects are also considered. Governing equations for the transition dynamics are formulated by employing the Lagrange's equation, and are expressed as nonlinear differential equations. We present comparison between the model results and their experimental counterparts. Numerical simulations show that the hysteretic dynamics of both the mechanical and thermal fields are successfully modelled by the proposed model.

422

Nacre-Like Composites Reinforced by Layered Architectures of Self-Assembled Ceramic Nanoparticles

Jia Yan, Zhanjun Wu, Dalian University of Technology (China).

Nacre, a structure found in many molluscan shells, has a brick-mortar-bridges microstructure where inorganic calcium carbonate layers are held together by organic protein "glue". This hybrid organic-inorganic lamellar structure of nacre shows nature's wonderful designs for strong and light materials, and may enlighten us some ideas for designing superlight and superstrong materials.

However, technically, it is very difficult to transcribe this nacre-like design into synthetic materials, partly because these layered microstructures need to be orderly and controllably replicated at a macroscopical scale. In present paper, we report a simple approach, which is ice templating, for building the sophisticated, nacre-like architectures. A sophisticated porous and layered architecture composed of self-assembled ceramic nanoparticles was prepared by unidirectional freezing an aqueous suspension of ceramic nanoparticles. It is concluded that ice platelets play a role of template, inducing the self-assembling of nanoparticles. The obtained porous lamellar ceramic was filled up with a second phase

by liquid or gas processing to obtain a dense composite, which possesses high mechanical strength and low density. Scanning electron microscope (SEM) characterization shows that the obtained composite has a brick-mortar-bridges microstructure, similar to that of natural nacre. It is expected that, as superstrong and superlight materials, these nacre-like composites can be applied in many fields including aerospace engineering and osseous tissue regeneration.

423

Study on Structural Health Monitoring for Composite Pressure Vessels Featuring FBG Sensors and Acoustic Emission

Zhanjun Wu, Xiaojin Zhang, Boming Zhang, Harbin Institute of Technology (China); Zhanjun Wu, Dalian University of Technology (China); Xiaojin Zhang, Shanghai Jiaotong University (China).

Composite pressure vessels are used in a wide variety of applications, which arises concern of safety issues. In this research, we studied structural health monitoring for composite pressure vessel using both fiber Bragg Gratings (FBG) and acoustic emission sensors. FBG sensors, electrical strain gauges and acoustic emission sensors were mounted on a composite filament pressure vessel. Then the vessel was subjected to cyclic hydraulic pressure loading. Both strain and acoustic emission were monitored during the loading process. It is found that the FBG sensors could accurately reveal the hydraulic pressure inside the vessel through surface strain measurement. Also, FBG sensors are sensitive to high strain gradient. Then stiffness degradation, which is considered a damage index for the composite vessel, was calculated with the measured strain data. Damage detection with acoustic emission was consistent with FBG measurements and thus verified each other.

424

Microstructure, Dielectric and Piezoelectric Properties of Lead-Free $0.948\text{Na}_{0.5}\text{K}_{0.5}\text{NbO}_3\text{-}0.052\text{LiSbO}_3$ Piezoelectric Ceramics

Wu Yang, Dengren Jin, Wenbiao Wu, Jinrong Cheng, Shanghai University (China).

Ferroelectric Potassium sodium niobate ($\text{Na}_{0.5}\text{K}_{0.5}\text{NbO}_3$) ceramics have been studied as promising lead-free piezoelectric ceramics. $0.948(\text{Na}_{0.5}\text{K}_{0.5})\text{NbO}_3\text{-}0.052\text{LiSbO}_3$ (KNN-5.2LS) showed excellent electrical properties, because it is around the composition with MPB. But the Q was reduced sharply and dielectric loss increased compared with KNN, so that it will be restricted in application in electronic devices. It was reported that Mn-doped KNN crystals exhibited a low leakage current density [Yoichi Kizaki, Defect control for low leakage current in $\text{K}_{0.5}\text{Na}_{0.5}\text{NbO}_3$ single crystals.] In this article, KNN-5.2LS doped with 1%mol (ZnO , CuO , MnO_2) was synthesized by conventional solid-state sintering. The effect of dopant (ZnO , CuO , MnO_2) on microstructure, dielectric, piezoelectric properties will be investigated.

425

Preparing and Study on Thermal-conductive Epoxy Resin Nanocomposites

Huixia Feng, Guohong Zhang, Liang Shao, Yang Zhao, Lanzhou University of Technology (China); Guohong Zhang, Yang Zhao, Jianhui Qiu, Akita Prefectural University (Japan).

EP/M was prepared successfully and the tensile strength and coefficient of heat conductivity were studied. With the increase of the padding dosage, the thermal-conductivity were added. The

tensile strength of EP/M were all enhanced while the top composites with the content of padding 20%.EP/M/OMMT was also prepared by adding the metal padding and second-inserting organic-bentonit to epoxy resin. It was seen that the two kinds of performance were enhanced. The coefficient of heat conductivity of EP/Ag/OMMT and the tensile strength of EP/Ni/ OMMT were the highest of all. The rupture surface of EP/M/OMMT were analysed with SEM.

426

Development of Novel Low Shrinkage Dental Nanocomposite

Yi Sun, Xiaorong Wu, Yanju Liu, Shouhua Sun, Harbin Institute of Technology (China); Weili Xie, Department of Stomatology, Harbin Medical University (China).

It has been the focus to develop low shrinkage dental composite resins in recent ten years. A major difficulty in developing low shrinkage dental materials is their deficiency in mechanical properties to clinical use. This paper reviews the present investigations of low shrinkage dental composite resins and attempts to develop a novel low shrinkage system with POSS incorporated. In this paper, it is especially interesting to evaluate the influences of shrinkage with different weight percentage of POSS (0~15wt %) incorporated in dental nanocomposite. Furthermore, infrared spectroscopic techniques and X-ray scattering were used to characterize their microstructures. Their mechanical properties are presented and shrinkage mechanisms are also discussed in this paper. The results show that the shrinkage decreases from 3.53 to 2.18 when 15wt% POSS is used. Therefore, the shrinkage of nanocomposites with POSS can be reduced effectively to improve marginal adaptation of the composite filling to the tooth cavity and to avoid recurrent caries. The mechanical properties of this novel system, such as strength, hardness and toughness, are also enhanced. Especially with 2wt% POSS incorporated, the best integrative improved effects are revealed that flexural strength increased 15%, compressive strength increased 12%, Viker's hardness increased 15% and fracture energy increased 56%.

427

Effect of Different Cross-Section Types on Mechanical Properties and Electromagnetic Properties of Carbon Fibers Reinforced Plastics

Ronggou Wang, Xin Liu, Wenbo Liu, Wang Sai, Harbin Institute of Technology (China); Yonggang Yang, Chinese Academy of Sciences (China).

To study the effect of different cross-section types on properties of carbon fibers, the microstructures of triangle-shape carbon fibers (TCF) and circle-shape carbon fibers (CCF) were investigated by scanning electron microscope, X-Ray Photoelectron Spectroscopy and X-ray diffraction. The mechanical properties and electromagnetic properties of carbon fibers reinforced plastics were also studied. Results show that their microstructures and tensile-strength were similar, while the imaginary part of complex dielectric constant and loss tangent of the triangle-shape carbon fiber reinforced plastics (TCFRP) are higher than those of the circle-shape carbon fiber reinforced plastics (CCFRP). The triangle-shape carbon fiber reinforced plastics have both the function of load bearing and the electromagnetic energy absorbing capability, and the composites will become promising radar absorbing structure material.

428

Research About Pulling Sensitive Characteristic of Carbon Fibre Reinforced Concrete and Security Self-Diagnosis of Beam

Joints

Longnan Huang, Xinbo Wang, Harbin Institute of Technology at Weihai (China); Dongxing Zhang, Harbin Institute of Technology (China).

Based on real-time diagnosis of health status of reinforced concrete beam joints, intellectual supervisory layer of carbon fiber reinforced concrete (CFRC) was set up at the bottom of girder structure. The intrinsic law of pulling sensitive characteristic of CFRC was studied and the electrical property collection and the stress transformation system of structure intellectual layer were established, which depended on the premise that the good electrical conductivity of carbon fiber and the defined correspondence between electric resistivity variation of carbon fiber and stress field carbon fiber situated were fully utilized. The security self-diagnosis of girder structure was acquired through online real-time monitoring and evaluation on electrical signal of intelligence layer from reinforced concrete beam joints.

429

Neural Modeling of the Dynamic Behavior of a Non-linear Model Frame Structure

Bin Xu, Zhigang Huang, Hunan University (China).

The identification of non-linear dynamic systems is increasingly becoming a necessity in every branch of engineering that deals with vibrating structures. Because the initiation and progress of damage in civil engineering is a typical nonlinear approach, identification methods which can deal with nonlinear system are crucial for efficient and dependent damage detection in structural health monitoring. In this study, a multi-storey frame structure model equipped with a magnet-orheological (MR) damper was designed and constructed to simulate the nonlinear behavior and was modeled with a neural network in a nonparametric way. Both numerical simulation study and vibration test are carried out to validate the performance of the proposed nonparametric modeling methodology and parametric model. Firstly, test on the MR damper employed in this study was carried out, and analytical parametric models for the MR damper including the Bingham model, the Dahl model and the Bouc-Wen model were established and were employed to simulate the structural dynamic response under different excitations. Then, the accuracy of the analytical parametric models for the nonlinear frame structure was tested by comparing the simulated response with raw experimental measurements under different excitations. Finally, the proposed neural networks based nonparametric model was established using a time regression input vector composing of raw dynamic response measurement of the model structure under a certain excitation. The performance of the nonparametric model was evaluated by comparing the prediction of the neural model with new data captured from the model structure but used neither in training nor in pruning phases. Discussions on the select of input and output variables and the topology of the neural network when different types of dynamic responses are available are made. Results show that the neural model provides an applicable way for identification of nonlinear dynamic structures.

430

Macro-strain Mode Based Parameters Identification for a Beam Structure with FBG Sensors

Bin Xu, and Chongwu Liu, Hunan University (China).

The development of optic fiber sensing technology provides easy way for the measurement of vibration-based strain of structures. As a typical optic fiber sensor, long-gauge Fiber Bragg Grating (FBG) sensors have been widely employed in civil engineering structures.

Therefore, the development of strain-based identification methods is crucial. In the previous study, a parameters identification and damage detection algorithm for a beam structure with the direct use of vibration-based macro-strain measurement time history with neural networks had been proposed and validated with experimental measurements. In this paper, comparing with the previous study, a damage locating and quantifying method was proposed using modal macro-strain vectors (MMSV) which were extracted from the dynamic macro-strain response time series from long-gage FBG sensors. The performance of the proposed methodology was tested with numerical simulation at first. Then, dynamic test on a simply-supported steel beam with different damage scenarios are carried out to verify the effectiveness and accuracy of the proposed method. The results were also compared with the time domain identification methods proposed previously and show that the method proposed in this study can accurately locate and quantify damages.

431

A Novel Valveless Micropump

Songmei Yuan, Lutao Yan, Qiang Liu, School of Mechanical Engineering and Automation (China).

Microelectro mechanical system (MEMS) technology has become focus of attention because of their promising commercial applications and its growth to respond to the market demand in many fields, such as micro-actuators, filters, sensors, accelerometers, etc. As one of the key devices of microfluidics, micropumps present precisely controlled flow rate and actually, they have been widely used in different areas (drug delivery, chemical synthesis, localized cooling of electronic circuits, microbiology, biological detection, clinical analysis in medicine, and inkjet printing). In this paper, a new valveless micropump has been designed, fabricated and tested.

The construction of a new valveless micropump is proposed. The micropump adopted piezoelectric transducer as the actuator, which produce bending deformation and volume change in pump chamber. In order to make full use of the kinetic energy, two inclusive chambers are actuated by one and the same PZT. The vibration modals and natural frequencies are obtained by means of FEM (Finite Element Method). The result show that the first modal is the best step for the piezoelectric transducer and the work frequency is 34053 Hz.

Characteristic of the micropump is measured. The experimental results indicate that the flow rates is linear to the driving voltage, because the driving voltage directly corresponds to the amplitude and the blocking force which provide a larger volume change inside the chamber. The micropump achieves the maximal output capability when the driving frequency is close to the natural frequency. The maximum flow rate is 110 μ l/min with an applied voltage of 100V when the frequency is around 34 KHz, in good agreement with theory.

432

A Novel Nanosilica-Reinforced Waterborne UV-Curable Material

Tong Zhang, Wenjian Wu, Biru Hu, National University of Defense Technology (China).

A novel multifunctional UV-curable waterborne polyurethane-acrylate(WPUA) was prepared with isophorone diisocyanate(IPDI), pentaerythritol triacrylate(PETA), polycaprolactone diols(PCL) and dimethylol propionic acid (DMPA). The chain structure of the WPUA was identified by ¹H NMR spectra. After that, the nanosilica modified with KH570 was dispersed in WPUA, and the effects were studied with dispersion and dispersion cast fil It was

found that the modified nanosilica was dispersed into WPUA hybrid nanocomposites homogeneously and stably. And the particle size was increased and its performances like hardness, abrasion resistance and thermal stability were improved with the addition and increasing amount of silica, while the curing speed was reduced.

433

Effects of Precipitation on the Damping Capacity of Fe-13Cr-2.5Mo Alloy

Xiaofeng Hu, Xiuyan Li, Lijian Rong, Yiyi Li, Chinese Academy of Sciences (China).

Fe-Cr based high damping alloys (HDA) have been systematically studied because of their high corrosion resistance and mechanical strength, and were applied to suppress mechanical vibration and noise in many industrial fields. In present paper, influences of precipitation on the damping capacity of Fe-13Cr-2.5Mo (mass fraction) based alloys have been investigated. Dynamic mechanical analyzer (DMA) was used to investigate the damping behavior at temperature $t=35^{\circ}\text{C}$, and in the range of strain amplitude $\varepsilon =10^{-6}$ and 10^{-5} . Field-emission scanning electron microscope (FESEM) with X-ray energy dispersive spectrometer (EDS) was used to observe microstructure and the compositions of precipitations. The results show that damping capacity of Fe-Cr-Mo based alloys is more significantly correlated with intragranular precipitations than with grain-boundary precipitations. Fe-Cr-Mo annealed at 1100°C for 1h followed by furnace cooling (FC) with fewer intergranular precipitations, exhibits the highest damping capacity. With the increase of annealing temperature, amount of intragranular precipitations increases and damping capacity of Fe-Cr-Mo alloy decreases. Addition of Ti or Cu inhibits the precipitation of grain-boundary precipitations, but promotes the intragranular precipitations in the alloy distinctly, so the damping capacity of Fe-Cr-Mo-1Ti or Fe-Cr-Mo-0.5Cu is slightly lower than that of Fe-Cr-Mo alloy. After addition of 1.0% Nb, there are abundant carbides of (Nb,Mo)C, which obviously deteriorates damping capacity of Fe-Cr-Mo-1Nb at low strain amplitude. But at higher amplitude, damping increases more rapidly and possesses the highest damping capacity, which suggests that more precipitations in Fe-Cr-Mo based alloys can interact with dislocations and generate an amplitude-dependent damping Q_{dis}^{-1} at high amplitude.

434

Study on Acceleration Detection Based FBG and Narrow Laser

Dianheng Huo, Tongyu Liu, Jun Chang, Xiaohui Liu.

Introduce a system based on optical fiber sensing technology. In this system, using 3MHz narrow DFB laser as a light source and FBG as a sensor, we can change the wavelength of the laser by adjust the laser's temperature, so the system can auto-scan and scout the working point on 3dB of FBG to get high sensitivity using single-chip-micyoco. We also design a high sensitivity FBG acceleration sensor; get the sensor's frequency character and linearity through experiments. This system can detect 0.1mg, so it will be used to detect micro-seism and other vibration signal.

436

Electrorheological Properties of Core/Shell Structural Titanate Nanotube @Acetamide Suspension with Various Prepared Processes

Yuchuan Cheng, Jianjun Guo, Xuehui Liu, Gaojie Xu, Ping Cui, Chinese Academy of Sciences (China).

Electrorheological (ER) fluids are smart materials whose rheological properties can be easily controlled through a changing

external electric field. There is very wide range of potential application for ER fluids in various areas, including the automotive industry, robotics, hydrature, damping and military. Since the phenomenon of electrorheology was discovered by W. M. Winslow in 1947, many researches about ER fluids have been performed.

A hydrothermal method was proposed to prepare titanate nanotubes (TNs) with the diameters of about 10 nm. Then these nanotubes were modified by acetamide via different self-assembled processes. The X-ray diffraction analyses, TEM, TG-DTA and FT-IR spectroscopy were used to determine the structure of the nanotubes. The results indicated that the acetamide molecules exist on the surface and inside of nanotubes. The different synthesis processes do not change the morphology of TN@acetamide nanoparticle, nevertheless they affect the interaction between amide and acetamide. The ER activity was studied by yield stress under and DC electric field. This one-dimensional nanoparticles ER fluid showed notable ER activity, which outlasted that of the spherical nanoparticles ER fluid. Furthermore, it was found that the ER effect was very sensitive to the interaction of molecules. The chemical bond between core and shell can enhance the ER activity of the sample.

437

A Novel Nano-Gripper Compliant Mechanism with Parallel Movement of Gripping Arms

Mahmoud Helal, Lining Sun, Liguo Chen.

Research and development of and on micro and nano sized objects and systems have received considerable interest the last few decades and have accelerated the last decade during the advent of nanotechnology. Compliant mechanisms (CMs) have made an enormous contribution in the design process of various fields such as for adaptive structures, hand-held tools, components in transportations, electronics, and surgical tools. The use of compliant mechanisms will help in reducing the number of components, which therefore decrease manufacturing cost and additionally increase the performance. Topology optimization has proven to be a powerful method for the conceptual design of structures and mechanisms. Topology optimization is the technique that finds the optimal layout of the structure within a specified design domain. This paper presents a nano-gripper which can realize a parallel movement of the gripping arms with possibility for simultaneous positioning of the gripped object. The topology optimization is applied for designing two-dimensional nano-gripper compliant mechanism with parallel movement of gripping arms. As objective function, the traditional mean compliance design problem is considered, where the objective is to find the material distribution that minimizes the mean compliance for a certain volume constraint. The optimization algorithm is implemented in ANSYS by using the ANSYS Parametric Design Language (APDL). The final optimal topology configuration of nano-gripper with parallel movement of gripping arms is shown and discussed.

438

Preparation and Characterization of a Novel Chitosan/BC Nanocomposite

Yuanyuan Jia, Weihua Tang, Fei Li, Shiru Jia, Tianjin University of Science and Technology(China).

This paper describes the biosynthesis of a novel chitosan-bacterial cellulose (Chitosan/BC) composite by adding chitosan hydrochloride to the culture medium of *Gluconacetobacter xylinus*. Water-soluble chitosan hydrochloride precipitates in the culture medium, probably due to the existence of peptone and yeast extract. A composite of bacterial cellulose and chitosan hydrochloride, was produced in situ using *Gluconacetobacter xylinus*. The chitosan is

bound to the lower side of the bacterial cellulose pellicle during the formation process. It is found that BC and Chitosan/BC samples show different color, the former being white and the latter light yellow. In addition, BC and Chitosan/BC samples have different dimensions. The thickness of Chitosan/BC is bigger than that of wet BC pellicle. The increased thickness of Chitosan/BC in comparison with BC is simply attributed to the incorporation of chitosan into BC. The wet Chitosan/BC is more rigid than unmodified BC, which was explained further by improved tensile strength of Chitosan/BC in both air-dried and reswollen states. The content of chitosan hydrochloride in Chitosan/BC composite was calculated by Kjeldahl nitrogen determination method. The morphology of Chitosan/BC composite was observed by SEM and compared with pristine BC. The pristine BC shows a fine 3-dimensional network. The morphology has been changed to some extent by the presence of chitosan. The incorporation of chitosan into bacterial cellulose was monitored via FTIR spectroscopy. The composite was further characterized by FTIR and XRD. Further work is underway to gain insights into the mechanisms governing the experimental phenomena.

439

A Study on Preparation of NiZnCu ferrite/TiO₂ Nanocomposite and its Properties

Guijuan Li, Shourui Fan, Xingwen Mu, Kang Wang, Changchun University of Technology(China).

NiZnCu ferrite/TiO₂ nanocomposite was prepared by sol-gel technique and high temperature calcinations with the nitrate of NiZnCuFe and tetrabutyl titanate as former body. The properties of NiZnCu ferrite/TiO₂ nanocomposite were characterized and analyzed by IR, UV, TEM, SEM, XRD, VSM, Mössbauer Spectrum etc. The results showed that nanocomposite had a better magnetic properties and absorptive function of UV.

440

Shape Memory and Mechanical Behavior of Poly L-lactide/Poly E-Caprolactone Biodegradable Polymer Blends

Maryam Amirian, Wei Cai, Ali Nabipour Chakoli, Jie He Sui.

Poly L-lactide (PLLA) bioresorbable implants have advantages in repair and regeneration of healing tissues, because PLLA is biodegradable, biocompatible, and has proper mechanical performance. However, one of the drawbacks of PLLAs for biomedical applications is their brittleness. One of the most practical strategies for tuning the properties of PLLA is blending with Poly ε-caprolactone (PCL). Both of PLLA and PCL have shape memory effect. In this work, we have studied the shape memory and mechanical behavior of PLLA/PCL blends. The samples with various content of each component were prepared by solution casting. The amounts of PLLA in blends are between 100 wt% and 60wt%. Differential scanning calorimetry (DSC) and dynamic mechanical analysis of PLA/PCL blends show two glass transition temperature and two melting points at positions close to the pure components revealing phase separation. The melting point of each component in the composite is upper than the melting point of its pure composition. The DSC analysis shows one crystallization temperature below the melting point of PCL component the time of cooling of PLLA/PCL blend. The X-ray diffraction analysis showed the both crystalline phase of PLLA and PCL in composite blend. The first shape memory analysis, angle deformation using bending tests, show that the PLLA/PCL (80 wt% PLLA and 20 wt% PCL) blend has the most shape recovery between other blends and pure polymers for both first and second cycle of tests. The second shape memory analysis, strain deformation using tensile tests, show that the PLLA/PCL (80 wt%

PLLA and 20 wt% PCL) blend has the most shape fixity but the PLLA/PCL (60 wt% PLLA and 40 wt% PCL) has the most shape recovery.

442

Ti Doping induced Phase Transformation in Multiferroic BiFeO₃ Ceramics

Yibin Li, Xiaodong He, Harbin Institute of Technology (China); Thirumany Sritharan, Xian Hui Koh, Sam Zhang, Nanyang Technological University (Singapore).

Ti-doped bismuth ferrite (BiFe_{1-x}Ti_xO₃, x=0, 0.05, 0.1, 0.15 and 0.2) ceramics were synthesized by a solid-state reaction and their multiferroic properties were investigated. X-ray diffraction patterns reveals that Ti doping caused phase transformation from rhombohedral structure in pure BiFeO₃ ceramic to tetragonal structure in Ti-doped BiFeO₃ ceramics. At low Ti concentration (0 ≤ Ti ≤ 0.1), there is no secondary phase is resulted in due to Ti incorporation. However, at higher Ti concentration, like x ≥ 0.1, the Ti-rich phase was formed. Moreover, Ti incorporation dramatically reduced the leakage current of BiFeO₃ ceramics. The ferroelectric and magnetic measurements were carried out to confirm the multiferroic nature of the system.

444

Experimental Investigation on Structure with Recentering Shape Memory Alloy Damper

Hui Qian, Huai Chen, Zhengzhou University (China); Hui Qian, Hongnan Li, Dalian University of Technology (China); Gangbing Song, University of Houston (USA).

Superelastic shape memory alloys (SMAs) are a class of materials that have the ability to undergo large deformations while reverting back to their original shape through removal of stress. The unique material can be utilized as key components for seismic energy dissipation in earthquake engineering. In this paper, an innovative recentering SMAs-based damper (RSMAD) is proposed. Cyclic tensile-compressive tests on the damper with various pre-strain under different loading frequency and displacement amplitude are conducted. To assess the effectiveness of the damper in reducing dynamic response of structures subjected to strong seismic excitations, an extensive experimental program and main results of shaking table tests performed on reduced-scale steel frame model with and without RSMAD are presented. In the shaking table tests, several representative seismic signals as well as white noise motion are used as input energy. The comparisons of dynamic behaviors, i.e. storey displacements, interstorey drifts and storey accelerations, of structural model with and without RSMAD under seismic loading are conducted. The results show that RSMAD is effective in suppressing the dynamic response of building structures subjected to strong earthquakes by dissipating a large portion of energy through their hysteretic loops. Moreover, the structures are able to undergo strong earthquakes without remarkable residual drift due to the re-centering feature of the damper.

445

Genetic Algorithm-based Multiobjective Optimal SMA Damping System for Seismic Structures

Wenjie Ren, Hebei University of Technology (China); Liqiang Wang, Tianjin University of Technology and Education (China).

Special devices for the passive control of vibrations can significantly improve the performance of structural systems subjected to earthquake excitations. Where and how many devices are placed on a structure will have a significant effect on the ability to reduce the response of the structure. Some optimal methods were

designed based on certain assumption, i.e. the number of devices was not included in the optimization problem but determined in advance. This paper discusses a new multiobjective optimal design of an SMA system for seismically excited buildings.

An improved algorithm based on the two-branch tournament genetic algorithm (GA) is presented to solve a multiobjective optimal problems (MOP). The improved algorithm evaluates individuals on their dominance that is measured by sign fitness functions, which forces the better performing individuals to win their competition, maintains appropriate diversity and induces a little higher search pressure toward ideal solutions. Besides, less computational effort is taken in the new algorithm, attributed to individuals of each generation being evaluated in one run of the tournament, regardless of the dimension of objectives. Based on the dominance rules, a penalty objective function is defined for a constrained MOP, considering an individual status (feasible or infeasible), position in a search space, and distance from a Pareto optimal set.

Superelastic shape memory alloy (SMA) is a viable candidate for use in the structural control field due to its large recoverable strain range, high damping capacity, extraordinary fatigue resistance and excellent corrosion resistance. A SMA system should be arranged in such a way that the system can effectively control the response of the structure with a low cost. Nondimensionalized peak inter-story displacement and number of the device are considered as the two objective functions for multiobjective optimal design of the SMA system. The aforementioned multiobjective GA is used to obtain the design parameters of the SMA system.

446

Optical Properties of Subwavelength Wiregrid Polarizer Designed for GaN-based LED

Guiju Zhang, Bing Cao, Qin Han, Chinghua Wang, Soochow University (China); Ke Xu, Chinese Academy of Sciences (China).

A theoretical simulation is presented on the optical transmission and polarized extinction ratio through subwavelength wiregrid polarizer for GaN-based LED. The micro-polarizers are specially designed based on Rigorous Coupled Wave (RCW) method for operation wavelengths of blue light (470nm) and green light (520nm) with metal wiregrid on the GaN substrate. The TM transmittance and the extinction ratio of TM and TE transmittances are influenced by period, thickness and duty cycle of the metal wiregrid. Silver and aluminum metal film grating are separately used for optimization design to improve the optical properties at the visible wavelengths. Simulation results show that, as the thickness of the metal grating decreases, the coupled light shifts the TM transmittance peak to shorter wavelength. As the same time, the extinction ratio remains a high value. TM transmittance coefficients separately greater than 95% and 97% with extinction ratios greater than 33dB are achieved for GaN-based aluminum grating and silver grating at the wavelength 470nm. And TM coefficients are greater than 92% and 96% with extinction ratios greater than 33dB, respectively at the wavelength 520nm. The thicknesses and periods of the metal grating are with sizes less than 300nm, which are under subwavelength structures. The numerical results are useful for designing and fabricating novel photonic nanostructure devices.

447

Effect of Polyhedral Oligomeric Silsesquioxane (POSS) on Elastic Properties of Polyethylene at Different Temperatures Using Isothermal-Isobaric Molecular Dynamics Simulations

Jun Lia, Yi Sun, Fanlin Zeng, Harbin Institute of Technology (China)

The influences of the polyhedral oligomeric silsesquioxane (POSS) on the elastic properties of the polyethylene at different temperatures were studied using molecular dynamics simulations. Ethylene monopolymer and ethylene copolymerized with 1 mol% 1-(9-deceny)-3,5,7,9,11,13,15-heptaethylpentacyclo[9.5.1.13,9.15,15.17,13]octasiloxane were simulated under 1 atmosphere pressure and at the temperature range 200K-450K. In the simulations, the Consistent Valence Force Field (CVFF) was used to describe the interactions of atoms. The NPT ensemble was employed, which was implemented using Nosé-Poincaré thermostat and metric-tensor pressostat. As a symplectic algorithm, the generalized leap frog scheme was adopted for time integrator. From specific volume versus temperature plots, the glass transition temperature (T_g) of polyethylene is a little less than 400K, which is in good agreement with that from experimental measurement. In the same way, the T_g of the ethylene-POSS polymer is obtained. It reveals that the POSS units have little effect on the glass transition temperature. Meanwhile, the elastic stiffness matrices were computed via the stress and strain fluctuation method. The results show that the modulus of polyethylene is greatly improved by the POSS units at all tested temperatures. The improvement effect increases as the temperature rises. The modulus of the ethylene-POSS polymer is 20% greater than the polyethylene at 200K and 50% greater at 450K. Based on the analysis of the potential energy, it is concluded that the variation of the coulomb energy introduced by the POSS units is the main reason to explain the improvement of the elastic properties of the ethylene-POSS with respect to the polyethylene.

448

Damage monitoring of composite pressure vessel with thin metal liner

Junqing Zhao, Rongguo Wang, Xiaodong He, Wenbo Liu, Harbin Institute of Technology (China).

The composite pressure vessel with thin metal liner has the advantage of both composite and metal. Due to the difference of elastic strain limits of composite and metal, there are problems of the compatibility of deformation. The surface strain of the pressure vessel is measured by Fiber Bragg gratings under water pressure. Acoustic emission method is used to monitor the damage state of loading and unloading process of the vessel. The mechanical properties and damage states during the loading and unloading process are analyzed based on the experimental results.

451

Modeling the shape memory effect of shape memory polymer

Bo Zhou, Guangping Zou, Harbin Engineering University (China); Yanju Liu; Jinsong Leng, Harbin Institute of Technology (China).

Shape memory polymer (SMP) is able to retain a temporary shape, which is formed by the deformation in a high temperature, through cooling it to a low temperature, and recover his original shape through heating to a high temperature. SMP was successfully utilized in the applications of heat shrinkable tubes, wraps, foams and self-adjustable utensils. Recently, it begins to be applied in the areas of biomedical devices, deployable space structures and micro-systems. Wide engineering applications demand effective and simple theoretical models which express the shape memory effect of SMP. It is not easy to model the mechanical constitutive behavior of SMP theoretically because the properties of polymer much depend on time and temperature.

In this paper, dynamic mechanical analysis (DMA) tests are performed to investigate the relationship between mechanical properties and temperature of the styrene-based SMP during the transition from glassy state to rubbery state. Tensile tests at various

constant temperatures are conducted to investigate the stress-strain-temperature relationship of the styrene-based SMP. A new material parameter function is established to describe the relations between temperature-dependent material parameters and temperature during the glass transition between the glassy state and rubbery state of the styrene-based SMP. A new thermo-mechanical constitutive equation is developed to express the stress-strain-temperature relationship of the styrene-based SMP from a practical viewpoint. Numerical calculations illustrate that the new material parameter function and thermo-mechanical constitutive equation well predict the thermo-mechanical process realizing the shape memory effect of the styrene-based SMP such as high-temperature deformation, shape fixity, and shape recovery.

452

Application of Support Vector Machine Based on Pattern Spectrum Entropy in Fault Diagnostics of Bearings

Rujiang Hao, Shijiazhuang Railway Institute; Zhipeng Feng, University of Science and Technology Beijing; Fulei Chu, Tsinghua University (China).

Rolling element bearings are among the most important and frequently encountered components in the vast majority of rotating machines, their carrying capacity and reliability being crucial for the overall machine performance. Therefore, the fault diagnosis and identification of rolling element bearings has been the subject of extensive research. This paper presents a novel pattern classification approach for the fault diagnostics of rolling element bearings, which combines the morphological multi-scale analysis and the "one to others" support vector machine (SVM) classifiers. Morphological pattern spectrum describes the shape characteristics of the inspected signal based on the morphological opening operation with multi-scale structuring elements. The pattern spectrum entropy and the barycenter scale location of the spectrum curve are extracted as the feature vector presenting different faults of the rolling element bearings, which are more effective and representative than the kurtosis value and the enveloping demodulation frequency spectrum. The "one to others" SVM algorithm is adopted to distinguish six kinds of fault bearing signals which were measured in the experimental test rig running under eight different working conditions. The recognition results of the SVM are ideal and more precise than that of the artificial neural network even though the training sample is few. The combination of the morphological pattern spectrum parameter analysis and the "one to others" multi-class SVM algorithm is suitable for the on-line automated fault diagnosis of the rolling element bearings. This application is promising and worth well exploiting.

453

Thermal Shock of Silicon-Based Materials Under Multi-Pulsed Intense Laser Radiation

Haiming Huang, Xiaoliang Xu, Yue Sun, Beijing Jiaotong University (China)

The silicon-based materials are widely used in MEMS. The purpose of this paper is to investigate the thermal shock property of silicon-based materials with the multi-pulsed laser using the theoretical deduction and a case analysis. The most important feature of this paper is that we take the non-Fourier effect into consideration. Based on the Generic Fourier law and Thermo-elastic Theory, the analytic expressions of the temperature field and the thermal stress field of silicon-based materials under the multi-pulse heat flow were deduced. What's more, through a case study, we find that the relaxation time is also an important factor in this thermal shock property. Finally, we think that it is necessary considering the non-Fourier effect of semi-infinite body

under the high energy laser irradiation, because it has the obvious thermal shock. The conclusion is useful for the micro-fabrication technology in the fields of MEMS.

454

Wireless Energy Transmission Through a Sealed Wall Using the Acoustic-Electric Interaction of Piezoelectric Ceramics

Hongping Hu, Yuantai Hu, Huazhong University of Science and Technology (China); Hongping Hu, Yuantai Hu, Xuedong Chen, University of Science and Technology (China)

We propose a system to transmit and store electric energy by using transmitting element, a chargeable battery, and a rectifier together with a dc-dc converter to connect the two components as an integrated system. The transmitting element is modeled by two piezoelectric transducers. One is as the driving transducer for generating acoustic wave; the other is as the receiving transducer for converting the acoustic energy into electric energy. A dc-dc converter employed in the storage circuit is to match the optimal output voltage of the receiving transducer with the battery voltage for efficient charging. A synchronized switch harvesting on inductor (SSHI) in parallel with the receiving transducer is introduced to artificially extend the closed circuit interval of the rectifier. This analysis extends a previous one by considering that influence of wall thickness which always exists in the application. The characteristics of the energy-transmitting element are studied. Performance of the energy-transmitting element is optimized by synthetic adjusting parameters of the element, and carefully choosing input frequency of electric source.

455

Generalized Rayleigh Surface Waves in a Functionally Graded Piezoelectric Material (FGPM) Layered Structure

Xiaoshan Cao, Feng Jin, and Tianjian Lu, Xi'an Jiaotong University (China)

The propagation behavior of generalized Rayleigh surface waves in a transversely isotropic functionally graded piezoelectric material (FGPM) layer/elastic substrate layered structure is taken into account. Phase velocity equations for electrically open and shorted at the free surface are obtained analytically. Influences of graded variation of material parameters on dispersion relations of Rayleigh surface waves and corresponding electro-mechanical coupling factor are quantified. Further research concerned with the particles' displacement properties in the FGPM layer for the Rayleigh wave propagation. Results obtained may provide theoretical guidance for designing surface acoustic wave devices based on deep insight into the characters of Rayleigh-type surface waves.

456

Electroelastic Stress in an Electrostrictive Material with Charged Surface Electrodes

Quan Jiang, Cunfa Gao, Nanjing University of Aeronautics and Astronautics (China); Quan Jiang, Nantong University (China).

Field singularities of collinear electrodes on the surface of a half-infinite electrostrictive solid are studied in terms of the complex variable method. Firstly, the general solutions for the potential functions of electric fields and stresses are derived for the case of collinear electrodes based on analytical continuation method, and then explicit results are given for the cases of one and two electrodes, respectively. Numerical calculations are also made to discuss the effects of applied electric loading on the field singularities near the electrodes. It is found that even at the low level of applied electric loading, considerable high stresses will be induced around the electrodes, especially at the tip of electrodes,

and moreover for the cases of multiple electrodes, the distribution of electric fields and stresses is more complicated than the case of a single electrode.

457

Transient responses of finite piezoelectric hollow cylinder under torsional excitation

H. M. Wang, Department of Mechanics, Zhejiang University (China)

An exact elastodynamic solution is obtained for a finite piezoelectric hollow cylinder under torsional excitation. The cylinder is made of 622 crystal class and is traction free at the two ends. Also, the cylinder is fixed at the external surface and is subjected to dynamic shearing stress and time dependent electric potential at the internal surface. In axial direction, the trigonometric series expansion technique is first introduced to guarantee the solution satisfy the end conditions. Then the governing equations for the new variables about radial coordinate r and time t are derived. By means of the normal mode expansion method, the solution for torsional vibration is finally obtained. Numerical investigations are presented. According the obtained results, the dynamic behaviors of the finite piezoelectric hollow cylinder are analyzed.

458

Analysis of Functionally Graded Circular Piezoelectric Bimorph By Fem Using Matlab

R.Q. Xu, B.L. Shao, Zijingang Campus Zhejiang University (China)

Circular piezoelectric bimorph has been successfully used in numerous types of microdevices, such as actuators for flowcontrol applications, transducers for acoustic applications, and in locomotion of robotic systems, energy harvesting and active structural health monitoring applications. Recently, the concept of the functionally graded material is introduced to improve properties and increase lifetime by selectively grading the elastic, piezoelectric, and/or dielectric properties along the thickness of a piezoceramic. However, even for the simple case of homogeneous circular piezoelectric geometry, analytical treatments are severely limited. This study established a sub-parametrical element to model the functionally graded circular piezoelectric bimorph, which consisting of functionally graded piezoelectric layer, bonding material and electrode. Both axisymmetric and non-axisymmetric cases can be considered in this element as well as static and dynamical behaviors. MATLAB is used to implement the whole FEM program and gives some numerical examples to demonstrate the presented method.

459

The Analysis of FBAR with the Consideration of Film Piezoelectric Properties

Ji Wang, Jiansong Liu, Jianke Du, Dejin Huang, Ningbo University (China)

The vibration frequency analysis of film bulk acoustic resonators (FBAR) is based on the assumption of layered infinite plates vibrating at working mode, which can be the extensional or thickness-shear depending on the original design. A transcendental equation is used to determine the vibration frequency with given materials and plate thicknesses. Similar to the analysis and design of quartz crystal resonators of thickness-shear type, frequency equations and displacements in the films can be used for the calculation of resonator properties which are important for

improvement and modeling. By expanding the formulation to include the piezoelectric effect, we shall also be able to obtain the electrical field as a vital addition to mechanical solutions. Of course, the piezoelectric effect will also be included in the frequency and displacements. The solutions can be used to calculate the electrical circuit parameters of a resonator. We study the vibrations of layered FBAR structures for both extensional and thickness-shear modes and the solutions also include the electrical field under an alternating voltage. With these equations, solutions, and further formulations on the electrical circuit properties of FBAR, we can establish a systematic procedure for the analysis and design, thus completing the currently empirical methodology in resonator development. These one-dimensional formulation based on the infinite plate assumption can be further improved through the consideration of finite plates and numerical solutions based on the commonly used finite element analysis. These studies will be the basis for the formulation and calculation of electrical circuit parameter extraction that is highly demanded as FBAR technology is expanding quickly to other applications. The accurate analysis and resonator property calculation will contribute to the sophistication of FBAR technology with improved design procedure and performance.

460

Vibrations of Layered Plates and Applications in the SMR Resonator Analysis

Ji Wang, Jiansong Liu, Jianke Du, Dejin Huang, Ningbo University (China)

Thin film acoustic wave resonators are typical layered structures consisting of piezoelectric and metal films serving as essential elements of vibration and excitation. Such a layered structure can be analyzed accordingly for the proper selection of the thicknesses of thin films based on the vibration frequency and resonator property. In recent studies on thin film acoustic wave resonators, especially the film bulk acoustic wave resonators (FBAR) and solidly mounted resonators (SMR) types, extensive fabrication and characterization efforts have been contributing to the development of many novel products and processing technology. The recently renewed global interests on the FBAR technology also expect the design of resonators can be done through sophisticated analysis with wave propagation and circuit theories. These requirements have motivated our studies on the vibrations of layered piezoelectric structures with applications in the FBAR resonator analysis and design. Based on the justified assumption that the microstructure of FBAR can also be treated as infinite plates, the vibration frequencies of the extensional and thickness-shear types are calculated from layered models with perfectly bonded interfaces. The calculated frequencies are in good agreement with experimental data. We now extend the analysis to SMR structures, which have much more bonded layers of piezoelectric and metal films, with the same assumption of infinite plates and perfect interfaces. The vibration solutions are given in terms of frequency and displacements. These results can be used for the proper determination of the film thicknesses and materials based on the resonator property which can be calculated from mechanical vibrations.

462

Exact Analysis of Longitudinal Vibration of a Nonuniform Piezoelectric Rod

W.Q. Chen, Zhejiang University (China); C.L. Zhang, Zhejiang University (China)

Piezoelectric rods are frequently used as transformer, known as Rosen transformer. This report shows that the equations of motion

governing the free longitudinal vibration of a nonuniform piezoelectric rod can be reduced to those that can be solved analytically by using suitable variable substitutions. Exact analytical solutions to determine the longitudinal natural frequencies and mode shapes for the nonuniform rod are derived. Numerical examples are given to show the effect of geometric non-uniformity on the dynamic characteristics of the rod.

463

Development and Implementation of a Remote Real-time Monitoring System for Cable Force of Tianjin Yonghe Cable-Stayed Bridge

Hongwei Li, Hui Li, Jinping Ou, Harbin Institute of Technology (China); Guohui Liu, Tianjin Highway Engineering Design Institute (China); Jinping Ou, Dalian University of Technology, (China)

Bridge cables are used as critical structural components for cable-stayed bridges. It is essential to identify and monitoring the cable force of cable-stayed bridges in real time and continuously. In this paper, the design of a remote real-time cable force monitoring system including both hardware and software components are realized and the specifications of the system are also presented. The system was implemented in the Tianjin Yonghe cable-stayed bridge located in Tianjin, China, to remotely monitor the cable force of the bridge and provide the condition assessment of the cables to the users via Internet. Experiences with this system demonstrate how effective low cost system provides a tremendous cost savings in terms of travel time, maintenance, and repair costs. This paper will also discuss the monitoring system and provides a preliminary analysis based on the data acquired from this system.

464

Non-Classical Generalized Deformable Theory for Functionally Graded Ultra-Thin Films

C.F. Lv, Zhejiang University (China); C.W. Lim, City University of Hong Kong (HongKong, China); W.Q. Chen, Zhejiang University (China)

A generalized refined theory including surface effects is developed for functionally graded (FGM) ultra-thin film. The classical generalized shear deformable theory is adopted to model the film bulk, while the bulk stresses on the surfaces are required to balance the surface stresses, which are determined according to the linear theory of surface elasticity. As a result, a non-classical generalized deformable theory is developed. A simply supported thin film in cylindrical bending is considered as an example to illustrate the application of the present theory. It is established that the shape function and the deflection exhibit significant size-dependence as the film thickness falls below micro-scales. By comparing to the Kirchhoff plate theory including surface effects, the necessity of the present theory for FGM thin films is solidly validated.

466

Smart Fiber Reinforced Plastic Composites Based on Fiber Optic Sensing

C.Q. Yang, Y.S. Tang, S. Shen, W. Hong, Southeast University (China); Z.S. Wu, Ibaraki University (Japan).

Smart materials have attracted worldwide attention both in research and application fields in recent years, among which the smart fiber reinforced plastic (FRP) composite is an important branch. In this paper, the development and application of smart FRP composite based on fiber optic sensing is briefly reviewed. The FRP composite is characterized by excellent mechanical property as well as high corrosion resistance and long-term durability, such as

its high strength/modulus ratios, which is suitable to be structural material. In the smart FRP composite, the structural elements are the reinforcing fibers and polymers, and the active elements are optic fibers. The active optic fibers may be optic FBG (Fiber Bragg Grating) sensors or traditional optic fibers. The FBG sensors are characterized by a high sensing accuracy and dynamic measurement; while, the traditional optic fibers analyzed with Brillouin scattering techniques are characterized by a distributed and continuous sensing. Consequently, the smart FRP composite based on optic fiber sensing are characterized by excellent mechanical and sensing properties as well as good designability. They can be used in many engineering fields, such as aerospace, civil and mechanical engineering.

467

Mathematical Characterization of the Hetero-structures of the Composites of Polyacene Quinone Radical Polymers and Sulfonated Polyurethanes Based on the Dielectric Studies

Dan Zhu, Nanjing Normal University (China); Juan Zhang, Masaru Matsuo, Nara Women's University (Japan); Chunye Xu, University of Washington (USA).

The sulfonated polyurethane (PUI) and polyacene quinone radical polymers (PAQRs) are synthesized and the composites of them are prepared with the contents of PAQRs is varied from 10 wt.% to 50 wt.%. The dielectric percolation threshold of the composites appears around 30% weight ratio (30 wt.%) of PAQR. PUI and the composites obtain high dielectric constant and loss, which is explained from the view of the polarization processes and the microscopic structures of the materials. The high dielectric constant is due to the polar sulfonate groups of PUI and the nomadic polarization in PAQR, as well as the interfacial polarization at the interface between the PAQR and PUI, and the contact effect occurring at the surface of the sample to the electrode. The dielectric loss is resulted from the conduction and the impedance to the orientation of the huge polarizing species from the space charges at the interfaces between the filler grains and the matrix. The structural diagrams and the equivalent circuit model are established for the composite below and above percolation, and the corresponding computational fitting is done for the dielectric responses of the composites. The parameters obtained from the fitting provide quantitative evaluations on the structural morphology and charge densities of the interface between PAQR and PUI, which correlate with the compatibility and the interaction between the two phases, and provide the origin of the deviation from the Debye dispersion in the dielectric behavior of the composites.

468

The Calculation of Dynamic Stress Intensity Factor of an Interfacial Under Uniform Speed Expanding Impacting Loading

Jin Cheng, Baoke Guo, Li Zhang, Harbin Institute of Technology (China)

Multi-layered structure and composite materials have been used broadly and lots of defects of interface are inevitably in them. Among of all defects, crack plays an important role for the damage of the materials. In engineering, interfacial crack surfaces often produce complicated impact each other under loadings. These additive impacting loadings have great effects to the damage of cracked structures. In this paper, the dynamic stress intensity factor of an interfacial crack between two homogeneous isotropic half infinite mediums produced by the uniform speed expanding impacting loading is calculated. Fourier and Laplace transforms are employed to simplify the general wave equations into ordinary

differential equation. Consider the zero initial and boundary conditions, the formal solution in double transform domains are obtained. The Cauchy singular integral equation of dislocation density function (DDF) is derived through Fourier integral inversion. By expanding DDF into Jacobi polynomials with weight function, the solution of DDF in Laplace transform domain is obtained numerically. Subsequently, the dynamic stress intensity factors of crack tips are expressed using the solution. To determine the dynamic stress intensity factors in time domain, a new efficient adaptive method of Laplace numerical inversion is used. Finally, as an example, the two half finite mediums takes Al alloy and steel, respectively. The numerical results of dynamic stress intensity factor are calculated and displayed graphically.

469

Magnetic Field Activation of Shape Memory Polymer Networks Containing Micron Nickel Powder

Jinsong Leng, Harbin Institute of Technology (China); Dawei Zhang, Northeast Forestry University (China)

Shape memory refers to the ability of certain materials to remember a shape, on demand, even after rather severe deformations. The most common material exhibiting such a property is nitinol, a nickel-titanium alloy of which the shape-memory effect is produced by a solid state phase transformation. In recent years, shape memory polymers have received increasing attention because of their low cost, low density, high shape recoverability and easy processability, compared to conventional shape-memory alloys. Basic principles of the shape memory effect in macromolecule materials can be well described by their elastic modulus-temperature behavior. At temperatures above the T_g , the polymer achieves a rubbery elastic state where it can be easily deformed without stress relaxation by applying external forces over a time-frame $t < \tau$, where τ is a characteristic relaxation time. When the material is cooled below its T_g , the deformation is fixed and the deformed shape remains stable. The predeformed shape can be easily recovered by reheating the material to a certain temperature higher than the T_g . An alternative shape memory polymer is styrene-type polymer which has been studied by several researchers. The styrene-type shape memory polymer which has two phases or showing cross-linked structure may show the shape memory effect. This paper is concerned about the synthesis of shape memory polystyrene copolymer and the investigation of the influence of the radiation dose on its shape memory effect. As one of novel actuators in smart materials, shape memory polymers (SMPs) have been investigated intensively. Styrene copolymer with proper cross-linking degree can exhibit shape memory effect (SME). In this paper, the shape memory effect of radiated polystyrene copolymer was investigated by shape recovery ability including shape recovery rate and efficiency. The radiation dose of styrene copolymer was determined by changed radicalization time. The glass transition temperature (T_g) of styrene copolymer was measured by Dynamic Mechanical Analysis (DMA). The shape memory performance of styrene copolymer with different radiated dosage was also evaluated. Results indicated that the shape memory polymer (SMP) was synthesized successfully. The T_g increased from 60°C to 65°C followed by increasing the radiation dose. Moreover, the SMP experienced good SME and the largest reversible strain of the SMP reached as high as 150%. When heating above $T_g+30^\circ\text{C}$ (different copolymers performed different T_g), the shape recovery speed of the copolymers increased with increasing the radiation dose. However, the recovery speed decreased with increasing the radiation dose at the same temperature of 95°C.

470

Novel Deployable Morphing Wing based on SMP Composite

Kai Yu, Jinsong Leng, Harbin Institute of Technology (China)

As a novel kind of smart materials, SMP composite has many advantages such as high strain recovery, low density, low cost, easy shaping procedure and easy control of recovery temperature. In this paper, a new kind of deployable morphing wing base on SMP composite is designed and tested. While the deployment of the morphing wing still relies on the mechanisms to ensure the recovery force and the stability performance, the deploying process tends to be more steady and accurate by the application of this smart material, which overcomes the inherent drawbacks of the traditional one, such as harmful impact to the flight balance, less accuracy during the deployment and complex mechanical masses. On the other hand, SMP composite is also designed as the wing's filler. During its shape recovery process, SMP composite stuffed in the wing helps to form an aerofoil for the wing and withstand the aerodynamic loads, leading to compressed aerofoil of the wing recovers its original shape. This kind of design can minimize the wing's volume for continently storage in a limited space. To demonstrate the feasibility and the controllability of the designed deployable morphing wing, primary tests are also conducted, including the deploying speed and actuating efficiency as the main testing aspects. Finally, Aerodynamic characteristics of the designed morphing wing are calculated by using CFD software. Wing's deformation under the air loads is also analyzed by using the finite element method to validate the flight stability in different situations.

471

Electroactive Shape Memory Polymers Composites and Their Applications

Xin Lan, Haibao Lv, Yanju Liu, Jinsong Leng, Shanyi Du, Harbin Institute of Technology (China)

As a novel smart material, shape memory polymers (SMPs) are a class of stimuli responsive materials, which recover the original shapes from large deformation when subjected to an external stimulus. The SMPs have not fully reached their technological potential, largely due to that the actuation of shape recovery in thermal-responsive SMPs is normally only driven by external heat. Thus, electro-activate SMP has been figured out and its significance is increasing in years to come. This review focuses on the progress of electro-activate SMP composites. Special emphases are given on the filler types that affect the conductive properties of these composites. Then, the mechanisms of electric conduction are addressed. Finally, the corresponding applications are presented.

472

Thermalmechanical Properties of Thermoset Shape-Memory Polymer Nanocomposite Filled with NanoCarbon Powders

Xin Lan, Yanju Liu, Jinsong Leng, Harbin Institute of Technology (China)

This paper concerns the thermalmechanical properties of thermoset styrene-based shape-memory polymer (SMP) nanocomposite filled with nanosized carbon powders. With an increase of the incorporated nano-carbon powders of the SMP composite, its glass transition temperature (T_g) decreases, and its storage modulus as well as thermal conductivity increases. Due to the high micro-porosity and homogeneous distributions of nano-carbon powders in SMP matrix, the SMP composite shows good electrical conductivity with a percolation of about 4 %. This percolation threshold is slightly lower than that of many other carbon based conductive polymer composites. Consequently, due to the relatively

high electrical conductivity, a sample filled with 10 vol% nano-carbon powders shows a good electroactive shape recovery performance heating by a low voltage above a transition temperature of about 65°C.

473

Electromechanical stability Analysis of Dielectric Elastomer

Liwu Liu, Yanju Liu, Shouhua Sun, Zhen Zhang, Kai Yu,, and Jinsong Leng, Harbin Institute of Technology (China)

The dielectric elastomer film will encounter electrical breaking-down frequently in its working state due to the coupling effect of electric field and mechanical force field. Referring to the electromechanical coupling system stability theory of dielectric elastomer proposed by Suo and Zhao, the electromechanical stability analysis of dielectric elastomer has been investigated. According Suo's theory, the free energy function of dielectric elastomer can be represented by the principle of superposition. Unstable domain of electromechanical coupling system of Neo-Hookean type silicone was analyzed by R. Díaz-Calleja et al. In the current work, the elastic strain energy function with two material constants was used to analyze the stable domain of electromechanical coupling system of Mooney-Rivlin type silicone, and the results seem to support R. Díaz-Calleja's theory. These results provide useful guidelines for the design and fabrication of actuators based on dielectric elastomer.

474

Variable Camber Wing Based on Pneumatic Artificial Muscles

Weilong Yin, Yijin Chen, Libo Liu, Jinsong Leng, Harbin Institute of Technology (China)

As a novel bionic actuator, pneumatic artificial muscle has high power to weight ratio. In this paper, a variable camber wing based on the pneumatic artificial muscle is developed. Firstly, the experimental setup to measure the static output force of pneumatic artificial muscle is designed. The relationship between the static output force and the air pressure is investigated. Experimental result shows the static output force of pneumatic artificial muscle decreases nonlinearly with increasing contraction ratio. Secondly, the finite element model of the variable camber wing is developed. Numerical results show that the vertical displacement and deflection angle of the trailing-edge increase linearly with increasing external load and limited with the maximum static output force of pneumatic artificial muscles. Finally, the variable camber wing model is manufactured to validate the variable camber concept. Experimental results show that the wing camber increases with increasing air pressure.

475

A Preliminary Study on Anti- γ -irradiation Performance of Epoxy Shape Memory Polymer with Various Hardener Content

Xuelian Wu, Yanju Liu, Jinsong Leng, Harbin Institute of Technology (China).

Shape memory polymer (SMP) is a new class of smart material which receives increasing attention in recent years. In this paper, in addition to the fabrication of a new series of epoxy SMPs with various hardener contents, the thermo-mechanical properties of the polymers both under/no gamma irradiation conditions were investigated and compared systematically. The radiation source is Co-60 and the total dosage of radiation is 1×10^4 Gy. Changes of network structures of the polymers was investigated by Fourier Transform Infrared spectroscopy. The effect of gamma irradiation on thermo properties of the polymers was studied by Differential Scanning Calorimetry (DSC). The influence of gamma irradiation

on mechanical properties and thermo-mechanical of the polymers was investigated by tensile test and Dynamic Mechanical Analysis respectively. Further, effect of gamma irradiation on shape memory effect of the polymers was compared too. Results show that the epoxy SMPs possesses good chemical stability, as the types of chemical groups doesn't change with gamma irradiation. Glass transition temperature (T_g) of irradiated polymers determined by DSC decreases 5-7°C compared with that before radiation. For each polymer before/after gamma radiation, no considerable change have been found in the curves of the storage modulus, loss modulus and $\tan \delta$ as a function of temperature, respectively. And tensile strength decreases from 15% to 30% while elongation at break is stable with the gamma radiation. Of particular attention is that the irradiated polymers can recover its initial shape fully which is same with that of polymer before gamma radiation, while the former shows quicker shape recovery speed than that of the latter. Results indicate that, the epoxy SMPs prepared in the study possess not only good thermo-mechanical properties but unique anti-gamma irradiation performance. Therefore, the results are significant for the application of SMP in aerospace fields.

476

Design of a Morphing Airfoil Using Aerodynamic Shape Optimization

Yuemin Yu, Jinsong Leng, Yanju Liu, Harbin Institute of Technology (China)

Recent advances in new smart materials science and actuation technologies have led to interest in morphing airfoils. The research discussed in this paper focuses upon the shape design of morphing airfoil sections. A designer can select the airfoil shapes with improved aerodynamic performance at the design conditions. The NACA 4412 sections is used as initial airfoil. An aerodynamic shape optimization computer program based on a computational fluid dynamics (CFD) solver with the Spalart-Allmaras turbulence model and a sequential quadratic programming algorithm is used in order to obtain a set of optimal airfoils at the different stages of air vehicle. The aerodynamic shape optimization program is used to obtain the airfoil that has the optimal aerodynamic characteristics at each one of stages of flight. Once the optimal airfoils at each stage of flight are obtained, the results are analyzed in order to gain a better understanding of the most efficient initial airfoil configuration. The results show that a very thin airfoil could be used as the initial configuration. Furthermore, a morphing mechanism that controls the camber and leading edge thickness of the airfoil will almost suffice to obtain the optimal airfoil at most operating conditions.

477

Dielectric Properties of Carbon Nanotube/Silicone Elastomer Composites

Zhen Zhang, Jinsong Leng, Liwu Liu, Shouhua Sun, Yanju Liu, Harbin Institute of Technology (China).

Dielectric elastomers have received a great deal of attention recently for effectively transforming electrical energy to mechanical work. Their large strains and conformability make them enticing materials which can be applied in many domains: biomimetics, aerospace, mechanics, medicals, etc. In order to maximize actuator performance, the dielectric elastomer actuators should have a high dielectric constant and high dielectric breakdown strength. Here we have investigated the increase in permittivity of a commercial silicone elastomer by the addition of carbon nanotube. The percolation threshold of the composites is obtained to be low and the elastic modulus also remains low. Experimental results suggest that for the case of conductive filler

particle-elastomer matrix interaction, actuation strain increases with increasing carbon nanotube content.

478

Fabrication and Properties of Shape-Memory Polymer Coated With Conductive Nanofiber Paper

Haibao Lv, Jinsong Leng, Yanju Liu, Harbin Institute of Technology (China); Jan Gou, University of Central Florida (USA)

A unique concept of making shape-memory polymer (SMP) nanocomposites from carbon nanofiber paper was explored in this study. The essential element of this method was to design and fabricate carbon nanofiber paper with well-controlled and optimized network structure of carbon nanofibers. In this study, carbon nanofiber paper was prepared under ultrasonicated processing and vapor press method, while the dispersion of nanofiber was treated by BYK-191 dispersant. The morphologies of carbon nanofibers within the paper were characterized with scanning electron microscopy (SEM). In addition, the thermo-mechanical properties of SMP coated with carbon nanofiber paper were measured by the differential scanning calorimetry (DSC) and dynamic mechanical thermal analysis (DMTA). It was found that the glass transition temperature of nanocomposites was slightly depressed determined by DSC, while the storage modulus was obviously enhanced in comparison with that of pure styrene-based SMP. Additionally, the thermal and electrical conductivity of nanocomposites were measured, and experimental results revealed that the conductive properties of nanocomposites were significantly improved, resulting in short response time to direct heating and electrical current.

479

Modeling Thermo-Mechanical Behaviors of Reinforced Shape Memory Polymer Under Cyclic Loads

Bo Zhou, Guangping Zou, Xin lan, Jin-Song Leng, Yan-Ju Liu, Harbin Institute of Technology (China)

Shape memory polymer (SMP) is able to keep a temporary shape formed through high-temperature deformation at a low temperature, and recover its original shape by heating to a critical temperature, which is called as shape memory effect. SMP experiences lower stress during deformation and demonstrates much larger recoverable strain. Early applications of SMP included heat shrinkable tubes, wraps, foams and self-adjustable utensils. Recently, SMP has begun to be applied in the areas of biomedical devices, deployable space structures and micro-systems. With the development and application of SMP, the reinforced SMP was also fabricated and investigated to overcome the limitations of SMP such as low strength, low stiffness, low recovery stress, electric insulation, and so on. Reinforced SMP has been playing an important role in deployable structures, such as deployable space antenna, truss and solar arrays in space industry, due to its superexcellent shape memory effect. It is of great interest to investigate thermo-mechanical behaviors of reinforced SMP.

In this paper, styrene-based fiber reinforced SMP is fabricated to improve the thermo-mechanical properties of the pure SMP. DMA tests are conducted on the reinforced SMP and pure SMP to investigate the influences of the reinforcement in the reinforced SMP on the glass transition behavior. Static three-point bending tests are performed to investigate the stiffness and strength of the reinforced SMP and pure SMP at room temperature. Cyclic three-point bending tests are carried out to investigate the material training effects of the reinforced SMP and pure SMP. Based on the experimental results, a training evolutionary equation is established to describe the material training effect of the reinforced SMP and pure SMP. Numerical calculations show the training evolutionary

equation can predict the material raining effect of the reinforced SMP and pure SMP.

480

Recent Advances in Shape Memory Polymers and Their Multifunctional Composites

Yanju Liu, Xin Lan, Jinsong Leng, Shanyi Du, Harbin Institute of Technology (China)

Shape-memory polymers (SMPs) have been one of the most popular subjects under intensive investigation in recent years, due to their many novel properties and great potential. These SMPs by far surpass shape-memory alloys and shape-memory ceramics in many properties, e.g. easy manufacture, programming, high shape recovery ratio and low cost, and so on. This paper firstly presents the definition and fundamentals of SMPs. Then, various types of shape memory polymers, their composites and corresponding applications are presented. Specially, a novel method is developed to use infrared laser to actuate the SMP through the optical fiber embedded into the SMP. Furthermore, a series of fundamental investigations of electroactive SMP are conducted. Electrically conductive fillers are utilized as the fillers to improve the electrical conductivity of polymer, and then the shape recovery is performed.

481

A Novel Time Division Multiplexing Fiber Bragg Grating Sensor Interrogator for Structural Health Monitoring

Yongbo Dai, Jinsong Leng, Gang Deng, Harbin Institute of Technology (China)

A novel fiber Bragg grating (FBG) sensor system for Structure Health Monitoring (SHM) is proposed in this paper. The proposed sensor technique is based on time division multiplexing (TDM). A semiconductor optical amplifier (SOA) connected in a ring cavity is used to serve as a gain medium and switch. The SOA is driven by a pulse generator which switch on the SOA at different periods, as a switch to select the reflected pulses from a particular sensor. The FBG sensors have identical center wavelengths and can be deployed along the same fiber. This technique relieves the spectral bandwidth issue and permits the interrogation of up to 100 FBGs along a fiber. The sensor system has a fast signal process and control unit, which have a typical scan frequency in 50 Hz and self-adaptive measurement for simple sensor array installation.

482

Reliability Assessment of Long Span Bridges based on Structural Health Monitoring: Application to Yonghe Bridge

Shunlong li, Hui Li, Jinping OU, Hongwei Li, School of Civil Engineering, Harbin Institute of Technology (China); Jinping Ou, School of Civil and Hydraulic Engineering, Dalian University of Technology (China)

This paper presents the reliability estimation studies based on structural health monitoring data for long span cable stayed bridges. The data collected by structural health monitoring system can be used to update the assumptions or probability models of random load effects, which would give potential for accurate reliability estimation. The reliability analysis is based on the estimated distribution for Dead, Live, Wind and Temperature Load effects. For the components with FBG strain sensors, the Dead, Live and unit Temperature Load effects can be determined by the strain measurements. For components without FBG strain sensors, the Dead and unit Temperature Load and Wind Load effects of the bridge can be evaluated by the finite element model, updated and calibrated by monitoring data. By applying measured truck loads and axle spacing data from weight in motion (WIM) system to the

calibrated finite element model, the Live Load effects of components without FBG sensors can be generated. Then first order reliability method (FORM) is employed to estimate the reliability index of main components of the bridge (i.e. stiffening girder). Furthermore, practical damage situations are considered to evaluate the influence of certain elements' failure on the reliability of undamaged components.

483

Prewarning of the China National Aquatics Center using Johnson Transformation based Statistical Process Control

Deyi Zhang, Yuequan Bao, Hui Li, Jinping Ou, Harbin Institute of Technology (China); Jinping Ou, Dalian University of Technology (China)

Structural health monitoring (SHM) is regarded as an effective technique for structural damage diagnosis, safety and integrity assessment and service life evaluation. SHM techniques based on vibration modal parameters are in-effective for space structure health maintenance and the statistical process control (SPC) technique is a simple and effective tool to monitor the operational process of structures. Therefore, employing strain measurements from optical fiber Bragg grating (OFBG) sensors, the Johnson transformation based SPC is proposed to monitor structural health state and some unexpected excitations on line in this paper. The large and complicated space structure-the China National Aquatics Center is employed as an example to verify the proposed method in both numerical and experimental aspects. It is found that the Johnson transformation can effectively improve the quality of SPC for SHM process, and it can clearly and effectively monitor structural health state and detect the unexpected external load happened in structures.

484

Damage Identification Method based on Fractal Dimension and Shannon Entropy

Yong Huang, Hui Li, Yongchao Yang, Harbin Institute of Technology (China)

Fractal geometry has been widely used to describe irregular phenomena such as damage in the structure as a new mathematical tool. However, most of structural damage identification methods based on fractal theory have the drawback of not being robust to noise which restricts their practical application. A new high noise robust damage identification method based on fractal dimension is presented in this paper. The damage index was deduced from the Katz's fractal dimensions of certain sampling points with arithmetic of Shannon entropy. The selection of sampling points in the sliding windows for calculating damage index is also studied and it can be regarded as a trade-off between the peak value generated by the damage and the stability of the damage index curve. As a validation, the proposed method is applied to detect damage in a simply supported beam by numerical and experimental study. The successful detection of the damage in the beam demonstrates that the method is capable of estimating the location of the damage. Noise stress tests are also carried out to demonstrate the strong robustness of the method under the influence of noise with appropriate sampling points in the sliding windows. The new fractal-based index is a promising damage identification method.

485

Numerical Methods for Investigation of Elastic Waves in Piezoelectric Structures

Xu Han, Hunan University (China).

With the phenomenal progress of the hi-tech frontier technology

such as ultrasonic dimensioning measurement, nondestructive examination, a preferable understanding of the electro-elastic waves in piezoelectric media is of practical and exploratory significance for its engineering application. Among the relevant researches which already abound in domestic and global academics with considerable achievements emerging in recent years, an effective numerical method, which confers the augmented functionality for analysis of wave propagation in piezoelectric media, is one of the research hotspots with raising prevalence. In this paper, a numerical-analytical method is suggested to deal with the investigation of electro-elastic coupled transient responses and characteristic wave surfaces in piezoelectric structures. The layered elements are introduced to represent the physical model of the piezoelectric structures, which slashes the generated nodes compared with the FEM methods. The governing equations are determined by Hamilton Principle with consideration of the coupling between the elastic and electric field in each element. The displacement and electro-potential are discretized along the thickness direction which fairly well maintains the accuracy of the simulation for analysis of the laminated or shell-type structures. The modal analysis and Fourier transformation with respect to dependent coordinates in the wave propagation directions are introduced to formulate the corresponding representations of elastic and electric fields in wave-number domain, which delivers the augmented efficiency and convenience in numerical computation for the solutions of the governing differential equations could be obtained by the integration with respect to wave-number. Six surfaces (phase velocity surface, phase slowness surface, phase wave surface, group velocity surface, group slowness surface, and group wave surface) are proposed to illustrate the characteristic of waves in piezoelectric structures. The mechanical and electrical responses can be obtained by performing the inverse Fourier transformation. Numerical examples are presented to analyze the wave propagation in an actual piezoelectric structure, and demonstrate the efficiency and accuracy of the present method.

486 Electromechanical Stability of Dielectric Elastomer Undergoing Large Deformation

Liwu Liu, Yanju Liu, Shouhua Sun, Zhen Zhang, Kai Yu, Jinsong Leng, Harbin Institute of Technology (China)

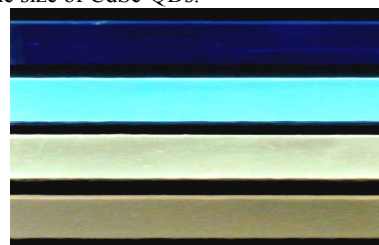
Dielectric elastomers are one of the important electroactive polymers used as actuators in adaptive structures due to their outstanding abilities to generate very large deformations while subjected to an external electric field. In this paper, Mooney-Rivlin elastic strain energy function with two material constants is used to analyze the electromechanical stability performance of dielectric elastomer. This elastic strain energy together with the electric energy incorporating linear permittivity is the main item to construct the free energy of the system. Particular numerical results are also calculated for further understanding of the dielectric elastomer's typical stability performance. The proposed model offers great help in guiding the design and fabrication of actuators featuring dielectric elastomers.

488 Synthesis and Optical Properties of Transparent and Light-Emitting Silicone Nanocomposites

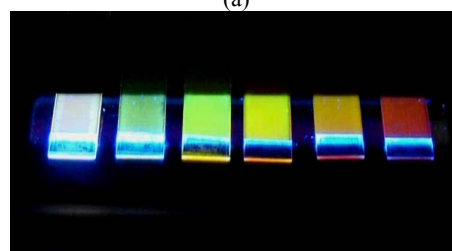
Yang Yan, Shaoyun Fu, Technical Institute of Physics and Chemistry, Chinese Academy of Sciences (China)

Due to the unique optical properties of transparent luminescent nanocomposites, they have shown a great potential to be applied in optoelectronic devices, light-emitting diodes and paints. Combination of transparent polymers and quantum dots (QDs)

leads to development of functional transparent and light-emitting polymer composites that have unique photoluminescent properties. In this paper, ZnO-QDs, ZnO-QDs/SiO₂ and CdSe-QDs were used to synthesize silicone nanocomposites with interesting fluorescent properties. Moreover, ZnO/SiO₂ nanoparticles were also employed to examine the effect of their size and composition on the transmittance of silicone nanocomposites. ZnO-QDs with different sizes were synthesized via a sol-gel method and then the transparent ZnO-QDs/silicone nanocomposites were subsequently prepared via the solution direct-mixing method. ZnO-QDs/silicone nanocomposites with different sizes of ZnO-QDs can emit different colors as shown in Figure 1a just like ZnO-QDs alone do, indicating that the nanocomposites can be prepared with adjustable luminescence by controlling the size of ZnO-QDs. ZnO-QD/SiO₂ (Z-S) nanoparticles were prepared by hydrolyzing TEOS within the ZnO-QD containing ethanol solution. Silica, which enwrapped ZnO-QDs, can effectively prevent the aggregation and growth of quantum dots. The Z-S composite particles containing different sized ZnO-QDs show different emission peaks. Then transparent Z-S/silicone nanocomposites were successfully prepared in terms of the matrix-filler RI matching principle and the best transmittance was achieved when ZnO-QDs content in Z-S composite nanoparticles was about 47 wt%. Z-S/silicone nanocomposites have the similar fluorescence and phosphorescence properties as Z-S composite particles do. While it is difficult to get red fluorescence from ZnO-QDs, CdSe-QDs, with the bulk bandgap of 1.72 eV, can be prepared with full color emission. CdSe-QDs with different sizes were prepared by a solvothermal method. Small CdSe quantum dots with emission in blue region were gained by an oxidation etching approach using H₂O₂ as oxidant. The CdSe/silicone nanocomposites were prepared via solution mixture method. The optical properties of CdSe/silicone nanocomposites with different sizes of CdSe-QDs and different contents of CdSe-QDs were studied. CdSe/silicone nanocomposites with different size of CdSe-QDs can emit lights with different colors as shown in Figure 1b, indicating that the transparent CdSe/silicone nanocomposites with adjustable luminescence can be prepared by controlling the size of CdSe-QDs.



(a)



(b)

Figure 1 Digital photos of (a) the neat silicone and the silicone nanocomposites containing 0.4 wt% ZnO-QDs of different sizes (from top to bottom: neat silicone, 1.95, 3.08 and 3.99 nm) under the excitation of UV light at $\lambda = 302$ nm and (b) of the CdSe-QDs/silicone nanocomposites containing CdSe with different diameters (from left to right: 3.60, 4.24, 4.43, 4.86, 5.32 and 6.55 nm) under UV light ($\lambda = 365$ nm).

Non-contact Dynamic Displacement and Vibration Measuring Technology using Laser Doppler Vibrometer

Ting Liu, Huan Liu, Hui Zhu, A.K.Asundi, Yunfeng Song, Sunny Instruments Singapore Pte.Ltd. (Singapore); Hui Zhu, A.K. Asundi, Nanyang Technological University (Singapore)

LDV (Laser Doppler Vibrometer) is one of the most efficient devices used in non-contact vibrating measurement. In this paper a simple but efficient calibration method for LDV is introduced. It is widely used in industry such as MEMs, hard-disk fabrication. And different measured object need different precision and different range. So calibration for a LDV is quite important. It determines the occasion that can be used. The purpose of this paper is to provide industries a suitable calibration method to reduce the cost and simplify the procedure of calibration and offer a reference for LDV applications.

Finite Analyse on New Structure of Integrated Core Sandwich Composites

Guo Yi, Yanju Liu, Jinsong Leng

The integrated core sandwich composites' layers are fabricated by the pillars which composited fibre and resin. These materials have shown excellent activate properties including low-quality, high-rigidity and strong, etc. In order to predict the macroscopic elastic constants of this structure accurately, a unit cell geometric model is presented. Then the macroscopic elastic constants are obtained using this finite element model. For the verification of the proposed finite element model, numerical results of macroscopic elastic constants' analysis are compared with those of experimental test results.